SAPIENZA
UNIVERSITÀ DI ROMA

*Raihan Rahmat Rabi*

# PROPOSAL OF AN ENERGY-BASED METHOD FOR THE DESIGN OF PASSIVE ENERGY-DISSIPATIVE BRACES

*PhD Thesis*
*XXXII Cycle*

*Supervisor*

*Prof. Ing. Giorgio Monti*

*PhD in Structural Engineering*

**Acknowledgements**

I would like to thank my supervisor Prof. Ing. Giorgio Monti and co-supervisor Dr.Vincenzo Bianco for their expertise, ideas, feedback, time and encouragement.

I want to express my gratitude to my family, particularly my parents who helped and encouraged me throughout my whole life.

I am grateful to the Ministry of Foreign Affairs of Italy for their continuous financial assistance during my PhD research.

Raihan Rahmat Rabi

**TABLE OF CONTENTS**

# CHAPTER 1

# INTRODUCTION

# 1 Introduction

## *1.1 Background*

Recent earthquakes have highlighted the urgency and importance of rehabilitating seismically deficient structures to achieve an acceptable level of performance. This can be achieved either by reducing the load effect to the existing structures, or by improving their strength, stiffness, and/or ductility. Over the past 20 years, significant advancements have been made in the research and development of innovative materials and technologies for improving the seismic performance of existing structures through rehabilitation processes.

Seismic protection of existing structures represents nowadays one of the main research and professional fields in structural engineering.

Many examples of bad and unsatisfactory structural performance, particular in case of reinforced concrete (RC) structures, were due to several reasons such as bad quality of materials, rough execution, lack of appropriate design of local details and inadequate code provisions. Besides, even if in very few cases, failures have also occurred in steel buildings during the well-known 1994 Northridge and 1995 Kobe earthquakes, due to unexpected brittle local behavior of connections as opposed to the large dissipative capacity expected by structural designers [1]. Following such experiences, research efforts have been addressed to the definition of both new proper constructional details to enhance the structural ductility [2] and to the revision of the current design procedures in seismic zones to better correlate the available plastic capacities with the actual seismic demands. As a result of these efforts, a new concept and design method has been introduced during the last years. It is represented by the so-called 'Damage Tolerant Structures' approach that differs from the common seismic structural design. In fact, the latter is based on the well-known concept to entrust the energy dissipation role under strong earthquakes to the plastic deformation capacity of beams and columns, with a consequence damage of primary structural elements even for moderate-intensity earthquakes. On the other hand, the 'Damage Tolerant Structures' approach consists in the use of special seismic protection sacrificial devices, which modify the dynamic properties of the primary structure and/or increase its dissipative capacity, thus controlling and reducing the dynamic response of the whole structure. The control of the dynamic response can be obtained through passive, active and hybrid protection systems.

The interest of this study is mainly turned to passive control systems, where the fundamental period and damping capacity of the structure equipped with protection devices remains constant during the seismic motion, without the intervention of any external power source, as instead happens in the active and hybrid control systems.

Among several passive control systems, ductile steel bracing systems have been studied.

Use of steel bracing is an effective strategy for the global-level strengthening and stiffening of existing buildings. Concentric or eccentric bracing schemes can be used in selected bays of an RC frame to increase its lateral resistance. The main advantage of

this method is that a rehabilitation of the foundation may not be required because steel bracings are usually installed between existing members. However, load increase on the existing foundation is still possible at the bracing locations, so that the foundation must be nonetheless evaluated. In addition, the connection between the existing concrete frame and the bracing elements should be carefully treated because connections are vulnerable during earthquakes. Several researchers have reported successful results when using steel bracing to upgrade RC structures [3] [4].

Extensive research is done in developing procedures for the design of passive energy dissipative bracing systems grounded on various concepts, i.e., force-based, displacement-based and energy-based. In this study, a new energy-based approach for the design of energy dissipative braces (EDBs) is proposed and its efficiency is compared with several recent design approaches available in the literature.

## *1.2 Motivation and scope of the research*

Existing reinforced concrete (RC) frame buildings with non-ductile detailing usually show a considerable risk during earthquakes. This type of building suffered severe damage and was responsible for most of the life losses during major Italian seismic events, such as the 1981 Irpinia earthquake. Several technical solutions are currently available for the mitigation of earthquake risks, going from active to passive dissipating devices as well as base isolation. The use of steel in seismic retrofitting and upgrading of existing constructions has long been studied [5,6]. Systems based on steel are generally very useful in those situations characterized by the absence of purposely-designed lateral-load resisting structures. A correct design of these systems is based on the idea of eliminating/reducing the plastic deformation demand to the existing structure by adding supplemental energy dissipating devices. Among these systems, metal-based technologies are often considered as the most satisfactory technical solutions, because of the effectiveness, practicality and economy. Metal solutions mainly consist in adding new structural elements (generally in form of braces), which collaborate with the existing structure, by varying its static scheme and operating at global level as supplemental energy dissipation passive systems, thus acting as a sort of ductile hysteretic fuse.

In the last years, steel dissipative bracing systems have been widely and successfully used as complementary structural elements, and sometimes also as substitutive elements of other lateral load resisting systems under seismic actions. In fact, a number of studies proved their significant effectiveness on the structural performance under wind and seismic loads. Both eccentric braces and buckling-restrained braces are characterized by a stable and compact hysteretic response, providing large energy dissipation capacity. These dissipative bracing systems are designed to dissipate most of the energy input by a strong earthquake and if they are damaged, they make post-earthquake rehabilitation easier, since these devices are designed to be replaceable. In eccentric braced frames (EBFs), forces are transferred to the brace members through bending and shear forces developed in the ductile steel link. The link is a beam element delimited by the braces. Links are designed to yield and dissipate energy while preventing buckling of the brace members.

Moreover, bolted connections between the link ends are suggested, in order to facilitate replacement of dissipative zones (links) after a damaging earthquake, which reduces repair costs. In case of buckling-restrained braces (BRBs), the avoidance of global compression buckling allows to solve the problem of the limited ductility of classic concentric bracings. They are made of very slender steel plates, forming the core of the BRB, which are allowed to yield both in tension and in compression. These slender plates are inserted in between steel rectangular or square hollow section profiles, which provide the restraining effect against lateral buckling. In the most classical form, the restraining tube is filled with concrete and an un-bonding layer is placed at the contact surface between the core plates and the filling concrete, thus the name of this version 'unbonded brace'. However, 'only-steel' solutions have been proposed, with two or more steel tubes in direct surface contact with the yielding steel plates. In the latter case, the restraining tubes can also be connected by bolted joints, thus allowing an easy inspection and maintenance during the lifetime or after a damaging earthquake.

Nowadays, many passive energy dissipative bracings design methodologies are available in literature, which follows various design concepts such as displacement-based approaches or energy-based approach. This study is focusing on:

a) *Analysis of the pros and cons of existing procedures for the design of Energy Dissipative Braces (EDBs),*
b) *Proposal of a new energy-based approach.*

This research is also significant to provide a practitioning engineer with a more comprehensive, easy-to-apply and more reliable method for the design of EDBs.

## *1.3 Organization of the thesis*

This thesis is organized in the following way:

In Chapter 2 the gravity-load-designed (GLD) structures are explained, the main deficiencies of non-engineered or structures built prior to the enforcement of seismic design codes are reviewed, in order to understand the need for retrofitting.

Chapter 3 is dedicated to the introduction of steel bracing systems and its various types used for retrofitting of existing buildings and in the design of new buildings. Moreover, some recent applications of these systems in Europe, particularly in Italy, are shown.

Chapter 4 is divided in two parts: in part 1 the seismic performance assessment methods known as N2 and the capacity spectrum method are thoroughly explained; part 2 presents the currently available methodologies for the design of passive energy dissipative devices developed on various design philosophies such as displacement- and energy-based concepts and their drawbacks are highlighted.

Chapter 5 presents the proposed energy-based methodology for the design of EDBs. In this Chapter, several important concepts such as input and hysteretic energy of SDoF system, inelastic input and hysteretic energy spectra and optimum strength distribution

philosophy are discussed. All of these concepts are essential to understand the conceptual bases of the proposed methodology.

Chapter 6 presents the application of the selected and proposed design procedure for EDBs on three 2D frames. The frames are subjected to nonlinear static and nonlinear dynamic analysis. The results of pre-retrofitted and post-retrofitted frames are discussed, and a comparison is done.

Chapter 7 presents the conclusions and outcome of the thesis.

# CHAPTER 2

# SEISMIC BEHAVIOUR
# OF GRAVITY-LOAD-DESIGNED STRUCTURES

# 2 Seismic Behavior of Gravity-Load-Designed (GLD) Structures

## *2.1 Introduction*

RC buildings represent a consistent part of the world construction heritage (in Italy over 50%) and a remarkable part of them has been built either without the application of seismic codes or adopting inadequate provisions of anti-seismic design. In Italy, more than a half of such patrimony has been built before 1971, when the observance of specific technical provisions for the seismic zones foreseen by Law 64/74 became obligatory. In that period the design of RC buildings was based on the use of the Law 1684/1962, which did not give any specific indication on constructional details (minimum amount of steel bars, stirrups, etc.) and regularity prerequisites able to guarantee an acceptable behavior of constructions under earthquakes.

For these reasons, the evaluation of the overall capacity of existing RC buildings is an important topic both in the engineering practice and in the research field, for both the assessment of the seismic vulnerability and the choice of opportune retrofitting solutions. To achieve this goal, the effects of past earthquakes on constructions help understand the seismic behavior of RC structures with non-ductile details and to identify possible retrofitting strategies. In detail, during violent seismic events (e.g., Irpinia 1980, Turkey 1999, Greece 1999) an unsatisfactory behavior of such structures has been observed, especially those designed only under gravitational loads, when seismic classification was not still introduced. Framed RC structures designed without adequate seismic rules and therefore able to exclusively withstand vertical loads (Gravity Load Design, GLD) show in many cases a deficient behavior characterized by a low ductility of beam-to-column joints and the absence of an appropriate resistance hierarchy able to provide collapse mechanisms of global type. Other observed problems were generally represented by the lack of in-plane and/or in-elevation regularity, the elevated torsional deformability and the presence of short columns, which determine an overall unsatisfactory seismic behavior.

Based on these circumstances, the key concepts of modern seismic codes are based on the achievement of the following objectives:

- prevent non-structural damage under seismic events of moderate intensity, which can frequently occur during the life of the structure,

- prevent structural damage, reducing the non-structural one, under seismic events of moderate intensity, which can happen less frequently,

- avoid structural collapse under high intensity earthquakes.

These prerequisites identify different performance levels for the structures, according to the methodology of the "Performance Based Design", in the certainty that the principal purpose of the different design criteria is to allow the evaluation of the desired performances of the structure under the applied load conditions. All these considerations underline a sequence of problems in the evaluation of the seismic behavior of the existing RC structures. Generally, all resistant mechanisms resulting either of brittle type or sensitive to the cyclic degradation have to be correctly evaluated by means of adequate calculation models in order to obtain reliable results in the

evaluation of the actual seismic performance. In this context, by evaluating the constructional details of RC structures designed under vertical loads only, the deficiencies reported in Figure 2.1 can be mainly recognized.

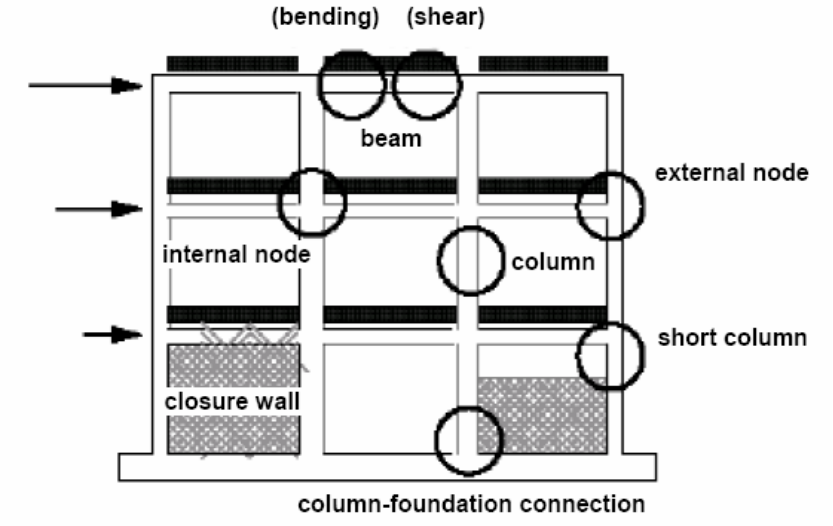


*Figure 2.1:Building designed for gravity loads*

## *2.2 The structural conception of 70s and 80s buildings*

The structural typology of RC frames of non-seismic buildings reached his "maturity" in the period between '70s and '80s. Many studies carried out on a number of RC buildings realized before 1970 have underlined as the calculation formalities of the structural elements conceived for withstanding gravitational loads do not differ significantly from the ones designed after the introduction of the law 1086/71. The main constructional differences between the structural typologies characterizing these two constructive epochs are represented by the adopted materials.

The design of this kind of building was developed by initially defining the position of the beams (generally deep beams) at each storey only with reference to the needs to support vertical loads. Thus, plane frames were realized along only one of the main orthogonal directions of the plan (usually the longitudinal one). The further needs "to close" the building with walls gave rise to perimeter frames and some internal frames (e.g. in the staircase area) along the other direction.

For standardization and simplicity reasons, the deep beams in a storey were made adopting the same transversal section. But, due to the fact that the beams were designed only for carrying vertical loads, they were the same also along the whole height of the buildings, giving rise to a unique typical structural plan for all the storeys. This plan differed at each story only for the cross-section of the columns, which obviously grew going from the upper to the lower levels. The staircase was usually made with a knee sloping beam supporting cantilever steps (and then subjected to torsional actions too). Therefore, the staircase structure on the whole behaved as a very stiff frame, due to the knee beam, which represents a sort of bracing for the frame, usually oriented along the transversal direction of the building plan, in parallel with the floor structure. Nevertheless, this structural scheme, even if providing lateral stiffness in one direction, gives rise to stocky columns (in both directions) which could be prone to dangerous brittle shear failure when the building is subjected to significant horizontal actions.

The floor structure was designed with reference to vertical loads only. Nevertheless, the current technology provided the thin upper slab with some weak reinforcements (transversal distribution reinforcement), in order to distribute concentrated load. Sometimes, when the constructional process was particularly accurate, also one or two transversal girders were made, with the scope to both better distribute any concentrated load and face transversal boundary effects. Even if no conceptual reference to floor diaphragm effect was made at that time, this effect is naturally performed by the slab, but limited by its resistance related to the small thickness of concrete and to the amount and continuity of the reinforcements. Generally, the columns had rectangular cross-section. The small dimension of the cross-section was ever not greater than 30-40 cm, in order to hide the columns in the perimeter walls. Consequently, the stiff direction (the depth) of the columns resulted in the plane of the perimeter walls, providing the building with a quite good distribution of the column stiffness along both the main direction of the plan for withstand horizontal loads, even if the designer usually did not consider these loads. In short, the design criteria used for proportioning the structural elements can be summarized as following:

- the beam cross-sections and reinforcements were sized with reference to only vertical loads. A simple continuous beam model was usually adopted, neglecting the rotation constraint given by the columns. The standardization of the cross-sections provided the beams of the transversal plan direction (which carried very low vertical loads) with significant overstrength;

- the columns were dimensioned on the base of axial forces only, neglecting any bending moment, considering a reduced value of the concrete compressive nominal strength (70%). The longitudinal (vertical) steel reinforcement area was defined as the 0.5 - 1.0% of the cross-section gross area. The allowable stresses method was used for safety verifications. Besides, this method is used in Italy also nowadays, even if it cannot be adopted for seismic design of structures and for seismic upgrading design anymore. It is well known that the allowable stress method (ASM) and the ultimate limit states method (ULSM) give quite the same results only for members in bending without reinforcement in compression [7]. In fact, the ULSM differs practically from ASM (in axial stress verifications) just for considering the reinforcement in compression more effective. For this reason, if we analyze and verify by means of ULSM an existing building, which has been designed without considering seismic actions but adopting the ASM, we should find an amount of over-strength in the columns (originally dimensioned only for compressive forces) that is greater than in the beams (originally verified only in bending). It can be said that the adoption of ASM provides the structure with a sort of capacity design, which is nowadays one of the most important criteria in seismic design. The foundation system was usually made by plinths based directly on the ground or on piles. Usually, the plinths were not connected one another, without any concerns on possible relative horizontal displacements among the column bases. Only on the perimeter of the building and around the staircase there were beams, connecting the plinths, in order to sustain the heavy perimeter walls of the basement. Anyway, the connections among internal columns should have been difficult to realize, because the columns usually were not aligned, particularly along transversal direction.

When continuous foundation beams were used instead of plinths, they were placed along the same alignment of the supporting beams of the floors, i.e. in longitudinal direction. In this case the foundation system was completed by transversal beams (not supported by the ground) for sustaining the perimeter walls. It is worth to notice that the foundation system was originally designed without considering any seismic horizontal load, but with reference to the effects of the maximum vertical loads. On the contrary, in case of seismic upgrading of the building, the foundation shall be verified for the effects of high horizontal (seismic) loads and reduced vertical loads (as prescribed by EC8 or by new Italian Code). For this reason, the amount of reinforcing interventions on the foundation system could be more limited than on the rest of the structure. The most sensitive aspect in seismic analysis and upgrading of existing building is the quality of detailing and materials, which directly influences both strength and ductility of beams and columns. Particularly the beam-to-column joints (panel zones) and the end zones of beams and columns were usually realized without any specific attention: they are generally affected by lack of stirrups and of re-bars anchorage, which lower in significant way the ductility capacity of the structural members. As far as the quality of materials is concerned, fortunately it is not very difficult to determine the compressive resistance of concrete and the typology and yield strength of re-bars, even if by means of destructive in-situ tests. Anyway, the quality level of the material used in that period results usually acceptable, even if the use of smooth rebar can be detected in few cases.

## *2.3 The structural inadequacy of GLD RC structures and relevant typical damages during seismic event*

Usually, the structural system of existing RC buildings is composed by resisting frames placed in one direction only, perpendicular to the floor slab orientation. Such frames are usually made of emergent beams, but in some cases, beams having the same depth of the slab are of concern. Therefore, in the other direction they are connected by the slab only, without any specific beam. The structural elements of these constructions are designed without any reference to the effect of horizontal forces, including explicitly also the wind action too. As a consequence, flexible resisting systems having a very poor ductility have been adopted. The typical lacks GLD buildings, according to the evidences reported in previous experimental and theoretical studies [8] are:

1. *Inadequate structural scheme*

In fact, GLD buildings are characterized by the absence of a coherent structural configuration, without the proper presence of continuous frames in the two main plan directions Figure 2.2.

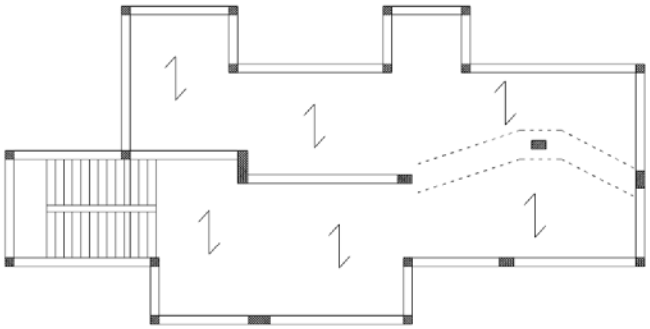

*Figure 2.2: Typical GLD plan, irregular and chaotic*

2. *Lack of in-plan regularity and an elevated torsional deformability*

This deficiency is mainly due to a large eccentricity between the centroid of stiffness and the centroid of floor masses (as shown in Figure 2.3). As a result of this inadequate plan configuration, torsional coupling effects may concentrate the lateral forces in some perimetric frames, thus resulting in an excess of local ductility demand.

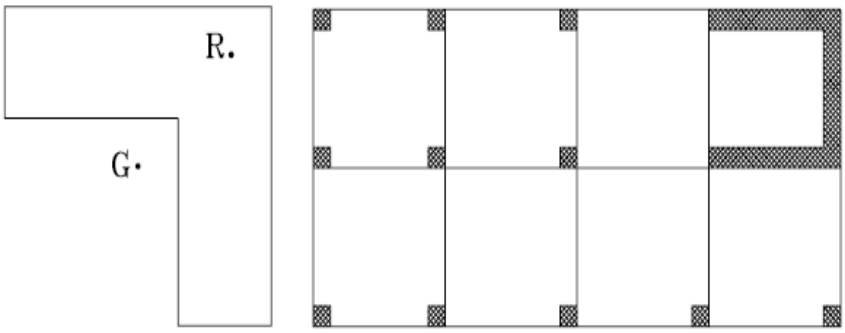


*Figure 2.3: In plan irregularity*

3. *Lack of in-elevation regularity*

This issue derives from typical architectural needs. It generally consists in an irregular distribution in elevation of lateral resisting systems. This improper structural configuration implies the concentration of ductility demand (and, as a consequence, of structural damages) in one or in a few stories. It is possible to identify two different types of elevation irregularity: an in-plane discontinuity irregularity and an out-plane discontinuity irregularity. In detail, an in-plane discontinuity irregularity shall be considered to exist in any primary element of the lateral-force-resisting system whenever a lateral-force resisting element is present in one story, but does not continue (as shown in Figure 2.4a), or is offset within the plane of the element, in the story immediately below (as shown in

Figure 2.4b). An out-of-plane discontinuity irregularity shall be considered to exist in any primary element of the lateral-force-resisting system when an element in one story is offset out-of-plane relative to that element in an adjacent story, as depicted in Figure 2.5.

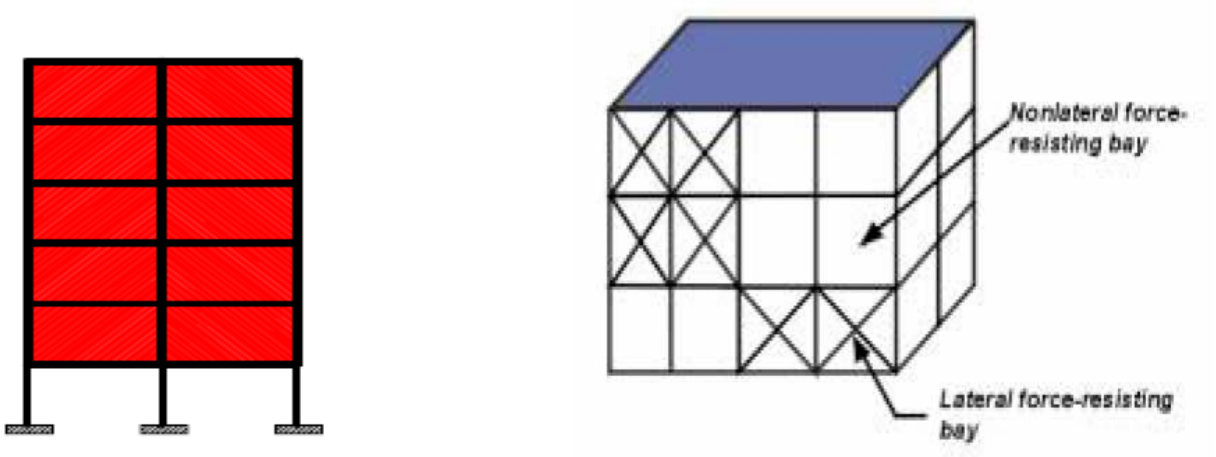


*a)* *b)*

*Figure 2.4: In-plane discontinuity irregularity in elevation (FEMA 356)*

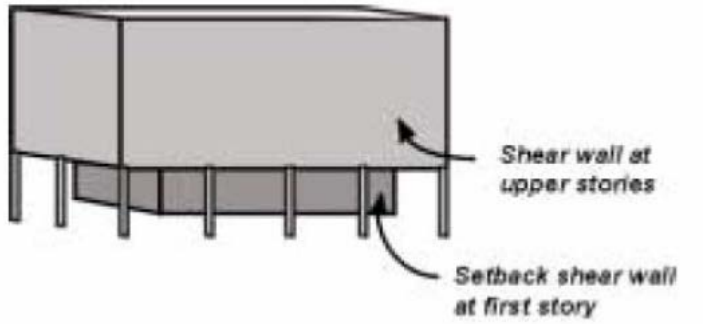


*Figure 2.5: Out-plane discontinuity irregularity in elevation (FEMA 356)*

As mentioned above, the result of irregularity in elevation consists in a concentration of the structural damages in a few stories, thus resulting in a so-called soft story or in a weak story. Generally speaking, a soft story is one that shows a significant decrease in lateral stiffness from that immediately above. A weak story is one in which there is a significant reduction in strength compared to that above. The condition may occur at any floor but is most critical when it occurs at the first story, because the forces are generally greatest at this level. Therefore, if all the stories are approximately equal in strength and stiffness, the entire building deflection under earthquake forces is distributed approximately equally to each story. If the first story is significantly less strong or more flexible, a large portion of the total building deflection tends to concentrate there, with consequent concentration of forces at the second-story connections Figure 2.6.

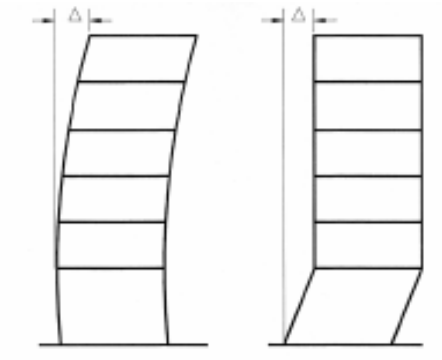

*Figure 2.6: Soft-Story mechanism formation*

In more detail, the soft-story problem may result from four basic conditions. These are summarized as follows:

- *Discontinuous load paths, created by a change of vertical and horizontal structure at the second story (*
- *Figure 2.4 and Figure 2.5)*
- *A first-story structure significantly taller than upper floors, resulting in less stiffness and more deflection in the first story (Figure 2.7a).*
- *An abrupt change of stiffness at the second story, though the story heights remain approximately equal. This is caused primarily by material choice: the use, for instance, of heavy precast concrete elements above an open first story (Figure 2.7b), or, more commonly in residential buildings, the presence of stiff masonry infill walls in the RC frame (Figure 2.7c)*

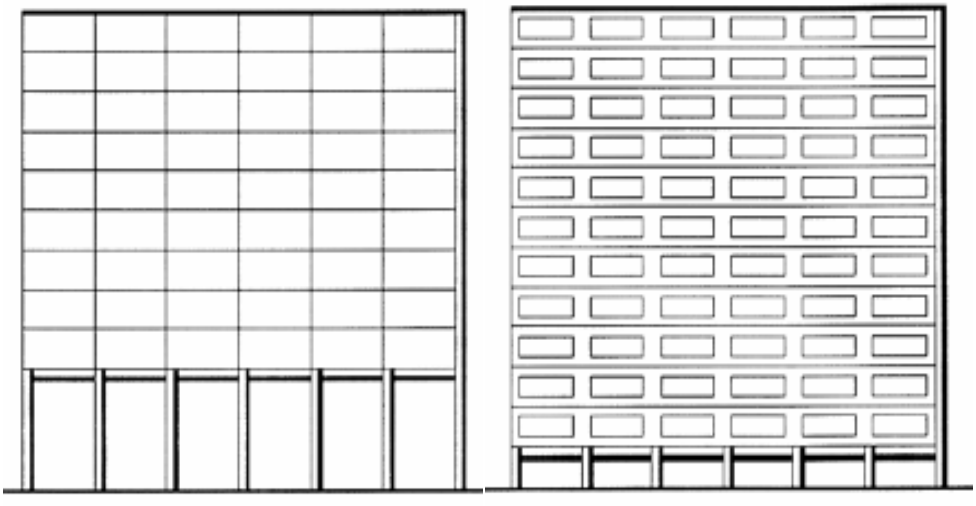

*a)* *b)*

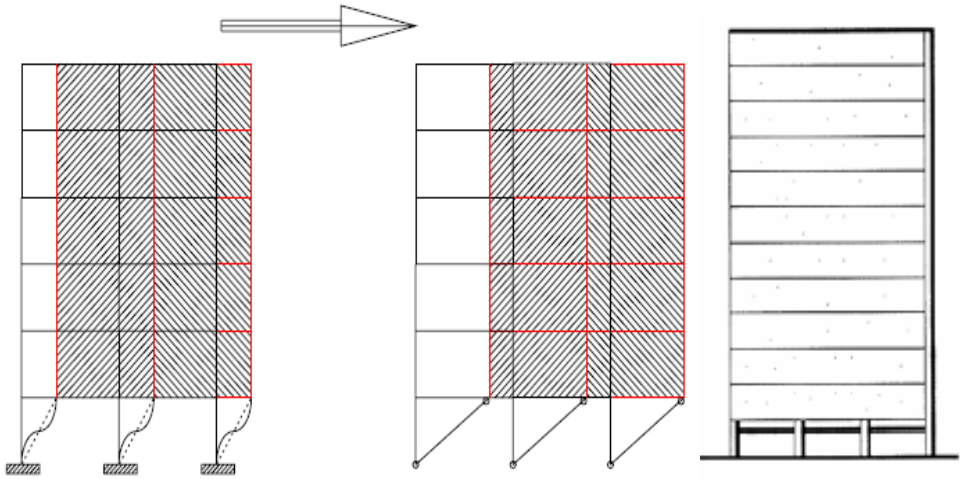

c ) d)

*Figure 2.7: Typical motivating causes for soft-story mechanism*

Typical damages and collapse mechanisms induced by soft story formation are summarized in Figure 2.8 through Figure 2.9.

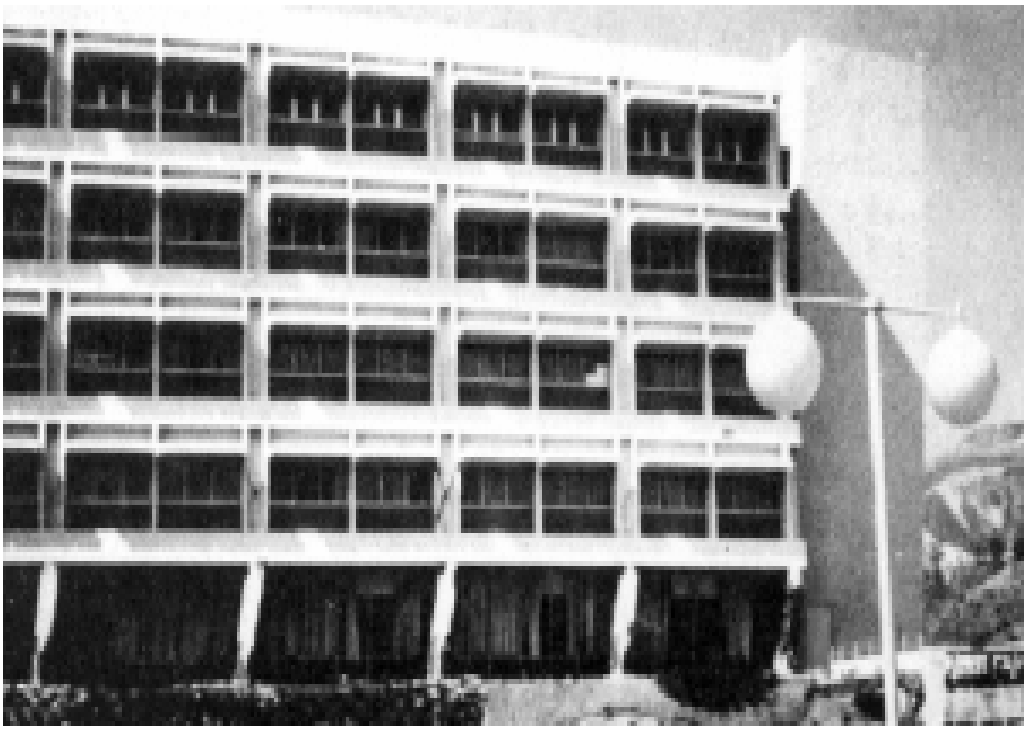

a)

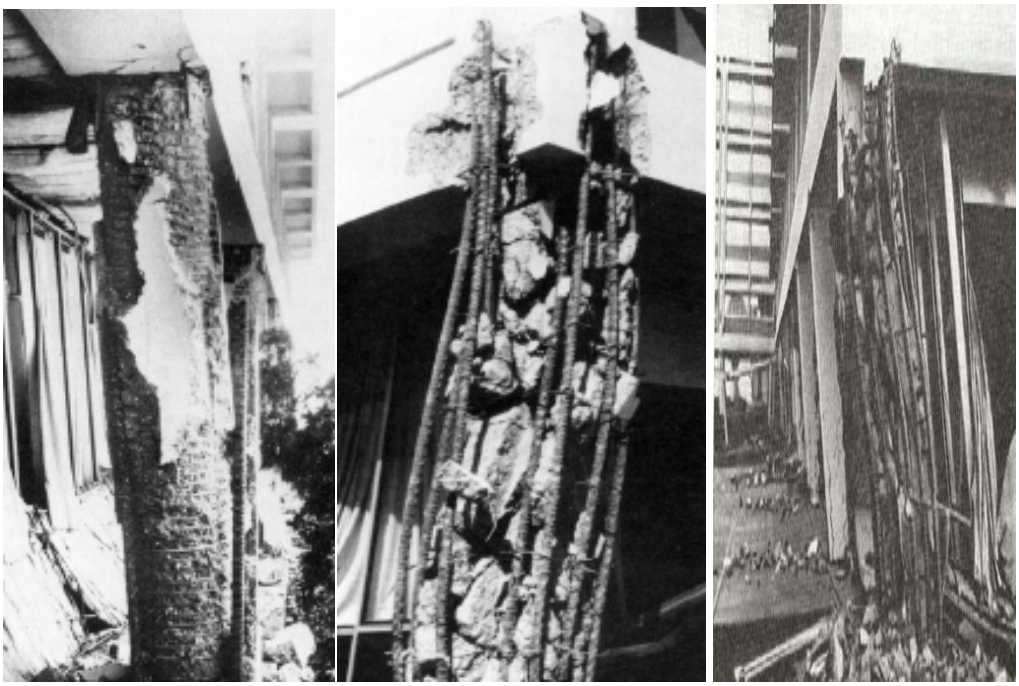

*b)* *c)* *d)*

*Figure 2.8:Damage to columns due to the formation of a soft story in the 4- story Olive View Hospital building during the February 9, 1971 San Fernando, California, earthquake: a wing of the building showing approximately 60cm drift in its first story (a); spirally reinforced concrete column in first story (b); tied rectangular corner column in first story (c, d).*

*Figure 2.9: Irpinia earthquake (1980), the global collapse of an hospital building due to formation of a soft story and poor local details.*

*3. Inadequate local details and lack of ductility.*

A good design concept is the proper detailing of members and their connections to achieve the requisite strength and ductility. Such detailing should aim at preventing non-ductile failures, such as those associated with shear and with bond anchorage. In fact, dynamic response to strong earthquakes, characterized by repeated and reversed cycles of large-amplitude deformations in critical elements, tends to concentrate deformation demands in highly stressed portions of yielding members. Hence, it is clear the great importance of proper detailing of potential hinging regions. Indeed, the experience and observation have shown that properly designed, detailed, and constructed reinforced-concrete buildings can provide the necessary strength, stiffness,

and inelastic deformation capacity to perform satisfactorily under severe earthquake loading.

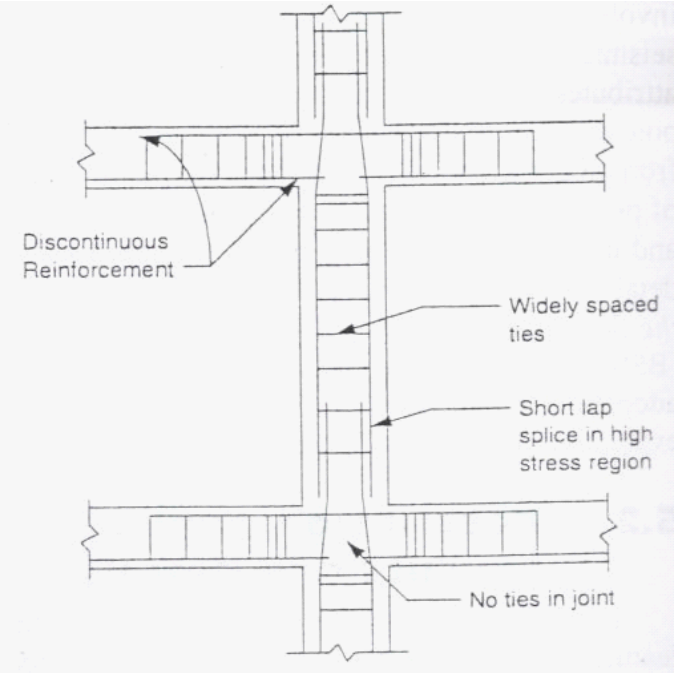


*Figure 2.10: Typical deficiencies in local details (ATC 40)*

In case of GLD RC structures, significant lacks in local details can be usually recognized Figure 2.10. Therefore, an accurate list of typical local deficiencies is summarized as follows:

- *Discontinuous transverse stirrups in beams and columns, largely spaced and not well bent inside the cross section. An insufficient reinforcement of the concrete in terms of bars and stirrups may induce undesirable brittle failures in the zones prone to develop plastic hinges. As an example in this sense, Figure 2.11 shows typical shear cracks due to the absence of adequate transverse reinforcement in a beam;*
- *Incorrect positioning of steel rebars and/or improper bars bending details. An example in this sense is shown in Figure 2.12 and Figure 2.13, where it is clearly highlighted the concrete cover spalling due to an incorrect positioning of bended steel rebars in a staircase flight and the detachment between the staircase flight and half pace;*

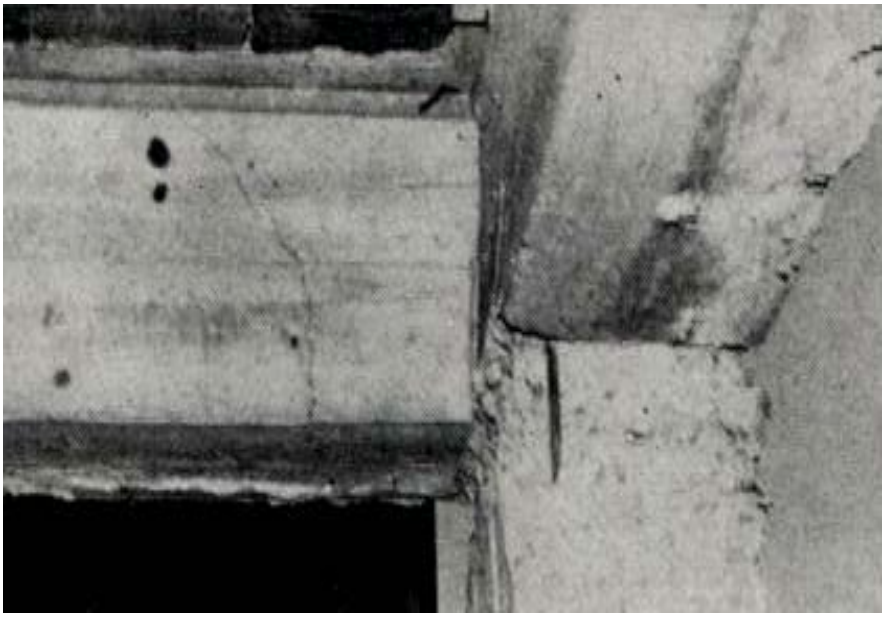

*Figure 2.11: Irpinia earthquake (1981), shear failure due to the absence of adequate transverse reinforcement in a beam.*

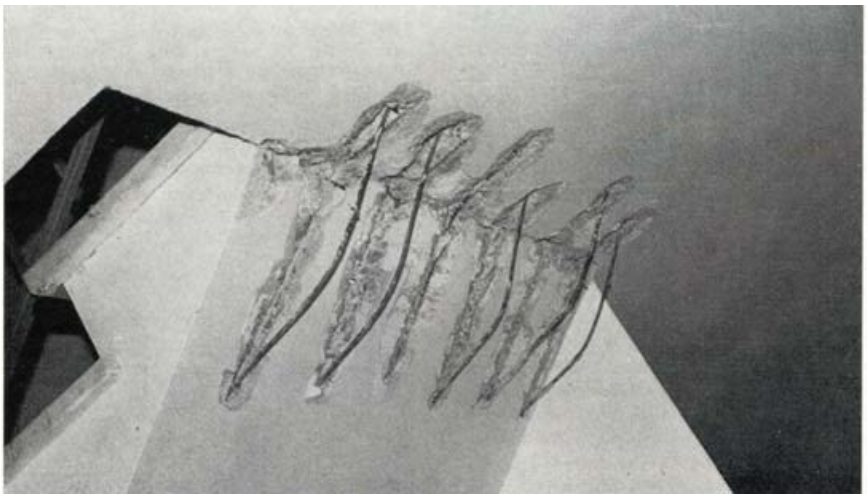

*Figure 2.12: Irpinia earthquake (1981), concrete cover spalling due to an incorrect positioning of bended steel rebars in a staircase flight.*

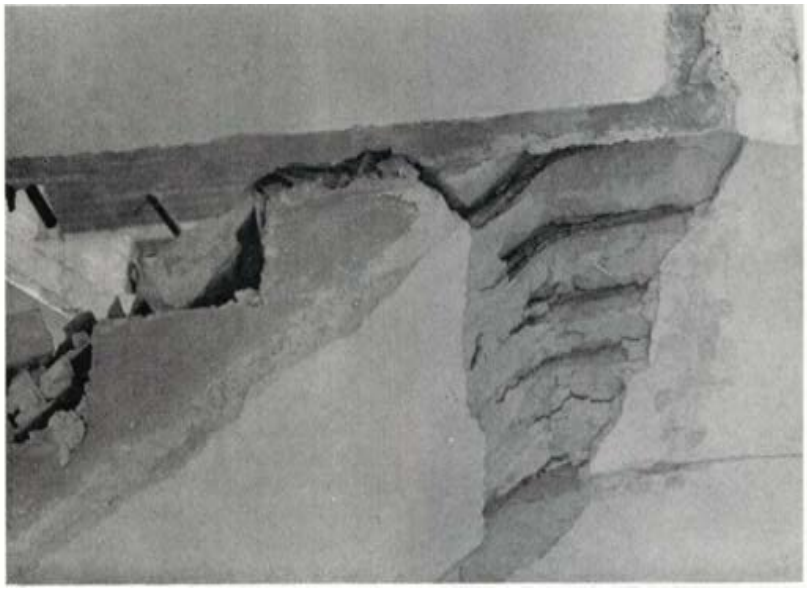

*Figure 2.13: Irpinia earthquake (1981), detachment between the staircase flight and half pace.*

- *Insufficient anchorage and incorrect overlaps of the longitudinal steel rebars. The scarce care of these details may induce strong damage concentration with one single large crack forming for each plastic hinge, thus indicating strong fixed-end rotation effects at large plastic story drift angles. This can be particularly evident for plastic hinges at the base of columns, where the presence of the lap-splice joint of the longitudinal steel reinforcement was present (Figure 2.14).*

*Figure 2.14: Fixed-end rotation at the base of column*

- *Eccentricities in beam to column joints;*
- *Scarce care of the resumptions of concrete casting of columns;*
- *The weakness of the columns in comparison to the beam, which can determine a soft-storey mechanism. This local deficiency is very common in GLD RC structure. In fact, in these structures the columns are usually designed to resist vertical loads. Consequently, the design bending actions can be considered*

*negligible respect to column axial loads. As a consequence, the results of this design process are slender columns with scanty amount of longitudinal and transverse steel reinforcement. This improper details induce a significant damage concentration in both column ends, usually characterized by concrete crushing and rebar buckling, thus assuming the so-called sharpened pencil shape (as shown from Figure 2.15a Figure 2.15g);*

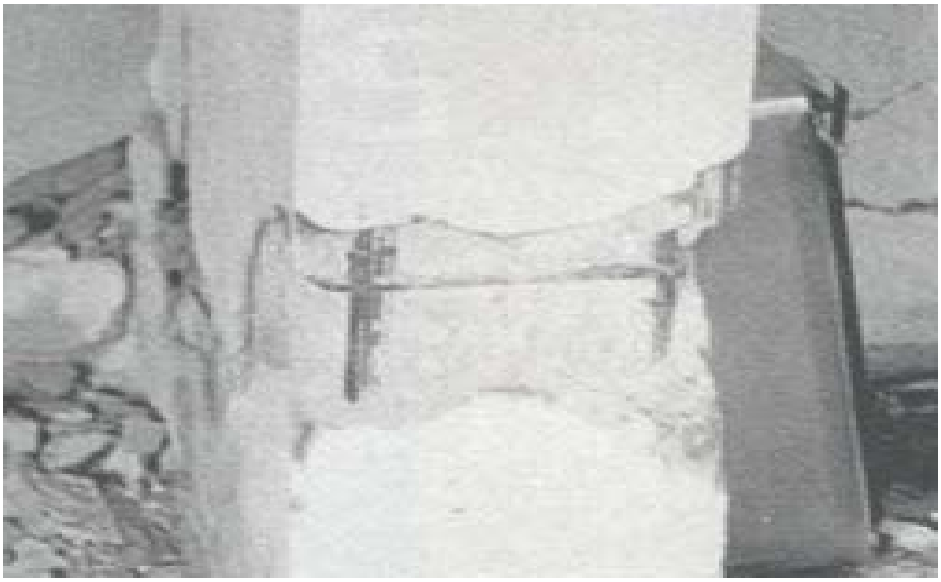

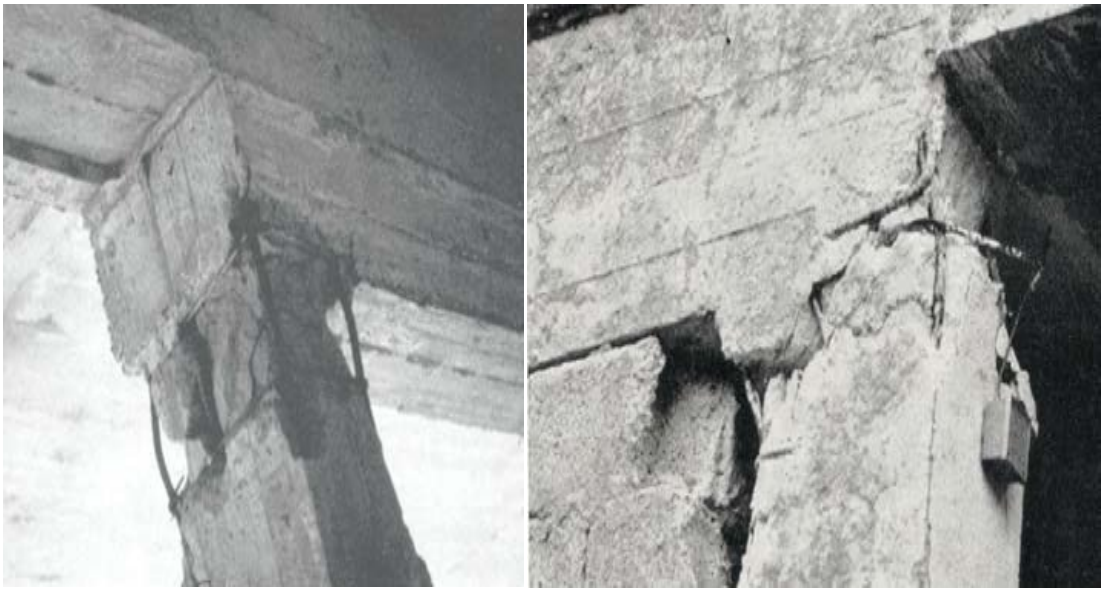

*Figure 2.15: Irpinia earthquake (1981), typical column failures due to inadequate local details and to weakness of the columns in comparison to the beam (continued).*

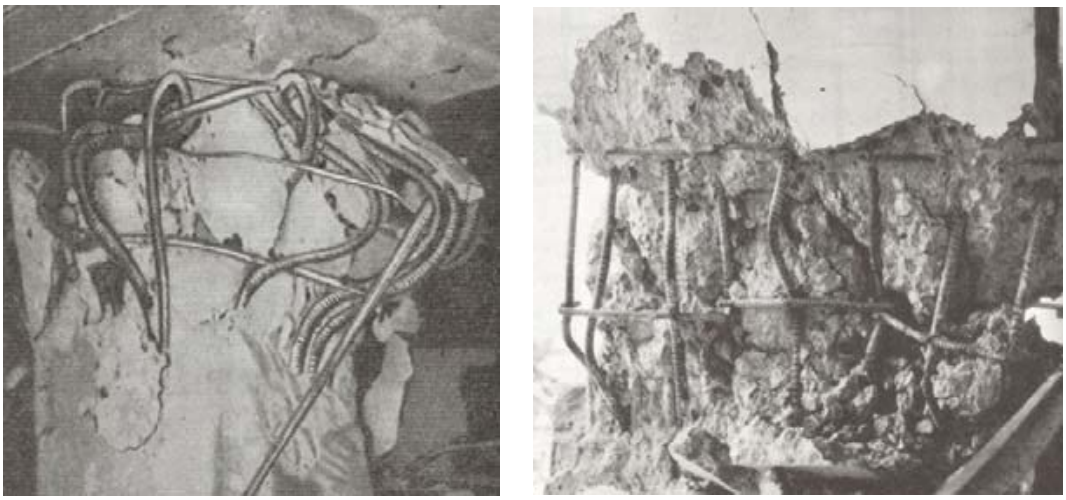

*Figure 2.16: Irpinia earthquake (1981), typical column failures due toinadequate local details and to weakness of the columns in comparison to the beam*

Absence of suitable confinement (that is transversal reinforcement) of beam-to-column joints and discontinuous bending reinforcement in correspondence of connections. Beam-column joints are critical elements in frame structures. These elements can be subjected to high shear and bond-slip deformations under earthquake loading. Beam-column joints have to be designed so that the connected elements can perform properly. This requires that the joints be proportioned and detailed to allow the columns and beams framing into them to develop and maintain their strength as well as stiffness while undergoing large inelastic deformations. A loss in strength or stiffness in a frame

resulting from deterioration in the joints can lead to a substantial increase in lateral displacements of the frame, including possible instability due to P-delta effects. The design of beam-column joints is primarily aimed at (i) preserving the integrity of the joint so that the strength and deformation capacity of the connected beams and columns can be developed and substantially maintained, and (ii) preventing significant degradation of the joint stiffness due to cracking of the joint and loss of bond between concrete and the longitudinal column and beam reinforcement or anchorage failure of beam reinforcement. Of major concern here is the disruption of the joint core as a result of high shear reversals. As in the hinging regions of beams and columns, measures aimed at ensuring proper performance of beam-column joints have focused on providing adequate confinement as well as shear resistance to the joint. The forces acting on a typical interior beam-column joint in a frame undergoing lateral displacement are shown in Figure 2.17. It is worth noting in Figure 2.17a that each of the longitudinal beam and column bars is subjected to a pull on one side and a push on the other side of the joint. This combination of forces tends to push the bars through the joint, a condition that leads to slippage of the bars and even a complete pull through in some test specimens. Slippage resulting from bond degradation under repeated yielding of the beam reinforcement is reflected in a reduction in the beam-end fixity and thus increased beam rotations at the column faces.

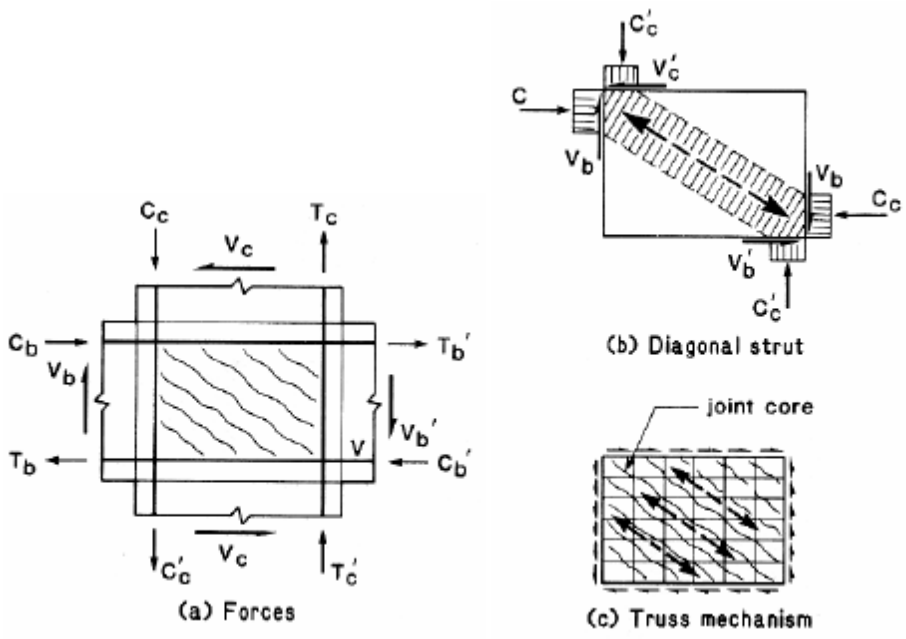


*Figure 2.17: Forces and postulated shear-resisting mechanisms in a typical interior beam-column joint: forces acting on beam-column joint (a); diagonal strut mechanism (b); truss mechanism (c).*

This loss in beam stiffness can lead to increased lateral displacements of the frame and potential instability. Two basic mechanisms have been postulated as contributing to the shear resistance of beam—column joints. These are the diagonal strut and the joint truss

(or diagonal compression field) mechanisms, shown in Figure 2.17b and c respectively. After several cycles of inelastic deformation in the beams framing into a joint, the effectiveness of the diagonal strut mechanism tends to diminish as through-depth cracks start to open between the faces of the column and the framing beams and as yielding in the beam bars penetrates into the joint core. The joint truss mechanism develops as a result of the interaction between confining horizontal and vertical reinforcement and a diagonal compression field acting on the elements of the confined concrete core between diagonal cracks. Ideally, truss action to resist horizontal and vertical shears would require both horizontal confining steel and intermediate vertical column bars (between column corner bars). Experimental tests cited in [9] indicate that where no intermediate vertical bars are provided, the performance of the joint is worse than where such bars are provided. Tests of beam-column joints [10] in which the framing beams were subjected to large inelastic displacement cycles have indicated that the presence of transverse beams (perpendicular to the plane of the loaded beams) considerably improves joint behavior. Results reported in [10] show that the effect of an increase in joint lateral reinforcement becomes more pronounced in the absence of transverse beams. However, the same tests indicated that slippage of column reinforcement through the joint occurred with or without transverse beams. The use of smaller diameter longitudinal bars has been suggested [11] as a means of minimizing bar slippage. Another suggestion has been to force the plastic hinge in the beam to form away from the column face, thus preventing high longitudinal steel strains from developing in the immediate vicinity of the joint. This can be accomplished by suitably strengthening the segment of beam close to the column (usually a distance equal to the total depth of the beam) using appropriate details, as a combination of heavy vertical reinforcement with crossties, intermediate longitudinal shear reinforcement, and supplementary flexural reinforcement and haunches. However, as shown in Figure 2.18 and Figure 2.19, during past earthquakes the absence of these contrivances resulted in severe damage in beam-to column joints, characterized by slipping phenomena of the bars, especially in case of employment of smooth bars without enough extremity hooks, that especially occurred in the external joints, which appear to be the most critical parts of the structure, but also in the intermediate ones, in case of not continuous longitudinal reinforcements. Besides, the absence of adequate quantity of stirrups at the beam-to-column intersection, due to the high shear stresses determined the collapse of the joints.

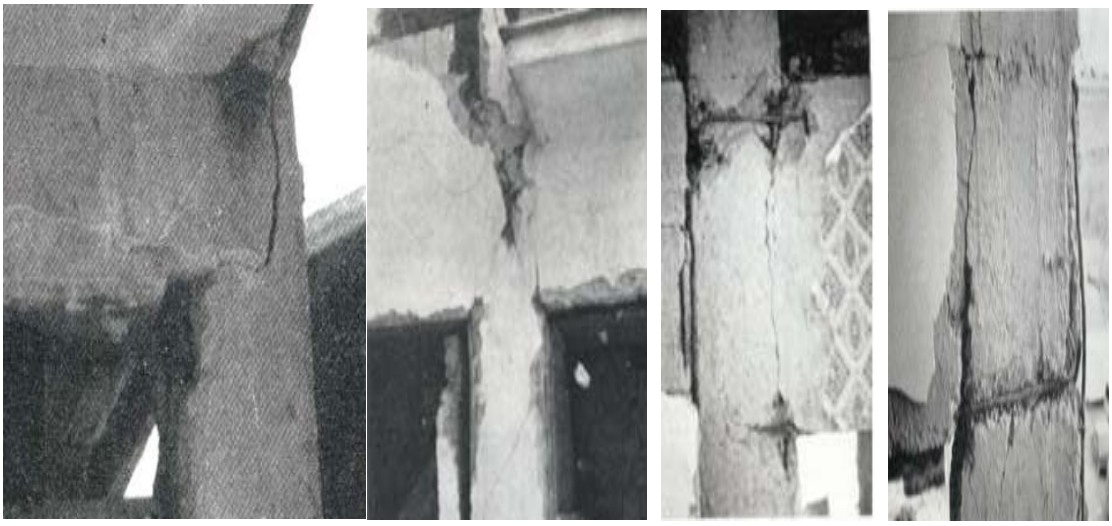

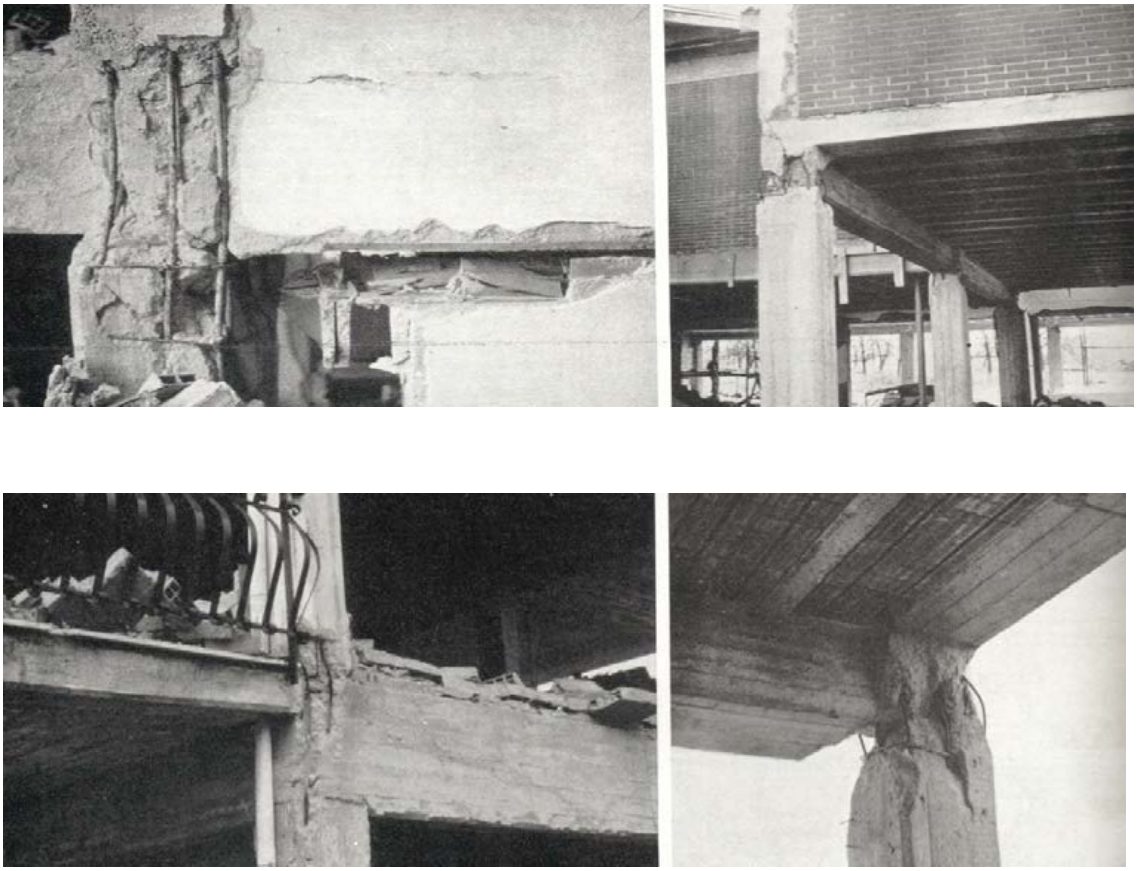

*Figure 2.18: Irpinia earthquake (1981), beam-to-column joint failures.*

*Figure 2.19: Kobe earthquake (1995), beam-to-column joint failure.*

# CHAPTER 3

# STEEL ENERGY DISSIPATIVE BRACING SYSTEM

# 3 Steel Energy Dissipative Bracing systems

## *3.1 Introduction*

Among the possible solutions to retrofit an existing structure, bracing systems are simple and effective, especially when story drifts need to be limited. The idea is to design systems that are strong enough to resist the seismic forces and light enough to keep the existing structural elements far from needing further strengthening. Furthermore, if these systems could be installed quickly and eliminate the need to disrupt the occupants of existing structures, they would be even more desirable (e.g., in the context of hospitals retrofitting). Steel braces can be considered as one of the most efficient solutions for resisting lateral forces due to wind and earthquakes, because they provide complete truss action. The common way for seismic protecting both new and existing framed structures is traditionally based on the use of concentric steel members arranged into a frame mesh (Concentrically Braced Frame – *CBF*), according to single bracing, cross bracing, chevron bracing and any other concentric bracing scheme. Even if such systems possess high lateral stiffness and strength for wind loads and moderate intensity earthquakes, some drawback have to be taken into account, concerning the unfavorable hysteretic behavior under severe earthquake, due to buckling of the relevant members, which generally causes poor dissipation behavior of the whole system (see Figure 3.1).

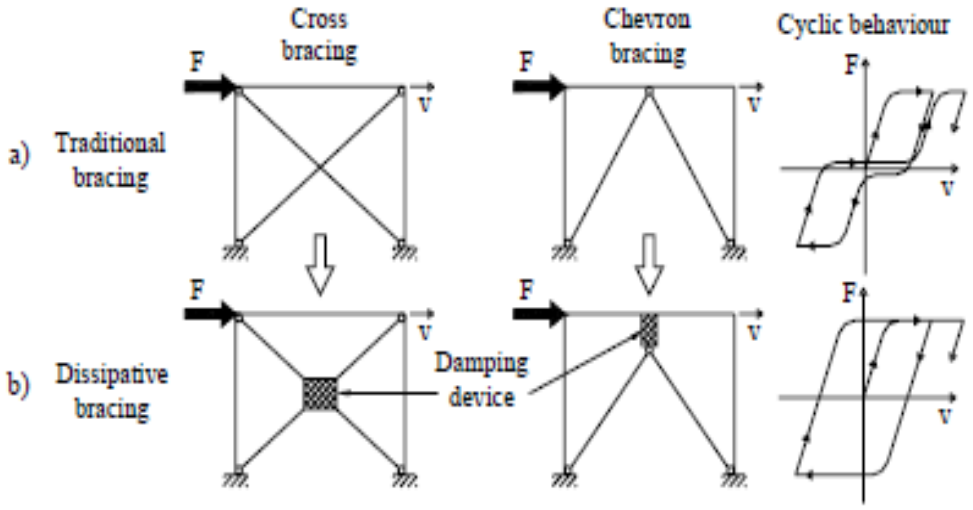


*Figure 3.1: Traditional and dissipative bracings*

For the seismic retrofitting of structure, in addition to the strengthening of the existing frame, the global seismic response of the structures should be improved too and increase its dissipative capacity. To address the aforementioned drawback the buckling and premature rupture of the braces should be avoided. This can be achieved by using some dissipative dissipate devices with the conventional bracing system that can dissipate the seismic energy before inflicting damage to the primary structure.

In Figure 3.1 some of the dissipative braces are schematically shown. Overall, the bracing system are very viable solution for the seismic retrofit of structures because it

can improve the systems strength, stiffness and energy dissipation capacity, improving its performance in future earthquakes.

Another advantage of using energy dissipative steel braces is that the devices mounted on the elastic brace can be easily replaced after being damaged in earthquake. The design of the system is done in such a way that it can be inspected and control the condition of the devices after each seismic event. Some other advantages include inexpensiveness (since they are mad of ordinary steel working) and can be easily removed and assembled in a structure.

The usage of these dissipative and damping devices has been proposed and implemented worldwide. The traditional cross bracing is a simple damping system, that can be designed in such a way that the plastic mechanism of the braces is formed and exploited before it buckles. While a dissipative bracing system is formed by inserting a dissipative device between the joint of the diagonal member and the beam (Figure 3.2a).

The simplest scheme is based on the transformation of a conventional concentric brace into an eccentric brace (EB) by means of a steel link, which is fixed to the beam and pin-joined to the diagonals (see Figure 3.2b). In this way the typical Y-shaped eccentric brace behaves as a passive control device, since the inelastic cyclic behavior of the link element allows a large amount of the input energy to be dissipated without any damage of the external framed structure. In fact, the basic design principle of the system is that, while plastic deformations occur in the dissipative device, the diagonals have to remain elastic both in tension and in compression.

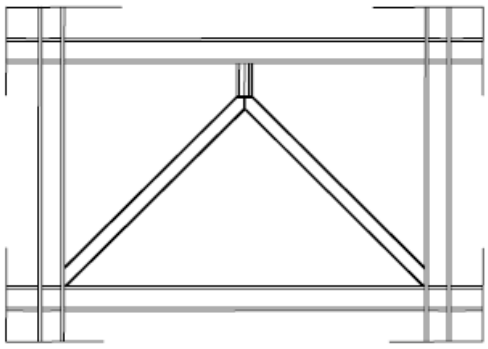

a. Y-braced eccentric braces

b. Conventional steel link

*Figure 3.2: Typical Dissipative chevron bracing system*

The cyclic performance of conventional bracings is also improved by the usage of a special type bracing members, which are called Buckling-Restrained Braces (BRBs) [12]. See Figure 3.3

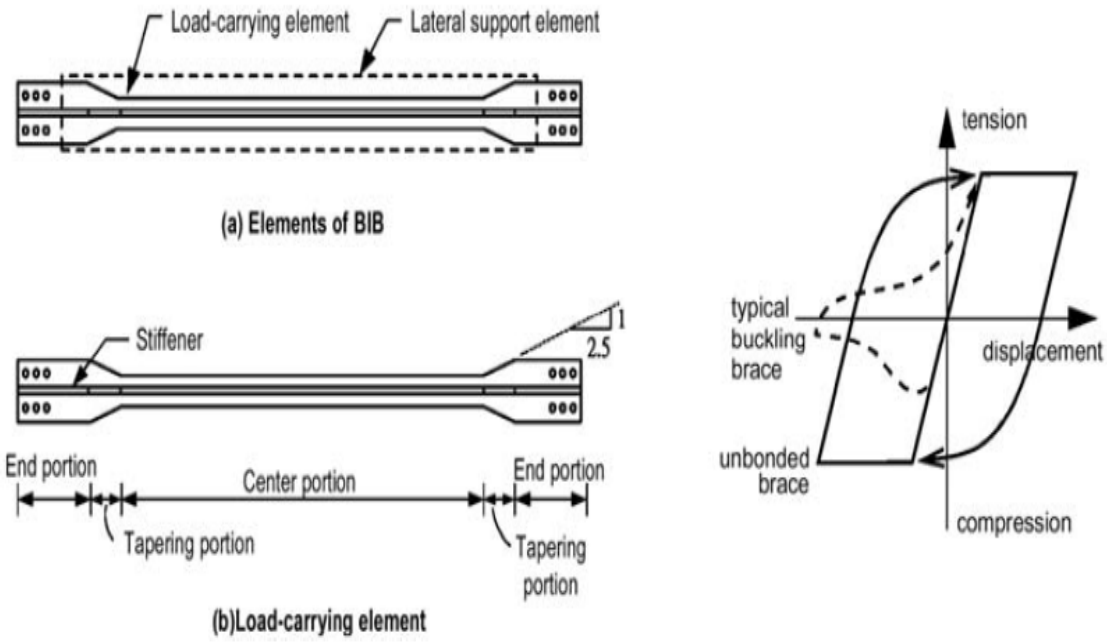


*Figure 3.3: Typical Buckling Restrained Bracing system and relevant cyclic behavior*

These dissipative systems are made of the special trusses composed by a steel core, as load carrying element, and placed inside a lateral support element, in order to obtain a buckling restrained bracing. The load carrying element is responsible for working under tensile and compressive axial forces while the lateral support element prevents the load carrying element from buckling when it is compressed, thanks to the appropriate lateral restraining mechanism.

The global and local buckling of the brace is avoided by the flexural strength and stiffness of the lateral support, resulting in axial yielding in both tension and compression. Therefore, a stable hysteretic behavior is utilized to capture the response of the BRB without any pinching and/or degradation of strength and stiffness up the failure, which is caused by the tensile rupture following significant necking of the steel core.

The present research utilizes BRBs as passive Energy Dissipative Braces (EDBs). Hence, the BRB characteristic and its advantages in comparison to a traditional bracing system will be discussed in detail.

## *3.2 Buckling Restrained Braces (BRBs)*

Among seismic performance upgrading systems, there are several options normally available, one of which is to employ energy dissipation devices, such as friction, viscoelastic and metallic dampers, buckling-restrained braces (BRBs), etc. Energy input by a strong earthquake, since these devices are designed to be replaceable.

BRBs can be a good system for protecting reinforced concrete (RC) structures from severe earthquake damage. BRBs provide stable energy dissipation capacity in both tension and compression. In addition, BRBs represent the effective solution to the problem of the limited ductility of classic concentric bracing, thanks to the avoidance of global compression buckling. BRBs are characterized by the ability of bracing elements to yield inelastically in compression as well as in tension. As shown in Figure 3.4, BRBs are characterized by a stable hysteretic behavior and, differently from traditional braces; they permit an independent design of stiffness, strength and ductility properties.

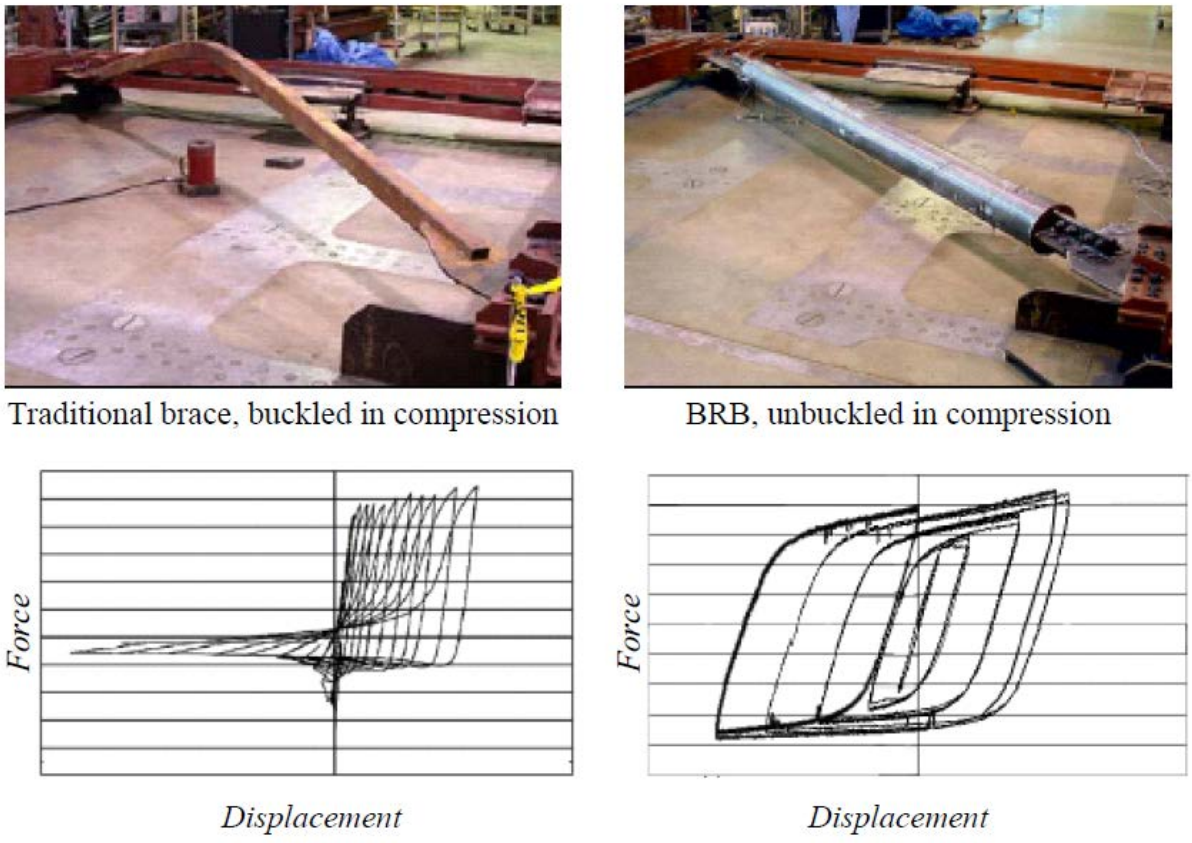


*Figure 3.4: Traditional Brace vs BRB*

This behavior is achieved through limiting buckling of the steel core within the bracing elements. The axial strength is decoupled from the flexural buckling resistance; in fact, the axial load is confined to the steel core, while the buckling restraining mechanism resists overall brace buckling and restrains high-mode steel core buckling (rippling).

The first studies about inhibiting global buckling of braces in compression were developed by [13]. They developed a pioneering buckling restrained system in which braces (made of steel flat plates) were sandwiched between a pair of precast reinforced concrete panels Figure 3.5.

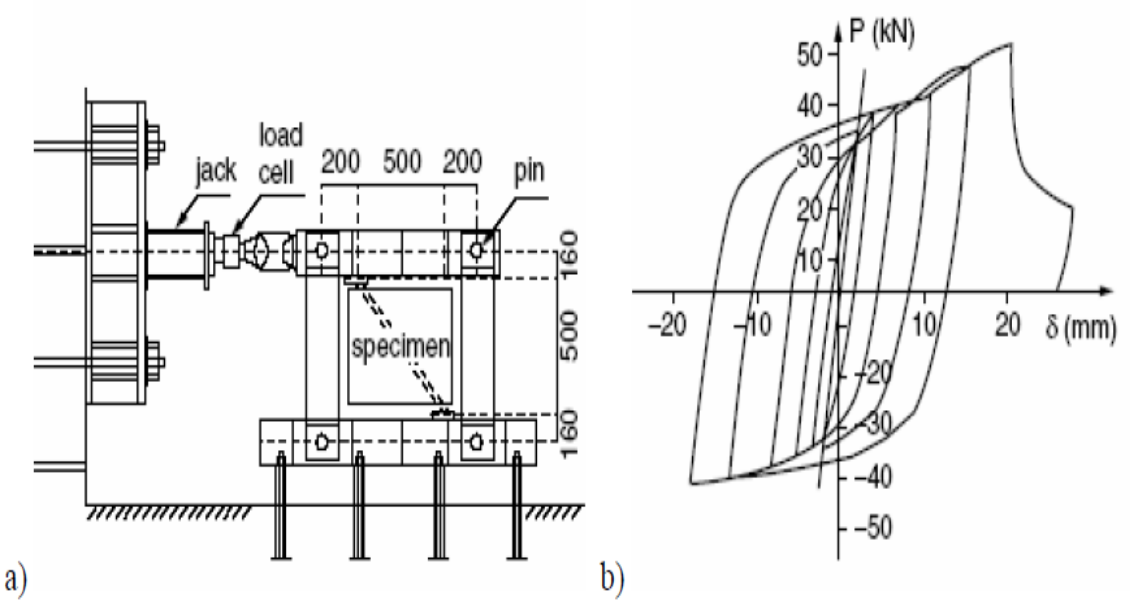


*Figure 3.5: BRB performance test, a) Test setup b) Hysteresis Behaviour*

Extending the concept of [13] , various developments on BRBs with a steel core confined by a steel casing were made in Japan from the second part of the 1970s up to 1990s. Among the first researchers, [14] studied and tested the first example of a steel brace able to dissipate energy without buckling. This early type of BRB consisted of a conventional brace encased in a square steel pipe filled with mortar. These braces were characterized by few stable hysteretic characteristics, because of the transverse deformation of the mortar resulted in permanent void space that were large enough to allow local buckling. [15] conducted tests on similar braces, which were wrapped in reinforced concrete, with the concrete kept from adhering to the internal brace by use of a shock-absorbing material. It was found however, that under repetitive loading, the concrete cracks and its buckling restraining effect diminishes [16]. This concept was further refined by [17] and [16] and lead to the so called unbonded brace Figure 3.6.

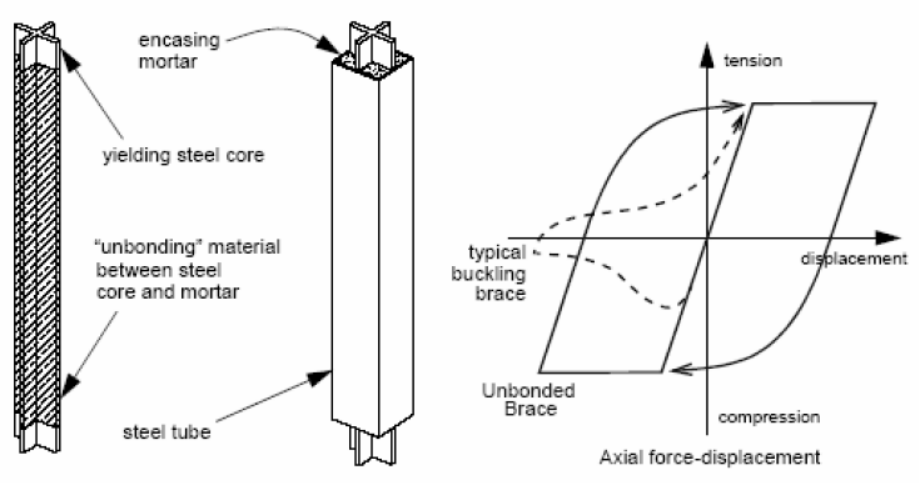


*Figure 3.6: Geometrical scheme of a typical unbonded Brace.*

In Italy, BRBs have been successfully adopted for seismic protection of one building of the University of Ancona Figure 3.7.

*Figure 3.7: University of Ancona (Italy)*

Different types of BRBs Figure 3.8 have been studied, all based on the basic concept to use tubes for restraining lateral displacements while allowing axial deformations of the core.

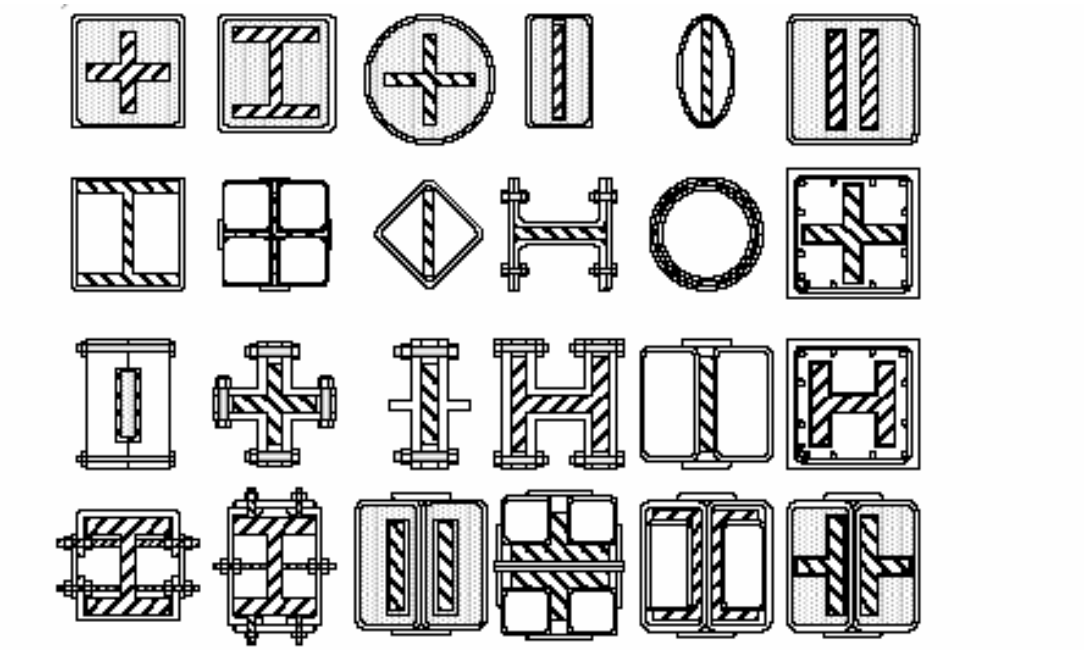

*Figure 3.8: Typical Types of BRBs*

In the most classical form, the restraining tube is filled with concrete and an unbonding layer is placed at the contact surface between the core plates and the filling concrete, thus this version is called ‘unbonded brace’. The unbonding material both ensures the brace to freely slide inside the buckling restraining unit and lets transverse expansion of the brace to take place when the brace yields in compression. ‘Only-steel’ solutions have been also proposed, with two or more steel tubes in direct contact with the yielding steel plates. In the latter case, the restraining tubes can also be connected by bolted steel connections, thus allowing an easy inspection and maintenance during the life-time or after a damaging earthquake [18]. An adequate gap size between the brace and the restraining tubes is also required in case of “only-steel” BRBs, in order to provide the necessary space for relative deformation between both members. The BRB technology is currently ongoing a strong development, with a growing number of buildings using buckling restrained braces as primary lateral force-resisting system. This strong development is also testified by several research studies which are ongoing in the US, Taiwan, Japan [18–20] and in Italy too [3,21]. In particular, in USA three industry-proprietary BRBs have been developed. These BRBs feature a steel core encased in a concrete-filled steel hollow tube. Chronologically, the first patented BRB uses flat or cruciform steel core with bolted end splice connections (Figure 3.9). To facilitate erection, holes on the gusset plate and brace are oversized; faying surfaces of the gusset and connection plates were also sandblasted to reduce the number of high-strength bolts, and hence the length of gusset connection. Satisfactory performance has been demonstrated from both uniaxial testing and sub assemblage testing [22].

The second industrialized patent uses a pin-and-collar assembly at each end of the brace (Figure 3.10). The use of a pin connection at the gusset plate isolates the brace from any moment or shear that could be transmitted because of frame drift. Also, by directly connecting the brace to the gusset by using a pin, the overall connection length is

reduced, resulting in a long yielding core that reduces the axial strain. The pin also reduces the number of pieces being connected. The collar assembly adds to the overall stability of the brace by preventing out-of-plane buckling of the core section extending beyond the confining unit. The third industrialized development uses a prismatic steel core along the entire length of the brace; each end is reinforced with welded stiffeners for the bolted splice connection with oversized holes for ease of erection. Uniaxial testing [22] has also been conducted to verify the cyclic performance.

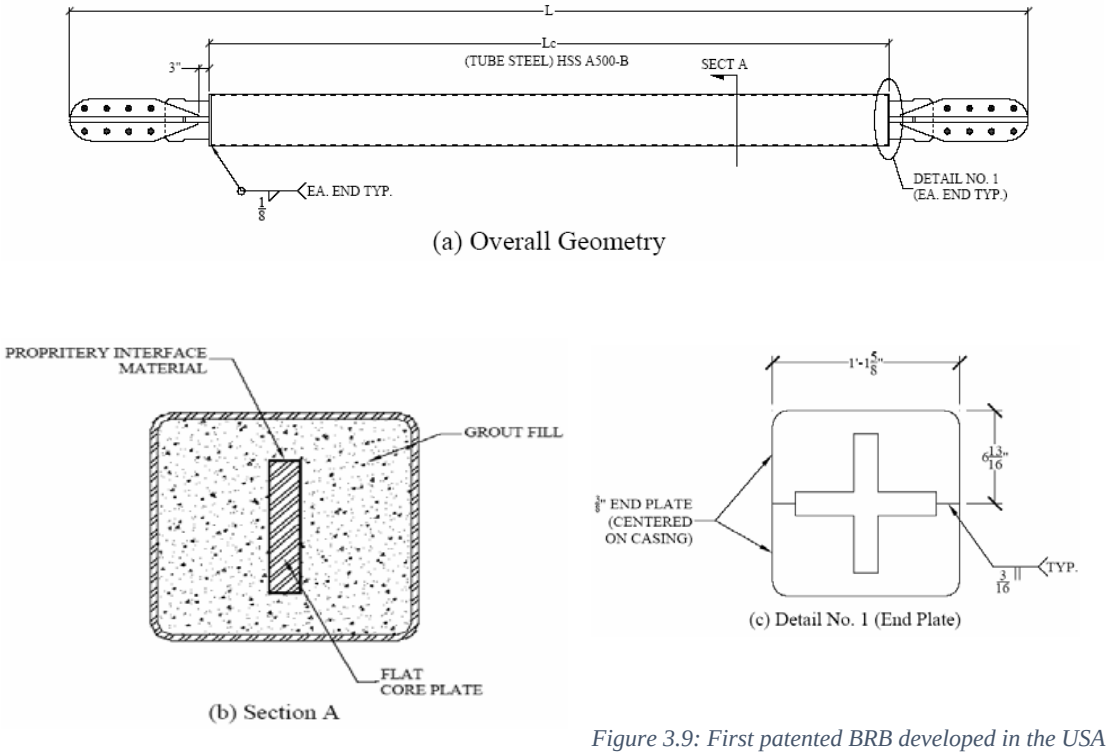


*Figure 3.9: First patented BRB developed in the USA*

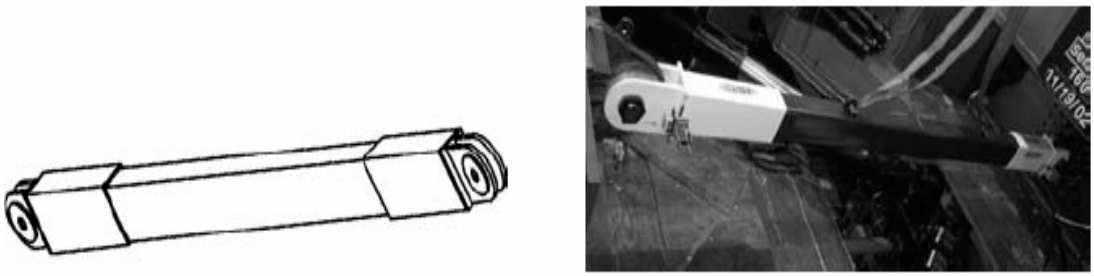

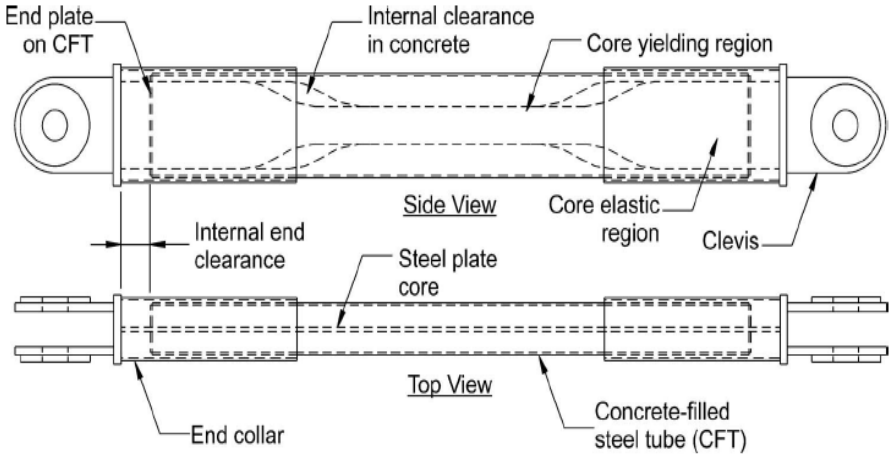


*Figure 3.10: Second patented BRB developed in the USA*

Parallel to US applications, in Taiwan [23] studied the cyclic behavior of a type of BRB with low-yield strength steel. The brace, called buckling-inhibiting brace (BIB), used a concrete-filled tube to confine the steel plate (Figure 3.11). A layer of silicon grease was used a debonding material. The adopted low-yield steel did not have a well-defined yield plateau, but the ultimate strain was very high (>50%). For the first time a stopper at the center of the load-carrying element that was inserted into the core in order to center the buckling-restrained system and to prevent it from slipping down.

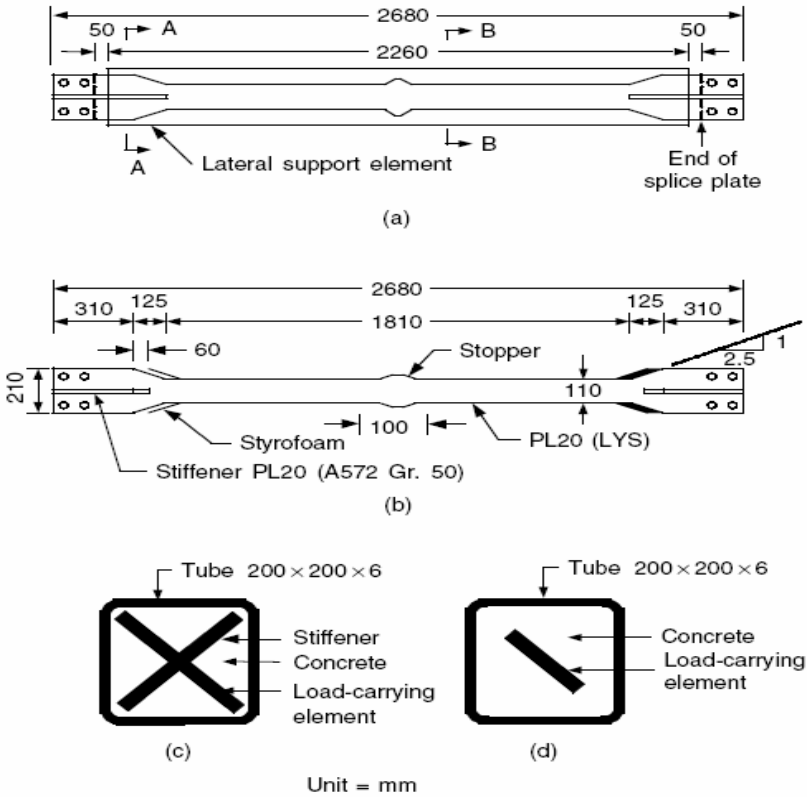


*Figure 3.11: Details of Buckling inhibiting brace; a) overall view; b) load carrying element; c)A-A section; d) B-B section (Chen et al.)*

The experimental studies on this typology showed that the maximum compressive strength was much higher than the maximum tensile strength. As a result, [23] suggested that this type of bracing be used in a diagonal configuration, not V or inverted-V configuration. [23] also investigated the steel-only BRBs with built-up steel sections as the buckling restraining mechanism.

[18] studied the effect of unbonding material on the cyclic response of BRBs. A total of 10 identical braces were tested, the only difference being the unbonding materials used. They demonstrated that the axial load difference $\Gamma = (C_{max} - T_{max})/T_{max\ is}$ equal to $2\varepsilon$, where $C_{max}$ and $T_{max}$ are the maximum compressive and tensile brace strengths at a given axial deformation level, while $\varepsilon$ is the axial brace strain. The above equation shows that $\Gamma$ is about 4% for $\varepsilon = 2\%$. But the test results show much higher $\Gamma$ values, precisely 30% for $\varepsilon = 2\%$. Other than the Poisson's effect, factors such as friction between steel core yielding element and mortar also contribute to a higher brace strength in compression cycles.

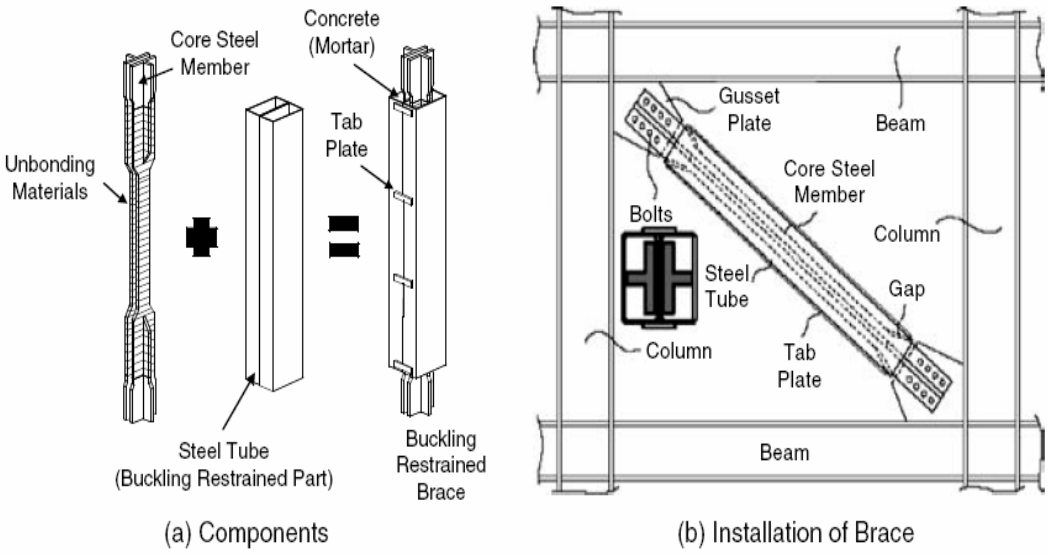


*Figure 3.12: Double tube buckling restrained brace*

Moreover, to reduce the size of the connections and to improve the constructability in the field, double-tube BRBs have been developed and extensively tested by [18] (Figure 3.12). Each brace is composed of two identical parts. Each part comprises a steel core, which is either a plate or a structural tee, encased in a rectangular steel tube. Both ends of the steel core are tee-shaped, thus each part of the brace can be conveniently connected in the field to the gusset in the same manner as the conventional double-T brace is connected to gusset plate connections. [18] proposed a detachable BRB type, to provide the possibility of disassembling the BRBs for inspection after an earthquake or during the lifetime. They studied several configurations of bolted connection for joining together the restraining tubes. Their test results suggest that the all metallic and

detachable BRBs can stably sustain severe cyclic increasing and constant fatigue inelastic axial strain reversals.

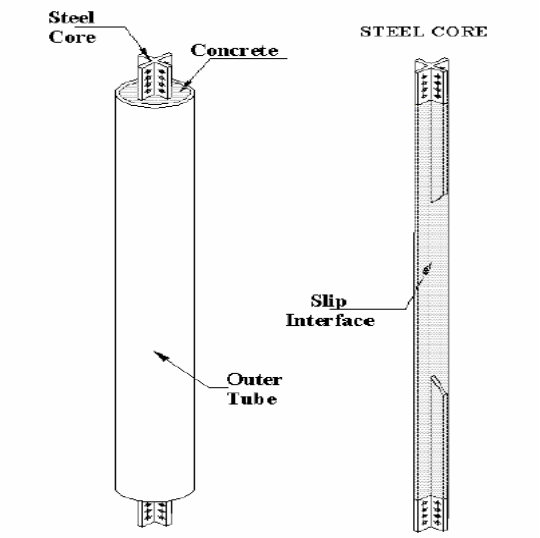


*Figure 3.13: Scheme of Italian patented BRB*

In Italy, the first studies about BRBs are relatively recent. Both unbonded and only steel BRBs have been studied. One Italian unbonded proprietary BRB type has been developed (Figure 3.13 ). It is very similar to the Japanese typologies; in fact, it is made of a steel rectangular core restrained by a steel sleeve infilled by high strength mortar. These BRBs (called Buckling Restrained Axial Damper or BRAD) have been successfully adopted for seismic protection of one building of the Faculty of Engineering of Ancona [24]. It represents the first professional application of buckling restrained braces in Italy and Europe (Figure 3.14).

*Figure 3.14: Two BRBs installed in the new building of the university of Ancona*

### 3.2.1 BRB design concept

Yielding of this special type of bracing occurs when the plastic strength of the core steel plates is achieved. The axial stiffness is determined by the combination of two or more springs in series, having the axial stiffness of the internal core and terminal tapered plates. Length and size of the latter can be independently fixed to some extent. In any case, the possibility to avoid compression buckling allows very slender steel plates to be used as core of the BRB, with a relatively low plastic strength and without impairing the system ductility. In this way, yielding of the BRB can be regulated to very low interstory drifts, thus permitting the dissipative action to be activated soon. The basic principle, that characterizes the BRB response, is based on the possibility of decoupling of the axial-resisting and flexural-resisting aspects in the compression field. In fact, the steel core plate must resist axial stresses, while buckling resistance is provided by a sleeve, which may be of steel, concrete or composite. Figure 3.15 shows the parts which constitute a common BRB. It is possible to divide the core into three zones: the yielding zone, that has a reduced cross section area within the zone of lateral restrain provided by the sleeve (zone C); the transition zones, which have a larger area than the one of the yielding zone, and similarly restrained (zone B); the connection zones, which extend past the sleeve and connect to the frame by means of gusset plates (zone A).

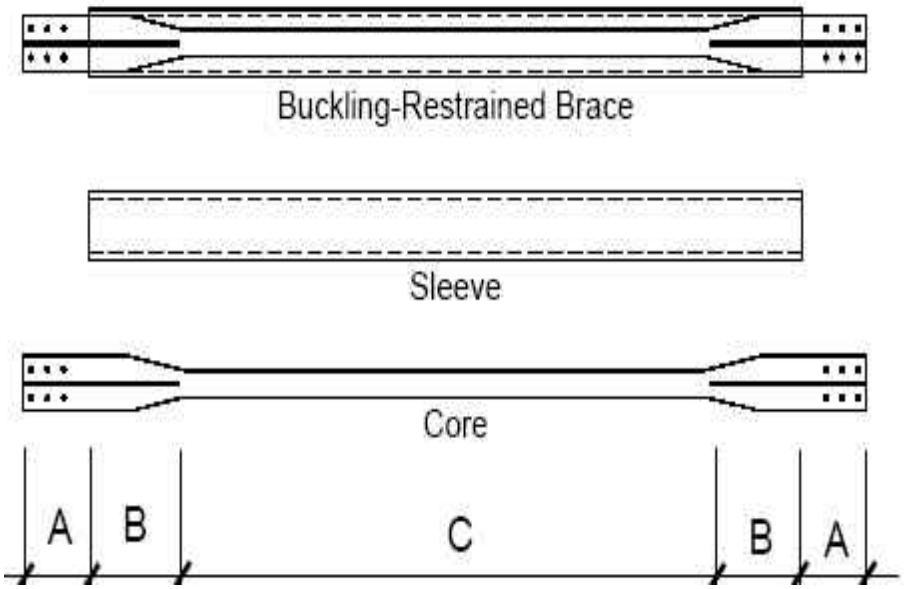


*Figure 3.15: Schematic view of a typical BRB element*

### 3.2.2 Mechanical Properties of BRBs

In order to properly confine the BRB inelastic deformations inside the restraining tube, the cross-sectional area ($A_c$) of the energy dissipation core segment ($L_c$) is smaller than that of the end joint regions ($L_j$).

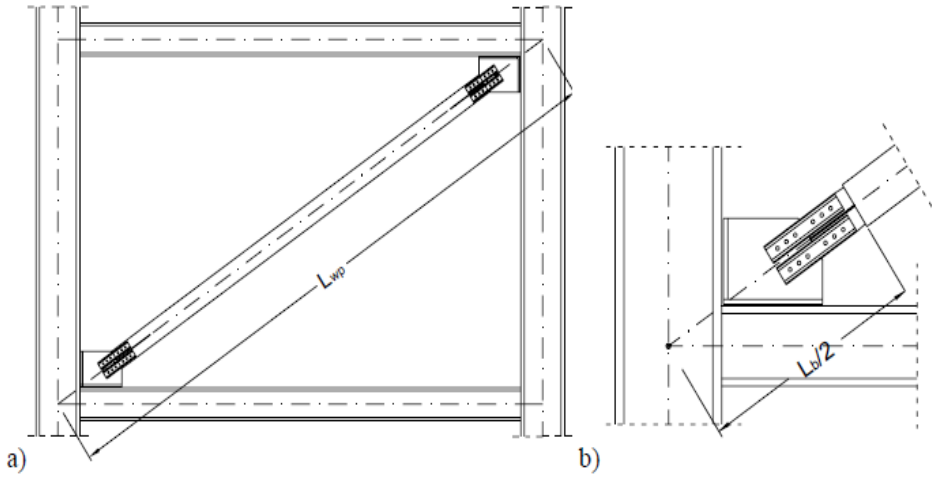


*Figure 3.16: Dimensions of theoretical BRB length (node-to-node length); a) effective length of BRB b) tsai et al (2004)*

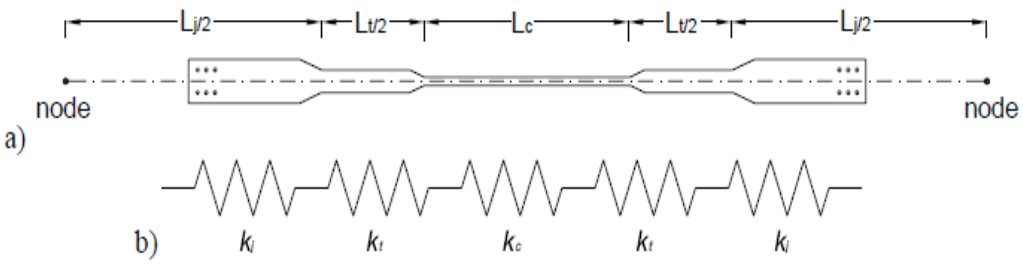


*Figure 3.17: Profile of steel core member in BRB*

A schematic configuration of a BRB in the frame is illustrated in Figure 3.16, in which $L_c$ and $L_{wp}$ represent the core length and the node-to-node length, respectively. Between the end and the core segment, a transition region can be deviced as illustrated in Figure 3.17. Moreover, referring to Figure 3.17b, it is confirmed by tests [25,26] that the effective stiffness, $K_e$ of the BRB, considering the variation of cross sectional area along the length of the brace, can be accurately predicted by:

$$K_e = \frac{1}{\sum \frac{1}{k_i}}$$

which simply combines axial stiffness of three axial springs connected in series.

### 3.2.3 BRB modelling

The BRB response can be simulated with bi-linear axial force-deformation relationship [18], or adopting the more accurate Bouc-Wen model (1976) [27]. In particular, in case of Bouc-Wen model, the nonlinear hysteretic behavior of a BRB can be approximated by Eq (3.1) :

$$N_t = \alpha K_{u(t)} + (1-\alpha) K u_y z_t \tag{3.1}$$

where $u_t$ is the axial deformation of the brace, $K$ is the brace elastic stiffness, α is the ratio of the post-yielding to elastic stiffness, $u_y$ is the yield displacement, and $Z_t$ is a hysteretic dimensionless quantity governed by the following differential equation:

$$u_y \dot{Z}_t + \gamma |\dot{u}_t| |\dot{Z}_t| |\dot{Z}_t|^{n-1} + \beta \dot{u}_t |\dot{Z}_t|^{\dot{n}} - \dot{u}_t = 0 \tag{3.2}$$

In the Equation (3.2), β, γ and $n$ are dimensionless quantities that control the shape of the hysteretic loop. This hysteretic model was originally proposed by Bouc (1971) for $n$=1, and subsequently extended by Wen (1975, 1976) and used in random vibration studies of inelastic systems. When parameter $n$ assumes large values (say $n$>10) the transition from the elastic to the post yielding regime is sharp and the Bouc-Wen model reasonably models bilinear behavior.

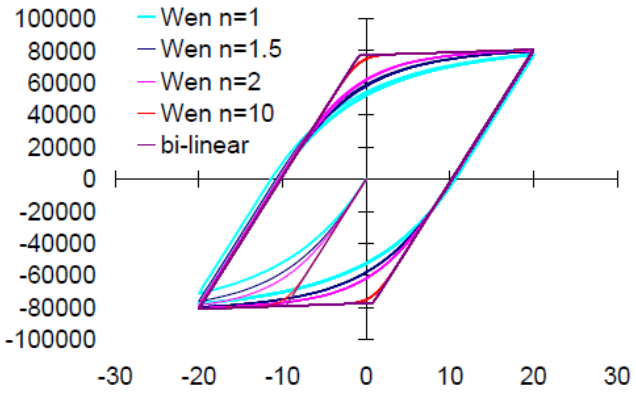


*Figure 3.18: Comparison of different hysteretic models to simulate the inelastic behavior of BRBs.*

In Figure 3.18 this aspect is clearly shown comparing the hysteretic Bouc-Wen model with different values of "*n*" compared with the bilinear axial force-axial deformation model. In particular, according to [27] the value of "*n*" that better match the experimental cyclic behavior of BRBs is for $n$=1 with a post-yield to elastic stiffness ratio of about 0.025 the initial elastic one.

# CHAPTER 4

# SEISMIC UPGRADING OF EXISTING RC BUILDING BY MEANS OF DISSIPATIVE BRACINGS: STATE OF THE ART

# 4 State of the art

This Chapter is divided in two sections, The first section is dedicated to an overview of structural performance assessment, with a discussion about two widely known methods (N2 and capacity spectrum), while the second section will deal in detail with the literature procedures for the design of passive energy dissipative braces.

## *4.1 Brief overview of the assessment methods*

There are numerous methods proposed in the literature for the assessment of structures. The most commonly used are:

1. *N2 method*
2. *Capacity spectrum method*

### 4.1.1 N2 method

The development of the N2 method started in the 1980s [28,29] at the University of Ljubljana. The N stands for nonlinear analysis and 2 for two mathematical models. The basis of the method came from the Q-model proposed by [30], which was improved in 1996 by [31]. The N2 method was extended to bridges [32]. In 1999, the N2 method was formulated in the acceleration-displacement format [33] , which combines the advantages of the graphical representation of the capacity spectrum method developed by Freeman with the practicality of inelastic demand spectra. The method is actually a variant of the capacity spectrum method based on inelastic spectra. The N2 method was included in Eurocode 8 [34] as the recommended nonlinear static procedure. The steps of the original version of the N2 method are described herein.

The steps of the original version of the N2 method are described herein:

1. *Step 1: Data*

A MDOF model of the building is developed including the nonlinear force deformation relationships for structural elements under monotonic loadings. An elastic acceleration response spectrum is also required corresponding to the seismic action under consideration (Figure 4.1).

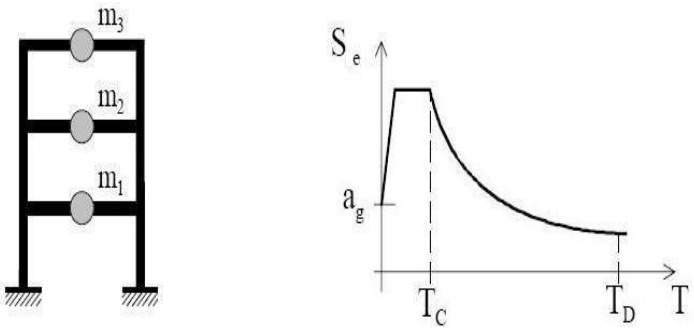


*Figure 4.1:MDoF frame and elastic response spectra*

2. *Step 2: Seismic demand in AD (acceleration-displacement) format*

The seismic demand is defined with a response spectrum in the format acceleration displacement (ADRS). For SDOF, the displacement spectrum can be computed from the acceleration spectrum using Eq (4.1.1).

$$S_d = \frac{T^2}{4\pi^2} S_e \qquad (4.1.1)$$

Where $\boldsymbol{S_e}$ and $\boldsymbol{S_d}$ are the values for the elastic acceleration and displacement spectrum, respectively, corresponding to the period *T* and a fixed viscous damping ratio. Example of the elastic acceleration and displacement response spectrum are plotted together in the ADRS format in Figure 4.2

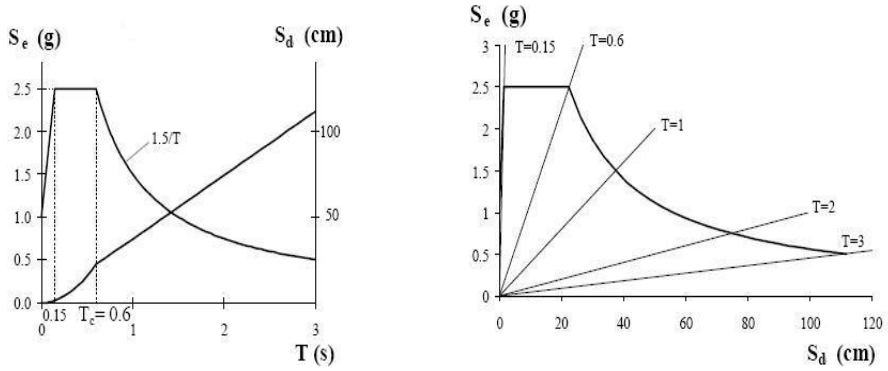


*Figure 4.2:Acceleration-Displacement response spectra (ADRS format)*

*3. Step 3: Pushover analysis*

A pushover analysis is performed, applying to the structure a monotonically increasing pattern of lateral forces, Figure 2.9. These forces represent the inertial forces induced in the structure by the ground motion. The N2 method uses a conventional non adaptive force-based pushover. Any reasonable distribution of lateral loads can be used in the N2 method. According to [35], the range of reasonable assumptions is relatively limited, and different assumptions lead to similar results. The Eurocode 8 recommends the use of at least two distributions: a first mode proportional load pattern and a uniform load pattern. The vector of the lateral loads *F* used in the pushover analysis proportional to the first mode is determined as in Eq (4.1.2):

$$F = pM\Phi \qquad (4.1.2)$$

The lateral force in the i-th level is proportional to the component $\Phi_i$ the assumed displacement shape $\Phi$, weighted by the story mass $m_i$ and it is obtained as given by Eq (4.1.3)

$$F_i = p\, m_i \Phi_i \qquad (4.1.3)$$

Note that the displacements are normalized in such a way that $\Phi_n = 1$, where n is the control node, i.e. the center of mass of the roof. Consequently $F_n = p\, m_n$.

The determination of these lateral loads is justified by the following reasons:

a) The distribution of lateral forces would be equal to the distribution of effective earthquake forces if the assumed displacement shape was exact and constant during the ground motion;

b) The lateral load definition allows a transformation from the MDOF to the SDOF system and vice-versa based on pure mathematics and without approximations as happens in FEMA237.

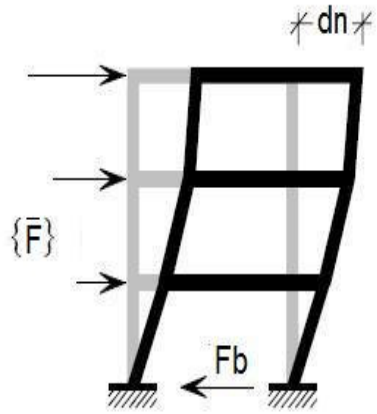


*Figure 4.3: lateral loads vector*

The vector of the lateral loads $F$ as shown in Figure 4.3 used in the pushover analysis with a uniform distribution is determined as in Eq (4.1.4):

$$F = pM$$

$$F_i = pm_i \qquad (4.1.4)$$

From the pushover analysis one obtains the nonlinear force-displacement relationship of the MDOF system called a capacity curve. The N2 method prescribes that this curve should represent the base shear $F_n$ and the displacement at the center of mass of the roof ($d_n$).

*4. Step 4: Equivalent SDOF system*

At this stage of the procedure, the MDOF structure should be transformed into an equivalent SDOF system. The procedure to determine the SDOF features is described herein.

The transformation of the MDOF to the SDOF system is made in the N2 method

using Eq. (4.1.5) and Eq. (4.1.6), see Figure 4.4:

$$d^* = \frac{d_n}{\Gamma} \qquad (4.1.5)$$

$$F^* = \frac{F_n}{\Gamma} \qquad (4.1.6)$$

Where $d^*$ and $F^*$ are the displacement and base shear of the SDOF system. $d_n$ and $F_n$ are the top displacement and base shear of the MDOF system.

The transformation factor $\Gamma$ from the MDOF to the SDOF model and vice-versa is defined according Eq. (4.1.7).

$$\Gamma = \frac{\Phi^T M 1}{\Phi^T M \Phi} \qquad (4.1.7)$$

The transformation factor $\Gamma$ is usually called the modal participation factor. Any reasonable shape of $\mathbf{\Phi}$ can be assumed. Herein, the elastic first mode shape will be considered. As was mentioned before, the displacement shape $\mathbf{\Phi}$ is normalized with respect to the center of mass of the roof. Therefore, the value of $\Phi_n$ is equal to 1.0, where *n* denotes the roof level.

The SDOF capacity curve is defined by the displacement of the SDOF ($d^*$) and the base shear of this system ($F^*$). Since both displacement and base shear of the MDOF are divided by the same factor $\Gamma$, the force-displacement relationship has the same shape. Therefore, the initial stiffness of the SDOF system is the same as the one defined by the base shear-top displacement capacity curve of the MDOF system.

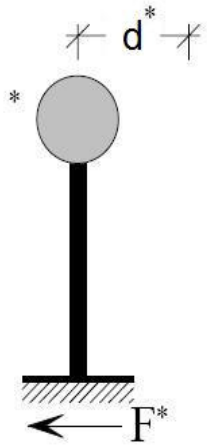


*Figure 4.4:Equivalent SDoF system*

Eurocode 8 prescribes a simplified elastic-perfectly plastic bilinear approximation of the SDOF capacity curve. Therefore, the post-yield stiffness of the bilinear approximation is equal to zero, as shown in Figure 4.5

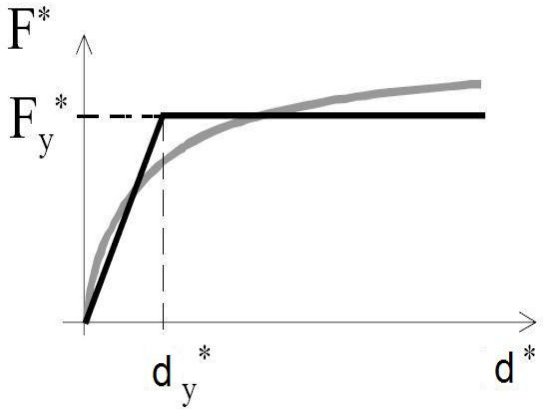


*Figure 4.5:Binlinearization of capacity curve*

The elastic period of the idealized bilinear SDOF system $T^*$ is computed according to Eq. (4.1.8).

$$T^* = 2\pi\sqrt{\frac{m^* d_y^*}{F_y^*}} \qquad (4.1.8)$$

Where $F_y^*$ and $d_y^*$ are the yield strength and displacement respectively.

*5. Step 5: Seismic demand for the equivalent SDOF system*

The seismic demand of the equivalent SDOF system can be calculated using the graphical procedures illustrated in Figure 4.6a for short period structures and in Figure 4.6b for medium and long period structures. In these figures the ADRS spectrum and the bilinearized SDOF capacity curve are represented in the same graph.

The capacity curve of the SDOF in the acceleration-displacement (AD) format is obtained by dividing the forces in the force-displacement curve by the equivalent mass $m^*$.

The target displacement of the structure with period $T^*$ and unlimited elastic behavior is given by Eq (4.1.9) :

$$d_{et}^* = S_e(T^*)\left[\frac{T^*}{2\pi}\right]^2 \qquad (4.1.9)$$

where $S_e(T^*)$ is the elastic acceleration response spectrum at the period $T^*$.

For the determination of the target displacement $d_t^*$ for structures in the short-period range and for structures in the medium and long period ranges, different expressions should be used as indicated below. The corner period between the short and medium period range is $T_c$ is the characteristic period of the ground motion, which is defined as the transition period between the constant acceleration section of the response spectrum (corresponding to the short period range) and the constant velocity segment of the response spectrum (corresponding to the medium period range).

a) For $T^* < T_C$ (short period range):

If $\frac{F_y^*}{m^*} > S_e(T^*)$ the response is elastic and thus Eq (4.1.10) is used for the determination of seismic demand:

$$d_t^* = d_{et}^* \qquad (4.1.10)$$

If $\frac{F_y^*}{m^*} < S_e(T^*)$ the response is nonlinear and Eq (4.1.11) is used to obtain target displacement :

$$d_t^* = \frac{d_{et}^*}{q_u}\left[1 + (q_u - 1)\frac{T_C}{T^*}\right] \geq d_{et}^* \qquad (4.1.11)$$

where $q_u$ is the ratio between the acceleration in the structure with unlimited elastic behavior $S_e(T^*)$ and in the structure with limited strength $\frac{F_y^*}{m^*}$

$$q_u = \frac{S_e(T^*)\, m^*}{F_y^*}$$

b) For $T \geq T_c$ (medium and long period range) the target displacement is determined by Eq(4.1.12)

$$d_t^* = d_{et}^* \qquad (4.1.12)$$

From Eq. (4.1.12) one can conclude that for the medium and long period range the equal displacement rule is applied. This means that the displacement of the inelastic system is the same as the corresponding elastic system for the same period.

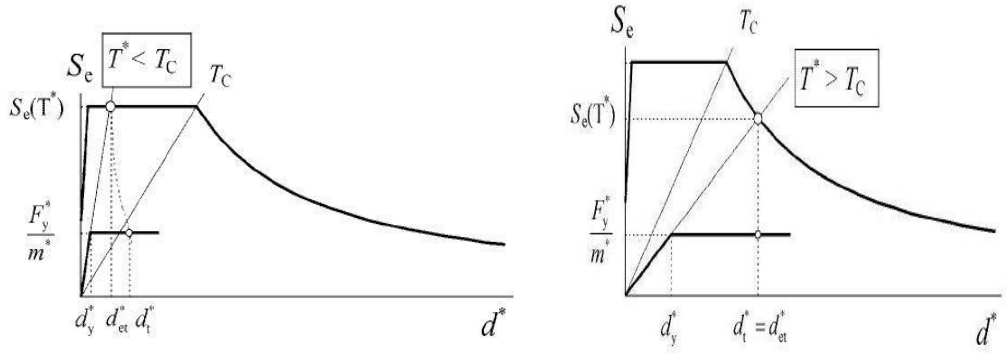


a) b)

*Figure 4.6:Seismic demand determination; a) short period structure; b) medium and long period structures*

The relation between different quantities can be visualized in Figure 4.6. The figures are plotted in acceleration-displacement format. Period $T^*$ is represented by the radial line from the origin of the coordinate system to the point in the elastic response spectrum defined by coordinates $d^* = S_e^*(T^*)\left(\frac{T^*}{2\pi}\right)^2$ and $S_e^*(T^*)$.

6. *Step 6: Global seismic demand for the MDOF model*

The target displacement of the MDOF system $d_t$ is calculated multiplying the target displacement of the SDOF obtained in step 5 by the transformation factor $\Gamma$, as given by Eq (4.1.13).

$$d_t = \frac{d_t^*}{\Gamma} \qquad (4.1.13)$$

### 4.1.2 Capacity spectrum method (CSM)

The capacity spectrum method is a very practical tool in the evaluation and retrofit of existing concrete buildings. It provides a graphical representation of the global force displacement capacity curve of the structure, comparing it with the response spectrum

that represents the earthquake. The graphical representation allows a clear understanding of how a building responds to an earthquake.

The CSM was developed to represent the first mode response of a structure based on the idea that the fundamental mode of vibration is the predominant response of the structure. For buildings in which the higher mode effects can be important, the results obtained with the CSM may not be so accurate.

In this section the capacity spectrum method (CSM) is briefly described, emphasizing the differences between the CSM-ATC40 and the CSM-FEMA440 features.

*1. Step 1: Data*

A MDOF model of the building must be developed including the nonlinear force-deformation relationship, as happens in the original N2 method.

*2. Step 2: Seismic demand in ADRS (acceleration-displacement response spectrum) Format*

Along the lines of what happens in the original N2 method, the seismic demand is defined with a response spectrum in the acceleration-displacement (ADRS) format. For a SDOF, the displacement spectrum can be computed using Eq (4.1.1). See Figure 4.2

*3. Step 3: Pushover analysis*

A conventional non-adaptive force-based pushover analysis is performed, applying to the structure a monotonically increasing pattern of lateral forces. In CSM the lateral forces applied have a first mode proportional distribution, calculated in the same way as the N2 method, see Eq. (4.1.2) and Eq (4.1.3).

From the pushover analysis one obtains the capacity curve that represents the base shear and the displacement at the center of mass of the roof.

*4. Step 4: Equivalent SDOF system*

The structural capacity curve expressed in terms of roof displacement and base shear is then converted into a SDOF curve in terms of displacements and accelerations, which is called the capacity spectrum. The transformations are made using Eq (4.1.14), (4.1.15), (4.1.16) and (4.1.17).

$$PF_1 = \frac{\sum_{i=1}^{N}(w_i\phi_{i1})/g}{\sum_{i=1}^{N}(w_i\phi_{i1}^2)/g} \qquad (4.1.14)$$

$$\alpha_1 = \frac{\sum_{i=1}^{N}[(w_i\phi_{i1})/g]^2}{\sum_{i=1}^{N}(w_i/g)\sum_{i=1}^{N}(w_i\phi_{i1}^2)/g} \qquad (4.1.15)$$

$$S_a = \frac{\frac{V}{W}}{\alpha_1} \qquad (4.1.16)$$

$$S_d = \frac{\Delta_{roof}}{PF_1\phi_{roof1}} \qquad (4.1.17)$$

where:

- *PF - modal participation factor for the first natural mode*
- $\alpha_1$ *- modal mass coefficient for the first natural mode*
- $\frac{w_i}{g}$ *- mass assigned to level i*
- $\phi_{i1}$ *- amplitude of mode 1 at level i*
- *N – Level N, the level which is the uppermost in the main portion of the structure*
- *V - Base shear*
- *W - building dead weight plus likely live loads*
- $\Delta_{roof}$ *- roof displacement (V and the associated* $\Delta_{roof}$ *make up points on the capacity curve)*
- $S_a$ *- spectral acceleration*
- $S_d$ *- spectral displacement (* $S_a$ *and the associated* $S_d$ *make up points on the capacity spectrum)*

Figure 4.7 shows that the participation factor and the modal mass coefficient vary according to the relative interstorey displacement over the height of the building. For example, for a linear distribution of interstorey displacement along the height of the building, $\alpha_1 = 0.8$ and $PF_1\phi_{roof1} = 1.4$.

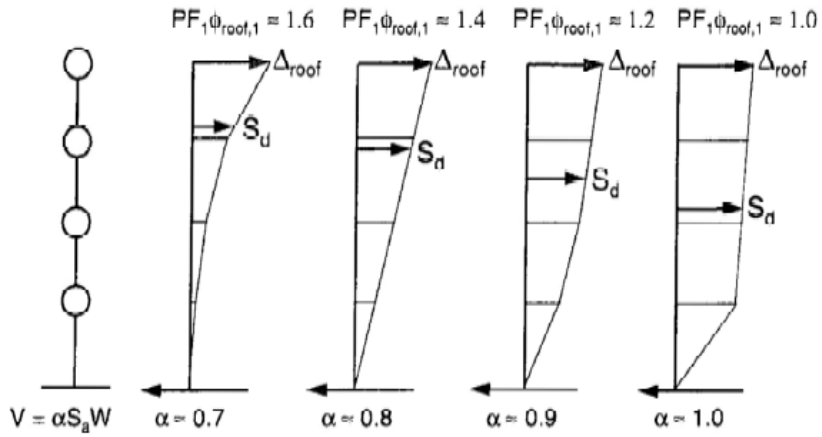


*Figure 4.7:Variation of participation factor and modal mass coefficient due to the varying load shape*

To convert the MDOF capacity curve into the SDOF capacity curve in the ADRS format (capacity spectrum), first it is necessary to calculate the modal participation factor $PF_1$ and the modal mass coefficient $\alpha_1$ using Eq (4.1.14) and Eq (4.1.15). Afterwards, for each point of the MDOF capacity curve ($\Delta_{roof}$, $V$ ) calculate the associated point ($S_a$ , $S_d$) of the capacity spectrum according to Eq (4.1.16) and Eq (4.1.17).

As mentioned, both CSM and N2 method consider a single control node for the SDOF characterization, usually the center of mass of the roof. In the N2 method both displacements and the forces of the MDOF are divided by the same Gama factor that depends on the mass of each story, the modal displacement at each floor normalized to the roof's center of mass and of the equivalent mass, in order to obtain the SDOF curve force *vs.* displacement. The CSM (ATC40 and FEMA440) uses two different

coefficients for the transformation of displacements and the accelerations, in order to calculate the SDOF curve in terms of acceleration vs. displacement. Note that, if one divides the SDOF forces in the N2 method by the equivalent mass (as defined by the method) in order to get the SDOF curve in the acceleration vs. displacement format, the equation of the SDOF accelerations will be the same as the one presented by ATC40 and FEMA440. The equations of the SDOF displacement transformation are the same as in Eurocode 8, ATC40 and in FEMA440.

*5. Step 5: Calculation of the target displacement*

The demand spectrum, with which the SDOF capacity curve will be intersected, must have an ADRS format (acceleration-displacement response spectrum). The calculation of the target displacement is an iterative process, where it is necessary to estimate a first trial performance point. For this purpose, there are several options one can use:

a) The first trial performance point can be estimated as the elastic response spectrum displacement corresponding to the elastic fundamental period. The response spectrum is defined for the viscous damping level considered (in buildings one usually considers 5%)

b) Consider a first trial equivalent damping value, for example 10%, and calculate the respective reduction factor. Multiply the elastic spectrum by this reduction factor and intersect the capacity curve with the reduced spectrum. The intersection corresponds to the first trial performance point. The capacity curve is then bilinearized for this point, and a new effective damping can be computed and hence a new reduction factor can be applied. The new intersection between the capacity curve and the new reduced spectrum leads to a new performance point. If the target displacement calculated is within a tolerable range (for example within 5% of the displacement of the trial performance point), then the performance point can be obtained. Otherwise the iterative process continues until one find convergence. Figure 4.8 represents the process schematically. The difference between the ATC40 guidelines and the FEMA440 report lies in the estimation of damping and in the computation of the response spectrum's reduction factor.

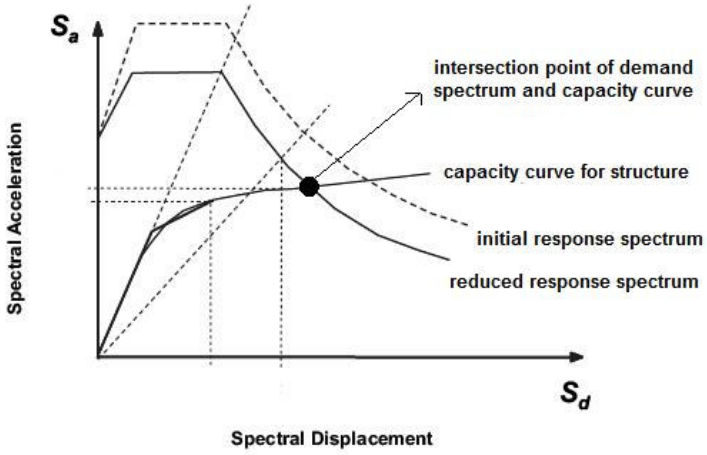


*Figure 4.8:Perforamce point determination in capacity spectrum method*

*6. Step 6: Determination of MDOF response parameters in correspondence to the Performance Point (converted from SDOF to MDOF)*

At this stage of the procedure, one should go back to the MDOF pushover curve to the point corresponding to the value of the SDOF target displacement (calculated in the previous step) multiplied by the transformation factor. For this step, one should take the building's performance results, such as deformations, interstorey drifts and chord rotations.

The specificities of both guidelines, ATC40 and FEMA440 in computing the effective damping and the reduction factor are explained as follows.

### 4.1.3 CSM-ATC40

The Procedure A of the ATC40 guidelines to calculate the target displacement was used in this work. It was previously described in step 5 of the procedure.

#### 4.1.3.1 Estimation of damping and reduction of the response spectrum

When a structure subjected to a ground motion enters the inelastic range, the associated damping is a combination of a viscous damping and a hysteretic damping. Hysteretic damping is related to the area inside the loops that are formed when the earthquake force (base shear) is plotted against the structure displacement. This guideline defines an equivalent viscous damping to represent this combination and it can be calculated using Eq (4.1.18).

$$\beta_{eq} = \beta_1 + 5 \qquad (4.1.18)$$

When this expression is applied to existing reinforced concrete buildings, which are not typically ductile, it overestimates realistic damping levels. To overcome this problem,

ATC40 introduces the concept of effective viscous damping that can be obtained by multiplying the equivalent damping by a modification factor *k* , as given by Eq (4.1.19)

$$\beta_{eff} = \kappa\beta_1 + 5 \quad (4.1.19)$$

- $\beta_{eq}$ *- equivalent viscous damping*
- $\beta_{eff}$*- effective viscous damping*
- $\kappa$ *- damping modification factor*
- $\beta_1$*- hysteretic damping represented as equivalent viscous damping*
- *5 – 5% viscous damping inherent in the structure (assumed to be constant)*

The hysteretic damping represented as equivalent viscous damping can be calculated according to Chopra [36]:

$$\beta_1 = \frac{1}{4\pi}\frac{E_D}{E_{so}} \quad (4.1.20)$$

- $E_D$ *- energy dissipated by damping*
- $E_{so}$ *- maximum strain energy*

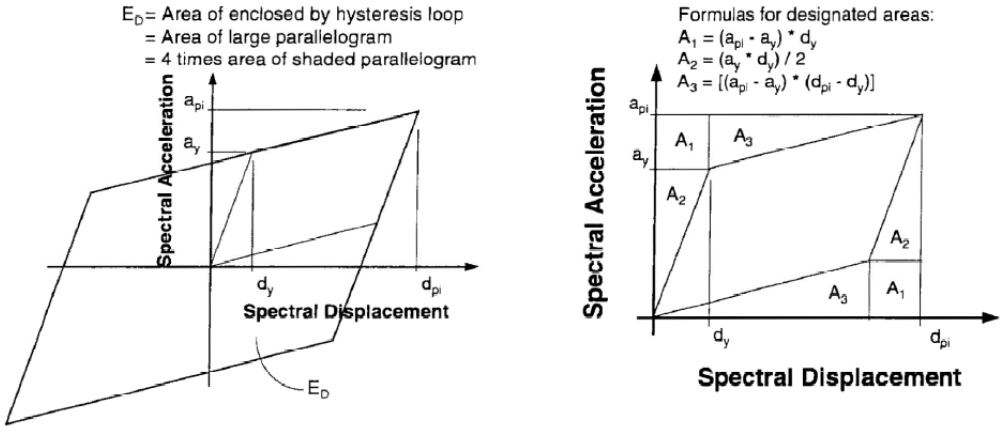


*Figure 4.9:Hysteresis curve*

Therefore, $\beta_1$ can be written as follows:

$$\beta_1 = 63.7\frac{a_y d_{pi} - d_y a_{pi}}{a_{pi} d_{pi}} \quad (4.1.21)$$

where $a_{pi}$ and $d_{pi}$ correspond to a trial performance point, for instance the intersection between the capacity curve and the demand spectrum. The capacity curve should be bilinearized at this trial point, considering a post-yield stiffness. $a_y$ and $d_y$ correspond to this bilinear curve yielding point. Hence, the effective damping can be written as Eq (4.1.22):

$$\beta_{eff} = 63.7\kappa\frac{a_y d_{pi} - d_y a_{pi}}{a_{pi} d_{pi}} + 5 \quad (4.1.22)$$

The damping modification factor *k* measures the extent to which the actual building hysteresis is well represented by the parallelogram illustrated in Figure 4.9 , either initially, or after degradation.

#### 4.1.3.2 Numerical Derivation of Spectral Reduction

The spectral reduction factors are calculated as shown in Eq (4.1.23) and Eq (4.1.24).

$$SR_A = \frac{3.21-0.68\ln(\beta_{eff})}{2.12} = \frac{3.21-0.68\ln\left(63.7\kappa\frac{a_y d_{pi}-d_y a_{pi}}{a_{pi}d_{pi}}+5\right)}{2.12} \geq 0.44 \qquad (4.1.23)$$

$$SR_A = \frac{2.31-0.41\ln(\beta_{eff})}{1.65} = \frac{2.31-0.41\ln\left(63.7\kappa\frac{a_y d_{pi}-d_y a_{pi}}{a_{pi}d_{pi}}+5\right)}{1.65} \geq 0.56 \qquad (4.1.24)$$

One should multiply the response spectrum by these factors to reduce it.

The performance point is then obtained as the intersection between the reduced response spectrum and the capacity curve as shown in Figure 4.10:

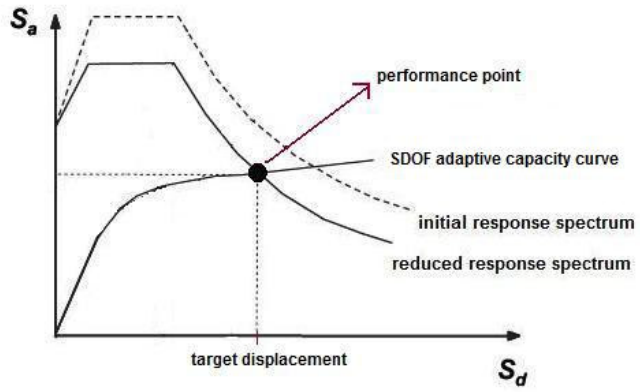


*Figure 4.10:Performace point attainment in capacity spectrum method*

## *4.2 Retrofitting of R/C structures using passive energy dissipative braces: Literature Review*

In recent years, several innovative low-damage strategies for controlling the seismic response of buildings have been developed and put into practice. One of these considers the adoption of passive control approach, consisting in the use of Energy Dissipative Bracing (EDB) systems inserted into the structural frame. These systems are characterized by special devices able to dissipate large amounts of energy during a seismic event and significantly reduce the interstorey drifts of the braced structures.

As the aim of this work is to improve the current EDBs design methodologies and propose a more innovative and easy-to-use methodology, a few more recently developed proposals for the design of EDBs are thoroughly analyzed and their pros and cons are discussed.

In this section three procedure are explained, namely:

a) Seismic retrofit of reinforced concrete frame buildings with hysteretic bracing systems: by A. Di Cesare and F.C. Ponzo [37]
b) A design procedure of dissipative braces for seismic upgrading structures: by A. Bergami and C. Nuti [38]
c) An energy-based method for seismic retrofit of existing frames using hysteretic dampers: by A. Benavent-Climent [39]

The first two design procedures are based on the N-2 and the capacity spectrum method, respectively, aimed at reducing the top displacement of the building while the third design procedure is based on the concept of energy-balance. These procedures are explained in detail in the following sections.

### 4.2.1 Seismic retrofit of reinforced concrete frame buildings with hysteretic bracing systems: by A. Di Cesare and F.C. Ponzo [37]

The design procedure for retrofitting framed buildings with EDBs proposed by Di Cesare-Ponzo is based on NLSA method, as described in the Italian and European seismic codes [34,40]. This method combines the pushover analysis of a multi-degree-of-freedom (MDOF) model with the response spectrum analysis of an equivalent single degree- of-freedom (SDOF) system to provide an estimation of the global nonlinear displacement response exhibited by the structure under strong earthquakes [34,40,41]. The procedure imposes a maximum top displacement as function of the considered seismic input and regularizes the stiffness and strength along the height of the braced building by following the regularity criteria provided by seismic codes, achieving a quite uniform distribution of story displacements and controlling the maximum interstorey drifts which must remain under the target limit.

The procedure, synthesized in Figure 4.11, evaluates the mechanical characteristics of the dissipative bracing system first for the equivalent SDOF system and then determines the characteristics of the braces along the building elevation. The distribution of dissipative braces inside the structural frames is function of the real geometry and position with the purpose to involve most of the devices in the energy dissipation with the same ductility demand. The optimal ranges for the design parameters are determined by referring to the results of experimental tests [42,43] and applications to real buildings [44,45]. As explained in the following, the symbols reported in Figure 4.12 refer to equivalent SDOF systems of: elastoplastic structure (S); elastoplastic bracing system (DB); elastic braced structure (E(S + DB)); elastoplastic braced structure (EP(S + DB)).

*1. Step 1: (evaluation of the equivalent SDOF system of the bare structure).*

The first step of the procedure is aimed at determining the mechanical characteristics of the equivalent SDOF system of the bare structure. The capacity curves can be determined through NLSA for both main directions of the building. At least two lateral

load distributions should be applied (both uniform and modal pattern), in both the positive and negative direction, considering also 5% accidental eccentricity of the center of mass of each story.

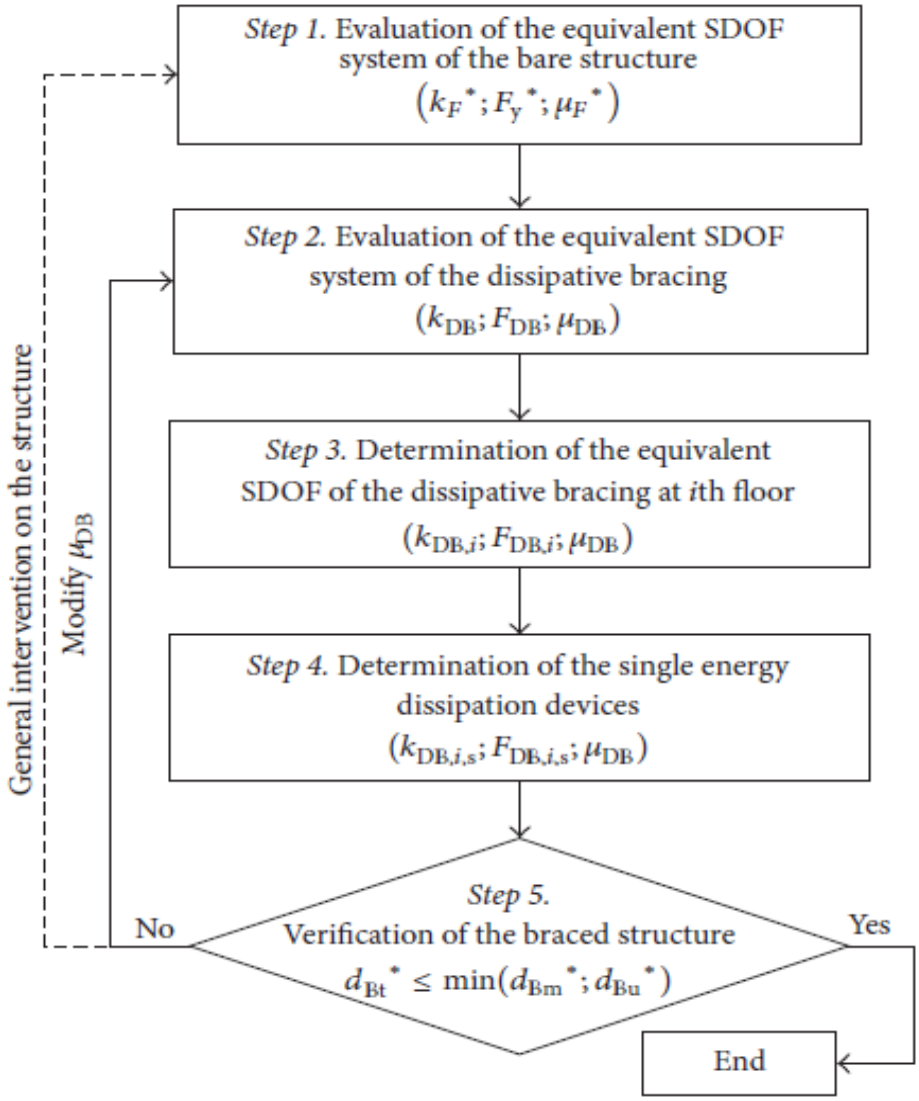


*Figure 4.11: Design flow chart of the procedure*

The idealized elastoplastic force-displacement relationship of the structure (S) is defined by the transformation factor $\Gamma$, the equivalent mass $m^*$, the yield force $F_y^*$ the yield displacement $d_y^*$ (or the elastic stiffness $k_f^* = \frac{F_y^*}{d_y^*}$, and the ultimate displacement $d_u^*$ (or the maximum ductility $\mu_f^* = \frac{d_u^*}{d_y^*}$).

*2. Step 2: Evaluation of the equivalent SDOF system of the dissipative bracing*

The characteristics of the equivalent SDOF of the bracing system are determined by an iterative subroutine, applied separately for each main direction. The damped bracing

(DB) system has been idealized as an elastoplastic system defined by the yield force $F_{DB}$, the elastic stiffness $k_{DB}$, and the design ductility $\mu_{DB}$.

a) Assuming a maximum displacement $d_{BM}^*$ of the equivalent SDOF system of the braced structure EP(S + DB), evaluated in correspondence of the Basic Design Earthquake (BDE), the target ductility $\mu_*$ of the existing structure (S) is defined by:

$$\mu^* = \frac{d_{Bm}^*}{d_y^*} \leq \mu_f^* \qquad (4.2.1)$$

If the aim of the design is that the structure remains in elastic range ($\mu^*$= 1), then $d_{Bm}^* \leq d_y^*$. Otherwise, a limited inelastic capacity of the existing structure can be exploited, in that case $1 < \mu^* \leq 1.5 - 3$, for brittle or ductile mechanism, respectively, and then $d_y^* < d_{Bm}^* \leq d_u^*$.

b) Assuming a design ductility 'DB of the equivalent SDOF of the bracing system (DB), the optimal ductility values range between 4 and 12, consistently with the properties of the considered hysteretic device and the Serviceability Design Earthquake (SDE) [46–49]. Those values refer to the in-series composition of the Hysteretic Damper (HD) and the rigid bracing truss (R). They allow the devices for responding elastically at the Serviceability Design Earthquake (SDE) and with a nonlinear behavior at BDE. The ultimate displacement of the equivalent bracing $d_{DBu}$ is assumed to be equal to the maximum displacement $d_{Bm}^*$ , and then the yield displacement of the equivalent SDOF of the bracing system (DB) $d_{DBy}$ is given by:

$$d_{DBy} = \frac{d_{Bm}^*}{\mu_{DB}} \qquad (4.2.2)$$

c) The yield force $F_{DB}^j$ of the equivalent SDOF of damped bracing (DB) system at the jth step is the unknown of the procedure. The elastic stiffness of the DB system $k_{DB}^j$ is determined by:

$$k_{DB}^j = \frac{F_{DB}^j}{d_{DBy}} \qquad (4.2.3)$$

The trilinear curve S + DB is obtained by summing in parallel the equivalent structure (S) and bracing system (DB).The equivalent period $T_B^{*j}$ and the elastic displacement $d_{DBe}^{*j}$ of the equivalent SDOF system of the braced structure (EP(S +DB)) are evaluated by Eq (4.2.4), (4.2.5) (see Figure 4.12), where the elastic stiffness $k_B^{*j}$ and yield force $F_{By}^{*j}$ of the equivalent (EP(S + DB)) are determined by the idealized elastoplastic of the braced structure (S + DB).

$$T_B^{*j} = 2\pi\sqrt{\frac{m^*}{k_B^{*j}}} \qquad (4.2.4)$$

$$d_{Be}^{*j} = S_{e\left(T_B^{*j}\right)} \left[\frac{T_B^{*j}}{2\pi}\right]^2 \qquad (4.2.5)$$

d) At the 2nd step, the target displacement $d_{Bt}^{*j}$ for the equivalent (EP(S + DB)) of the Basic Design Earthquake (BDE) is determinate as function of the period of the braced structure $T_B^{*j}$ and $T_C$ the upper limit of the period of the constant spectral acceleration branch [34,40], as follows:

*i)* *If $T_B^{*j} < T_C$ short-period range, then $d_{Bt}^{*j}$ is determined from the equal energy criteria between the elastic (E(S +DB)) and elastoplastic SDOF of the braced structure (EP(S + DB)). Then, $d_{Bt}^{*j}$ can be expressed as the equality of the area underlying the elastic and elastoplastic oscillator curves; see Figure 4.12*

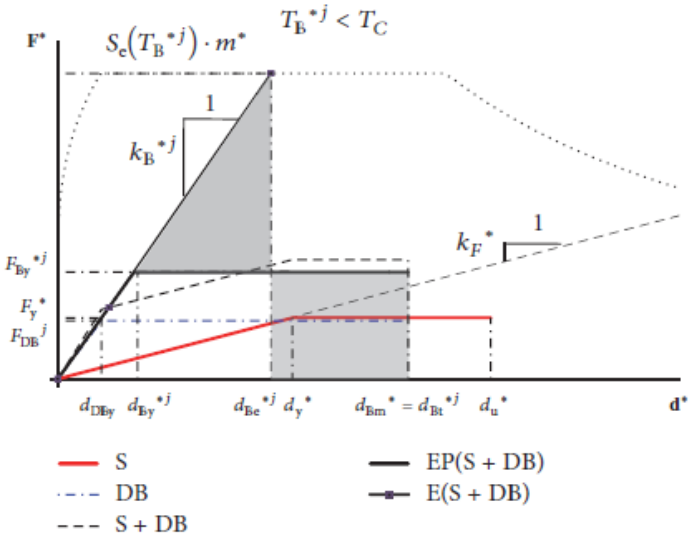


*Figure 4.12: Step 2 for short period structures*

*Generally, the target displacement evaluated by equal energy criteria results more conservative than the displacement evaluated by NLSA; see Step 5. This conservative design assumption is due to the stiffening effect of bracing into the structural frames.*

*ii)* *If $T_B^{*j} > T_C$ medium/long-period range, then $d_{Bt}^{*j}$ is determined from the equal displacement criteria between the elastic (E(S + DB)) and elastoplastic (EP(S + DB)) oscillators of the braced structure; that is, $d_{Bt}^{*j} = d_{Be}^{*j}$ ; see Figure 4.13.*

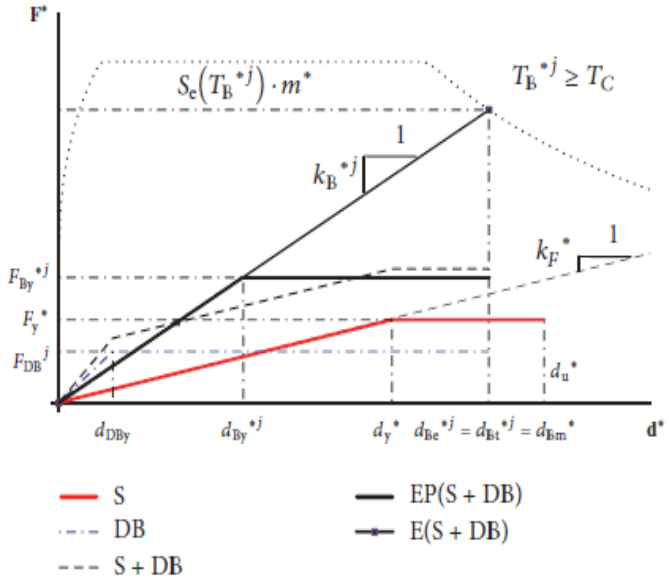


*Figure 4.13: Medium and long period structures*

*If the target displacement $d_{Bt}^{*j}$ is much different from the maximum displacement $d_{Bm}^*$ , bigger than an imposed tolerance value$\left| d_{Bt}^{*j} - d_{Bm}^* \right| < \varepsilon$, the iterative subroutine is applied. An updated value of the yielding force $F_{DB}^{j+1}$ of the equivalent DB system is evaluated and Sub steps (2c) and (2d) are repeated. Usually the procedure converges in a few iterations.*

3. *Step 3: Determination of the characteristics of the dissipative bracing at storey i:*

The characteristics of the equivalent SDOF dissipating system, determined in the previous step, are distributed along the height of the building achieving the substantial satisfaction of the criteria of regularization in elevation for the braced structure, as defined by [40]. The distribution maximizes the efficiency of the bracing system and no single floor will exhibit excessive interstorey displacements. This should always be avoided in a regular building, as being connected to damage of structural and nonstructural elements and to the activation of weak or soft storey mechanism.

The stiffness $k_{DB,i}$ of the equivalent bracing of the storey *i* is determined hypothesizing that the ratio between the stiffness at each storey of the bare frame $k_{F,i}$ and that of the relative bracing $k_{DB,i}$ is proportional to the ratio $r_k$ between the elastic stiffness of the equivalent bare structure $k_F^*$ and the elastic stiffness of the bracing systems $k_{DB}$ as shown by Eq (4.2.6). The stiffness of the storey i of the original structure $k_{F,i}$ can be calculated from the interstorey displacement $\Delta_{s,i}$ generated by linear static analysis (LSA) applying a distribution of horizontal seismic forces $F_i$ to each storey.

$$k_{DB,i} = r_k k_{f,i} \qquad (4.2.6)$$

where:

- $r_k = \frac{k_{DB}}{k_F^*}$
- $k_{F,i} = \frac{1}{\Delta_{si}} \sum_i^{n_p} F_i$

In case of irregular distribution in elevation of the stiffness of the retrofitted building at the end of the design procedure, the contribution of the bracing system in terms of stiffness must be modified with the aim of regularizing the braced structure. To this end, reference is made to the criteria for regularity in elevation of the building set out in the codes [34,40].The stiffness of equivalent bracing $k_{DB,i}$ at the storey $i$ can be modified following the iterative procedure, valid for buildings having a number of storeys $n_s \geq 2$, as reported in the following.

For $i = n_s \dots, 2$

If $\Delta k_{tot,i}^j > 0.3, \quad k_{DB,i}^j = m_k k_{tot,i-1}^{j-1} - k_{F,i}$

If $\Delta k_{tot,i}^j < -0.1, \quad k_{DB,i-1}^j = \frac{k_{tot,i-1}^{j-1}}{M_k} - k_{F,i}$ (4.2.7)

If $-0.1 \leq \Delta k_{tot,i}^j \leq 0.3,$

$k_{DB,i}^j = k_{DB,i}^{j-1}$ , $k_{DB,i-1}^j = k_{DB,i-1}^{j-1}$,

where $\Delta k_{tot,i} = \frac{(k_{tot,i-1} - k_{tot,i})}{k_{tot,i-1}}$ is the variation of the stiffness of the reinforced structure at the $i^{th}$ storey with respect to lower floor; $k_{tot,i} = k_{f,i} + k_{DB,i}$ is the total stiffness of the $i^{th}$ storey of the braced structure; $m_k$ and $M_k$ are the stiffness correction factors to be taken in the following range of values $0.1 \leq m_k \leq 1$ and $1.1 \geq M_k \geq 1$ , $j = 1, \dots n_s$ is the step of iteration.

In the same way, the yield force $F_{DB,i}$ of the equivalent bracing at the $i^{th}$ storey is determined in the hypothesis that the ratio between the yield force at each floor of the bare frame $F_{y,i}$ and that of relative bracing $F_{DB,i}$ is distributed proportionally to the ratio $r_k$ between the strength of equivalent bare structure $F_y^*$ and the strength of equivalent bracing $F_{DB}$ systems. The yield force $F_{y,i}$ of the $i^{th}$ storey of the bare structure can be calculated in a simplified manner starting from the displacements at the elastic limits $d_{y,i}$ determined by redistributing the displacement at elastic limit of the original structure $d_y^*$ as a function of the ratio between the interstorey displacement $\Delta_{si}$ and the total elastic displacement $S_{TOT}$ calculated by means of LSA.

$F_{DB,i} = r_F F_{y,i}$ (4.2.8)

where:

- $r_F = \frac{F_{DB}}{F_y^*}$

- $F_{y,i} = k_{F,i} d_{y,i}$

- $d_{y,i} = \frac{\Delta_{si}}{s_{TOT}} d_y^*$

When the ratio among the actual storey resistance of the bare frame and the resistance required by the analysis of the reinforced building varies non-proportionally (more than 20%) between adjacent storeys, the yield force $F_{DB,i}$ of storey $i$ of equivalent bracing system could be modified following the iterative procedure, valid for building having a number of storeys; $n_S \geq 2$, reported in the following.

For $i = 2, \dots, n_s - 1$

If $\Delta\rho_i^j < 0.8$

$$F_{DB,i}^j = \frac{m_F\left(F_{y,i-1} - F_{DB,i-1}^{j-1}\right)V_{Ed,i}}{V_{Ed,i-1}} - F_{y,i}$$

If $\Delta\rho_i^j > 1.2$ (4.2.9)

$$F_{DB,i}^j = \frac{M_F\left(F_{y,i-1} + F_{DB,i-1}^{j-1}\right)V_{Ed,i}}{V_{Ed,i-1}} - F_{y,i}$$

If $0.8 \leq \Delta\rho_i^j \leq 1.2$,

$F_{DB,i}^j = F_{DB,i}^{j-1}$

where $\Delta\rho_i = \frac{\rho_i}{\rho_{i-1}}$ is the variation of the ratio $\rho_i$ at the $i^{th}$ floor with respect to lower floor; $\rho_i = \frac{(F_{y,i} + F_{DB,i})}{V_{ED,i}}$ is the ratio between storey resistance of the bare frame and resistance required by the analysis of the reinforced structure at the $i^{th}$ floor; $V_{ED,i}$ is the design shear force of storey $i$ required by the analysis of the reinforced structure; $m_f$ and $M_f$ are the strength correction factors to be taken in the following range of value $0.8 \leq m_f \leq 1$ and $1.2 \geq M_F \geq 1$ from small to large irregularities in elevation of the original structure; $j = 1, \dots, n_s$ is the step of iteration.

In framed buildings, the stiffness and strength variations should not vary disproportionately between adjacent storeys. In the design of the dissipative bracing system, the corrections factors have been adopted in order to reduce the irregularities in elevation of the original structure and to contain the variation of stiffness and strength of the braced structure in the following range of values $-10\% < \Delta k_{tot,i} < 30\%$ and $-20\% < \Delta\rho_i < 20\%$, respectively.

*4. Step 4: Determination of the single energy dissipation device*

The characteristics of the single dissipating brace $k_{DB,i,s}$ , $F_{DB,i,s}$ , $\mu_{DB}$ are finally defined starting from the equivalent dissipative bracing system of $i^{th}$ storey, as function of the number and slope of the braces, given in Eq (4.2.10), (4.2.11).

$$k_{DB,i,s} = \frac{k_{DB,i}}{n_{DB,i}} \frac{1}{\cos^2 \emptyset_s} \quad (4.2.10)$$

$$F_{DB,i,s} = \frac{F_{DB,i}}{n_{DB,i}} \frac{1}{cos\emptyset_S} \quad (4.2.11)$$

where $n_{DB,i}$ is the number of damped braces in the floor, $\emptyset_s$ is the angle between the single brace and the horizontal.

The preliminary design of the bracing elements is based on the yielding forces of the dissipative damper. Increased reliability is required for the dissipative bracing system. This shall be affected by applying a magnification factor $\gamma_X = 1.2$ on the yielding forces of each dissipative damper unit to avoiding either any buckling phenomena for compression condition or yielding in tension under the Maximum Considered Earthquake (MCE) loading, as defined by codes [34].

The stiffness and ductility characteristics of the single Hysteretic Damper (HD) depend on the stiffness $k_{R,i,s}$ of the single rigid bracing truss (R) at the story $i$ , as defined in:

$$F_{DB,i,s} = F_{HD,i,s};$$

$$K_{DB,i,s} = \frac{k_{HD,i,s} k_{R,i,s}}{k_{HD,i,s} + k_{R,i,s}} \quad (4.2.12)$$

$$\mu_{DB} = \frac{k_{HD,i,s} + k_{R,i,s}\mu_{HD}}{k_{HD,i,s} + k_{R,i,s}}$$

where $K_{DB,i,s}$ , $F_{DB,i,s}$ , $\mu_{DB}$ are the stiffness, the yield force, and the ductility of each Hysteretic Damper (HD).

Typically, ductility of devices $\mu_{HD}$ based on steel yielding can reach values greater than 20, displaying stable behavior for an adequate number of cycles [50]. In order to dissipate a good amount of energy reaching adequate values of ductility demanded to dissipating devices, the rigid support will be chosen considering a stiffness ratio $\frac{k_{R,i,s}}{k_{HD,i,s}} \geq 2$.

*5. Step 5: Verification of the braced structure*

The design procedure ends with the verification of the braced structure for the BDE. NLSA have been performed considering the MDOF model, which includes the nonlinear behavior of the dissipative brace elements. The iterative procedure stops if the target displacement $d_{Bt}^*$ of the braced structure, modified considering a transformation factor $\Gamma_B$ and the equivalent mass $m_B^*$ , satisfies the condition

$$d_{Bt}^* \leq \min(d_{Bm}^*; d_{Bu}^*) \quad \text{if } T_B^* < T_C \quad (4.2.13)$$

$$d_{Bt}^* = \frac{d_{Be}^*}{q_{B^*}} \left[1 + \frac{(q_B^* - 1)T_C}{T_B}\right] \geq d_{Be}^* \quad \text{if } T_B^* \geq T_C \quad (4.2.14)$$

$$d_{Bt}^{*} = d_{Be}^{*} \qquad (4.2.15)$$

where $q_B^* = \frac{S_{e(T_B^*)} m_B^*}{F_{By}^*}$ is the ratio between the acceleration in the braced structure with unlimited elastic behavior and with limited strength ; $d_{By}^*$ , $d_{Bu}$ are the yield and the ultimate displacements of the braced structure; $\mu_B^* = \frac{min(d_{Bm}^*; d_{Bu})}{d_{By}^*}$ is the ductile capacity of the braced structure.

If Eq (4.2.13) is not satisfied, the iterative procedure of Step 2 is applied by increasing the design ductility of the dissipative bracing $\mu_{DB}$ in Substep (2b) and/or assuming a maximum displacement equal to the target displacement $d_{Bt}^*$ determined in Step 5, instead of $d_{Bm}^*$ assumed in Substep (2a). Moreover, in case of verification not satisfied, specific intervention to the structural elements (beams, columns, and/or beam to column joints) could be required in order to increase the capacity of the bare frame and the procedure restart from Step 1.

It is worth noting that the application of the NLSA is allowed in the hypothesis that the requirements laid out in the codes for the use of this analysis method are respected (regularity criteria). As shown in the following, a correct positioning of the dissipating braces usually determines the achievement of regularity conditions. Otherwise, it should be necessary to perform a nonlinear dynamic analysis for the safety verification of the braced structure (Step 5).

### 4.2.2 A design procedure of dissipative braces for seismic upgrading of structures: by A. Bergami and C. Nuti

This procedure is a displacement-based retrofitting methodology, which is used to determine the characteristics (brace stiffness, brace strength and ductility) of the energy dissipative braces required for the retrofitting of structures. It's an iterative strategy that emphasizes on the assessment of braced-structure's response through capacity spectrum method and reiterating the design process in case the capacity does not meet the demand, as shall be seen later in detail.

Considering a braced structure, as in Figure 4.14a, being its capacity curve represented by the curve S+B of Figure 4.14b , one can assume that this latter is the sum of the capacity curves of the structure (S) and of the bracing system (B): therefore, the latter can be obtained subtracting S from S+B. This assumption is relatively accurate for design purposes and holds true when the increase of axial forces in the columns is small, in fact the structural behavior of S does not changes after retrofitting and is kept constant during the design process. In Figure 4.14b the capacity curve S is approximated as elasto-plastic as well as the capacity curve B: therefore, the curve S+B is tri-linear. Given the seismic action in term of response spectrum, for a given capacity curve S+B, one can obtain the structural response in term of displacement known the equivalent viscous damping $n_{eq,S+B}$ associated to each point of the curve S+B.

It is well known that the force-displacement behavior of a *BRB* (with *j* the generic device) can be modelled by a simple bilinear law characterized by the elastic axial stiffness $K'_{b,j}$ the yield strength $F'_{by,j}$ and the hardening ratio $\beta_{b,j}$.

$K'_{b,j}$ , $F'_{by,j}$, $D'_{by,j}$ and $\beta_{b,j}$ depend on mechanical properties of the selected devices ($D'_{by,j}$ is the axial displacement at yielding) while the length $l_{b,j}$ and the inclination $\emptyset_{b,j}$ of each brace can be determined referring to both geometric characteristics of the structure and brace distribution Figure 4.15.

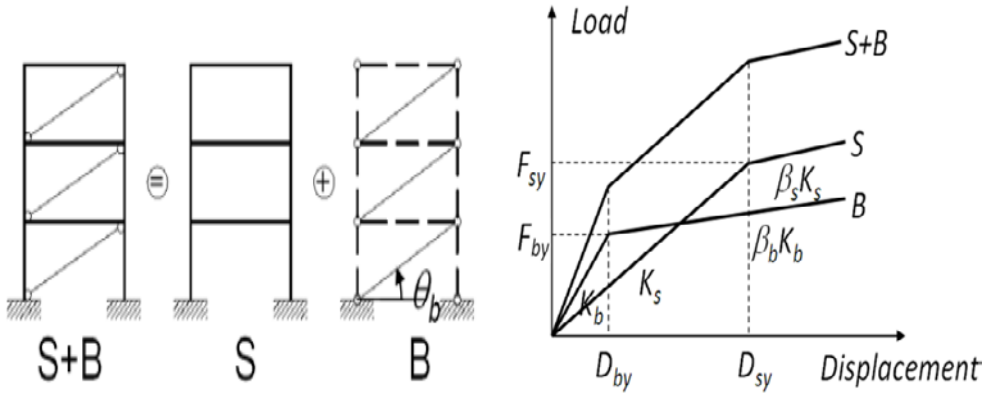


*a)* *b)*

*Figure 4.14: Existing structure and bracing system; a) Bare frame and bracing system's configuration; b) Combined response of bare frame and bracing system in terms of force-displacement*

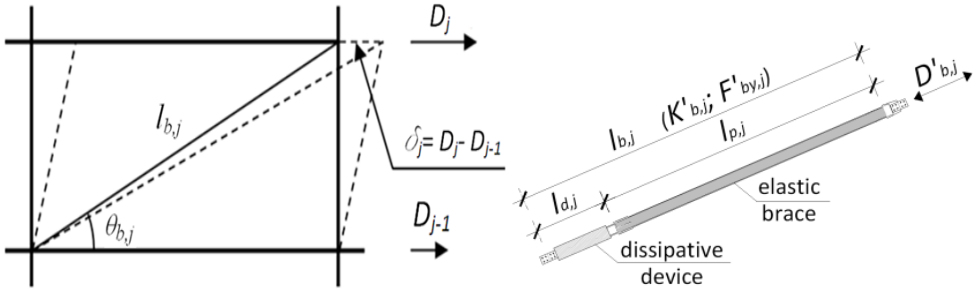


*Figure 4.15:Deformed shape of a generic single part of the braced frame*

Being $K_{b,j}$, $F_{by,j}$, $D_{by,j}$ the horizontal components of stiffness, yield strength and displacement at yield of the bracing system *B* respectively, they can be expressed as follow:

$$K_{b,j} = K'_{b,j} Cos^2 \Theta_{b,j} \quad (4.2.16)$$

$$F_{by,j} = F'_{by,j} Cos \Theta_{b,j} \quad (4.2.17)$$

$$D_{by,j} = \frac{D'_{by,j}}{Cos \Theta_{b,j}} \quad (4.2.18)$$

Objective of the design is the definition of the following variables:

a) The Plano-altimetric configuration of the bracing system that influences device sizing as it modifies the braced frame deformed configuration both in the linear range as well as beyond the plastic limit;
b) The axial stiffness $K'_{b,j}$ of each brace;
c) The yielding limit of each brace ($D'_{by,j}$, $F'_{by,j}$ in terms of axial components or $D_{by,j}$, $F_{by,j}$ in terms of horizontal components) that is the point beyond which the system B becomes dissipative. It thus influences both resistance and energy dissipation capacity of the braced structure. In Figure 4.14 a representation of the cited parameters is given referring, for simplicity, to a bilinear relationship of the horizontal components of load and displacement for both S and B;
d) The hardening ratio $\beta_{b,j}$ of the bracing system that affects both resistance and dissipative capacity of the braced structure.

It is evident that if the dissipative system yields before the structure itself ($D_{by}<D_{sy}$) the efficiency of the intervention will increase, therefore this should and will be a basic assumption.

Moreover, the designer, once defined the desired performance for the structure in terms of top displacement, can decide to avoid or accept plastic deformations of the existing structural elements. With reference to Figure 4.14 three ranges of displacement can be identified on the capacity curve.

The first segment corresponds to a displacement range below the point of first yielding of the bracing system ($D < D_{by}$): in this range both the structure and the braces are elastic and therefore total damping of *S+B* coincides with the inherent damping $\nu_I$ offered by the original structure ( $\nu_{tot} = \nu_I$).

It is a matter of fact that, in case one uses very stiff braces, total damping could be even smaller than the original inherent damping due to the large increase of elastic energy. Entering in the second branch, beyond first yielding of *B*, the structure *S* is still elastic ($D_{by} < D \leq D_{sy}$) and the bracing system dissipate energy: therefore total damping is the sum of the inherent plus the one due to braces dissipation ($\nu_{tot} = \nu_I + \nu_{eq,B}$). This latter displacement range can be assumed as acceptable at least for frequent earthquakes. Finally, if it is accepted that also the structure yields ($D>D_{sy}$), total damping of *S+B* is the sum of the inherent damping and the damping offered by both the bracing system and the structure itself ($\nu_{tot} = \nu_I + \nu_{eq,B} + \nu_{eq,S}$). This latter situation is often the case: many existing structures have been designed to resist to vertical loads only or, at most, to very small horizontal forces. In general yielding of *S* can be accepted for rare earthquakes and excluded for frequent earthquakes in order to limit damage. It is now useful to express each limit state of interest in terms of displacement $D^*$. The same $D^*$ can be obtained adopting different retrofitting combinations of stiffness, strength and consequently dissipation.

The first parameter to be determined is the stiffness of the braces (additional stiffness). Different criteria to distribute the additional stiffness are proposed in scientific literature: constant at each story, proportional to story shear, proportional to interstorey

drifts of the original structure. In this work the latter is assumed and therefore, given the interstorey drift $\delta_j$ the stiffness $K'_{b,j}$ corresponding to each storey of the bracing system is:

$$K'_{b,j} = K_{global}\, c_{b,j} \tag{4.2.19}$$

where:

$$c_{b,j} = \frac{\delta_j}{\max_j\{\delta_j\}} \tag{4.2.20}$$

Each brace is a composite element realized by coupling an elastic element (usually a steel profile) with a dissipative device in series. The latter will determine the desired yielding force whereas the former will be designed to assure the desired stiffness of the series

#### 4.2.2.1 Evaluation of the equivalent viscous damping

As mentioned in the previous section, a specific energy dissipated by the structure and the braces corresponds to each deformation reached by the structure, be it with or without dissipative braces; the dissipated energy can be expressed in terms of equivalent viscous damping. Referring to the formula proposed by Chopra [36], the equivalent viscous damping of the structure at the generic displacement *D* can be expressed as follows

$$\nu_{eq,S} = \frac{1}{4\pi}\frac{E_{D,s}}{E_{S,S}} \tag{4.2.21}$$

All the parameters of the Eq (4.2.21) can be easily determined from the capacity curve: $E_{D,s}$ is the energy dissipated in a single cycle of amplitude *D* and $E_{S,S}$ is the elastic strain energy corresponding to the displacement *D*. Referring to an equivalent bilinear capacity curve (it can be determined from the capacity curve using one of the methods available in literature) terms of Eq. (4.2.21), considering an ideal elasto-plastic hysteretic cycle, can be determined as follow:

$$E_{D,s} = 4(F_{sy}D - D_{sy}F_{s(D)}) \tag{4.2.22}$$

$$E_{S,S} = \frac{1}{2}DF_{S(D)} \tag{4.2.23}$$

- $D$ - *The displacement reached from the structure*
- $F_s(D)$ - *The force corresponding to D (the force is the base shear)*
- $D_{sy}$ - *Displacement at yielding*
- $F_{sy}$ - *The yielding force (base shear at yielding)*

It is well known that the hysteretic cycle of a real structure differs from the ideal cycle, therefore this difference can be taken into account adopting a corrective coefficient $c_S$ for the structure and $c_B$ for the braces ($c$ = 1 for the ideal elasto-plastic behavior). Therefore:

$$E_{D,S} = \chi_S E_{D,S}^{bilinear} \quad (4.2.24)$$

$$E_{D,B} = \chi_S E_{D,B}^{bilinear} \quad (4.2.25)$$

with $E_{D,S}^{bilinear}$ the energy dissipated by the ideal hysteretic cycle of the dissipative brace.

Parameter $c_S$ can be determined referring to the provisions of [41]. For the braces the assumption of $c_B \approx 1$ has been considered reasonable: in fact, according to [51] , the force-displacement relationship of a *BRB* can be idealized as a bilinear curve. However different values can be adopted, if the case, with no difference in the procedure. The procedure assumes a bilinear curve characterized by a yielding force equal to the yielding traction force (the maximum compressive strength of *BRBs* is slightly larger than the maximum tensile strength due to the confining effect of the external tube): the hysteretic cycle obtained is elasto-plastic but precautionary smaller than the real one. Than the evaluation of the equivalent viscous damping of the braced structure $\nu_{eq,S+B}$, to be added to the inherent damping $\nu_I$ (usually $\nu_I = 5\%$ for r.c. structures and $\nu_I = 2\%$ for steel ones), can be obtained using the following expression:

$$\nu_{eq,S+B} = \frac{1}{4\pi}\frac{E_{D,S+B}}{E_{S,S+B}} = \frac{1}{4\pi}\left[\frac{\chi_S E_{D,S}^{bilinear}}{E_{S,S+B}} + \frac{\chi_B \sum_j E_{D,B,j}^{bilinear}}{E_{S,S+B}}\right] \quad (4.2.26)$$

$$\nu_{eq,S} = \chi_S \frac{1}{4\pi}\frac{E_{D,S}^{bilinear}}{E_{S,S+B}} \quad (4.2.27)$$

$$\nu_{eq,B} = \chi_B \frac{1}{4\pi}\frac{\sum_j E_{D,B,j}^{bilinear}}{E_{S,S+B}} \quad (4.2.28)$$

where is the energy dissipated by the dissipative braces placed at level $j$. Eq (4.2.26) can be generalized assuming that $E_{D,B,S} = \sum_i E_{D,B,i}^{bilinear}$ with $E_{D,B,i}$ the energy dissipated by the $i$ braces placed at level $j$.

Note that $\nu_{eq,S}$ and $\nu_{eq,B}$ are obtained by dividing the dissipated energy, determined from the capacity curve of *S* or *B* respectively, by the elastic strain energy of the braced structure, determined from the curve of *S*+*B*.

#### 4.2.2.2 Design procedure

In previous section the main aspect of the evaluation of seismic response of a structure with *BRBs* were explained. In this section the procedure is detailed.

The procedure is based on the capacity spectrum method: the target is expressed in terms of displacement. Iteration is required since the addition of braces modifies structural response and the capacity curve must be updated as long as the characteristics of the new braces are defined.

Moreover, the energy dissipated by the braces is considered additional to the dissipative capacity of the structure, computed on the capacity curve of the original one.

Structural response is obtained reducing the design spectrum on the base of the damping of the braced structure $\nu_{tot}$.

$$\nu_{tot} = \nu_I + \nu_{eq,B} + \nu_{eq,S+B} \quad (4.2.29)$$

In a displacement-based design perspective the performance desired is selected at first as the displacement (target displacement) corresponding to a selected limit state for a given seismic action. Then the required total effective damping needed to make the maximum displacement not larger than the target one is determined. The additional damping, due to bracing, is estimated as the difference between total damping and hysteretic damping of the structure without braces. The characteristics of the braces to guarantee the required additional damping are finally determined. This is an iterative procedure; the main steps follow:

1. *Step1: Seismic action definition*

Define the seismic action: the seismic action is defined in terms of elastic response acceleration spectrum ($T$-$S_a$).

2. *Step 2: Definition of target displacement*

Select the target displacement: the target displacement is selected (for example the top displacement $D_t^*$) according to the performance desired (limit state).

3. *Step 3: Obtain the capacity curve*

Define the capacity curve: the capacity curve of the braced structure S+B, in terms of top displacement and base shear ($D_t$-$V_b$), is determined via pushover analysis. The pushover analysis can be easily performed using a software for structural analysis: many different force distributions can be adopted selecting the best option for the specific case (e.g. modal shape load profile).

If a modal shape load profile has been selected it is important to underline that the modal shape is influenced by the bracing system and consequently, at each iteration, the load profile must be updated to the modal shape of the current braced structure. Notice that, at the first iteration, the structure without braces is considered and therefore the capacity curve obtained will be fundamental for the evaluation of the contribution offered by the existing structure to the braced structure of the subsequent iterations.

4. *Define the equivalent bilinear capacity curve*

The capacity curve is approximated by a simpler bilinear curve $D_t$-$F_{s+b}$ that is completely defined by the yielding point ($D_{s+b,y}$, $F_{s+b,y}$) and the hardening ratio $\beta_{s+b}$ (at the first iteration the parameters correspond to $D_{s,y}$, $F_{s,y}$, $\beta_s$ of the existing building).

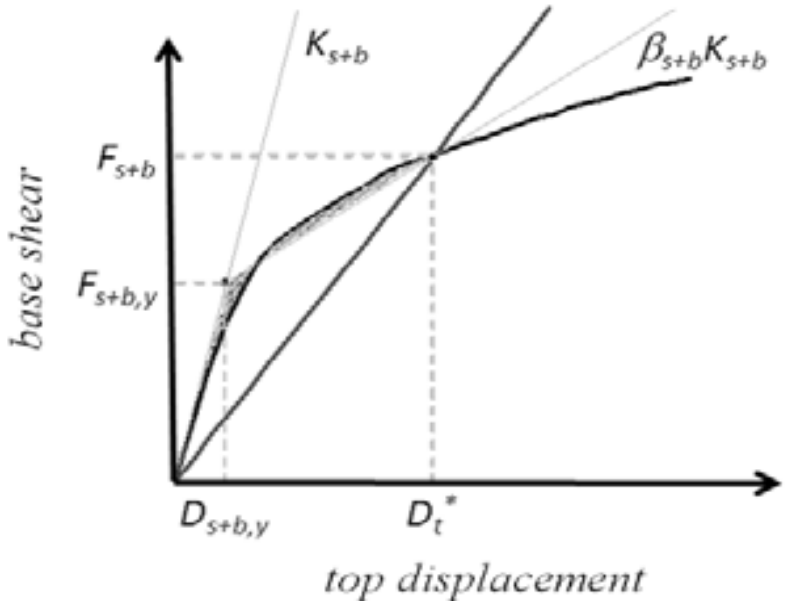


*Figure 4.16:Evaluation of the equivalent bilinear capacity curve*

*5. Define equivalent single degree of freedom*

MDOF system is converted in a SDOF system by transforming the capacity curve into the capacity spectrum ($S_{dt} - S_a$ )

$$S_{dt} = \frac{D_t}{\Gamma \emptyset_t} \quad (4.2.30)$$

$$S_a = \frac{F_{S+B}}{\Gamma L} \quad (4.2.31)$$

where $\Gamma$ is the participation factor of the modal shape $\emptyset$.

The modal characteristics of the braced structure may change at every iteration due to new brace characteristics.

*6. Evaluate the required equivalent viscous damping*

The equivalent viscous damping $\nu_{eq,S+B}^*$ of the braced structure to meet the displacement of the equivalent SDOF system and the target spectral displacement $S_{dt}^* = \frac{D_t^*}{\Gamma \emptyset^T}$ is determined.

According to the Capacity Spectrum Method the demand spectrum is obtained reducing the 5%damping response spectrum by multiplying for the damping correction factor *h* that is function of $\nu_{tot}$.

$$\eta = \sqrt{\frac{10}{5+\nu_{tot}100}} = \frac{S_{\nu_{eff}}}{S_{5\%}} \quad (4.2.32)$$

From Eq (4.2.32) one obtains the damping $\nu_{tot}^*$ needed to reduce displacement up to the target displacement $S_{dt}^*$.

$$\nu_{tot}^{*} = 0.1\left(\frac{S_{5\%}}{S_{dt}^{*}}\right)^{2} - 0.05 \qquad (4.2.33)$$

*7. Evaluate the equivalent viscous damping contribution due to the naked structure*

The contribution to damping of the structure $\nu_{eq,s(Dt^{*})}$ can be determined from being $D_{t^{*}}$ the top displacement corresponding to $E_{D,S}^{bilinear}$ and $E_{S,S+B}$ that are the energy dissipated by S and the elastic strain energy of S+B ($E_{D,S}^{bilinear}$ and $E_{S,S+B}$ are determined from the capacity curve of S and S+B respectively).

*8. Evaluate the additional equivalent viscous damping contribution due to braces*

Given $\nu_{tot(D_t^{*})}^{*}$ from Eq (4.2.33) the equivalent viscous damping needed to be supplied by the braces $\nu_{eq,B(D_t^{*})}^{*}$ is evaluated from Eq (4.2.26) and Eq (4.2.29) as follows

$$\nu_{eq,B(D_t^{*})}^{*} = \nu_{tot(D_t^{*})}^{*} - \nu_{eq,S(D_t^{*})}^{*} - \nu_I \qquad (4.2.34)$$

*9. Dimensioning of the braces*

Once the required equivalent viscous damping $\nu_{eq,B(D_t^{*})}^{*}$ has been evaluated from Eq (4.2.34) axial stiffness and yielding strength required to achieve the desired additional damping can be determined with the same procedure previously adopted for the structure (Step 7). The energy dissipated by the braces inserted at each $j_{th}$ level can be expressed as:

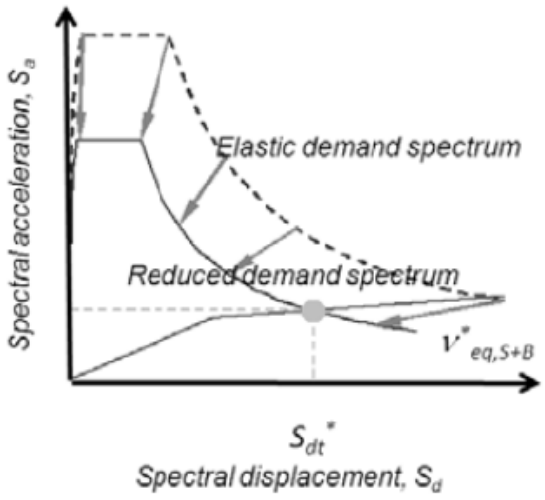


*Figure 4.17: Evaluation of the equivalent viscous damping needed to achieve the target performance point*

$$E_{D,B}^{bilinear} = \sum_{j=1}^{n} 4(F'_{by}\delta'_{j} - \delta'_{y,j}F_{b,j(\delta_j)}) \qquad (4.2.35)$$

being $\delta'_{y,j}$ the component of the interstory drift $\delta_j$ at jth of the n floors along the axis of the brace ($\delta'_{y,j}$ is the axial displacement corresponding to yielding of the device).

The axial displacement of the damping brace at the $j^{th}$ floor $\delta'_{bj}$ can be determined from its inclination angle $\theta_{b,j}$ and interstory drift $\delta_j = D_j - D_{j-1}$; therefore $\delta'_{bj} = \delta_j Cos\theta_{bj}$.

The dissipative brace is usually constituted of a dissipative device (such as the BRB) assembled in series with an extension element (e.g. realized with a steel profile) in order to connect the opposite corners of a frame Figure 4.18.

Therefore, being $K'_{b,j}$ and $K'_{by,j}$ the equivalent stiffness of the spring series in the elastic and plastic range respectively, $a = \frac{K_{e,j}}{K_{d,j}}$ the ratio between the elastic stiffness of the steel profile and of the device and $\beta_{d,j}$ the ratio between stiffness after and before yielding of the dissipative device, the following expression can be derived:

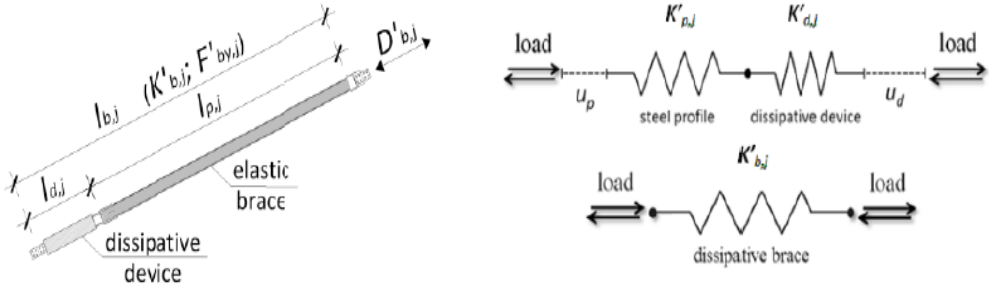


*Figure 4.18:Dissipative device assembled in series with an extension element (i.e a steel profile): equivalent model of spring in series and equivalent single spring model*

$$K'_{b,j} = \frac{K'_{d,j}}{\frac{1}{\alpha_j}+1};\ K'_{by,j} = \frac{\beta_{b,j}K'_{d,j}}{\frac{\beta_{b,j}}{\alpha_j}+1};\ \alpha_j = \frac{K'_{p,j}}{K'_{d,j}} \tag{4.2.36}$$

$$F'_{b,j} = F'_{by,j} + \left(\delta'_j - \delta'_{y,j}\right)\frac{\beta_{b,j}K'_{d,j}}{\frac{\beta_{b,j}}{\alpha_j}+1} \tag{4.2.37}$$

$$\delta'_{y,j} = \frac{F'_{by,j}}{K'_{b,j}} = \frac{F'_{by,j}}{K'_{d,j}}\left(\frac{1}{\alpha_j}+1\right) \tag{4.2.38}$$

Consequently, if there is one brace per direction and per floor, substituting Eq (4.2.37) into Eq (4.2.35) $\nu^*_{eq,B(D^*_t)}$ can be expressed in the following way:

$$\nu^*_{eq,B(D^*_t)} = \chi_B \frac{2}{\pi} \frac{\sum_{j=1}^{n} \left\{ F_{by,j} \delta'_{j-} \delta'_{y,j} \left[ F'_{by,j} + \left(\delta'_j - \delta'_{y,j}\right) \frac{\beta_{b,j} K'_{d,j}}{\frac{\beta_{b,j}}{\alpha_j} + 1} \right] \right\}}{F_{S,S+B(D^*_t)} D^*_{S,S+B}} \qquad (4.2.39)$$

where the $\delta'_j$ are determined from the pushover analysis for the top displacement $D_t$ and $\delta'_{y,j}$ that is the yielding displacement of devices, can be reasonable assumed as $\delta'_j \leq \frac{\delta'_{y,j}}{4}$.

$F'_{y,j}$ is, for each direction, the yielding force of the floor brace: once $\delta'_{y,j}$ has been defined $F'_{y,j}$. is consequently determined (4.2.38).

Thus, remembering Eq (4.2.19) and according to Eq (4.2.36), $K'_{d,j}$ can be expressed as follows:

$$K'_{d,j} = K_{global} c_{b,j} \left(\frac{1}{\alpha_j} + 1\right) \qquad (4.2.40)$$

Therefore substituting Eq (4.2.40) into Eq (4.2.39) $K_{global}$ can be determined as follows:

$$K_{global} = \pi \frac{\nu_{eq,B(D^*_t)} F_{s,s+B(D^*_t)} D_{s,s+B}}{2\, \chi_B\, C_1} \qquad (4.2.41)$$

with:

$$C_1 = \sum_{j=1}^{n} c_{b,j} \{ \delta'_{y,j}\, \delta'_j - \delta'_{y,j} [\delta'_{y,j} + \left(\delta'_j - \delta'_{y,j}\right) \frac{\beta_{b,j} \left(\frac{1}{\alpha_j} + 1\right)}{\frac{\beta_{b,j}}{\alpha_j} + 1}] \} \qquad (4.2.42)$$

A value of $a_j > 3$ is usual in applications, therefore $K'_{b,j} = \frac{3}{4} K'_{d,j}$ while the steel profile must be stronger (neither yielding nor buckling) than the device: for a given interstorey drift the larger is $a_j$ the larger are device displacements and hysteretic cycles. At this point all terms of Eq (4.2.41) are known so, from Eq (4.2.40) and (4.2.36) , the floor brace stiff nesses $K'_{b,j}$ can be defined (the yielding force $F'_{by,j}$ can be directly derived since the stiffness $K'_{b,j}$ and the yielding displacement $\delta'_{y,j}$ have been defined).

Though in this procedure referring to (4.2.39) it is important to underline that, in a general case, one can have *m* different braces for each level *j*. In fact, at the same level, each brace *i* can be characterized by its specific properties as a consequence, for example, of the geometry of the bays of the structural frame. Consequently (4.2.39) can be generalized as follows.

$$\nu^*_{eq,B(D^*_t)} = \frac{2}{\pi} \frac{\sum_{j=1}^{n} \sum_{i=1}^{n} \chi_{B,i} \left\{ F_{by,j,i}\, \delta'_{j-} \delta'_{y,j,i} \left[ F'_{by,j,i} + \left(\delta'_j - \delta'_{y,j,i}\right) \frac{\beta_{b,j,i}\, K'_{d,j,i}}{\frac{\beta_{b,j,i}}{\alpha_{j,i}} + 1} \right] \right\}}{F_{S,S+B(D^*_t)} D^*_{S,S+B}} \qquad (4.2.43)$$

*10. Check convergence*

One must repeat steps from 3 to 9 until the performance point of the braced structure converges to the target displacement with adequate accuracy.

### 4.2.3 An energy-based method for seismic retrofit of existing frames using hysteretic dampers: by A. Benavent-Climent

The method proposed by Benavent-Climent focuses on the seismic retrofitting of existing frames by adding hysteretic energy dissipating devices (EDDs). The procedure is based on the energy balance of the structure, and it is used to determine the lateral strength, the lateral stiffness and the energy dissipation capacity of the EDDs needed in each story to achieve prescribed target performance levels for a given earthquake hazard. The performance levels are governed by the maximum lateral displacement. The earthquake hazard is characterized in terms of input energy and several seismological parameters, and further takes into account the proximity of the earthquake to the source. This method deals with the effect of the EDDs explicitly in terms of hysteretic energy, bypassing equivalent viscous damping approximations, and directly quantifies the cumulative damage induced in the EDDs.

Before the methodology is further discussed, the background of energy-based design is hereby briefly presented:

#### 4.2.3.1 Background on energy-based design

The equation of motion of an inelastic single-degree-of-freedom system (SDOF) subjected to a unidirectional horizontal ground motion can be written as follows:

$$M\ddot{y} + C\dot{y} + Q_{(y)} = -M\ddot{z}_g \qquad (4.2.44)$$

where M is the mass, C is the damping coefficient, $Q_{(y)}$ is the restoring force, y is the relative displacement, $\dot{y}$ and $\ddot{y}$ its first and second derivatives with respect to time and $\ddot{z}_g$ is the ground acceleration. Multiplying Eq (4.2.44) by $dy = \dot{y}dt$ and integrating over the entire duration of the earthquake i.e. from $t = 0$ to $t = t_0$, the energy balance equation becomes:

$$W_k + W_\xi + W_s = E \qquad (4.2.45)$$

In the left-hand-side term, $W_k = \int \dot{y}M\ddot{y}dt$ is the kinetic energy, $W_\xi = \int C\dot{y}^2 dt$ is the damping energy, and $W_s = \int Q_{(y)}\dot{y}dt$ is the absorbed energy ,which is composed of the recoverable elastic strain energy, $W_{se}$ , and the irrecoverable plastic energy, $W_p$, i.e. $W_s = W_{se} + W_p$ . The right-hand-side term, $E = \int -M\ddot{z}_g\dot{y}dt$ is, by definition, the input energy, which can be expressed in the form of an equivalent velocity $V_E$ as:

$$V_E = \sqrt{\frac{2E}{M}} \qquad (4.2.46)$$

Since $W_k + W_{se}$ is the elastic vibrational energy $W_e$, the Eq (4.2.45) can be rewritten as:

$$W_e + W_p = E - W_\xi \qquad (4.2.47)$$

Further, $W_e + W_p$ can also be expressed in the form of an equivalent velocity $V_D$ so that:

$$W_e + W_p = \frac{MV_D}{2} \qquad (4.2.48)$$

Eq (4.2.47) holds also for a multi-degree-of-freedom system(MDOF) subjected to a unidirectional horizontal ground motion if the above expression for $W_k$, $W_\xi$, $W_s$ and E is replaced by $W_k = \int \dot{y}^T M\ddot{y}dt$, $W_\xi = \int \dot{y}^T C\dot{y}dt$, $W_s = \int \dot{y}^T Qdt$ and $E = -\int \dot{y}^T Mr\ddot{z}_g dt$ respectively. Here and, M is the mass matrix, C the damping matrix and Q(t) the restoring force vector; $\ddot{y}_{(t)}$ , $\dot{y}_{(t)}$ are the acceleration and velocity vectors relative to the ground respectively ;and represents the displacement vector $y_{(t)}$ resulting from a unit support displacement.

On the basis of numerous response analyses, [52] concluded that, in general MDOF damped inelastic systems, the total input energy supplied by the earthquake – and consequently $V_E$ – coincides approximately with that of an equivalent elastic SDOF system with mass M equal to the total mass of the MDOF system, and period T equal to that of its first vibration mode. This conclusion has been validated experimentally [53]. In the energy-based seismic design approach, the energy input spectrum in the form of equivalent velocity $V_E - T$ characterizes the loading effect of the earthquake. Design input energy spectra $V_E - T$ [52,54,55] have been proposed in past studies. The cumulative damage of the structure is strongly related to the plastic strain energy $W_p$. The sum of $W_p$ and the elastic vibrational energy $W_e$ is what Housner [56] called the energy that damages a structure subjected to seismic action. From Eq (4.2.45)-(4.2.48) it follows that for undamped systems $V_D = V_E$ ; otherwise, the difference between $V_D$ and $V_E$ is the energy dissipated by the inherent damping of the structure. Several empirical expressions have been proposed that allow us to obtain $V_D$ from $V_E$ [52,54,57]. Moreover, attenuation relationships have been established for use in energy-based seismic design [58] that directly provide $W_S$ – the absorbed energy – for a given earthquake magnitude, source-to-site distance, site class and ductility factor, in terms of an equivalent velocity $V_a$ defined by:

$$V_a = \sqrt{\frac{2W_S}{M}} \qquad (4.2.49)$$

Although $V_D - T$ spectra have been recently introduced in some building codes, characterization of the design earthquake in terms of energy input spectra $V_D - T$ is not as common for professionals as in the form of absolute acceleration spectra $S_a - T$. Energy input spectra in terms of $V_D - T$ can be obtained from the $S_a - T$ spectra on the basis of the following considerations: (i) over the range of damping ratios exhibited by actual structures — say less than 0.10 — the spectral absolute acceleration Sa of damped elastic SDOF systems is related to the pseudo-velocity spectral response, $S_{pv}$ , by the well known expression $S_a = \omega S_{pv}$ , where $\omega$ is the circular frequency. (ii)

Hudson [59,60] demonstrated that, except in the case of very long period oscillators, the spectral relative velocity, $S_v$ , differs very little from $S_{pv}$. (iii) Akiyama [52] showed that $S_v$ provides a good approximation of $V_D$, and validated Housner's [56] assumption that $V_D$ can be taken as equal to $S_V$ for the purposes of earthquake-resistant design.

#### 4.2.3.2 Modeling and design criteria

The application of this method requires the determination of the mass $m_i$ the lateral yield strength, $Q_{fy,i}$ , the initial stiffness $k_{f,i}$ of each story $i$ , and the fundamental period $T_1$ of the existing building (referred to as main structure in this method). This seismic retrofit strategy consists of adding hysteretic EDDs in each story. The existing structure and the added EDDs are arranged so as to form a dual system consisting of two inelastic springs connected in parallel as shown in Figure 4.19 .The lateral load displacement relationship $Q_{f,i} - \delta_i$, of a given $i^{th}$story of the main structure—without EDDs—under monotonic loading is represented by the elastic-perfectly plastic model shown with bold lines in Figure 4.19a. The lateral load– displacement relationship, $Q_{s,i} - \delta_i$, of a given $i^{th}$ story accounting only for the EDDs is also assumed to be of the elastic-perfectly-plastic type and is defined by the lateral yield strength $Q_{s,i}$ and the initial stiffness $k_{s,i}$ as shown in Figure 4.19b. The lateral shear force-interstory drift relationship of the entire building-device structure of a i-th story under monotonic loading, $Q_i - \delta_i$, is obtained by summing up the forces sustained by each element at a given displacement level $\delta_i$ , as shown in Figure 4.19c . The goals of the procedure are: (i) to determine the $Q_{sy,i}$ and $k_{s,i}$ of the EDDs needed in each story to achieve the required building performance levels for a given earthquake hazard; and (ii) to evaluate the energy dissipation demand on the EDDs. Usually, one of the objectives of the EDDs is to avoid inelastic deformations in the structural elements outside the EDDs, and many researchers consider this objective as one of the basic requirements for a system with EDDs [61,62]. Further, many existing structures were designed according to past seismic codes and their ductility, if any, is very limited. In the case of reinforced concrete frames, it is worth noting that although they do not have a large elastic range, especially if compared with steel frames, there is a range of lateral drift within which the behavior can be assumed to be ‘‘basically’’ elastic and the damage on the main frame would be null or negligible. Accordingly, it is imposed that

$$\delta_{max,i} \leq \delta_{fy,i} \qquad (4.2.50)$$

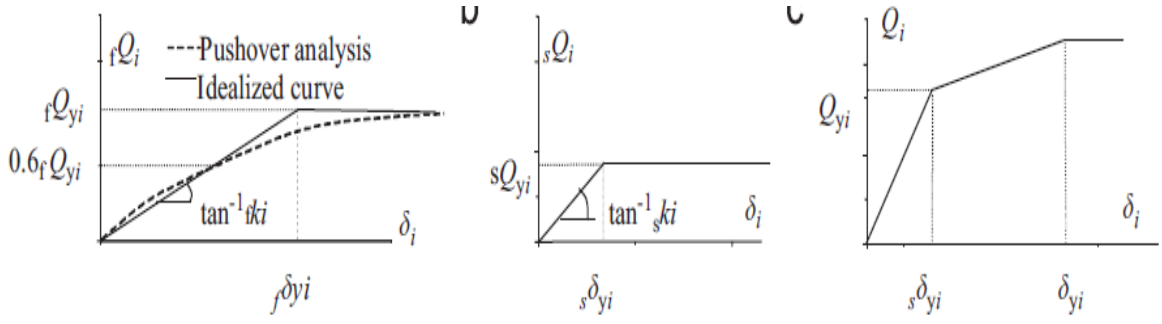

*a)* *b)* *c)*

*Figure 4.19:Idealized interstory drift-shear force curve of each stor; a) existing structure; b) Energy dissipating device; c) dual system*

where $\delta_{max,i}$ is the maximum interstory drift of the entire building-device structure and ($\delta_{f,y,i} = \frac{Q_{f,y,i}}{k_{f,i}}$ ) is the yielding interstory drift of the main structure. The condition imposed by Eq (4.2.50) is intended to avoid the severe degradation effects in the response of the main structure that may arise from stiffness degradation and deterioration as well as shear effects in some types of structures. In structures for which such degradation cannot be avoided, this method is not applicable. Such is the case, for example, of precast structures with slender columns and/or existing reinforced concrete frame systems designed primarily for gravity loads and with high shear degradation. Yet the proposed formulation is indeed applicable to symmetric structures or systems with prevalent translation modes of vibration. If the main existing structure has important irregularities that may place extraordinary displacement demand some elements due to torsional response, measures must be adopted to mitigate torsional effects. One such measure is to locate the EDD so that they can balance the stiffness and make the mas sand stiffness centers very close. The lateral yield strength of the entire building-device structure at the $i^{th}$ story, $Q_{y,i}$ , is simply:

$$Q_{y,i} = Q_{s,y,i} + \delta_{s,y,i} k_{f,i} \tag{4.2.51}$$

where $\delta_{s,y,i} = \frac{Q_{s,y,i}}{k_{s,i}}$ is the yield deformation of the EDDs installed in that story. The maximum lateral force sustained by the main structure, $Q_{f,max,i}$ , is $Q_{f,max,i} = \delta_{max,i} k_{f,i}$. For the building- device structure surviving the earthquake, the plastic strain energy accumulated in the i-th story, $W_{P,i}$ must not exceed the ultimate energy dissipation capacity of the EDDs installed in that story, $W_{u,i}$ . In turn, $W_{P,i}$ and $W_{u,i}$ can be expressed in the form of two non-dimensional coefficients, $\eta_i$ and $\eta_{u,i}$ defined by:

$$\eta_i = \frac{W_{pi}}{Q_{s,y,i}\delta_{s,y,i}} \tag{4.2.52}$$

$$\eta_{u,i} = \frac{W_{ui}}{Q_{s,y,i}\delta_{s,y,i}} \tag{4.2.53}$$

Thus the above condition can be written as:

$$\eta_i \leq \eta_{u,i} \tag{4.2.54}$$

#### 4.2.3.3 Formulation of the method

For the sake of convenience, $\delta_{max,i}$ , $Q_{y,i}$ , $Q_{max,f,i}$, $Q_{s,y,i}$ and $k_{f,1}$ will be also expressed herein in non-dimensional form by the plastic deformation ratio $\mu_i$, the shear-force

coefficients $\alpha_i$ , $\alpha_{max,f,i}$ , $\alpha_{s,i}$, and the stiffness ratio $\chi_1$, respectively,which are defined as follows:

$$\mu_i = \frac{(\delta_{max,i} - \delta_{s,y,i})}{\delta_{s,y,i}};\ \alpha_i = \frac{Q_{y,i}}{\sum_{k=i}^{N} m_k g};\ \alpha_{max,f,i} = \frac{Q_{max,f,i}}{\sum_{k=i}^{N} m_k g} \quad (4.2.55)$$

$$\alpha_{s,i} = \frac{Q_{s,y,i}}{\sum_{k=i}^{N} m_k g};\ \chi_1 = \frac{k_{f,1}}{k_{eq}}$$

Here N is the total number of stories, g is the acceleration of the gravity, and $k_{eq}$ is the stiffness of an equivalent SDOF system of mass $M = \sum m_j$ and period equal to the fundamental period of the main structure, $T_1$ i.e $k_{eq} = \frac{4\pi^2 M}{T_1^2}$

#### *4.2.3.3.1 Stiffness and strength distribution of the EDDs among the stories*

The ratio between the lateral stiffness provided by the EDDs and the lateral stiffness of the main structure in each story is referred to as:

$$K_i = \frac{k_{s,i}}{k_{f,i}} \quad (4.2.56)$$

There is no need to make $K_i$ equal in all stories, although this criterion has been used on occasion in the past. The lateral strength distribution of the entire building-devices structure, $\frac{Q_{y,i}}{Q_{y,1}}$ , can be expressed in terms of shear-force coefficients by $\bar{\alpha}_i = \frac{\alpha_i}{\alpha_1}$. The criterion adopted in this method to determine the $\bar{\alpha}_i$ distribution is to attain an even distribution of damage among the EDDs. The damage in the EDDs installed in a given story i can be characterized by the non-dimensional parameter $\eta_i$ defined by Eq (4.2.52) . Past studies [52] showed that the strength distribution $\bar{\alpha}_i$ that makes $\eta_i$ equal in all stories($\eta_i = \eta$ ) in a low-to-medium rise multi-story building subjected to seismic loads coincides approximately with the maximum shear-force distribution in an equivalent elastic undamped shear strut with similar lateral stiffness distribution along its height. The derivation of the ‘‘exact’’ shear-force coefficient distribution $\bar{\alpha}_i$ for an elastic undamped shear strut subjected to a design earthquake characterized by a bilinear $V_D - T$ spectrum is explained in detail. The ‘‘exact’’ solution cannot be expressed with simple equations, but it can be approximated for design purposes with the following expression:

$$\bar{\alpha}_i = \frac{\alpha_i}{\alpha_1} = \exp\left[\left(1 - 0.02\frac{k_{f1}}{k_{f,N}} - 0.16\frac{T_1}{T_G}\right)\bar{x} - \left(0.5 - 0.05\frac{k_{f,1}}{k_{f,N}} - 0.3\frac{T_1}{T_G}\right)\bar{x}^2\right] \quad (4.2.57)$$

Here $\bar{x} = \frac{(i-1)}{N}$, $k_{f,N}$ is the lateral stiffness of the uppermost N-th story of the main structure, whereas $T_G$ defines the change of slope of the $V_D - T$ bilinear spectra. $T_G$ may be called the predominant period of the ground motion [63].

Further, from the definition of $\alpha_{S,1}$ and $K_i$ given by Eq (4.2.55) and Eq (4.2.56), the following relation must hold so that the distribution of $\alpha_{S,1}$ be that given by (4.2.57):

$$\alpha_{S,i} = \bar{\alpha}_i \alpha_{S,1} \frac{K_i(K_1+1)}{K_1(K_i+1)} \quad (4.2.58)$$

Of course, instead of Eq (4.2.57), a more refined lateral strength distribution could be used from dynamic analysis by applying a trial and error iterative method. This would not alter the method at all. However, it implies selecting a set of earthquake records, conducting many nonlinear dynamic response analyses, and averaging the distribution derived for each record, which can be a very cumbersome process. Such a process should be used for systems with a degrading type of response under earthquake loading.

#### *4.2.3.3.2 Lateral strength to be provided by the EDDs of the first story*

Once the stiffness ratios $K_i$ and the lateral shear-force coefficient distribution $\bar{\alpha}_i$ are determined, the lateral shear force coefficient to be provided by the EDDs of the first story, $\alpha_{S,1}$, must be calculated in order to obtain the required lateral shear force coefficient of the EDDs in the other stories $\alpha_{S,i}$ with (4.2.58). The equations that govern the $\alpha_{S,1}$ required for a given seismic hazard and building performance level are derived next by establishing the energy balance of the structure.

When using EDDs the yield displacement $\delta_{s,y,i}$ of the EDDs is made smaller than that of the main structure, $\delta_{f,y,i}$ so that the EDDs begin dissipating energy before the main structure might yield. Moreover, $Q_{s,y,i}$ is commonly smaller than $Q_{f,y,i}$. As a result, the elastic strain energy stored by the EDDs is commonly negligible in comparison to that of the main structure, and the elastic vibrational energy of the whole building, $W_e$ can be approximated from the maximum shear force sustained by the main structure on the first story as follows:

$$W_e = \frac{M g^2 T_1^2}{4\pi^2} \frac{\alpha_{max,f,1}^2}{2} \quad (4.2.59)$$

From Eq (4.2.52) and taking into account the coefficients defined in Eq (4.2.55), the plastic strain energy accumulated in the i-th story $W_{p,i}$ can be expressed as follows:

$$W_{p,i} = \eta_i Q_{s,y,i} \delta_{s,y,i} = \eta_i \alpha_{S,i}^2 \left[\sum_{k=i}^{N} m_k g\right]^2 \frac{1}{k_{s,i}} \quad (4.2.60)$$

Provided that the strength distribution given by Eq (4.2.57) is adopted, the normalized plastic strain energy $\eta_i$ can be assumed equal in all stories, i.e. $\eta_i = \eta$. Thus, taking into account Eq (4.2.56) and using the non-dimensional parameters $\alpha_{s,i}$ and $\bar{\alpha}_i$ defined above, the total plastic strain energy dissipated by the EDDs of the whole structure, $W_p$, can be expressed in terms of the plastic strain energy dissipated by the EDDs of the first story, $W_{p,1}$, by introducing a new ratio $\gamma_1 = \frac{W_p}{W_{p,1}}$, which is obtained as follows:

$$\gamma_1 = \frac{W_p}{W_{p,1}} = \frac{\sum_{i=1}^{N} [\eta_i \alpha_{S,i}^2 (\sum_{k=i}^{N} m_k g)^2 \frac{1}{k_{s,i}}]}{\eta_1 \alpha_{S,1}^2 M^2 g^2 / k_{s,1}} = \sum_{i=1}^{N} \{[\bar{\alpha}_i (\sum \frac{m_j}{M}) \frac{(K1+1)}{(K_i+1)}]^2 \frac{k_{F,1} K_i}{k_{f,i} K_1}\} \quad (4.2.61)$$

Thus:

$$W_p = \gamma_1 W_{p,1} = \gamma_1 Q_{s,y,1}\delta_{s,y,1}\eta = \frac{\gamma_1 \alpha_{s,1}^2 M^2 g^2 \eta}{K_1 \chi_1 k_{eq}} = \frac{\gamma_1 \alpha_{s,1}^2 M g^2 \eta T_1^2}{4\pi^2 K_1 \chi_1} \quad (4.2.62)$$

Substituting Eq (4.2.59) in Eq (4.2.47) gives:

$$\frac{M_g^2 T_1^2}{4\pi^2}\left[\frac{\alpha_{max,f,1}^2}{2} + \frac{\gamma_1}{K_1\chi_1}\eta_s \alpha_{s,1}^2\right] = \frac{MV_D^2}{2} \quad (4.2.63)$$

Now, a new parameter $\alpha_e$ is introduced. $\alpha_e$ is defined as the base shear-force coefficient that the main structure should have in order to absorb by itself—i.e. without EDDs—the amount of input energy $\frac{MV_D^2}{2}$ supplied by the earthquake. The expression for $\alpha_e$ can be obtained placing $\alpha_{s,1} = 0$ in Eq (4.2.63) —this implies ignoring the EDDs—and solving for $\alpha_{max,f,1}^2 = \alpha_e$ , which gives:

$$\alpha_e = \frac{2\pi V_D}{g T_1} \quad (4.2.64)$$

Using Eq (4.2.64), Eq (4.2.63) can be rewritten as follows:

$$\frac{\alpha_{max,f,1}^2}{2} + \frac{\gamma_1}{K_1\chi_1}\eta_s \alpha_1^2 = \frac{\alpha_e^2}{2} \quad (4.2.65)$$

The relation between $\eta_i$ and $\mu_i$ is a key parameter in seismic design methodologies based on the energy concept, and it has been addressed in different ways in the past [53,64,65]. Based on the results of regression analyses performed with 128 near-fault and 122 far-field earthquake records, Manfredi et al. [66] proposed the following formulae for estimating the equivalent number of plastic cycles $n_{eq}$ at the maximum value of plastic excursion that a SDOF system of mass $m$ , elastic period $T$ and yielding force $F_y$ must develop in order to dissipate the total amount of hysteretic energy input by the earthquake

$$n_{eq} = 1 + c_1 I_d \sqrt{\frac{T_{NH}}{T}}\,(R-1)^{c_2} \quad (4.2.66)$$

Here $T_{NH}$ is the initial period of medium period region in the Newmark and Hall [67] spectral representation. $R$ is the reduction factor defined as $R = \frac{mS_a}{F_y}$ where $S_a$ is the elastic spectral acceleration. $I_d$ is a seismological parameter [68] defined by:

$$I_d = \frac{\int_0^{t_0} \ddot{z}_g^2 d_t}{PGA\ PGV} \quad (4.2.67)$$

where PGA and PGV are the peak ground acceleration and velocity, respectively. In Eq (4.2.66), Manfredi et al. [66] proposed to take $c_1 = 0.23$, $c_2 = 0.4$ for near-fault earthquakes; and $c_1 = 0.18$, $c_2 = 0.6$ for far-field earthquakes. In order to apply the Manfredi et al. equation to the this method, the multi-story structure is assimilated to an equivalent SDOF system with elastic period $T = T_1$, mass $m = M$ and $F_y = Q_{s,y,1} + k_{f,1}\delta_{s,y,1}$. Based on this equivalence, while taking into account that $S_a$ is approximately equal to $\left(\frac{2\pi}{T}\right)S_v$ , and that the elastic spectral velocity $S_v$ coincides approximately with $V_D$ [52,58], Eq (4.2.66) is rewritten as:

$$n_{eq} = 1 + c_1 I_d \sqrt{\frac{T_{NH}}{T_1}} \left( \frac{K_1 \alpha_e}{(K_1+1)\alpha_{s,1}} \right)^{c_2} \quad (4.2.68)$$

For the EDDs with elastic-perfectly-plastic characteristics dealt with in this study, $n_{eq}$ is, by definition [66]: $n_{eq} = \frac{W_{pi}}{Q_{s,y,i}(\delta_{max,i} - \delta_{s,y,i})}$ , which coincides with $\frac{\eta_i}{\mu_i}$. In the this method, the same $n_{eq} = \frac{\eta_i}{\mu_i}$ given by Eq (4.2.68)—is adopted for all stories. Since $\eta_i$ was also assumed as constant, $\eta_i = \eta$ , the maximum plastic deformation ratio $\mu_i$ has the same value $\mu_i = \mu = \frac{\eta}{n_{eq}}$ in all stories. On the other hand, since the condition given by Eq (4.2.50) was adopted, the maximum base shear-force coefficient of the main structure $\alpha_{max,f,1}$ is:

$$\alpha_{max,f,1} = \frac{\delta_{max,1} k_{f,1}}{Mg} \quad (4.2.69)$$

From the definition of $\mu_i = \mu$ – Eq (4.2.55) - particularized for the first story, it is obtained that $\delta_{max,1} = \delta_{s,y,1}(\mu + 1)$, and substituting in Eq (4.2.69) gives:

$$\alpha_{max,f,1} = \frac{\delta_{s,y,1} k_{f,1}(\mu+1)}{Mg} = \frac{\delta_{s,y,1} k_{s,1}(\mu+1)}{K_1 Mg} = \frac{Q_{s,y,1}(\mu+1)}{K_1 Mg} = \frac{\alpha_{s,1}(\mu+1)}{K_1} \quad (4.2.70)$$

Substituting Eq (4.2.69) in Eq (4.2.65) , recalling that $\mu = \mu_i = \frac{\eta}{n_{eq}}$ and solving for $\mu$ gives:

$$\mu = K_1 \left\{ \sqrt{\left( \frac{n_{eq}\gamma_1}{\chi_1} \right)^2 + \frac{2 n_{eq}\gamma_1}{K_1 \chi_1} + \frac{\alpha_e^2}{\alpha_{s,1}^2}} - \frac{n_{eq}\gamma_1}{\chi_1} \right\} - 1 \quad (4.2.71)$$

Noting that for the other stories $\mu = \frac{\delta_{max,i} - \delta_{s,y,i}}{\delta_{s,y,i}}$, using Eq (4.2.58) and (4.2.71) and solving for $\delta_{max,i}$ gives the equation that predicts the maximum displacement of a given story i:

$$\delta_{max,i} = \frac{\bar{\alpha}_i \alpha_{S,1}(K_1+1)(\sum_{j=1}^{N} m_j g)}{k_{f,i}(K_i+1)} \left\{ \sqrt{\left( \frac{n_{eq}\gamma_1}{\chi_1} \right)^2 + \frac{2 n_{eq}\gamma_1}{K_1 \chi_1} + \frac{\alpha_e^2}{\alpha_{s,1}^2}} - \frac{n_{eq}\gamma_1}{\chi_1} \right\} \quad (4.2.72)$$

#### *4.2.3.3.3 The procedure*

In the propsed method, the characteristics of the existing main structure-without EDDs- to be retrofitted( i.e. $m_i, k_{f,i}, \delta_{f,y,i}$ *and* $T_1$) are assumed to be known data. $m_i, k_{f,i}, \delta_{f,y,i}$ and $T_1$ can be estimated by using approximate formulae [52], or by creating a finite element based model and performing a pushover analysis using a triangular lateral load distributio. In the latter option a $Q_{f,i} - \delta_i$ curve is obtained for each story – the dotted line in Fig. 1a- from which $k_{f,i}$ and $\delta_{f,y,i}$ can be estimated by ising the secant stiffness at 60% of the yield strength, as suggested by FEMA 273 [69], and $T_1$ is obtained from and eignevalue analysis. The goal of the methodology is to determine the lateral stiffness $k_{s,i}$, lateral strength $Q_{s,y,i}$, and the normalized energy dissipation demand η of

the EDDs to be installed in each story, so that the entire building-device structure satisfies predtermined performance levels defined by the maimum allowed interstory drift, $\delta_{allow,i}$, for a given earthquake hazard characterized by $V_D, T_G, T_{NH}, I_d$ and the proximity to the source. The basic steps involoved in the procedure are as follows.

*1. Step 1*

Characteriaze the deisng earthquake in terms of a bilinear $V_D - T$ spectra defined by the maximum demand $V_{D,max}$ and the predominant period $T_G$- i.e. $V_D = TV_{D,max}/TG$ for $T < TG$, $V_D = V_{D,max}$ for $T \geq T_G$- and the values ofc the seismological parameters $I_d, T_{NH}, c_1 \; and \; c_2$.

*2. Step 2*

Prescribe the maximum interstroy drift allowed in each story, $\delta_{allow\,i,}$ in accordance with the acceptance criterai for building components at the targe building rehabilitation performance level.

*3. Step 3*

Calculate $\bar{\alpha}_i$, $\alpha_e$ and $\chi_1$ with the equations given above

*4. Step 4*

Choose a set of values for $K_i$, and compute $\gamma_1$, From $i = 1$ to $i = N$ proceed for each story as follows.

Starting with $\alpha_{S,1} = 0$ iterate in Eq (4.2.72)-Increasing the values of $\alpha_{S,1}$ until the predicted $\delta_{max,i}$ gets close to $\delta_{allow,i}$ within an acceptable tolerance (for example, 5% of $\delta_{allow,i}$). In these iteration, $\alpha_{S,1}$ shall not be larger the value given by the following expression so that $\delta_{s,y,i} \leq \delta_{f,y,i}$.

$$\alpha_{S,1} \leq \frac{\delta_{f,y,i} k_{f,i} K_1 (K_i + 1)}{\bar{\alpha}_i (K_1 + 1) \sum_{k=i}^{N} m_k g} \qquad (4.2.73)$$

If in a given story $i$ it is not possible to find a $\alpha_{S,1}$that makes $\delta_{max,i}$ close enough to $\delta_{allow,i}$, restart step 4 with larger values for $K_i$. Once the appropriate $\alpha_{S,1}$ is obtained, keep this value as $\alpha_{S,1,i} = \alpha_{S,1}$ and proceed with the next story. The parameter $\alpha_{S,1,i}$ represents the shear-force coefficient required for the EDDs of the first story so that the maximum interstory drift at the i-th story does not exceed the allowed limit $\delta_{allow,i}$.

*5. Step 5*

Select the maximum of the $\alpha_{S,1,i}$ i.e. $\alpha_{S,1,max} = \max\{\alpha_{S,1,i}\}$, which give the required lateral strength for the EDDs of the first story. Obtain the lateral required in the other stories, $\alpha_{S,i}$, by making $\alpha_{S,1} = \alpha_{S,1,max}$ in Eq (4.2.58). Calcualte the lateral stiffness $k_{s,i}$ and the lateral strength $Q_{s,y,i}$ required for the EDDs of each taking into account that $k_{s,i} = K_i k_{f,i}$ and $Q_{s,y,i} = \alpha_{S,i} \sum m_k g$.

As explained in section 4.2.2, the design procedure proposed by Nuti et al. [38] is based on the capacity spectrum method, which utilizes the equivalent viscous damping equation to design the required braces that reduces the interstorey displacements to the allowable limit. This concept is quite interesting and peculiar and it was for this reason

that the procedure was presented in this study. However,being an iterative procedure, it requires that in each iteration a non linear static analysis be carried out and the response be assessed using the capacity spectrum method. In general, it was observed that the final design of the braces is attained in a significant number of iterations. Therefore, the procedure was considered too lengthy and time-consuming and its implementation too complex to be followed by common practitioners. For these reasons, its application was not further considered in this thesis.

# CHAPTER 5

# PROPOSAL OF AN ENERGY-BASED PROCEDURE FOR THE DESIGN OF ENERGY-DISSIPATIVE BRACES

# 5 Proposal of an Energy-Based procedure for the design of Energy-Dissipative Braces (EDBs)

## *5.1 Introduction*

The seismic retrofitting of existing buildings requires taking into account several different factors, such as architectural constraints, the indirect cost due to closing of the building (or of part of it) for the duration of the retrofit work, or having to heavily reinforce the existing structure due to the increased seismic demand transferred onto it by the retrofit system.

Referring to the structural needs, it seems that the main concerns for structural designers are: 1) the limitation of lateral displacement in buildings under seismic action, and 2) the capacity to resist horizontal actions.

The use of innovative techniques for the seismic amelioration of existing RC buildings has been attracting the attention of both academic and technical communities since the second half of the previous century. Among these techniques there is the employment of passive energy dissipating devices that are mounted in series to metallic braces installed within the existing RC frames. Such energy-dissipating devices can be: 1) fluid-viscous, 2) viscoelastic, 3) elasto-plastic, 4) frictional, or 5) based on shape-memory alloys. The large number of devices available in the market is not accompanied yet, at least within the Italian Building Code, by a mature and detailed description of the design procedure, so that the practicing engineer who would like to suggest such technique is often discouraged by the necessity to refer to scientific publications. With the aim to contribute to fill this gap, an energy-based methodology is proposed, applied and compared with some of the most innovative design procedures available in the scientific literature to date.

This chapter presents the proposed methodology, and some important concepts such as input and hysteretic energy determination for SDoF systems, hysteretic energy distribution in MDoF systems, optimum strength distribution, which are essential in understanding and applying energy-based methods.

The efficiency of the proposed methodology is later assessed by applying it on three case studies. In order to make a comparative analysis of the proposed methodology, the same frames have been also designed by recently developed procedures for the design of the Energy Dissipative Braces.

The formulation of the proposed energy-based design procedure is grounded on the concept of optimum strength distribution explained by Akiyama [52]. Before the proposed procedure is explained, some concepts are discussed, which are significant in understanding, developing and applying the proposed procedure.

## *5.2 Commonly used seismic design procedures*

Despite some limitations and uncertainties, performance-based design procedures present the means to design structures able to resist seismic forces with an acceptable damage. The two most widely used conventional performance-based design procedures are the force–based design and displacement-based design methods. They are both fundamentally nonlinear static procedures (NSPs).

In the force-based design (FBD) method, a design seismic force for a target structure is specified on the basis of an elastic acceleration response spectrum. This seismic design force is called the design base shear. To account for the inelasticity (ductility effect), the design force of the target structure obtained from the elastic acceleration response spectrum is divided by a force-reduction factor. The structure is then designed for the reduced force, and the displacement can be checked so that the code-specified serviceability limits are met. Regardless, the FBD method is not without limitations and drawbacks. Smith and Tso [70] through their study on a large class of reinforced concrete members such as piers, flexural walls and ductile moment resisting fames claimed that force-based design procedure is inconsistent. They argued that the assumption that the stiffness of the lateral force resisting elements is essentially independent of their strength is inconsistent, since strength and stiffness are usually related. Moreover, the problems associated with this method, as pointed out in [71], are:

- *The elastic stiffness is not known at the start of the design process, and very approximate values have to be used.*
- *Foundation effects are generally ignored in force-based design and are difficult to incorporate in the design process as they affect both the elastic period, and displacement ductility demand.*
- *Even though the design force is calculated from an allowable displacement ductility factor, it does not properly address the force-displacement relationship of the structure.*

The displacement-based design (DBD) method, which is generally accepted to be a viable alternative to the FBD method, takes displacement as a design parameter as opposed to using base shear as in FBD. As a result, the important task in a DBD approach is to estimate the maximum displacement demand in a structure with reasonable simplicity and accuracy as a function of its local mechanical characteristics, such as member strain and deformation limits. FEMA 273's [69] displacement-based Coefficient Method is one of the currently available seismic DBD methods. The Coefficient Method modifies the linear elastic response of an equivalent single degree of freedom (SDOF) system by multiplying it by a series of coefficients to estimate a global displacement, commonly termed as the target displacement. This method uses an idealized force-displacement curve (pushover curve), which is a plot (for a given damping coefficient) of base shear versus roof displacement developed for a multiple degree of freedom (MDOF) structure. A corresponding spectral value for an effective period, $T_e$ , of an equivalent SDOF system is then obtained from an elastic response spectrum corresponding to a design ground motion. The target displacement is then calculated using an empirical formula that involves modifying coefficients and the

spectral value for the corresponding effective period. The effective period is obtained from an initial period of the structure and accounts for the loss of stiffness in the transition from elastic to inelastic behavior.

The accuracy of the DBD method is highly dependent on how closely the equivalent SDOF system and its corresponding MDOF system are related through the idealized pushover curve.

Recently, researchers have identified glitches in the use of roof displacement-based pushover curve. Enrique-Hernandez Montes et al. [72] noted that the use of roof displacement in generating the capacity curve can be misleading because the capacity curve so obtained sometimes tends to show the structure as a source of energy rather than absorbing energy. They suggested that an energy-based pushover analysis be used instead, whereby the lateral force is plotted against a displacement which is a function of energy. Manoukas et al. [73] also developed an energy-based pushover procedure for estimating structural performance under strong earthquakes. They showed through numerical examples that their procedure provides better results compared to those produced by other similar procedures.

In addition, neither the FBD method nor the DBD method can directly consider the cumulative damage effect that result from numerous inelastic cycles of the ground motion due to deterioration of the structure's hysteretic behavior. Moreover, the effect of earthquakes on structures should be interpreted not just as a force or displacement quantity, but as a product of both, i.e., in terms of input energy. This is the underlying concept for the inception of the energy-based seismic design (EBSD) method. EBSD is believed by many to be the next generation of seismic design methods.

## *5.3 Energy-based seismic design (EBSD) and its current status*

In chapter 4 the energy-balance equation and its components were briefly explained, so it will be repeated here in detail.

The equation of motion for a single-degree-of-freedom (SDOF) inelastic system subjected to a ground motion is given by

$$m\ddot{u} + c\dot{u} + f_S = -m\ddot{u}_g \qquad (5.1)$$

where $m$= mass of the system; $c$ = damping coefficient; $f_S$ = restoring force; $\ddot{u}_g$= ground

acceleration, and $\ddot{u}$, $\dot{u}$, $u$ are the relative acceleration, velocity, and displacement of the system with respect to the ground, respectively.

According to Uang and Bertero [74], the energy balance equation for an SDOF structure based on relative motion can be written as:

$$\int_0^t m\ddot{u}\,\dot{u}d_t + \int_0^t c\,\dot{u}\dot{u}d_t + \int_0^t f_s\,\dot{u}d_t = -\int_0^t m\ddot{u}_g\,\dot{u}d_t \qquad (5.2)$$

Eq (5.2) can be rewritten as

$$E_k + E_\xi + E_s = E_I \quad (5.3)$$

where:

- $E_k = kinetic\ energy = \int_0^t m\ddot{u}\,\dot{u}d_t = \frac{1}{2}m\dot{u}^2$
- $E_\xi = damping\ energy = \int_0^t c\,\dot{u}^2 d_t$
- $E_s = strain\ energy = \int_0^t f_S\,\dot{u}d_t$
- $E_I = relative\ input\ energy = -\int_0^t m\ddot{u}_g\,\dot{u}d_t$

$E_k$ in Eq (5.3) vanishes when the structure ceases to vibrate. $E_\xi$ is related to the inherent viscous damping of the structure and/or by any supplemental damping mechanism provided by the presence of any damping devices in the system. $E_s$ consists of two different types of energy: elastic strain energy, $E_E$, and hysteretic energy $E_H$. Elastic strain energy does not cause permanent damage to the structure. As its name indicates, it occurs as a result of elastic deformation of the structure and becomes zero when vibration of the structures stops. Hysteretic energy is related to the inelastic deformation the structure undergoes during the ground motion. Unless otherwise dissipated through some mechanism, hysteretic energy could inflict permanent damage to the structure.

The philosophy of EBSD thus primarily focuses on ensuring that structures are designed to meet the energy demand of an earthquake, i.e., the hysteretic energy. In EBSD, if the hysteretic energy demand of a structure due to an earthquake can be dissipated through a controlled inelastic deformation of the structure, the design is said to be satisfactory. Therefore, hysteretic energy is considered to be the main design parameter in energy based seismic design. Also, EBSD is believed to be a rational design approach for seismic design because it takes into account the accumulated earthquake-induced damage in the design procedure. Conversely, the viability of EBSD depends on the accuracy in developing inelastic design spectra for SDOF as well as on the ability of the equations relating input energy and hysteretic energy. Moreover, for MDOF structures, the way the hysteretic energy is distributed over the different levels of the structure is equally important to an accurate estimation of input and hysteretic energies.

In summary, EBSD attempts to ensure that the seismic energy demand is less than or at most equal to the capacity of the structure to dissipate it. The seismic energy demand is the total hysteretic energy, whereas the capacity of the structure is the allowable plastic energy of the structure. In lieu of any supplementary damping devices, the plastic energy is the amount of energy consumed in forming plastic hinges in the structure.

## *5.4 Input and hysteretic energies of SDoF systems*

### 5.4.1 Energy spectra for an inelastic SDoF system

Eq (5.3) is a statement of energy balance for an SDOF system. Alternatively, the energy balance can be expressed in terms of the total displacement of the SDOF system and in

this case the resulting input energy is called an absolute/total input energy $E_I$ and is given by Eq (5.4)

$$E_I = -\int_0^t m\ddot{u}_g \, \dot{u}_t dt \tag{5.4}$$

where $\dot{u}_t$ is the total velocity of the system; $m$ , $\ddot{u}_g$ are as defined before.

Bruneau and Wang [75] in their study on closed-form energy expression for an SDOF system subjected to rectangular and harmonic base excitations observed that there exists a close relationship between relative input energy and relative displacement. As a result, they recommended that a relative input energy formulation is preferred over an absolute formulation for assessing earthquake damage on structures. Henceforth, the relative input energy $E_I$ is used to quantify the energy content of an earthquake and is simply referred to as the input energy in this study.

Before Uang and Bertero [74] introduced the energy balance concept, a number of researchers have recommended different empirical formulae to estimate earthquake input energy. For instance, Housner [56] computed the input energy per unit mass of an SDOF system as follows

$$\frac{E_I}{m} = \frac{1}{2}(PSV)^2 \tag{5.5}$$

where *m* is mass of the structure and *PSV* is the pseudo-spectral velocity at the period of the SDOF. He was also the first to use an energy approach for seismic design. He used it in the design of an elevated water tank to resist a 1940 S00E component of El Centro accelerogram, and concluded that his equation is valid for both elastic and inelastic SDOF systems.

Akiyama [52], using Japanese design earthquakes, proposed the input energy per unit mass of an elastic SDOF structure due to a given earthquake as

$$\frac{E_I}{m} = \frac{1}{2}(V_e)^2 \tag{5.6}$$

where the value of the equivalent velocity, $V_e$ (cm/s), is given by

$$V_e = \begin{cases} 250T_n, & T_n < T_g \\ 250T_g, & T_n \geq T_g \end{cases} \tag{5.7}$$

where $T_n$ is the natural period of vibration of the structure (in second) and $T_g$ is the predominant period of the ground motion (in second). He showed that the predominant period of the ground motion is dependent on on-site soil characteristics.

Kuwamura and Galambos [63] proposed different expressions for $V_e$ in Eq (5.8) that took into account the severity and duration of an earthquake:

$$V_e = \begin{cases} \frac{1}{2}\sqrt{\frac{I_e}{T_g}T_n}, & T_n \leq T_g \\ \frac{1}{2}\sqrt{T_g I_e}, & T_n \geq T_g \end{cases} \tag{5.8}$$

where $I_e$ is the intensity of the accelerogram, computed as $I_e = \int_0^t \ddot{u_g}\, d_t$ and $t$ is the duration of the earthquake. Fajfar et al. [76] used 40 accelerograms and studied structures that fall within the constant velocity region of the response spectra. From their study, they proposed the expression given in Eq (5.9) for estimating earthquake input energy in such structures.

$$\frac{E_I}{m} = 2.2\, t_{dt}^{0.5}\, PGV^2 \tag{5.9}$$

where $t_{dt}$ is the strong motion duration as defined by Trifunac and Brady [77] and PGV is the peak ground velocity of the ground motion.

Decanini and Mollaioli [78] proposed two inelastic energy spectra, namely the input energy ($E_I$) and the hysteretic-to-input energy ratio ($E_H/E_I$). These spectra allow to evaluate the seismic demands in terms of maximum displacement and ductility. They further studied the influence of the inelastic behavior on the input energy spectra on the characteristic of the excitation, which is influenced by soil type, source-to-site distance and the seismic event magnitude.

For each soil class a characteristic period of vibration that separates the zone where the inelastic input energy is higher than the elastic one from that where the reverse occurs, is individuated. The design inelastic input energy per unit mass was derived according to the following relation:

$$E_{I\mu} = f_a A E_I \tag{5.10}$$

where $f_A$ denotes the normalized spectral ordinate and $AE_I$ represents the area under the elastic input energy spectrum in the range of periods between 0.05 and 4.0 s. This factor depends on the soil class, the source to site distance $D_f$ and the magnitude interval.

$$f_a = \frac{E_{I\mu}}{AE_I}\ [s^{-1}] \tag{5.11}$$

The design inelastic energy spectral shapes were individuated by smooth curves accounting for the fundamental trends and defined by simple mathematical relationships. The graph of the adopted inelastic spectral shape in Figure 5.1 consists of three regions characterized by the following patterns:

1. Linear variation for the highest frequencies;
2. Constant branch for the intermediate frequencies;
3. Decaying curve for the lowest frequencies, expressed an inverse function of the period.

The three regions are characterized by the following equations:

$$\begin{aligned} &T_O \le T \le T_1 && f_a = a + (p-a)(T - T_0)/(T_1 - T_0) \\ &T_1 \le T \le T_2 && f_a = p \\ &T \ge T_2 && f_a = p\left(\frac{T_2}{T}\right)^k \end{aligned} \tag{5.12}$$

Where $a$ represents the normalized specral ordinate correspoiding to the period $T_0$; $p$ is the maximum spectral value relative to the constant part of the spectrum; $T_1$ is the period corresponding to the beginning of the constant zone of the spectrum, $T_2$ is the period denoting the onset of the decaying branch; $k$ is a parameter governing the velocity of the decay.

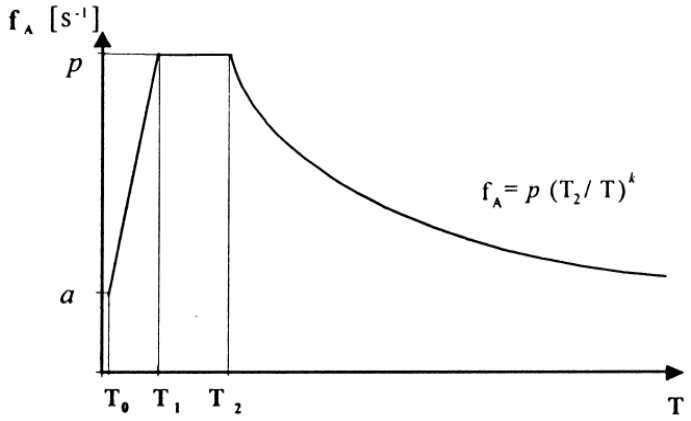


*Figure 5.1:Inelastic design input energy spectral shape*

### 5.4.2 Evaluation of hysteretic energy for SDoF systems

Housner [56] defined the input energy that contributes to the damage of a structure as the total seismic input energy $E_I$ less the energy dissipated through inherent damping, $E_\xi$. According to his definition, the damage energy, $E_D$ , can be written as

$$E_D = E_I - E_\xi \tag{5.13}$$

Theoretically, per Housner's [56] definition, the damage energy is the sum of the absorbed and kinetic energy. However, at the end of ground motion duration, the kinetic energy becomes small; consequently, the absorbed energy $E_a$, can be assumed to be approximately equal to the damage energy $E_D$. The expressions for the input energy $E_I$ and damage energy $E_D$, normalized by mass $m$ and expressed in terms of equivalent velocities are given as follows:

$$V_E = \sqrt{\frac{2E_i}{m}} \tag{5.14}$$

$$V_D = \sqrt{\frac{2E_D}{m}}$$

Akiyama [52], based on analyses of SDOF systems with elastic-perfectly plastic restoring force characteristics, proposed the following relationship between normalized input and damage energies as

$$\frac{V_D}{V_E} = \frac{1}{1+3\xi+1.2\sqrt{\xi}} \tag{5.15}$$

where $\xi$ is the damping ratio.

Fajfar and Vidic [76] did a parametric study on nonlinear elasto-plastic SDOF systems subjected to five different ground motions from different countries and proposed the following expression for systems with 5% damping.

$$\frac{V_D}{V_E} = \sqrt{\frac{0.9(\mu-1)^{0.95}}{\mu}} \qquad (5.16)$$

For a structure with damping ratio $\xi = 0.05$ , Manfredi [65] recommended the following expression be used to estimate hysteretic energy $E_H$, per unit mass

$$\frac{E_H}{m} = \frac{\mu_c - 1}{[1+1.5(\mu_c-1)^{0.8}]^2}\left(1 + 0.23 I_d \sqrt{\mu - 1}\right)\left(\frac{S_a}{\omega}\right)^2 \qquad (5.17)$$

He further suggested that for damping $\xi = 0.05$, the input energy and hysteretic energy can be related by

$$E_H = 0.72\frac{\mu_c - 1}{\mu_c} E_I \qquad (5.18)$$

Decanini and Mollaioli [78] provide a relationship between design input energy $E_I$ and hysteretic energy $E_H$ as given in Figure 5.2.

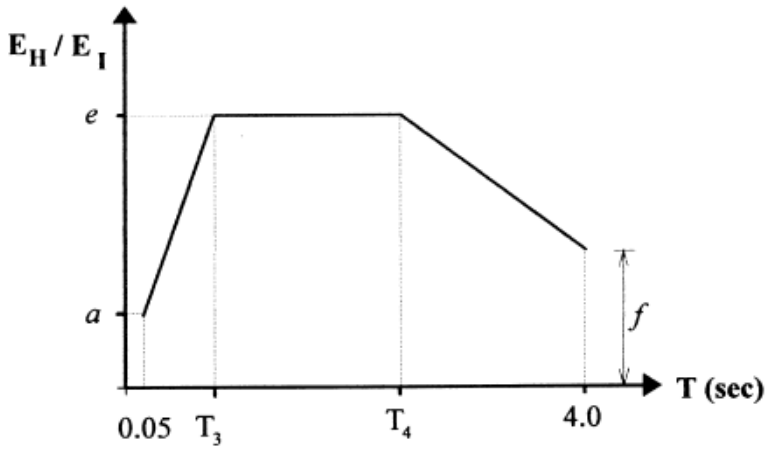


*Figure 5.2: Design spectral shape of $E_H/E_I$*

The period $T_4$ , corresponding to the end of the constant branch, shifts toward the low frequencies as ductility and soil stiffness decrease. The constant value of $E_H/E_I$ between $T_3$ and $T_4$ depends strongly on ductility, and to a small extent on the soil class. It can be shown that this value, indicated with $e$ , can be approximated by the following expression:

$$e = \frac{E_H}{E_I} = K_S \frac{\mu - 1}{\mu} \qquad (5.19)$$

where $K_s$ is a coefficient depending on the soil type, and assuming the values 0.75, 0.80, 0.90, respectively for soils $S_1$ , $S_2$ and $S_3$.

### 5.4.3 Hysteretic energy distribution

Using a statistical approach Shen and Akbas [79] investigated the hysteretic energy ( $E_H$ ) distribution over the height of a building and were not able to identify any consistent pattern. However, Akbas *et al* [80] from their study of regular frames with a damping ratio of ζ=0.02 concluded that hysteretic energy distribution along the height is linear. Ye *et al.* [81] counter argued that hysteretic energy distribution can be considered linear only for damping ratio ζ > 0.1 and proposed the linear equations shown in Eq (5.20) to distribute the $E_H$ over the building height for structures with damping ratio ζ > 0.1. It is imperative to note that such high damping could only be attained if supplementary damping devices are installed in the structure.

$$\frac{E_{H,i}}{E_H} = \begin{cases} \frac{2(N+1-i)}{N(N+1)}, & for\ N < 5 \\ \frac{2(N-i)}{N(N-1)}, & for\ N \geq 5 \end{cases} \tag{5.20}$$

where *N* is the total number of stories; *i* is the story of interest; $E_H$ and $E_{H,i}$ are the total and story *i* hysteretic energies, respectively.

Ye *et al*. [81] established a relationship between the peak story responses and plastic deformation energy $PE_i$ obtained from a pushover analysis. They proposed that the peak story responses and the corresponding story plastic deformation energy can be related by Eq (5.21). They further pointed out that there is a direct relationship between $E_H$ distribution and *PE* in MDOF systems and proposed an expression for $E_H$ distribution in MDOF systems as shown in Eq (5.22)

$$PE_i = (1-\alpha_i)(\mu_i - 1)F_{y,i}d_{y,i} \tag{5.21}$$

$$\frac{E_{H,i}}{\sum_{i=1}^{N} E_{H,i}} = \frac{PE_i}{\sum_{i=1}^{N} PE_i} \tag{5.22}$$

## *5.5 Optimum strength distribution concept*

Akiyama [52] suggested that buildings with medium height can be represented by shear struts. Shear deformations in a shear strut is demonstrated in Figure 5.3, where height at an arbitrary point is expressed by x and horizontal displacement is expressed by y. The shear force, Q, and the slope of deflection, $\frac{\partial y}{\partial x}$, are related by:

$$Q = G\ \frac{\partial y}{\partial x} \tag{5.23}$$

where G is the shear modulus

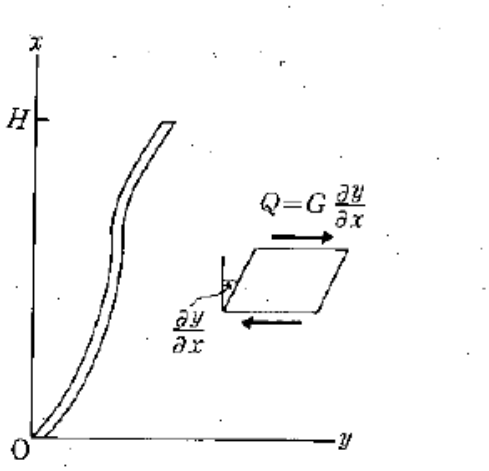


*Figure 5.3: Deformation in shear strut*

The vibrational equation for undamped elastic systems subjected to ground motion, $z_o$, is written:

$$m\frac{\partial^2 y}{\partial t^2} - \frac{\partial}{\partial x}\left(G\frac{\partial y}{\partial x}\right) = -m\frac{\partial^2 z_0}{\partial t^2} \quad (5.24)$$

The vibrational Eq (5.24) for a shear strut is solved and the shear force expression along the height of the strut is obtained:

$$Q_{j(x)} = \int_x^H mA_{(x)}\, d_x \quad (5.25)$$

where $A_{(x)}$ is the maximum absolute acceleration, $Q_{j(x)}$ is the shear force of the strut at $j^{\text{th}}$ mode, and $Q_{j(x)}$ is expressed in terms of a shear coefficient $\hat{\alpha}_{(x)}$ as:

$$\hat{\alpha}_{(x)} = \frac{Q_{(x)}}{g\int_x^H m d_x} \quad (5.26)$$

Setting $x = 0$, the shear force coefficient $\hat{\alpha}_{(0)}$ at the base is obtained.

The ratio $\bar{\alpha}_{(x)} = \frac{\hat{\alpha}_{(x)}}{\hat{\alpha}_{(0)}}$ is called the shear coefficient ratio.

Akiyama [52] further provides another expression to approximate the ratio $\bar{\alpha}_{(x)}$ with an exponential equation:

$$\bar{\alpha}_i = \exp\left[\left(1 - 0.02\frac{k_{f,1}}{k_{f,N}} - 0.16\frac{T_1}{T_G}\right)\bar{x} - \left(0.5 - 0.05\frac{k_{f,1}}{k_{f,N}} - 0.3\frac{T_1}{T_G}\right)\bar{x}^2\right] \quad (5.27)$$

where $k_{f,1}$ is the stiffness of the 1st story, $k_{f,N}$ is the stiffness of the $N^{\text{th}}$ story, $T_1$ is the fundamental period, $T_G$ is the predominant period, $\bar{x} = \frac{i-1}{N}$ and N is the story number.

–

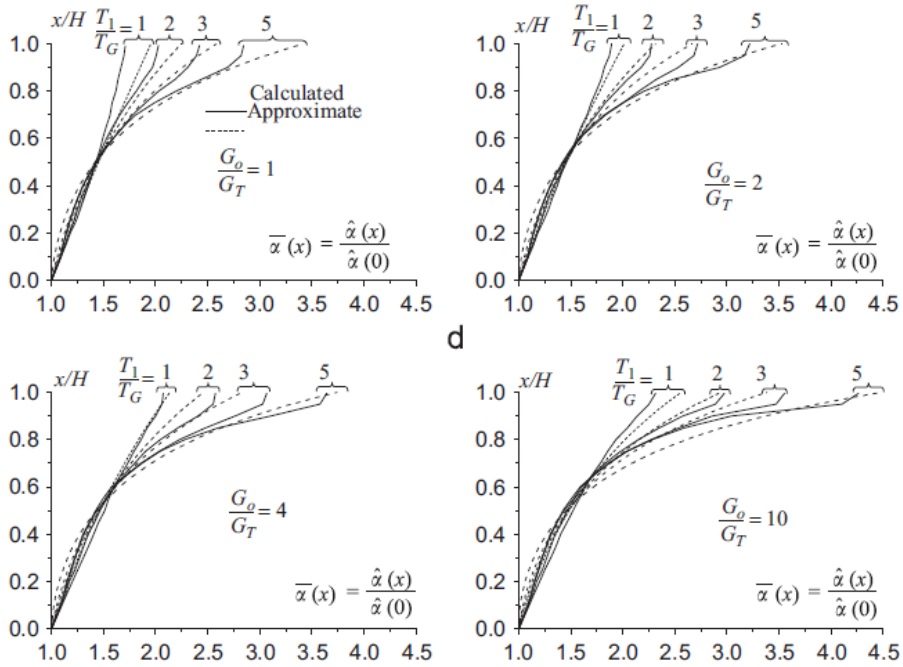


*Figure 5.4: Plot of actual and approximated shear force coefficient ratio $\bar{\alpha}_i$*

Eq (5.26) and (5.27) are plotted in Figure 5.4. It can be observed that the approximated ratio estimates the real ratio of shear coefficient to a good extent.

This strength profile allows one to design the story strength at the base and obtain the strength of the stories above as a function of the shear strength of story 1.

According to Akiyama [52] the optimum strength distribution is achieved when the shear coefficient ratio given by Eq (5.27) is satisfied.

Maintaining the optimum strength distribution avoids the damage concentration to occur at a story. The damage concentration occurs when the elastic vibrational energy is sufficiently small, the total input energy concentrates in the weakest story. Such energy concentration into one story of multi-story frames is responsible for forming the soft story mechanism, thus resulting in the collapse of the multi-story structure.

The methodology for the design of Energy Dissipative Braces (EDBs) proposed in this study is grounded on the concept of optimum strength distribution.

## *5.6 Proposed procedure for the design of energy dissipative braces (EDBs)*

In the previous section some important concepts such as inelastic input energy $E_I$, demand hysteretic energy $E_H$, energy distribution in a multi-story frame and optimum strength distribution concept were explained. Understanding of all these concepts are essential for the proposed procedure.

The proposed procedure's formulation is based on the energy-balance equation and further exploits the optimum strength distribution profile for the design of hysteretic energy dissipative braces.

The procedure is explained in a stepwise manner by starting from the energy balance equation. Thus Eq (5.3) is rewritten:

$$E_I = E_k + E_\xi + E_s + E_H \tag{5.28}$$

where $E_I$ is the total input energy, $E_k$ is the kinetic energy, $E_s$ is the recoverable elastic strain energy and $E_H$ is the irrecoverable hysteretic energy.

$E_H$ is associated to the damage of the structure and Housner [56] termed it as "damaging energy". Since poorly designed existing buildings are not capable to dissipate the plastic strain energy, in order to survive the design earthquake must be equipped with supplemental energy dissipative devices. Energy Dissipative Braces (EDBs) are mainly designed to dissipate the demand hysteretic energy, while the existing structure is intended to remain elastic and to dissipate the elastic vibrational energy ($E_k + E_s$). Figure 5.5 shows the schematic of a structure equipped with EDBs.

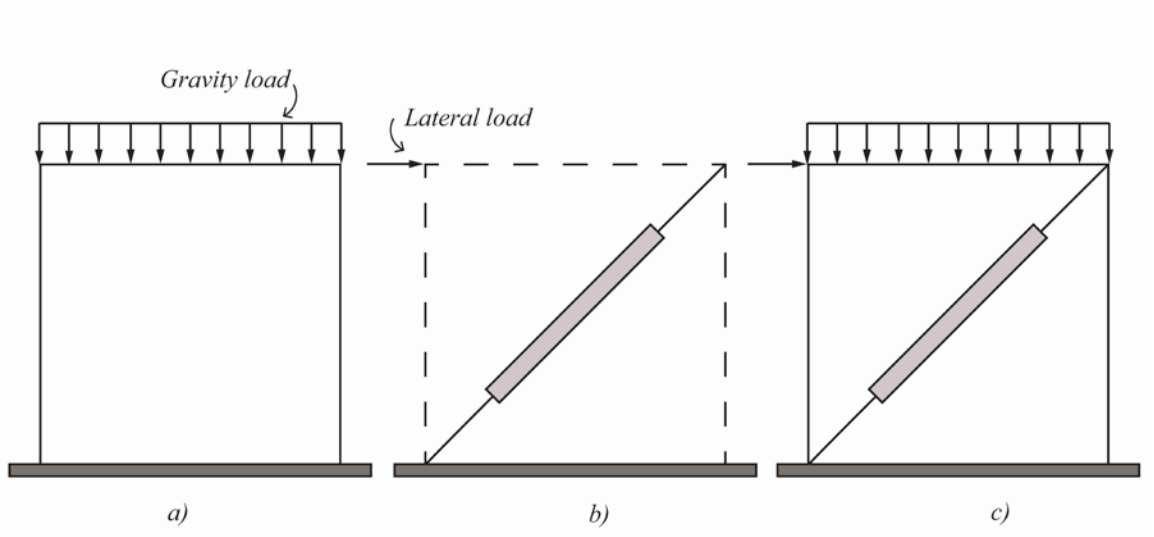


*Figure 5.5: Schematic of a frame equipped with EDBs*

For the structure to survive an earthquake, the demand hysteretic energy accumulated at a particular storey $E_{H_i}$ must be smaller than the energy dissipation capacity of the EDBs $W_{P_i}$ in that storey.

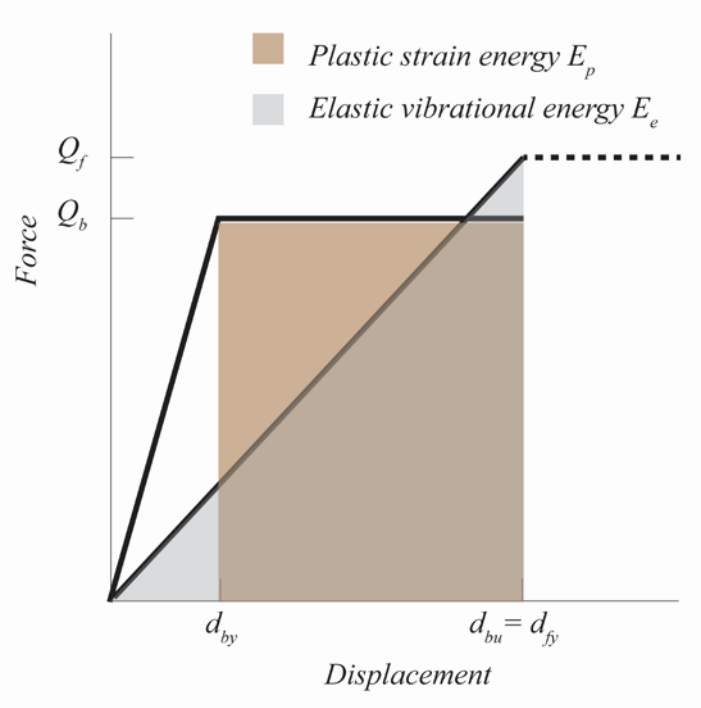


*Figure 5.6: Plastic strain energy dissipation capacity of EDBs $W_P$ and Elastic Vibrational Energy dissipation capacity $W_e$ of the existing structure*

The strain energy $E_s$ is made of two parts; recoverable elastic strain energy $E_{se}$ and irrecoverable plastic strain energy $E_p$, so that the Eq (5.28) is rewritten:

$$E_e + E_p = E_D \tag{5.29}$$

- $E_e = E_{Se} + E_k$
- $E_p = E_S - E_{se}$
- $E_D = E_I - E_\xi$

The objective is to keep the existing structure elastic that dissipates the elastic vibrational energy $E_e$ while designing the EDBs to dissipate the demand hysteretic energy $E_H$.

For the structure to dissipate the demand hysteretic energy imparted by the earthquake, it should be always maintained that:

$$Energy\ Dissipation\ Capacity\ of\ EDBs\ (E_p) \geq Demand\ Hysteretic\ Energy\ E_H$$

Considering Figure 5.6, the left side of the equation is obtained as simply the rectangular area:

$$E_P = n_{eq} Q_{b,y} (d_{b,y} - d_{f,y}) \tag{5.30}$$

The number of equivalent plastic cycles $n_{eq}$ is a very fundamental parameter, which keeps the near fault and far-field earthquake effects into account. Manfredi et al. [66] define it as the number of plastic cycles at the maximum value of plastic excursion that

the structure must develop in order to dissipate the total amount of hysteretic energy $E_H$ and proposed the following equation for obtaining $n_{eq}$.

$$n_{eq} = 1 + c_1 I_d \sqrt{\frac{T_{NH}}{T_1}} (R-1)^{c_2} \quad (5.31)$$

- $I_d$ *Manfredi's index*
- $T_{NH}$ *initial period of medium period region in the Newmark and Hall spectral representation [67]*
- $T_1$ *Fundamental period of the structure*
- $c_1$ *and* $c_2$ *Coefficients to take into account the near field and far-field effects*
- *R -Strength reduction factor*

Initially choosing a certain amount of ductility ($\mu$) for the EDBs and equating the demand $E_H$ with the capacity $E_P$ the required strength of the EDBs is obtained:

$$Q_b = \frac{E_H}{n_{eq}(d_{b,y} - d_{f,y})} \quad (5.32)$$

Since the objective is to get the design strength of the story at the base, the Eq (5.32) is specialized for story 1, thus:

$$Q_{b,1} = \frac{E_{H,1}}{n_{eq}(d_{s,y,1} - d_{f,y,1})} \quad (5.33)$$

In the previous section it was explained that $\bar{\alpha}_i$ is the ratio between the shear coefficient at $i^{th}$ story $\alpha_i$ and the shear coefficient at $1^{st}$story $\alpha_1$, which can be also simplified as:

$$\bar{\alpha}_i = \frac{\alpha_i}{\alpha_1} = \frac{Q_{bi}}{Q_{b1}} \Gamma_i \quad (5.34)$$

- $\bar{\alpha}_i$ *; Shear force coefficient ratio*
- $\alpha_i = \frac{Q_{syi}}{\sum_{k=i}^{n} m_k g}$ *; shear force coefficient at* $i^{th}$ *story*
- $\alpha_1 = \frac{Q_{sy1}}{\sum_{k=1}^{n} m_k g}$*; shear force coefficient at story 1*
- $\Gamma_i = \frac{\sum_{k=1}^{n} m_k g}{\sum_{k=i}^{n} m_k g}$

Now, using the shear strength ratio $\bar{\alpha}_i$ estimated by Eq (5.27), the shear strength at $i^{th}$ story $Q_{b,i}$ is obtained:

$$Q_{b,i} = Q_{s,y,1} \frac{\bar{\alpha}_i}{\Gamma_i} \quad (5.35)$$

The shear strength determined in Eq (5.35) is the required strength at the $i^{th}$ story to balance the energy dissipated and the demand hysteretic energy at that story.

Since the ductility at all stories is kept equal ($\mu_i = \mu$), the stiffness of the bracing system at $i^{th}$story can be obtained as following:

$$k_{s,i} = \frac{Q_{b,i}}{d_{b,y,i}} \quad (5.36)$$

- $d_{b,y,i} = \frac{\Delta_{max,i}}{\mu}$
- $\Delta_{max,i}$ *: the maximum displacement of story* $i$

$\Delta_{max,i}$ is obtained as the minimum between the yield displacement of existing structure $d_{fy,i}$ and the allowable interstorey drift $\Delta_{allowable,i}$ of the story $i$

$$\Delta_{max,i} = min\left(\Delta_{allowable,i}\ ,\ \delta_{yi}\right) \quad (5.37)$$

The yield story displacement $\delta_{yi}$ is determined through understanding the moment-curvature relationship of the vertical members and their force-displacement curve. It can be done using various software that use fiber sections, which can be time consuming. In this study, for obtaining moment-curvature curves of column sections, closed-form equations proposed by Monti [82] are scripted in MatLab and the capacity of individual columns in terms of force-displacement are obtained. Since the column section in a story are parallel elements, their capacity summation provides the capacity of the story, hence the yield displacement of the individual story $\delta_{yi}$ is known.

The procedure is iterative, initially a certain value of ductility is assumed for the dissipative devices and the design procedure is followed, the demand hysteretic energy is iterated since the fundamental period $T_1$ will change with the insertion of the braces, thus the demand hysteretic energy needs to be updated at each iteration until the following condition meets:

$$E_H^i - E_H^{i-1} \leq tolerance$$

- $i$ *- is the number of iterations*
- *The tolerance can be assumed as <5 percent.*

The design of the braces is accepted when the desired drifts are achieved:

$$d_i \leq \Delta_{max,i} \quad (5.38)$$

In case Eq (5.38) is not satisfied, this is due to the smaller value of ductility which limits the hysteretic energy dissipation capacity of the braces, thus the design procedure is repeated with higher values of $\mu$.

The flow chart below summarizes the overall design steps of the proposed procedure:

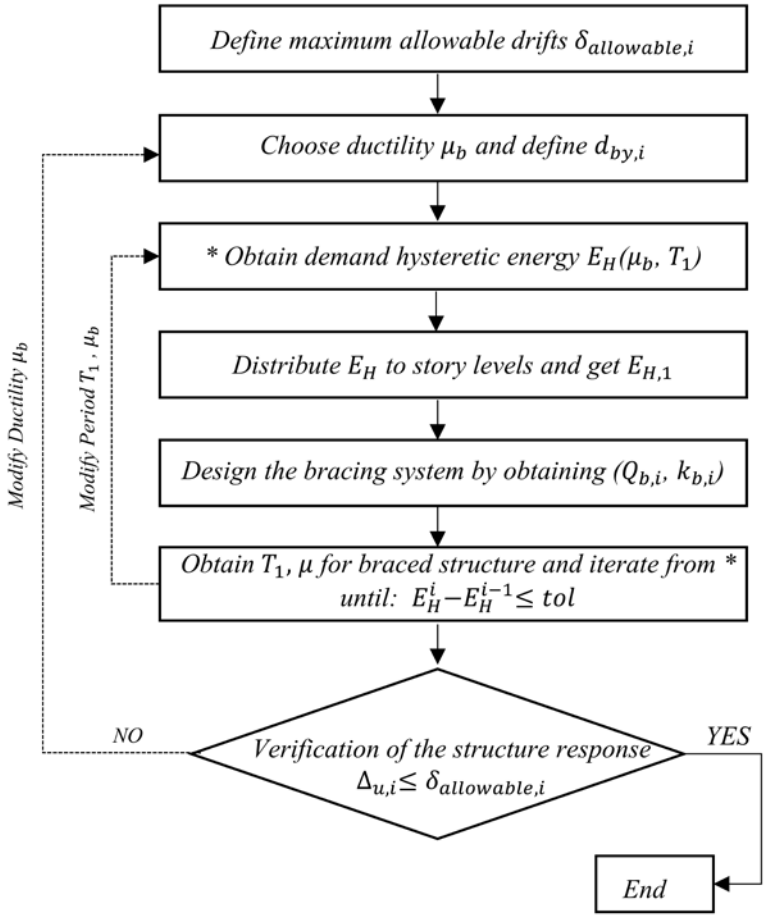
Define maximum allowable drifts $\delta_{allowable,i}$
Choose ductility $\mu_b$ and define $d_{by,i}$
* Obtain demand hysteretic energy $E_H(\mu_b, T_1)$
Distribute $E_H$ to story levels and get $E_{H,1}$
Design the bracing system by obtaining ($Q_{b,i}$, $k_{b,i}$)
Obtain $T_1$, $\mu$ for braced structure and iterate from * until: $E_H^i - E_H^{i-1} \leq tol$
Verification of the structure response $\Delta_{u,i} \leq \delta_{allowable,i}$
NO
YES
Modify Ductility $\mu_b$
Modify Period $T_1$ , $\mu_b$
End

# CHAPTER 6

# APPLICATION OF SELECTED PROCEDURES FOR THE DESIGN OF EDBs AND COMPARISON WITH THE PROPOSED METHODOLOGY

# 6 Application of selected procedures for the design of EDBs and comparison with the proposed methodology

## *6.1 Introduction*

In this application section, two methods selected from the literature are presented and applied for comparison with the proposed method:

1. *A displacement-based design procedure for the EDBs by Ponzo-Di Cesare [83]*
2. *An energy-based design method for the EDBs by Benavent Climent [84]*

The objective of this study is to highlight pros and cons of these procedures and compare their outcomes with that obtained with the energy-based method proposed in Chapter 5.

In this Chapter, the efficiency of the proposed method is assessed and compared with the selected methods by applying them on three 2D frames. The results obtained from the non-linear static and non-linear dynamic analysis are presented and discussed.

It is worth mentioning that the formulation of the selected design methodologies and of the proposed method are all scripted in MatLab, attached in the appendix.

## *6.2 Case studies*

### 6.2.1 Description of the frames

Three reinforced concrete frames of 3, 5, and 9 stories have been analyzed. The bay length of each frame is 5.5 m and the height of all stories is 3 m, as shown in Figure 6.1. The inherent modal damping ratios are assumed to be 5% of the critical damping for linear static analysis, while for non-linear dynamic analysis Rayleigh's damping is used.

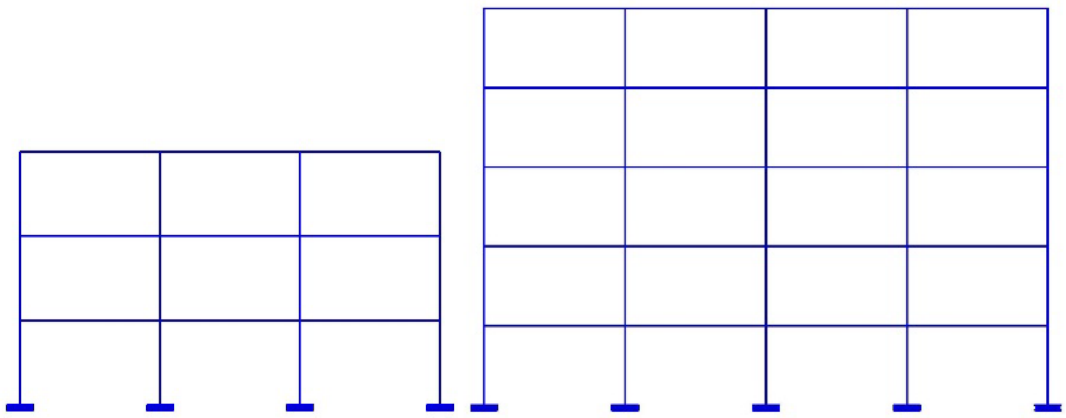

*a)* *b)*

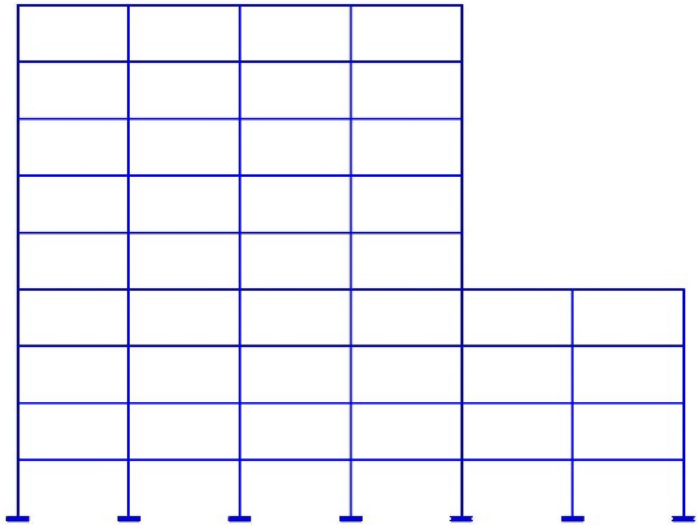

c)

*Figure 6.1: a) Case1: 3 bay 3 story frame; b) Case 2: 4 bay 5 story frame c) Case 3: 6 bay 9 story frame*

### 6.2.2 Structural modelling

The main structural elements of the frames are beams, columns, beam-column joints and the energy dissipative braces. The structural elements are modelled through interconnected frame elements with either lumped or distributed nonlinearities. At the element level, the material nonlinearities of beam-column members are modelled from lumped plasticity formulations to distributed plasticity formulations, as illustrated in Figure 6.2:

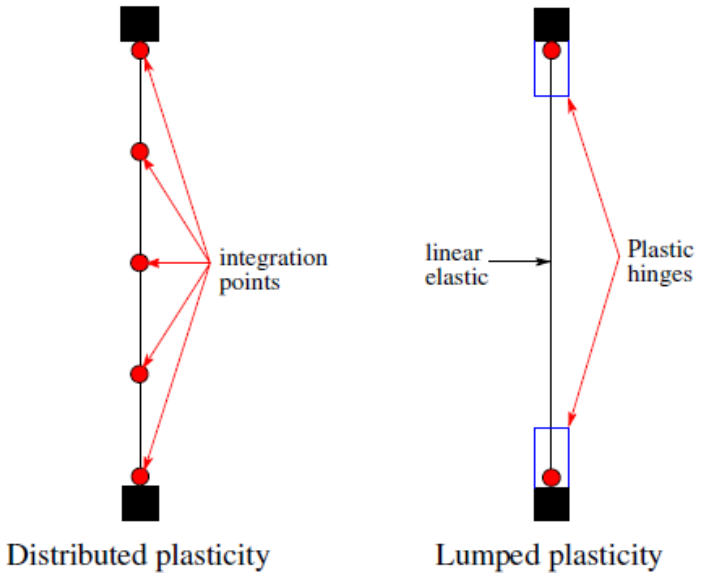


*Figure 6.2: Lumped and distributed plasticity*

In the lumped plasticity models, it is assumed that nonlinear behavior of the beam column members is concentrated at the ends or at pre-determined sections. It assumes

that the nonlinear behavior is located at the center of the plastic hinge zone, generally located at each end of the element.

The concrete uniaxial material model is based on the constitutive relationship proposed by Mander, *et al* [85]. Lateral transverse reinforcement confinement effect was incorporated as per [86]. Under uniaxial compression, the concrete strain corresponding to the point of unconfined peak stress was considered 0.002. For the concrete model, the tensile stress capacity was assigned as 0. The Poisson's ratio ($\nu_c$) of concrete under uniaxial compressive stress was assumed to be 0.2. The modulus of elasticity of concrete ($E_c$) was calculated using the empirical formula $E_c = 5000\sqrt{f_{ck}}$ , where $f_{ck}$ is the concrete compressive strength at 28 days. The specific weight of the concrete material ($\gamma_c$) was assumed as $24\frac{KN}{m^3}$.

Frame members were modeled with linear elastic elements, while inelastic deformations were concentrated at plastic hinge regions at member ends. The columns were fixed at the base, and the beam-column joints were considered infinitely rigid. Factors of 0.4 and 0.68 were applied to the moment of inertia of the beams and columns, respectively, to simulate cracked concrete properties, as per Eurocode-8 [34]. The following modelling features had to be implemented in the analysis as precisely as possible for improved accuracy of results:

- *Sectional moment-curvature and member moment-rotation or force-deformation relationships.*
- *Lengths of plastic hinge regions at member ends.*
- *Locations of link hinges with zero link length within each plastic hinge region at member ends,*
- *A hysteretic model that could trace the load reversal paths within each hysteresis loop.*
- *Sectional capacities of frame members were determined using computer software Response2000 [ ].*

Plastic hinge lengths for frame members $l_p$ were calculated according to Paulay and Priestley [87] as given by Eq (6.1):

$$l_p = 0.08L + 0.022d_b f_y \quad (6.1)$$

where $L$ is the member length between the critical section and the point of contraflexure (shear span), $d_b$ is the diameter of the longitudinal reinforcement in m, $f_y$ is the yield strength of reinforcement in MPa. The point of contra-flexure was assumed to occur at mid-length of clear span. The plastic hinges were defined at both ends of linear elastic frame elements.

The EDBs are modeled using link element in SAP2000 and a BRB hysteretic model is assigned for the nonlinear time history analysis as shown in Figure 6.3. The characteristics such as strength, stiffness and ductility of the EDBs were obtained using the aforementioned methodologies from the literature and the proposed methodology

explained in Chapter 5. The comparison of post-retrofitting response is done by carrying out pushover and non-linear time history analysis.

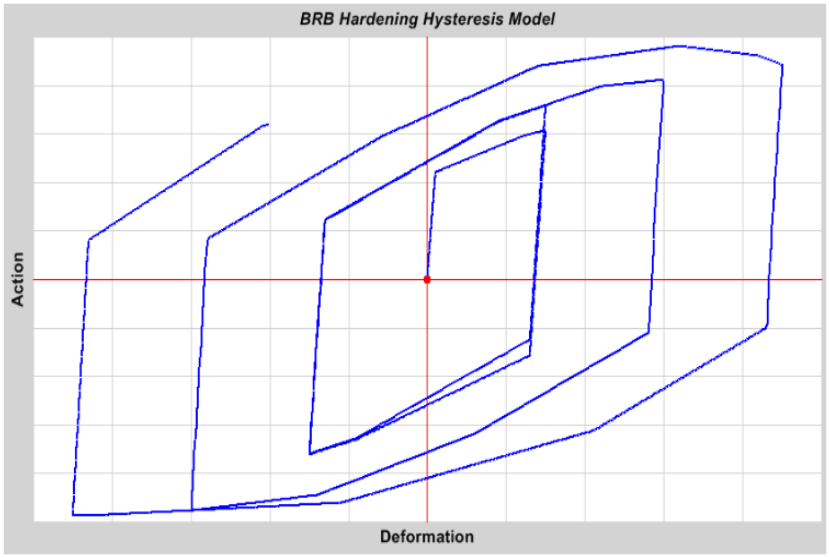


*Figure 6.3: BRB hysteresis model available in SAP2000 library*

### 6.2.3 Structural analysis

The structural response in the form of demand and capacity are evaluated through the static analysis such that the strength and deformation can be attained at various limit states, i.e. elastic, yielding, ultimate, and collapse states. If the damping and inertial effects are assumed as negligible, the static analysis is also considered as a special form of dynamic analysis. The material inelasticity and geometrical nonlinearity were considered in this method. Therefore, in earthquake engineering, the static analysis is one of the most common methods used for the seismic design.

In order to assess and retrofit the frames using the approaches selected in this study, besides the dynamic analysis, also linear static and non-linear static analysis (pushover) were used, whose main features are recalled in the following sections.

### 6.2.4 Equivalent static analysis

The seismic performance assessment of the RC structures can be investigated through a simplest analysis tool known as the equivalent static analysis, also referred as equivalent lateral force method (EFL). This method considered the material behave as linear elastic, i.e. material follows Hooks law, and geometrical nonlinearity which considers the second order (P-Δ) effects [88]. In this method, the inertial forces assumed to act during earthquakes are converted to equivalent lateral loads and these equivalent forces along with the gravity loads are applied at the nodes of the frame throughout the

height of the structures. In this method, generally two types of loads pattern, i.e. inverted triangular and parabolic load patterns were subjected, depending upon the fundamental period and vibration modes of the structures. The predetermined mode shapes are identified with the help of which the magnitudes of lateral forces in each storey are computed. Elnashai and Di Sarno (2008) [88] concluded that the first vibration mode is the dominant in the entire structures, and triangular load pattern considered in the equivalent static analysis for the estimation of the horizontal forces are approximately good and precise.

The steps performed for the equivalent static analysis as mentioned in [88] are as follows:

1. *Assume a lateral load pattern distribution.*
2. *Apply the gravity and horizontal loads.*
3. *Evaluate displacements and hence internal forces.*
4. *If scaled forces are used, the ensuing displacements also require scaling.*

The Equivalent lateral force method is used during the application of design methodology proposed by Ponzo-Di Cesare [37]. It is used in order to obtain drifts, strength and stiffness of the existing structure. The procedure by Ponzo-Di Cesare is explained in detail in Chapter 3.

### 6.2.5 Non-linear Static (pushover) analysis

The estimation of the strength and deformation demands in the structures before and after the insertion of the braces is evaluated through a pushover analysis and these demands are compared with the pre and post intervention capacity of the frames to identify the various performance levels of the structures. The performance assessment can be done through building response parameters, such as roof displacement, global drift, inter-storey drift, deformation in the structural and non-structural elements, and element and connection forces. It is observed from various literatures that some of the parameters, such as estimation of inter-storey drift and its distribution throughout the height, force and displacement demands on brittle and ductile members, identification of likely failure modes, global structural behavior due to effect of individual member strength deterioration, and so on, can be effectively attained, as opposed to elastic static and dynamic analyses.

The structural response evaluated from pushover analysis is generated assuming the system as the equivalent single degree of freedom (SDOF) and it is found that if single mode actually controls the response, then it remains constant in the time history as well.

The conventional pushover analysis consists of a constant lateral force or displacement pattern type to the structures under constant gravity loads. The material inelasticity and geometrical nonlinearity is considered in this method. The pushover analysis estimates the capacity of the structures in which certain functions acts to represent the inertial force due to earthquake ground motions. This method assumes the structures as in a

static equilibrium and incremental iterative solutions are introduced. The iteration proceeds until the program fails to converge when the state can be assumed to have reached the target displacement. The capacity curve is the plot of the global base shear $V_{base}$ plotted along the ordinate versus roof displacements, $\delta_{top}$ or global drift along the abscissa, representing the variation of the base shear capacity for corresponding roof displacements. Elnashai and Di Sarno [88] defined certain steps to carry out the conventional pushover analysis which are as follows.

1. *Apply the gravity loads in a single step.*
2. *Assume a lateral load pattern either in terms of displacement shape $\Phi$ or force vector $V$.*
3. *Select a controlling displacement node, e.g. the roof centre of mass for buildings.*
4. *Determine the vertical distribution of lateral forces $V_i = m_i \Phi_i$ if the displacement vector $\Phi$ has been selected in 2. Conversely, determine the vertical displacement distribution $\Phi_i$.*
5. *Compute the incremental - iterative solution of the static equilibrium equations. This step is repeated until the target performance level, e.g. the target displacement of the roof center of mass, is reached. The target displacement is intended to represent the maximum displacement likely to be experienced during the expected earthquake ground motion.*
6. *For structures that are not symmetric about a plan perpendicular to the applied loads, the lateral load or displacement pattern should be applied in both positive and negative directions.*
7. *Determine the base shear V base, top displacement $\delta$ top, the story shear $V_i$ and storey drift $\delta_i$*
8. *Plot the system ($V_{base}$ versus $\delta$ top) and the storey ($V_i$ versus $\delta_i$ / $h_i$) pushover curves.*

The frames are modeled in commercial FEM software SAP2000 2019. For conducting pushover analysis, a modal shape load profile was adopted and concentrated hinges as per the ASCE standards [89] definitions were assigned to the sections in both extremities. The ultimate rotational capacity of the plastic hinges is expressed as a function of reinforcement in the sections and the axial force capacity of the elements. The flexural stiffness of the sections is reduced by 50% in order to take into account the reduction of stiffness due to cracks in brittle materials as proposed by NTC-08 [40].

### 6.2.6 Seismic action

The intensity of the seismic actions is related to the basic seismic hazard of the site. Three parameters which define the seismic risk for a particular site are: peak ground acceleration $a_g$, amplification factor ($F_o$) and the period of the beginning of constant velocity portion of the spectra ($T_C^*$). The values of the mentioned parameters for the site of the building in our study is reported in Table 6.1 as a function of the mean return period $T_R$, determined as function of the nominal life $V_N$ of the structure and of its class

of use. The seismic response is further modified based on the soil type and the local topography: in our case the building sits on Type C soil and the site topography class is $T_1$ (flat surface). The response spectra for these parameters are then obtained for the site of the building corresponding to different limit states, as reported in Table 6.1 and plotted in

Figure 6.4.

| Limit State | $T_R$ (Years) | $a_g/g$ | $F_o$ | $T_{c^*}$ (sec) |
|---|---|---|---|---|
| SLO | 45 | 0.098 | 2.339 | 0.281 |
| SLD | 75 | 0.124 | 2.312 | 0.292 |
| SLV | 712 | 0.298 | 2.386 | 0.356 |

*Table 6.1: Seismic hazard parameters according to NTC2018*

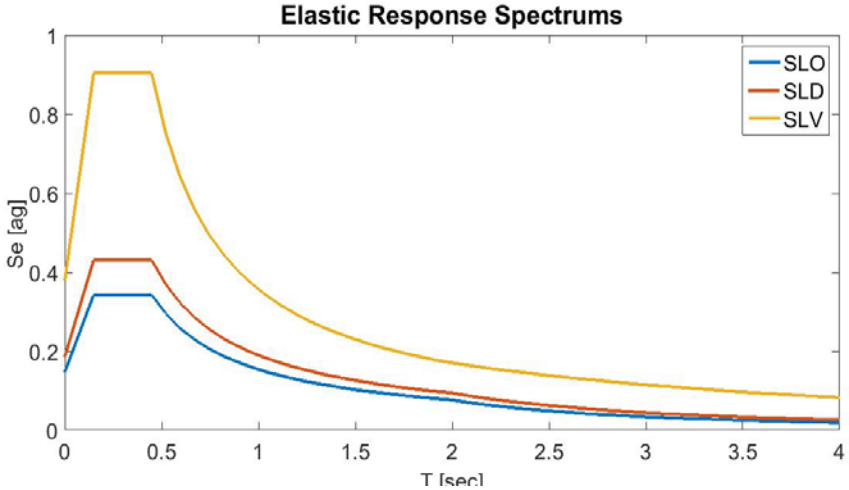


*Figure 6.4:Elastic response spectra for L'Aquila*

## *6.3 Pre- and post-intervention performance assessment and comparison of results*

The performance of unbraced frames is assessed through pushover analysis explained in section 6.2. The capacity curves are plotted in Figure 6.5. The first mode load profile is used in the pushover analysis. The frame sections were assigned concentrated plasticity according to ASCE [89].

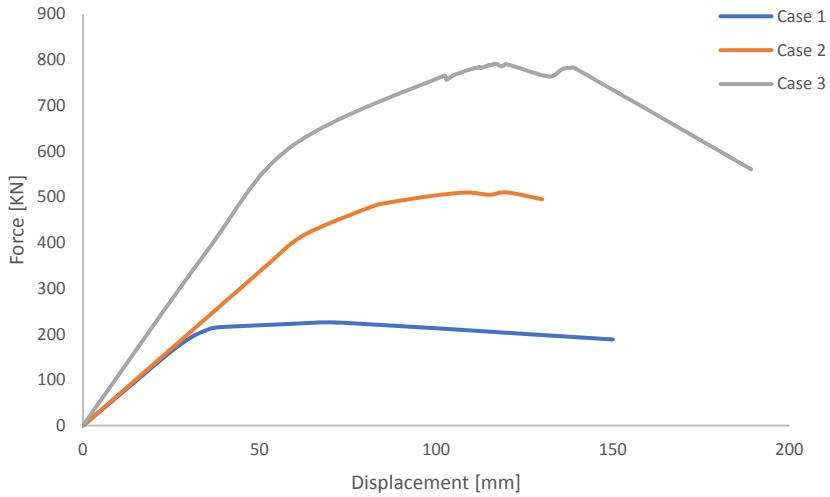


*Figure 6.5: Capacity curves of three cases (pre intervention)*

From the deformed shape of the case study frames after pushover analysis in Figure 6.6, it can be seen that the soft story mechanism is formed at the base for case 1, while in case 2 the damage is to somewhat distributed, but the story is ultimately failed. In case 3 which is irregular in height a soft story mechanism is formed at the mid height. This is expected since the design of the frame sections are not corresponding to the new seismic codes and lacks the required detailing, some deficiencies are the lack of stirrups in columns, strong beams and weak columns, no stirrups at the joints, etc.

The cases were deliberately chosen in a way that they exhibit three different failure modes:

1. *Frame in case 1 fails due to a soft story formation at the base*
2. *Frame in case 2 shows a relatively distributed failure but most of the damage occurs at the base*
3. *In case 3, due to the vertical irregularity, failure occurs at the mid-height*

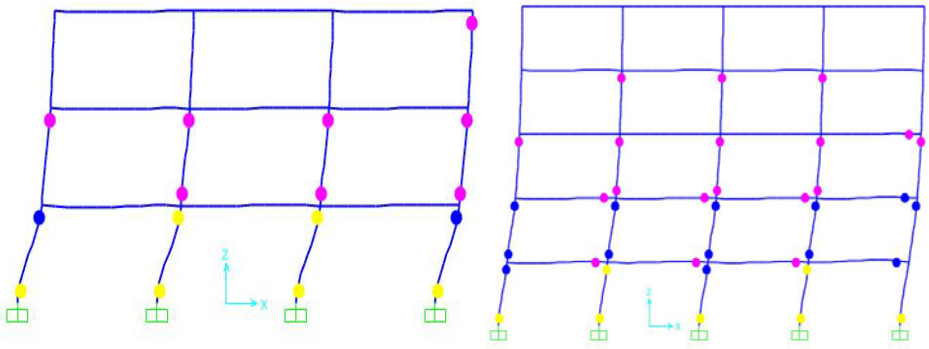

*a)* *b)*

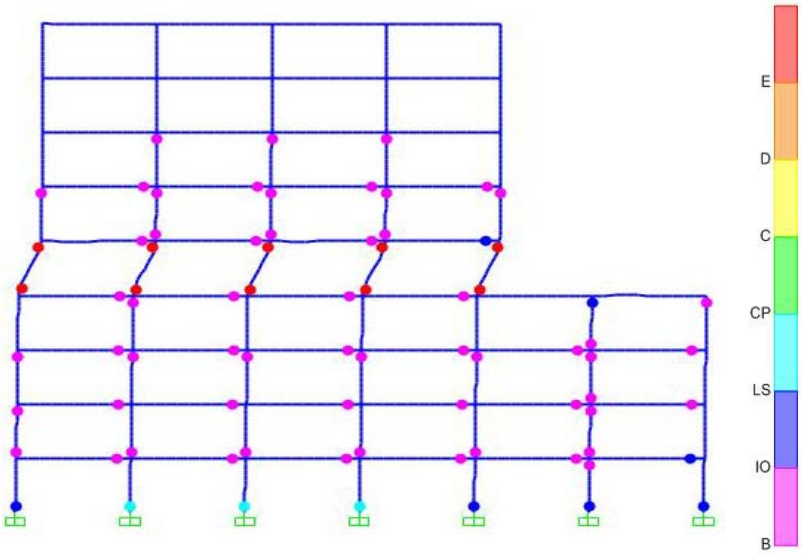


c)

*Figure 6.6: Deformed shape of case study frame; a) Case 1; b) Case 2; c) Case 3*

The target top displacement $d_{t^*}$ is chosen as the minimum of the sum of the allowable interstorey drifts $\Delta_i$ and the sum of the yield displacement of stories $\delta_{yi}$ .

$$d_{t^*} = \min\left(\sum_{i=1}^{n} \Delta_i \ , \sum_{i=1}^{n} \delta_{yi}\right) \qquad (6.2)$$

For these case studies, the allowable inter-story drift is taken to be 1% of the story height, which corresponds to the life safety limit states.

Since the damage is not distributed among the stories and it is concentrated at particular stories, this highlights the need for intervention in order to have a more uniform distribution of drifts that satisfy the seismic code requirements. Thus, the EDBs are designed with various methodologies and the response of the retrofitted frames is assessed through both non-linear static and non-linear dynamic analysis.

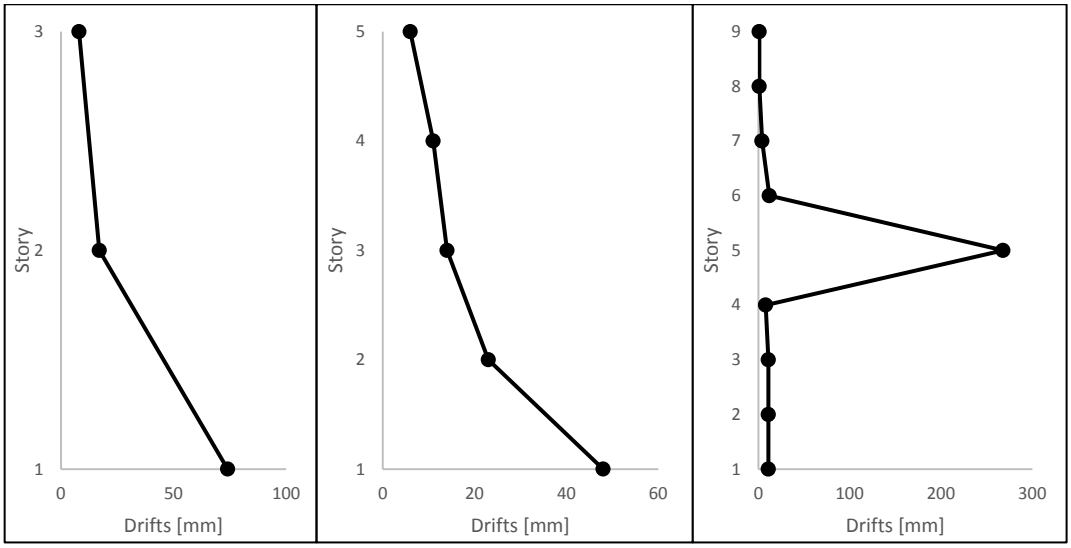


*a)* *b)* *c)*

*Figure 6.7: Drift Profile of unretrofitted frames; a) Case.1; b) Case.2; c) Case.3*

## *6.4 Post retrofitting response of the frames*

Two procedures proposed by Ponzo-Di Cesare [37] and Benavent-Climent [84] for the design of EDBs from the literature and the proposed methodology are applied in order to design the characteristics (Strength, Stiffness, Ductility) of EDBs and subsequently the efficiency of all three procedures are compared. The results are compared in terms of achieving allowable interstory drift profile, top displacement, and energy dissipation demand and capacity.

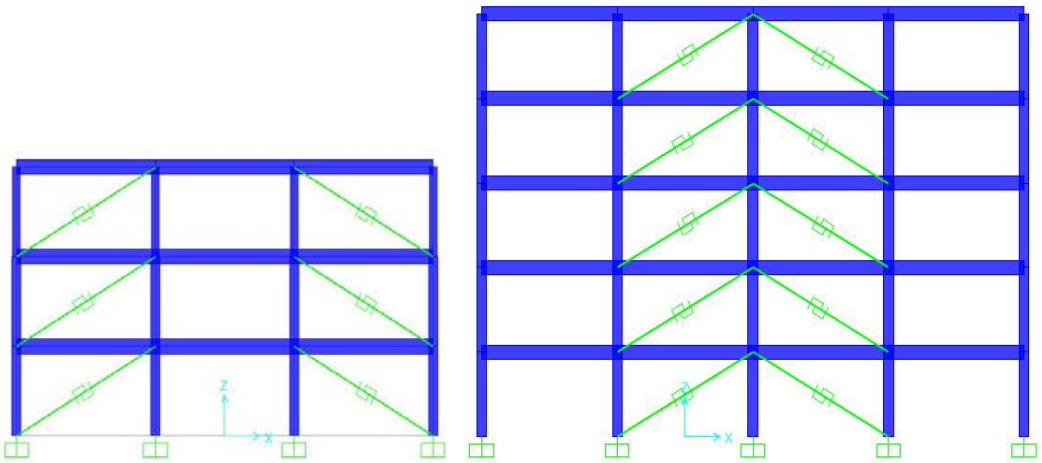

*a)* *b)*

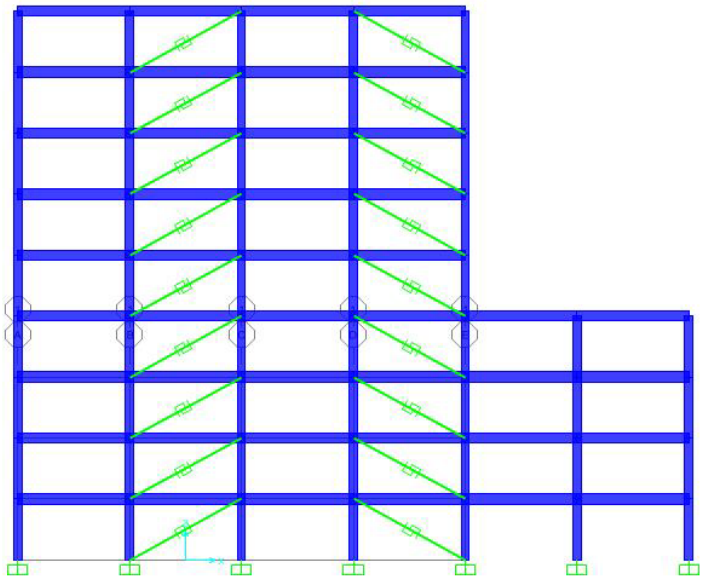

c)

*Figure 6.8: Braced Frames modelled in SAP2000; a) Case.1 b) Case 2; C) Case 3.*

The EDBs are then modeled with the designed characteristics as multi-linear link elements in Sap2000 as shown in

Figure 6.8 and subjected to non-linear static (pushover) and non-linear dynamic analysis.

It is essential to understand how the constitutive law that dictates the behavior of the EDBs are obtained. For example, the constitutive laws of the designed EDBs of case 1 in Figure 6.9 obtained through the selected and the proposed procedures is shown, which leads to the following observations:

1. *Ponzo-Di Cesare design procedure maintains the same stiffness for the bracing system throughout the height of the frames, while the yield displacement capacity of the braces is significantly different. In other words, the ductility of the stories is not equalized, which could result in damage being concentrated at a single story.*
2. *Benavent Climent procedure results in the design of a bracing system that has varying stiffness and ductility at all stories, causing an uneven distribution of the damage among the stories.*
3. *Since the damage concentrates at a relatively weaker story as demonstrated by Akiyama* [52] *and Paulay and Priestly* [87] *through a chain analogy, therefore the proposed procedure focuses to rectify the issue of damage concentration through distributing strength of the bracing system proportional to the demand and keeping the same ductility for all stories.*

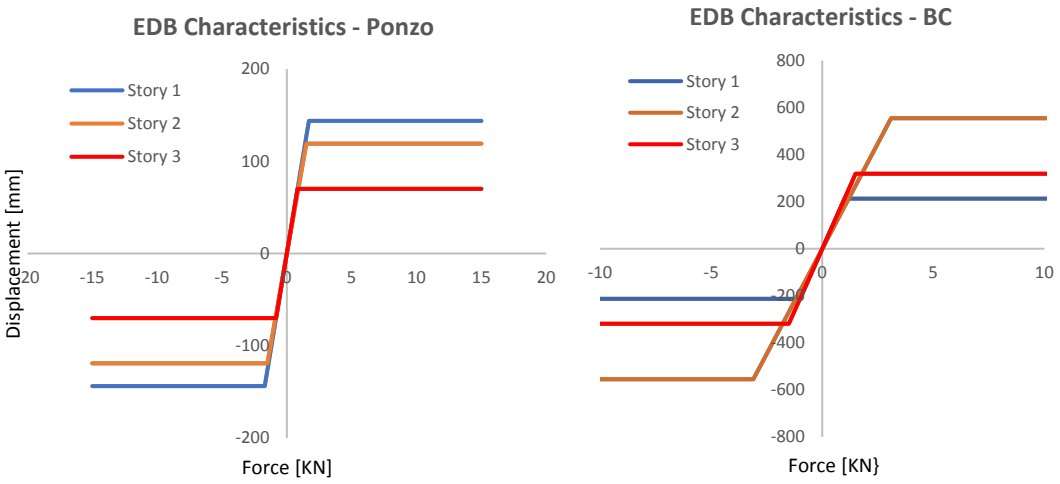


*a)* *b)*

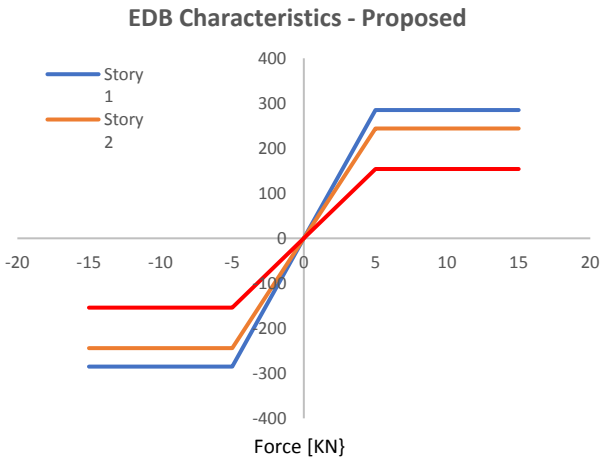


c)

*Figure 6.9: Constitutive laws of the bracing systems for Case.1; a) Ponzo-Di Cesare procedure; b) Benavent Climent's procedure; c) Proposed procedure*

Since the addition of the EDBs will result in the increment of the stiffness of the structures, it is of paramount importance to distribute the additional stiffness in a way that does not result in vertical irregularity, which in return may lead to an irregular drift profile and damage concentration.

The stiffness profile of the bracing systems obtained through these three procedures are shown in Figure 6.10.

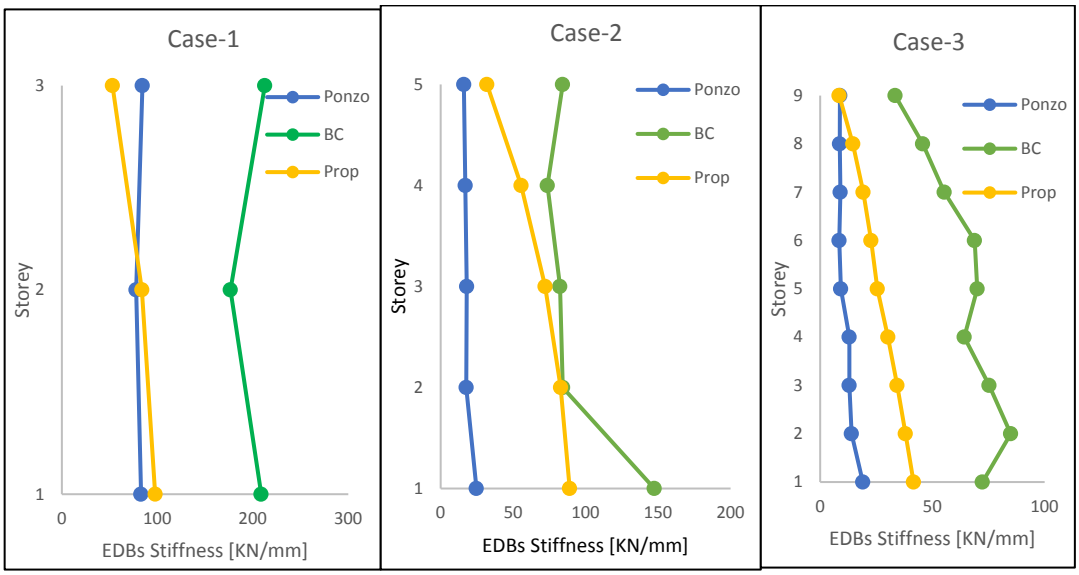


*Figure 6.10: Energy dissipative bracing system stiffness profile*

It is evident from the stiffness profiles in Figure 6.10 obtained through the three applied methodologies that:

1. *The methodology by Benavent-Climent results in irregular distribution of stiffness along the height of the structure, i.e., it does not follow a consistent stiffness distribution criterion. This inconsistency causes the damage concentration in a relatively weaker story. The case studies show that the first story in all three cases remains significantly less stiff, while the stories above are provided with much higher stiffness, causing the damage to occur at the ground floor by forming a soft story mechanism. It can be also noticed that the overall stiffness provided to the frames in all three case studies is comparatively much higher than the other design methodologies, which implies that EDB system will be more costly and less efficient.*

2. *Ponzo-Di Cesare chooses to distribute the equivalent SDoF bracing system's strength proportional to the story-strength of the original structure. This strength distribution criterion does not alter the existing structure's strength profile. In most cases the strength profile of the existing structures is not regular*

*or in other words the strength along the height is not optimum. Thus, the strength profile of the structure before the intervention and after the intervention remains the same, ultimately the irregularity of strength profile results in damage concentration at the significantly weaker story.*

3. *The proposed design methodology follows the optimum strength distribution concept, which makes sure that all stories evenly contribute to the dissipation of the demand energy, and as a result avoid the damage (energy) concentration at a single story.*

## *6.5 Pushover analysis of the retrofitted frames*

Non-linear static analysis is a useful tool to assess the response of the structures; this method of analysis is prescribed by ATC-40 [41] and FEMA-356 [90] for assessing the capacity of existing buildings.

In section 6.2 the process of modelling the nonlinearity of frame elements and carrying out pushover analysis was explained. The pushover analysis results for retrofitted frames are shown in Figure 6.11. These plots indicate that Benavent-Climent's procedure results in higher stiffness values for the EDBs in all three cases without maintaining a regular stiffness distribution criterion throughout the height of the structure.

Pushover curves of frames with EDBs plotted in Figure 6.11 indicate:

a) *Due to the presence of stiff EDBs designed with Benavent-Climent's methodology, the global demand of equivalent SDoF system is reduced and provides a conservative solution.*

b) *Ponzo's methodology seems effective in regular frames (Case 1, Case 2) while it fails to perform well for structures irregular in height (Case 3).*

c) *It can be observed from the capacity-demand curves of the braced frames designed with the proposed methodology that the performance point is closer than the other to the target displacement, thus proving its efficiency for both regular and irregular frames.*

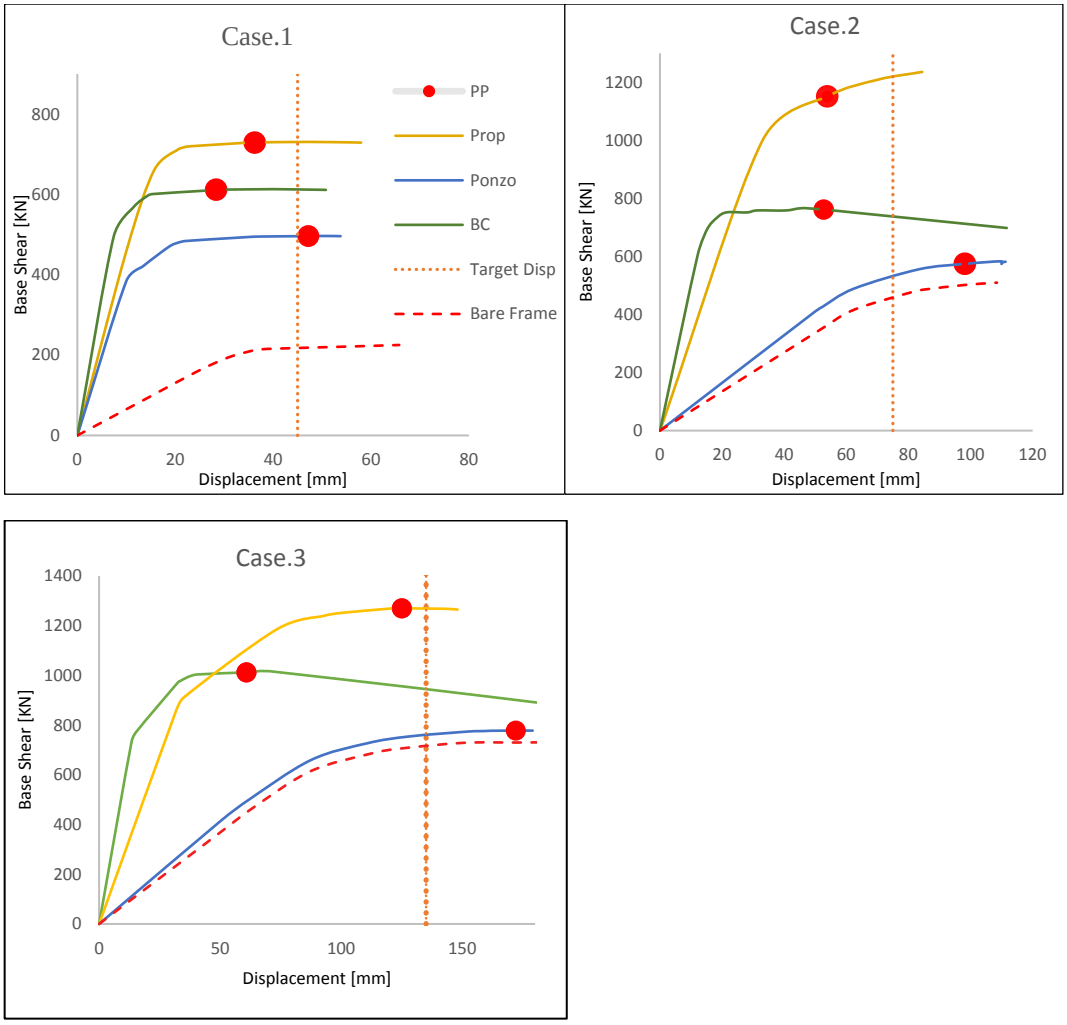


*Figure 6.11:Post-intervention Capacity Curves*

While capacity curves in Figure 6.11 represent the top displacement and base shear of equivalent SDoF system, it's of paramount importance to control and restrict the interstory drifts to the allowable limit. For this purpose, the interstory drifts are checked and plotted in

Figure 6.12.

The drift profile of the braced frames obtained from the pushover analysis at the performance point shows that:

a) *The interstorey drifts are exceeding the allowable limit in some storys for braced frames designed with both Ponzo-Di Cesare and Benavent Climent design methodologies.*

b) *The interstorey drifts of the braced frames designed with the proposed procedure are more uniform and well within the allowable limit and it also ensures the damage is not concentrated at a single story.*

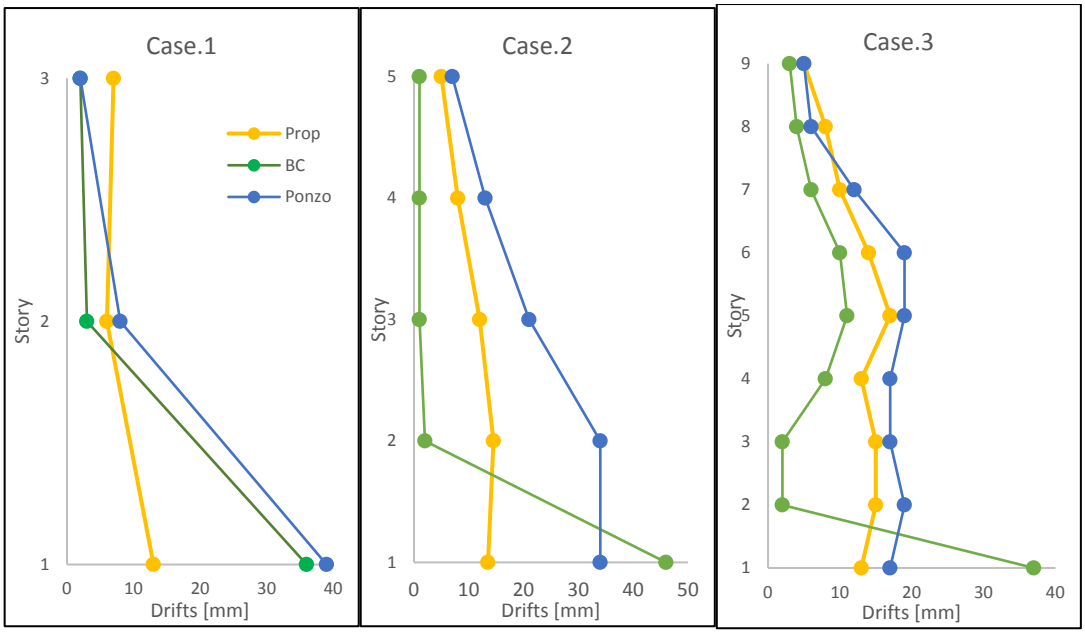


*Figure 6.12: Post-Intervention drifts from pushover analysis*

## *6.6 Non-linear dynamic analysis*

The braced frames were subjected to a design-spectrum-compatible artificial ground motion produced by SeismoArtif software. The ground motion is plotted in Figure 6.13.

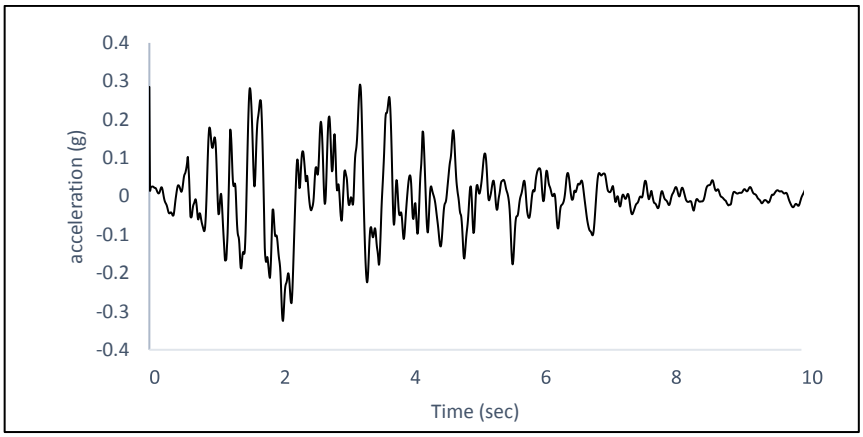


*Figure 6.13: Artificial accelerogram generated by SeismoArtif*

The seismic performance of the existing building after introducing the retrofit strategies was evaluated through the comparison of inter-storey drift profiles and story-wise energy distribution.

Figure 6.14 shows the distribution of inter-storey drift for frames retrofitted with selected and proposed design procedures. From the drift profiles the following results can be drawn:

1. *Benavent Climent design procedures results in irregular distribution of strength and stiffness along the height of the structures, thus causing the damage concentration at single story in all three cases.*
2. *The maximum drifts of case 1 and 2 designed with Ponzo's procedure ends up in damage concentration at the bottom and mid height respectively. This is due to the varying ductility capacities of the energy dissipative (bracing) system.*
3. *The proposed procedure adopts an optimum strength profile that distributes strength proportionaly to the demand and imposes equal ductility capacity at all stories, this leads to the damage being distributed among the stories and results in more uniform drift profile for all three cases.*

It is worth mentioning that, in the non-linear time history analyses, Rayleigh's damping was used. Since the insertion of the bracings will significantly increase the stiffness of the braced frame, the use of elastic stiffness in Rayleigh's damping will result in more conservative response, hence in this analysis, Rayleigh's damping is calculated considering the effective stiffness of the system.

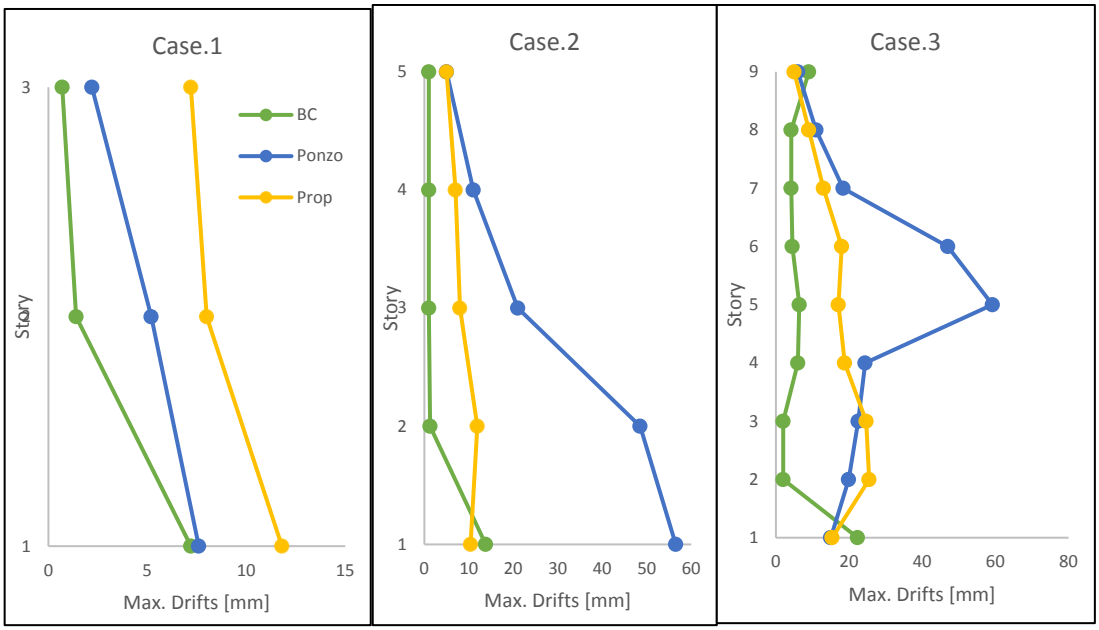


*Figure 6.14: Maximum drifts from non-linear time history analysis*

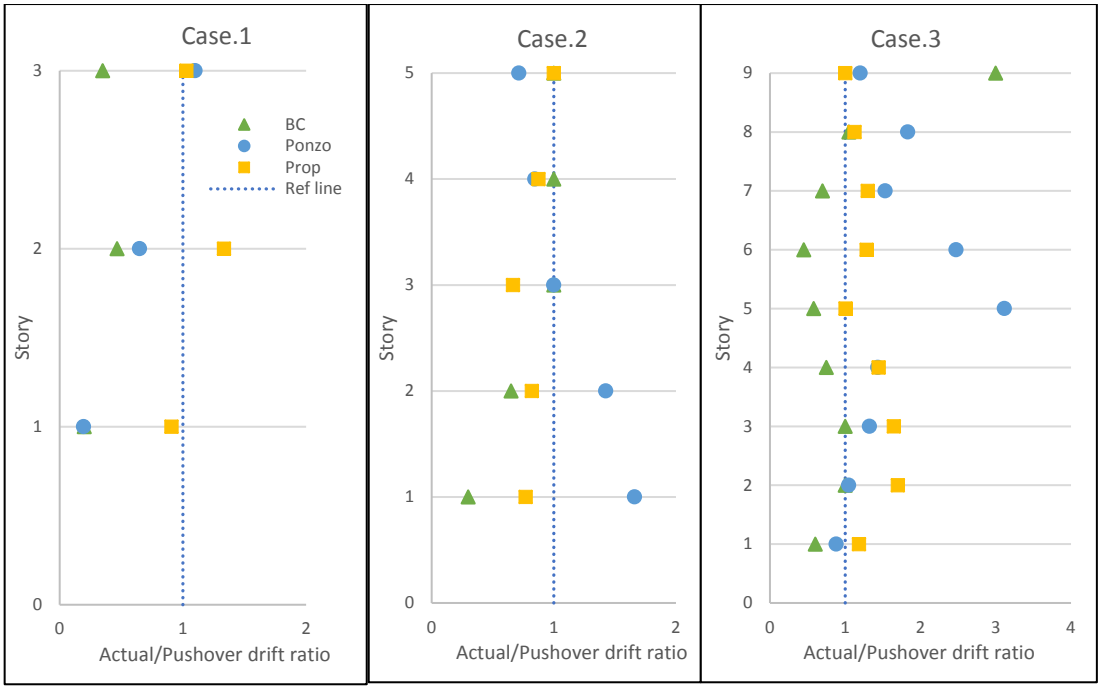


*Figure 6.15:NLTHA/Pushover drifts ratio*

The plot of the NLTHA/Pushover drifts ratio in Figure 6.15 shows that the drifts of the frames designed by proposed methodology are more closer to the reference line while the selected procedures are showing a disperse and more scattered data, confirming high discrepancy between the drifts obtained from pushover and non-linear time history analysis.

Furthermore, the hysteretic energy dissipated by the braces in each storey is calculated by summing up the energy dissipated by the braces installed in the story. The story-wise dissipated energy is plotted in Figure 6.16. The hysteretic energy dissipated by each storey is the accumulated energy dissipated by the braces installed in those stories.

In Figure 6.16, the hysteretic energy dissipated by the EDBs are shown, which clearly demonstrate that:

- *The frames retrofitted by Benavent Climent's procedure are dissipating almost the entire energy in story 1, which causes the soft story mechanism and leads to the collapse of the frame.*

- *Ponzo-Di Cesare procedure provides good energy distribution for case 1 but fails to do the same in case 2 and 3.*

- *The proposed procedure ensures an evenly distributed damage throughout the stories, so to attain a gradual failure and avoid damage concentration in all cases.*

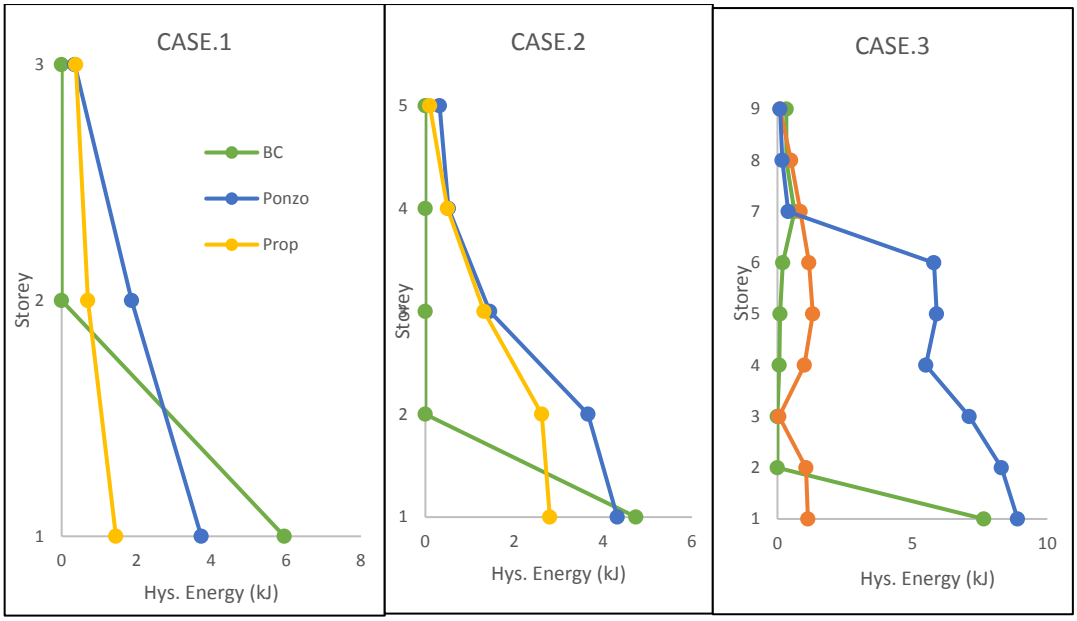


*Figure 6.16: Post intervention story wise hysteretic energy distribution*

# CHAPTER 7

# CONCLUSIVE REMARKS

# 7 Conclusive remarks

The study presented in this PhD thesis has been focused, first, on the study of various design methodologies available in the literature for the design of passive energy dissipative bracing systems and, subsequently, on the proposal of a new energy-based method, whose effectiveness has been the object of a comparative application.

The main reason for choosing this topic is that steel dissipative bracing systems are a simple and effective retrofitting technique. They work as sacrificial ductile fuses, performing as overall displacements reducers and limiting the inter-story drifts enough to reduce the structural damage. The advantage of bracing systems in retrofitting the structures is that they are strong enough to resist earthquake forces and light enough to avoid the need for strengthening of structural elements. Furthermore, these systems are easily installed and replaced after the they are damaged in an earthquake without disrupting the building's occupants.

These advantages elevate the significance of passive energy dissipative bracing systems as viable, feasible, reliable and effective solutions for seismic retrofit of existing structures.

As explained in detail in the relevant chapters, this study is focused on the proposal of an energy-based method for the design of energy dissipative braces and its comparison with two design methods selected from the literature, namely:

- *Displacement-based design method by Ponzo-Di Cesare*
- *Energy-based design method by Benavent Climent*

After a wide review of literature and explanation of significant concepts regarding energy-based design methodologies, a new energy-based design method is proposed in Chapter 5.

In order to evaluate the efficiency of the proposed method it was deemed necessary to compare the outcomes of the selected procedures from the literature with the proposed method, on three cases presented in Chapter 6.

In the validation of the post-retrofitting response of the three case studies, both pushover and non-linear dynamic analysis were used. Based on the results obtained, the following conclusions are drawn:

*a) Story-wise stiffness and strength distribution*

The procedures selected from literature fail to maintain the response regularity of frames and assigns additional stiffness/strength that ends up in vertical irregularity of the frames. Excessive strength/stiffness distribution is not only detrimental to the structure in terms of structural response but it's also directly proportional to the cost. The braces with higher stiffness/strength means higher costs. It was shown in Chapter 6 that during the design of the braces the additional strength should be assigned as a function of the demand, this concept is called optimum strength distribution which is employed in proposed procedure.

*b) Post-retrofitting drifts*

In order to compare the efficiency of the procedure, the drift profiles are obtained for the braced frames designed with both selected procedures and proposed procedure as reported in Chapter 6, which showed that both the selected procedures from the literature, to some extent fails to distribute the damage and obtain a uniform drift profile, while the proposed method results in more uniform drift profile and avoids the damage concentration at a single story, thanks to the optimum strength distribution. This is confirmed by pushover and non-linear dynamic analysis results.

*c) Story-wise energy distribution*

Non-linear dynamic analysis results showed that the proposed procedure assures the energy dissipation takes place at all stories which is one of the main principals in seismic design of structures, while in the frames designed by the selected procedures from literature the energy dissipation is either concentrated at a single story (particularly for Benavent-Climent method) or excessive dissipation in some stories (observed in frames designed by Ponzo-Di Cesare method).

# 8 References


[1] Mazzolani F 2000 *Moment resistant connections of steel frames in seismic areas: design and reliability*

[2] Berman J W and Bruneau M 2009 Cyclic testing of a buckling restrained braced frame with unconstrained gusset connections *J. Struct. Eng.* **135** 1499–510

[3] D'Aniello M 2006 Seismic upgrading of RC structure by steel eccentric bracing *Pollack Period.* **1** 17–32

[4] Corte G Della, D'Aniello M, Conference–First F M-P of X C and 2005 U Seismic upgrading of RC buildings using buckling restrained braces: full-scale experimental tests

[5] Mazzolani F 2006 Seismic upgrading of RC buildings by advanced techniques: The ILVA-IDEM research project

[6] Mazzolani F M 2008 Innovative metal systems for seismic upgrading of RC structures *J. Constr. Steel Res.* **64** 882–95

[7] Calderoni B, Lenza P, Sismica P R-I and 2000 U 2000 Prescrizioni normative e sicurezza sismica *USPI*

[8] Bracci J M, Reinhorn A M and Mander J B 1995 Seismic resistance of reinforced concrete frame structures designed for gravity loads: performance of structural system *ACI Mater. J.* **92** 597–609

[9] Park R 1986 DUCTILE DESIGN APPROACH FOR REINFORCED CONCRETE FRAMES. *Earthq. Spectra* **2** 565–619

[10] Hanson N and Conner H 1967 Seismic Resistance of Reinforced Concrete Beam-Column Joints *J. Struct. Div.* **93** 533–60

[11] Paulay T, Park R and Priestley M J N 1978 Reinforced Concrete Beam-Column Joints Under Seismic Actions. *J Am Concr Inst* **75** 585–93

[12] Chen C 1990 Development and experimental investigation of a ductile CBF system *Proceedings of the 4th national conference* vol 2 pp 575–84

[13] Wakabayashi, M., Nakamura, T., Katagihara, A., Yogoyama, H., & Morisono T 1973 Experimental study on the elastoplastic behavior of braces enclosed by precast concrete panels under horizontal cyclic loading (Parts 1 &2). In Summaries of technical papers of annual meeting (Vol. 6, pp. 121-8). *Archit. Inst. Japan* **6** 121–8

[14] Takeda Y, Kimura Y, Yoshioka K, Furuya N and Takemoto Y 1976 An Experimental Study on Braces encased in Steel Tube and mortal *Annu. Meet. Archit. Inst. Japan* 1041–2

[15] Mochizuki N, Murata Y, Ou N and Takahashi S 1997 An experimental study on buckling of unbonded braces under centrally applied loads *Annual Meeting of the Architectural Institute of Japan*

[16] Wada A 1997 Seismic design trend of tall steel buildings after the Kobe

earthquake *ci.nii.ac.jp*

[17] Watanabe A, Hitomi Y, Saeki E, Wada A and Fujimoto M 1988 Properties of brace encased in buckling-restraining concrete and steel tube *Proc. Ninth World Conf. Earthq. Eng.* **4** 719–24

[18] Tsai K-C, Lin S, Lai J-W, Hwang Y-C, Lin S-L and Weng C-H 2004 *RESEARCH AND APPLICATION OF DOUBLE-CORE BUCKLING RESTRAINED BRACES IN TAIWAN Acceleration Control Analysis and Synthesis of A Multiple Shaking Table Test System Considering Coupling Effect View project Reinforced Concrete Structures subjected to Blast and*

[19] Sabelli R and Aiken I 2004 *13 th World Conference on Earthquake Engineering U . S . BUILDING-CODE PROVISIONS FOR BUCKLING-RESTRAINED BRACED FRAMES : BASIS AND DEVELOPMENT*

[20] Wada A and Nakashima M 2004 *From Infancy To Maturity of Buckling Restrained Brace Research*

[21] Corte D and Mazzolani F M 2006 Full-Scale Tests of Advanced Seismic Upgrading Techniques for RC Structures *Proceedings of the Second fib Congress*

[22] Merritt S, Uang C-M and Benzoni G 2003 Subassemblage testing of COREBRACE buckling-restrained braces 108

[23] Chen C 2002 Recent advances of seismic design of steel buildings in Taiwan *Struct. Eng.*

[24] Antonucci R, Balducci F, Cappanera F and Castellano M G 2001 *Strutture prefabbricate con controventi dissipativi: l'esempio del nuovo polo didattico della Facoltà di Ingegneria dell'Università Politecnica delle Marche di Ancona* vol 1

[25] Lin M-L, Weng Y-T, Tsai K-C, Hsiao P-C, Chen C-H and Lai J-W 2004 *3 th World Conference on Earthquake Engineering PSEUDO-DYNAMIC TEST OF A FULL-SCALE CFT/BRB FRAME: PART 3-ANALYSIS AND PERFORMANCE EVALUATION*

[26] Tsai K C and Huang Y C 2002 Experimental responses of large scale BRB frames *Cent. Earthq. Eng. Res. Natl. Taiwan Univ.*

[27] Black C J, Makris N and Aiken I D 2004 Component Testing, Seismic Evaluation and Characterization of Buckling-Restrained Braces *J. Struct. Eng.* **130** 880–94

[28] Fajfar P and Fischinger M 1988 N2- A Method For Non-linear Seismic Analysis of Regular Buildings *Ninth World Conf. Earthq. Eng.* 111–6

[29] Fajfar P and Fischinger M 1987 Non-linear seismic analysis of RC buildings - Implications of a case study *Eur. Earthq. Eng.* **1** 31–43

[30] Saiidi M and Sozen M A 1981 Simple Nonlinear Seismic Analysis of R/C Structures *ASCE J Struct Div* **107** 937–52

[31] Fajfar P and Gašperšič P 1996 The N2 method for the seismic damage analysis

of RC buildings *Earthq. Eng. Struct. Dyn.* **25** 31–46

[32] Fajfar P, Gašperšič P and Drobnič D 1997 A simplified nonlinear method for seismic damage analysis of structures

[33] Fajfar P 1999 Capacity spectrum method based on inelastic demand spectra *Earthq. Eng. Struct. Dyn.* **28** 979–93

[34] EN 1998-1 2004 EN 8: Design of structures for earthquake resistance *Eur. Stand. (Design Struct. Earthq. Resist.* **1**

[35] Fajfar P 2000 A Nonlinear Analysis Method for Performance-Based Seismic Design *Earthq. Spectra* **16** 573–92

[36] Chopra A 1995 Dynamics of structures: theory and applications to earthquake engineering

[37] Di Cesare A and Ponzo F C 2017 Seismic Retrofit of Reinforced Concrete Frame Buildings with Hysteretic Bracing Systems: Design Procedure and Behaviour Factor *Shock Vib.* **2017**

[38] Bergami A V and Nuti C 2013 A design procedure of dissipative braces for seismic upgrading structures *Earthq. Struct.* **4**

[39] Benavent-Climent A 2011 An energy-based method for seismic retrofit of existing frames using hysteretic dampers *Soil Dyn. Earthq. Eng.* **31** 1385–96

[40] Ministero delle Infrastrutture 2008 D.M. 14/01/2008 - Nuove Norme Tecniche per le Costruzioni *Gazz. Uff.* **29**

[41] Applied Technology Council (ATC) 1996 ATC-40 Seismic Evaluation and Retrofit of Concrete Buildings **1** 612

[42] Di Cesare A, Ponzo F C, Nigro D, Dolce M and Moroni C 2012 Experimental and numerical behaviour of hysteretic and visco-recentring energy dissipating bracing systems *Bull. Earthq. Eng.* **10** 1585–607

[43] Palermo M, Silvestri S, Gasparini G and Trombetti T 2015 Crescent shaped braces for the seismic design of building structures *Mater. Struct. Constr.* **48** 1485–502

[44] Sorace S 2012 *Dissipative Bracing-Based Seismic Retrofit of R/C School Buildings* vol 6

[45] Sorace S, Terenzi G and Mori C 2016 Passive energy dissipation-based retrofit strategies for R/C frame water towers *Eng. Struct.* **106** 385–98

[46] Cardone D, Dolce M, Ponzo F C and Coelho E 2004 Experimental behaviour of R/C frames retrofitted with dissipating and RE-centring braces *J. Earthq. Eng.* **8** 361–96

[47] Dolce M, Cardone D, Ponzo F C and Valente C 2005 Shaking table tests on reinforced concrete frames without and with passive control systems *Earthq. Eng. Struct. Dyn.* **34** 1687–717

[48] Ponzo F C, Di Cesare A, Nigro D, Vulcano A, Mazza F, Dolce M and Moroni C 2012 Jet-pacs project: Dynamic experimental tests and numerical results

obtained for a steel frame equipped with hysteretic damped chevron braces *J. Earthq. Eng.* **16** 662–85

[49] Di Cesare A, Ponzo F C and Nigro D 2014 Assessment of the performance of hysteretic energy dissipation bracing systems *Bull. Earthq. Eng.* **12** 2777–96

[50] Dolce M and Marnetto R 2001 Energy dissipating coverplates for steel brace joints *Proceedings of the 5th World Conference on Joints, Bearings and Seismic Systems for Concrete Structures*

[51] Sabelli R 2004 Recommended provisions for buckling-restrained braced frames *Eng. J.* **41** 155–75

[52] Akiyama H 1985 Earthquake-resistant limit-state design for buildings

[53] Uang C-M and Bertero V V 1988 Use of energy as a design criterion in earthquake-resistant design *Earthq. Eng. Res. Cent.* **88** 77–90

[54] Benavent-Climent A, Pujades L G and López-Almansa F 2002 Design energy input spectra for moderate-seismicity regions *Earthq. Eng. Struct. Dyn.* **31** 1151–72

[55] Zahrah T F and Hall W J 1984 Earthquake Energy Absorption in SDOF Structures *J. Struct. Eng.* **110** 1757–72

[56] Housner G W 1956 Limit design of structures to resist earthquakes *Proc. 1st World Conf. Earthq. Eng.* 5.1-5.13

[57] Fajfar P and Vidic T 1994 Consistent inelastic design spectra: Hysteretic and input energy *Earthq. Eng. Struct. Dyn.* **23** 523–37

[58] Chou C C and Uang C M 2000 Establishing absorbed energy spectra - An attenuation approach *Earthq. Eng. Struct. Dyn.* **29** 1441–55

[59] Hudson D E 1956 Response spectrum techniques in engineering seismology *Proc. World Conf. Earthq. Eng.* 1–12

[60] Hudson D E 1962 *Some problems in the application of spectrum techniques to strong-motion earthqhuake analysis* vol 52

[61] Choi H and Kim J 2006 Energy-based seismic design of buckling-restrained braced frames using hysteretic energy spectrum *Eng. Struct.* **28** 304–11

[62] Dubina D, Stratan A and Dinu F 2008 Dual high-strength steel eccentrically braced frames with removable links *Earthq. Eng. Struct. Dyn.* **37** 1703–20

[63] Kuwamura H and Galambos T V. 1989 Earthquake load for structural reliability *J. Struct. Eng. (United States)* **115** 1446–62

[64] COSENZA and E. 1997 The Improvement of the Seismic-Resistant Design for Existing and New Structures using Damage Concept *Proc. Int. Work. Seism. Des. Methodol. Gener. Code* 119–30

[65] Manfredi G 2001 Evaluation of seismic energy demand *Earthq. Eng. Struct. Dyn.* **30** 485–99

[66] Manfredi G, Polese M and Cosenza E 2003 Cumulative demand of the earthquake ground motions in the near source *Earthq. Eng. Struct. Dyn.* **32** 1853–

[67] Newmark N and Hall W 1982 Earthquake Spectra and Design, EERI Monograph. Earhquake Engineering Institute

[68] … E C t and 1997 U 1997 The improvement of the seismic-resistant design for existing and new structures using damage concept *The International Workshop on Seismic Design*

[69] Building Seismic Safety Council (US) and Applied Technology Council 1997 NEHRP guidelines for the seismic rehabilitation of buildings:FEMA 273 *Fed. Emerg. Manag. Agency* 435

[70] Smith R and Tso W 2002 Inconsistency of force-based design procedure *J. Seismol. Earthq. Eng.* **4** 46–54

[71] Powell G H 2008 *Displacement-Based Seismic Design of Structures* vol 24

[72] Hernandez-Montes E, Kwon O S and Aschheim M A 2004 AN ENERGY-BASED FORMULATION FOR FIRST- AND MULTIPLE-MODE NONLINEAR STATIC (PUSHOVER) ANALYSES *J. Earthq. Eng.* **8** 69–88

[73] Manoukas G, Athanatopoulou A and Avramidis I 2011 Static pushover analysis based on an energy-equivalent SDOF system *Earthq. Spectra* **27** 89–105

[74] Uang C -M and Bertero V V. 1990 Evaluation of seismic energy in structures *Earthq. Eng. Struct. Dyn.* **19** 77–90

[75] Bruneau M and Wang N 1996 Some aspects of energy methods for the inelastic seismic response of ductile SDOF structures *Eng. Struct.* **18** 1–12

[76] Fajfar P, Vidic T and Fischinger M 1989 Seismic demand in medium- and long-period structures *Earthq. Eng. Struct. Dyn.* **18** 1133–44

[77] Trifunac M D and Brady A G 1975 *A STUDY ON THE DURATION OF STRONG EARTHQUAKE GROUND MOTION* vol 65

[78] Decanini L D and Mollaioli F 2001 An energy-based methodology for the assessment of seismic demand *Soil Dyn. Earthq. Eng.* **21** 113–37

[79] Shen J and Akbas B 1999 Seismic energy demand in steel moment frames *J. Earthq. Eng.* **3** 519–59

[80] Akbaş B and Shen J 2003 *Seismic behavior of steel buildings with combined rigid and semi-rigid frames* vol 27

[81] Ye L, Cheng G, Qu Z and Lu X 2012 *Study on energy-based seismic design method and application on steel braced frame structures* vol 33

[82] Monti G and Petrone F 2015 Yield and ultimate moment and curvature closed-form equations for reinforced concrete sections *ACI Struct. J.* **112** 463–74

[83] Cesare A Di and Ponzo F C 2017 Seismic Retrofit of Reinforced Concrete Frame Buildings with Hysteretic Bracing Systems: Design Procedure and Behaviour Factor

[84] Benavent-Climent A 2011 An energy-based method for seismic retrofit of existing frames using hysteretic dampers *Soil Dyn. Earthq. Eng.* **31** 1385–96

[85] Mander J B, Priestley M J and Park R 1988 Theoretical stress-strain model for confined concrete *J. Struct. Eng. (United States)* **114** 1804–26

[86] Mander J B, Nair B, Wojtkowski K and Ma J 1993 An Experimental Study on the Seismic Performance of Brick-Infilled Steel Frames With and Without Retrofit

[87] Paulay T and Priestley M 1992 *Seismic design of reinforced concrete and masonry buildings*

[88] Elnashai A S and Di Sarno L 2008 *Fundamentals of Earthquake Engineering* (John Wiley and Sons)

[89] ASCE- American Society of Civil Engineers 2000 Prestandard and Commentary for the Seismic Rehabilitation of Buildings *Rehabil. Requir.* 1–518

[90] Engineers R 2000 FEMA 356: Prestandard and Commentary for the Seismic Rehabilitation of Buildings, Report No

# APPENDIX

# MATLAB SCRIPTS FOR THE APPLICATION OF THE SELECTED AND PROPOSED PROCEDURE

## PROPOSED METHOD - CASE-1

```
clear
clc
close all
```

- Unbraced Structure Characteristics

```
Np = 3; % Number of stories
m_x(1) = 0.043 ; % Mass [KNxsec2/mm]
m_x(2) = 0.043;  %
m_x(3) = 0.043 ; %

Mass_matrix_1=[0.043 0 0  ; 0 0.043 0  ; 0 0 0.043];
Shape_vector_1=[0.4 0.8 1];
r=[1;1;1];
mass_starr_1=Shape_vector_1*Mass_matrix_1*r; % 1st mode effective mass
k_star_1 = 14.2; %[KN/mm] elastic stiffness
T_star_1 = 2*pi*sqrt(mass_starr_1/k_star_1); % [sec] SDFS's period in the X direction
wn_star_1= (2*pi)/T_star_1;

k_f_x(1) = 19.0; % [KN/mm] Story Stiffness of Existing structure
k_f_x(2) = 16.7; % [KN/mm]
k_f_x(3) = 20.1; % [KN/mm]

d_yf_x(1) = 20.0; % [mm] Yield displacement of stories
d_yf_x(2) = 20.0; % [mm]
d_yf_x(3) = 20.0; % [mm]

D_t_1 = 40; %[mm] minimum of Yield displacements of stories, chosen as max ultimate displ for
 Storey 1.
Mu = 4; % Ductility of the devices

n_eq = 4; % number of plastic cycles excursion
```

- Demand evaluation in terms of energy

```
ag_adim = 0.298 ; % [g]
Tc_star = 0.356 ; % []
F0 = 2.386 ; % [] maximum amplification factor
g = 9820; % mm/sec2

T_G_x = 0.5;     % [sec] predominant period
T1_x = 0.63; % [sec] calculated by an eignevalue analysis using intitial stiffness of the mem
bers

% Note that those parameters have been taken from CDS and already takes into account PVR(SLV)

% Soil type
cat_suolo = 3; % [Soil category from A to E i.e. from 1 to 5]
```

```
% Structural damping
Xsi = 5; % [%]

ST = 1.0 ;% [ ] topographic amplification factor

% stratigraphic amplification factor SS [] and soil-dependent coefficient CC []
if cat_suolo == 1
    SS = 1.0;
    CC = 1.0;
end
if cat_suolo == 2
    CC = 1.1 * Tc_star^(-0.2);
    aux = 1.4 - 0.4 * F0 * ag_adim;
    if aux>=1.0 && aux<=1.2
        SS = aux;
    elseif aux < 1.0
        SS = 1.0;
    elseif aux > 1.2
        SS =1.2;
    end
end
if cat_suolo == 3
    CC = 1.05 * Tc_star ^(-0.33);
    aux = 1.7 - 0.6 * F0 * ag_adim;
    if aux>=1.0 && aux<=1.5
        SS = aux;
    elseif aux < 1.0
        SS = 1.0;
    elseif aux > 1.5
        SS =1.5;
    end
end
if cat_suolo == 4
    CC = 1.25 * Tc_star^(-0.5);
    aux = 2.4 - 1.5 * F0 * ag_adim;
    if aux>=0.9 && aux<=1.8
        SS = aux;
    elseif aux < 0.9
        SS = 0.9;
    elseif aux > 1.8
        SS =1.8;
    end
end
if cat_suolo == 5
    CC = 1.15 * Tc_star^(-0.4);
    aux = 2.0 - 1.1 * F0 * ag_adim;
    if aux>=1.0 && aux<=1.6
        SS = aux;
    elseif aux < 1.0
        SS = 1.0;
    elseif aux > 1.6
        SS =1.6;
    end
end

Tc = Tc_star * CC; %[sec]
Tb = Tc/3; %[sec]
```

```
Td = 4.0 * ag_adim + 1.6; %[sec]
eta = sqrt(10/(5+Xsi)); % []
S = SS * ST ; % []

% Evaluating Elastic spectral acceleration for the structure- 5% damping
if T_star_1 >= 0 && T_star_1 < Tb
    Se_1_T_star_1 = ag_adim * g * S * eta * F0 * (T_star_1/Tb + (eta*F0)^(-1.0)*(1-T_star_1/T
b)); % [mm/sec2]
elseif T_star_1 >= Tb && T_star_1 < Tc
    Se_1_T_star_1 = ag_adim * g * S * eta * F0;
elseif T_star_1 >= Tc && T_star_1 < Td
    Se_1_T_star_1 = ag_adim * g * S * eta * F0 * (Tc/T_star_1);
elseif T_star_1 >= Td
    Se_1_T_star_1 = ag_adim * g * S * eta * F0 * (Tc * Td * T_star_1^(-2));
end


SV_5_Percent_x= Se_1_T_star_1/(wn_star_1); %mm 5% damped spectral displacement

E_I = 0.5 * (SV_5_Percent_x)^2 * mass_starr_1; %% Total input energy
E_H_tot = E_I * 0.72 * (1-(1/Mu))^0.7; %% Demadn Hysteretic Energy
```

- Distribution of E_H to story levels

```
E_H = zeros(1,Np);
if Np<5
    for i=1:Np
    E_H(i)=E_H_tot*(2*(Np+1-i)/(Np*(Np+1)));
    end
elseif Np>=5
    for i=1:Np
    E_H(i)= E_H_tot*(2*Np-1)/(Np*(Np-1));
    end
end


%
```

- Design Strength of EDBs at story 1

```
D_u_1 = d_yf_x(1); % Ultimate displacement of story 1
D_y_1 = D_u_1/Mu; % Yield displacement of storey 1
F_y_1 = E_H(1) / (n_eq *(D_u_1-D_y_1)); % Design strength of EDBs at First story [ KN]


%
```

- Distribtion of strength as a function of F_y_1 using Akiyama's formulation

```
alpha_bar_x = zeros(1,Np);    % shear coefficient ratio
for i = 1:1:Np
```

```
    % evaluate the alpha_bar_i for the i-th story and put it in the
    % corresponding cell of vector alpha_bar
    Aux_1_x = (1 - 0.02 * (k_f_x(1)/k_f_x(Np)) - 0.16 * (T1_x/T_G_x));
    Aux_2_x = 0.5 - 0.05 * k_f_x(1)/k_f_x(Np) - 0.3 * T1_x/T_G_x;
    % Auxiliary values to be input in the following expression for alpha_bar(e).
    % It is convenient to evaluate these once for all, since 1) they do not
    % depend on the counter "e", and 2) it is always good idea to split
    % long mathematical expressions to better check them!
    x_bar_x = (i-1)/Np;
    alpha_bar_x(i) = exp( ( Aux_1_x * x_bar_x) - Aux_2_x *(x_bar_x)^2 );
end

m_t(1)= m_x(1)+ m_x(2)+m_x(3);
m_t(2)= m_x(2)+m_x(3);
m_t(3)= m_x(3);

Gama_x = zeros(1,Np);
for i=1:Np
    Gama_x(i)=m_t(1)/m_t(i);
end

F_y = zeros(1,Np);  %%% Horizontal Component
for i=1:Np
    F_y(i)=F_y_1* alpha_bar_x(i)/Gama_x(i);
end


Nc_x =2 ;
alfa_c_x =31;

F_y_Axial = zeros(1,Np); %%% Axial Component of single brace strength
for i=1:Np
    F_y_Axial(i) =F_y(i) /(Nc_x * cosd(alfa_c_x));
end


K_s = zeros(1,Np);
for i=1:Np
    K_s(i)=F_y(i)/D_y_1;
end
```

---

*Published with MATLAB® R2018b*

## PROPOSED METHOD - CASE-2

```
clear
clc
close all
```

- Unbraced strcuture characteristics

```
Np = 5; % Number of stories
m_x(1) = 0.043 ; % KNxsec2/mm
m_x(2) = 0.043; %
m_x(3) = 0.043 ; %
m_x(4) = 0.043 ;
m_x(5) = 0.043 ;

Mass_matrix_1=[0.043 0 0 0 0 ; 0 0.043 0 0 0  ; 0 0 0.043 0 0; 0 0 0 0.043 0; 0 0 0 0 0.043];
Shape_vector_1=[0.2 0.47 0.71 0.89 1];
r=[1;1;1;1;1];
mass_starr_1=Shape_vector_1*Mass_matrix_1*r; % 1st mode effective mass
k_star_1 = 6.57; %[KN/mm] elastic stiffness
T_star_1 = 2*pi*sqrt(mass_starr_1/k_star_1); % [sec] SDFS's period in the X direction
wn_star_1= (2*pi)/T_star_1;

k_f_x(1) = 32.0; % [KN/mm]
k_f_x(2) = 22.5; % [KN/mm]
k_f_x(3) = 22.6; % [KN/mm]
k_f_x(4) = 20.1; % [KN/mm]
k_f_x(5) = 21.5; % [KN/mm]


d_yf_x(1) = 20.0; % [mm] Yield displacement of stories
d_yf_x(2) = 20.0; % [mm]
d_yf_x(3) = 20.0; % [mm]
d_yf_x(4) = 20.0;
d_yf_x(5) = 20.0;

D_t_1 = 40; %[mm] minimum of Yield displacements of stories, chosen as max ultimate displ for
 Storey 1.
Mu = 4; % Ductility of the devices

n_eq = 1; % number of plastic cycles excursion
```

- Demand evaluation in terms of energy

```
ag_adim = 0.298 ; % [] it actually is ag/g
Tc_star = 0.356 ; % []
F0 = 2.386 ; % [] maximum amplification factor
g = 9820; % mm/sec2

T_G_x = 0.5;     % [sec] predominant period
T1_x = 0.63; % [sec] calculated by an eignevalue analysis using intitial stiffness of the mem
```

```
bers

% Note that those parameters have been taken from CDS and already takes into account PVR(SLV)

% Soil type
cat_suolo = 3; % [from A to E i.e. from 1 to 5]
% Structural damping
Xsi = 5; % [%]

ST = 1.0 ;% [ ] topographic amplification factor

% stratigraphic amplification factor SS [] and soil-dependent coefficient CC []
if cat_suolo == 1
    SS = 1.0;
    CC = 1.0;
end
if cat_suolo == 2
    CC = 1.1 * Tc_star^(-0.2);
    aux = 1.4 - 0.4 * F0 * ag_adim;
    if aux>=1.0 && aux<=1.2
        SS = aux;
    elseif aux < 1.0
        SS = 1.0;
    elseif aux > 1.2
        SS =1.2;
    end
end
if cat_suolo == 3
    CC = 1.05 * Tc_star ^(-0.33);
    aux = 1.7 - 0.6 * F0 * ag_adim;
    if aux>=1.0 && aux<=1.5
        SS = aux;
    elseif aux < 1.0
        SS = 1.0;
    elseif aux > 1.5
        SS =1.5;
    end
end
if cat_suolo == 4
    CC = 1.25 * Tc_star^(-0.5);
    aux = 2.4 - 1.5 * F0 * ag_adim;
    if aux>=0.9 && aux<=1.8
        SS = aux;
    elseif aux < 0.9
        SS = 0.9;
    elseif aux > 1.8
        SS =1.8;
    end
end
if cat_suolo == 5
    CC = 1.15 * Tc_star^(-0.4);
    aux = 2.0 - 1.1 * F0 * ag_adim;
    if aux>=1.0 && aux<=1.6
        SS = aux;
    elseif aux < 1.0
        SS = 1.0;
    elseif aux > 1.6
```

```
        SS =1.6;
    end
end

Tc = Tc_star * CC; %[sec]
Tb = Tc/3; %[sec]
Td = 4.0 * ag_adim + 1.6; %[sec]
eta = sqrt(10/(5+Xsi)); % []
S = SS * ST ; % []

% Evaluating Elastic spectral acceleration for the structure- 5% damping
if T_star_1 >= 0 && T_star_1 < Tb
    Se_1_T_star_1 = ag_adim * g * S * eta * F0 * (T_star_1/Tb + (eta*F0)^(-1.0)*(1-T_star_1/T
b)); % [mm/sec2]
elseif T_star_1 >= Tb && T_star_1 < Tc
    Se_1_T_star_1 = ag_adim * g * S * eta * F0;
elseif T_star_1 >= Tc && T_star_1 < Td
    Se_1_T_star_1 = ag_adim * g * S * eta * F0 * (Tc/T_star_1);
elseif T_star_1 >= Td
    Se_1_T_star_1 = ag_adim * g * S * eta * F0 * (Tc * Td * T_star_1^(-2));
end


SV_5_Percent_x= Se_1_T_star_1/(wn_star_1); %mm 5% damped spectral displacement

E_I = 0.5 * (SV_5_Percent_x)^2 * mass_starr_1; %% Total input energy
E_H_tot = E_I * 0.72 * (1-(1/Mu))^0.7; %% Demadn Hysteretic Energy
```

- Distribution of E_H to story levels

```
E_H = zeros(1,Np);
if Np<5
    for i=1:Np
    E_H(i)=E_H_tot*(2*(Np+1-i)/(Np*(Np+1)));
    end
elseif Np>=5
    for i=1:Np
    E_H(i)= E_H_tot*(2*Np-1)/(Np*(Np-1));
    end
end
```

- Design Strength of EDBs at story 1

```
D_u_1 = d_yf_x(1); % Ultimate displacement of story 1
D_y_1 = D_u_1/Mu; % Yield displacement of storey 1
F_y_1 = E_H(1) / (n_eq *(D_u_1-D_y_1)); % Design strength of EDBs at First story [ KN]


%
```

- Distribtion of strength as a function of F_y_1 using Akiyama's formulation

```
alpha_bar_x = zeros(1,Np);    % initialize the vector containing the alpha adimensional value
s
for i = 1:1:Np
    % evaluate the alpha_bar_i for the i-th story and put it in the
    % corresponding cell of vector alpha_bar
    Aux_1_x = (1 - 0.02 * (k_f_x(1)/k_f_x(Np)) - 0.16 * (T1_x/T_G_x));
    Aux_2_x = 0.5 - 0.05 * k_f_x(1)/k_f_x(Np) - 0.3 * T1_x/T_G_x;
    % Auxiliary values to be input in the following expression for alpha_bar(e).
    % It is convenient to evaluate these once for all, since 1) they do not
    % depend on the counter "e", and 2) it is always good idea to split
    % long mathematical expressions to better check them!
    x_bar_x = (i-1)/Np;
    alpha_bar_x(i) = exp( ( Aux_1_x * x_bar_x) - Aux_2_x *(x_bar_x)^2 );
end


 m_t(1) = m_x(1)+m_x(2)+m_x(3)+ m_x(4)+m_x(5);
 m_t(2) = m_x(2)+m_x(3)+m_x(4)+m_x(5);
 m_t(3) = m_x(3)+m_x(4)+m_x(5);
 m_t(4) = m_x(4)+m_x(5);
 m_t(5) = m_x(5);


Gama_x = zeros(1,Np);
for i=1:Np
    Gama_x(i)=m_t(1)/m_t(i);
end

F_y = zeros(1,Np);  %%% Horizontal Component
for i=1:Np
    F_y(i)=F_y_1* alpha_bar_x(i)/Gama_x(i);
end


Nc_x =2 ;
alfa_c_x =31;

F_y_Axial = zeros(1,Np); %%% Axial Component of single brace strength
for i=1:Np
    F_y_Axial(i) =F_y(i) /(Nc_x * cosd(alfa_c_x));
end


K_s = zeros(1,Np);
for i=1:Np
    K_s(i)=F_y(i)/D_y_1;
end
```

---

*Published with MATLAB® R2018b*

## PROPOSED METHOD - CASE-3

```
clear
clc
close all
```

- Unbraced strcuture characteristics

```
Np = 9; % Number of stories
m_x(1) = 0.066 ; % Units of the mass are KNxsec2/cm
m_x(2) = 0.066 ; % Units of the mass are KNxsec2/cm
m_x(3) = 0.066 ; % Units of the mass are KNxsec2/cm
m_x(4) = 0.066 ; % Units of the mass are KNxsec2/cm
m_x(5) = 0.043 ;
m_x(6) = 0.043 ; % Units of the mass are KNxsec2/cm
m_x(7) = 0.043 ; % Units of the mass are KNxsec2/cm
m_x(8) = 0.043 ; % Units of the mass are KNxsec2/cm
m_x(9) = 0.043 ;

Mass_matrix_1=[0.066 0 0 0 0 0 0 0 0 ; 0 0.066 0 0 0 0 0 0 0 ; 0 0 0.066 0 0 0 0 0 0 ; 0 0 0
0.066 0 0 0 0 0 ; 0 0 0 0 0.043 0 0 0 0; 0 0 0 0 0 0.043 0 0 0; 0 0 0 0 0 0 0.043 0 0; 0 0 0
0 0 0 0 0.043 0; 0 0 0 0 0 0 0 0 0.043];

Shape_vector_1=[0.1 0.24 0.38 0.5 0.64 0.77 0.88 0.95 1];
r=[1;1;1;1;1;1;1;1;1];
mass_starr_1=Shape_vector_1*Mass_matrix_1*r; % 1st mode effective mass

k_star_1 = 7.02; %[KN/mm] elastic stiffness
T_star_1 = 2*pi*sqrt(mass_starr_1/k_star_1); % [sec] SDFS's period in the X direction
wn_star_1= (2*pi)/T_star_1;

k_f_x(1) = 44.2; % [KN/cm]
k_f_x(2) = 31.7; % [KN/cm]
k_f_x(3) = 31.0; % [KN/cm]
k_f_x(4) = 31.1; % [KN/cm]
k_f_x(5) = 22.3; % [KN/cm]
k_f_x(6) = 20.5; % [KN/cm]
k_f_x(7) = 21.06; % [KN/cm]
k_f_x(8) = 21.01; % [KN/cm]
k_f_x(9) = 21.35; % [KN/cm]

d_yf_x(1) = 20.0; % [mm] Yield displacement of stories
d_yf_x(2) = 20.0; % [mm]
d_yf_x(3) = 20.0; % [mm]
d_yf_x(4) = 20.0;
d_yf_x(5) = 20.0;
d_yf_x(6) = 20.0; % [mm]
d_yf_x(7) = 20.0; % [mm]
d_yf_x(8) = 20.0;
d_yf_x(9) = 20.0;

D_t_1 = 20; %[mm] minimum of Yield displacements of stories, chosen as max ultimate displ for
 Storey 1.
```

```
Mu = 4; % Ductility of the devices

n_eq = 3; % number of plastic cycles excursion
```

- Demand evaluation in terms of energy

```
ag_adim = 0.298 ; % [] it actually is ag/g
Tc_star = 0.356 ; % []
F0 = 2.386 ; % [] maximum amplification factor
g = 9820; % mm/sec2

T_G_x = 0.5;      % [sec] predominant period
T1_x = 1.5; % [sec] calculated by an eignevalue analysis using intitial stiffness of the memb
ers

% Note that those parameters have been taken from CDS and already takes into account PVR(SLV)

% Soil type
cat_suolo = 3; % [from A to E i.e. from 1 to 5]
% Structural damping
Xsi = 5; % [%]

ST = 1.0 ;% [ ] topographic amplification factor

% stratigraphic amplification factor SS [] and soil-dependent coefficient CC []
if cat_suolo == 1
    SS = 1.0;
    CC = 1.0;
end
if cat_suolo == 2
    CC = 1.1 * Tc_star^(-0.2);
    aux = 1.4 - 0.4 * F0 * ag_adim;
    if aux>=1.0 && aux<=1.2
        SS = aux;
    elseif aux < 1.0
        SS = 1.0;
    elseif aux > 1.2
        SS =1.2;
    end
end
if cat_suolo == 3
    CC = 1.05 * Tc_star ^(-0.33);
    aux = 1.7 - 0.6 * F0 * ag_adim;
    if aux>=1.0 && aux<=1.5
        SS = aux;
    elseif aux < 1.0
        SS = 1.0;
    elseif aux > 1.5
        SS =1.5;
    end
end
if cat_suolo == 4
    CC = 1.25 * Tc_star^(-0.5);
    aux = 2.4 - 1.5 * F0 * ag_adim;
    if aux>=0.9 && aux<=1.8
```

```
        SS = aux;
    elseif aux < 0.9
        SS = 0.9;
    elseif aux > 1.8
        SS =1.8;
    end
end
if cat_suolo == 5
    CC = 1.15 * Tc_star^(-0.4);
    aux = 2.0 - 1.1 * F0 * ag_adim;
    if aux>=1.0 && aux<=1.6
        SS = aux;
    elseif aux < 1.0
        SS = 1.0;
    elseif aux > 1.6
        SS =1.6;
    end
end

Tc = Tc_star * CC; %[sec]
Tb = Tc/3; %[sec]
Td = 4.0 * ag_adim + 1.6; %[sec]
eta = sqrt(10/(5+Xsi)); % []
S = SS * ST ; % []

% Evaluating Elastic spectral acceleration for the structure- 5% damping
if T_star_1 >= 0 && T_star_1 < Tb
    Se_1_T_star_1 = ag_adim * g * S * eta * F0 * (T_star_1/Tb + (eta*F0)^(-1.0)*(1-T_star_1/T
b)); % [mm/sec2]
elseif T_star_1 >= Tb && T_star_1 < Tc
    Se_1_T_star_1 = ag_adim * g * S * eta * F0;
elseif T_star_1 >= Tc && T_star_1 < Td
    Se_1_T_star_1 = ag_adim * g * S * eta * F0 * (Tc/T_star_1);
elseif T_star_1 >= Td
    Se_1_T_star_1 = ag_adim * g * S * eta * F0 * (Tc * Td * T_star_1^(-2));
end


SV_5_Percent_x= Se_1_T_star_1/(wn_star_1); %mm 5% damped spectral displacement

E_I = 0.5 * (SV_5_Percent_x)^2 * mass_starr_1; %% Total input energy
E_H_tot = E_I * 0.72 * (1-(1/Mu))^0.7; %% Demadn Hysteretic Energy
```

- Distribution of E_H to story levels

```
E_H = zeros(1,Np);
if Np<5
    for i=1:Np
    E_H(i)=E_H_tot*(2*(Np+1-i)/(Np*(Np+1)));
    end
elseif Np>=5
    for i=1:Np
    E_H(i)= E_H_tot*(2*Np-1)/(Np*(Np-1));
    end
end
```

- Design Strength of EDBs at story 1

```
D_u_1 = d_yf_x(1);
D_y_1 = D_u_1/Mu;
F_y_1 = E_H(1) / (n_eq *(D_u_1-D_y_1)); % Design strength of EDBs at First story [ KN]

%
```

- Distribtion of strength as a function of F_y_1 using Akiyama's formulation

```
alpha_bar_x = zeros(1,Np);    % initialize the vector containing the alpha adimensional value
s
for i = 1:1:Np
    % evaluate the alpha_bar_i for the i-th story and put it in the
    % corresponding cell of vector alpha_bar
    Aux_1_x = (1 - 0.02 * (k_f_x(1)/k_f_x(Np)) - 0.16 * (T1_x/T_G_x));
    Aux_2_x = 0.5 - 0.05 * k_f_x(1)/k_f_x(Np) - 0.3 * T1_x/T_G_x;
    % Auxiliary values to be input in the following expression for alpha_bar(e).
    % It is convenient to evaluate these once for all, since 1) they do not
    % depend on the counter "e", and 2) it is always good idea to split
    % long mathematical expressions to better check them!
    x_bar_x = (i-1)/Np;
    alpha_bar_x(i) = exp( ( Aux_1_x * x_bar_x) - Aux_2_x *(x_bar_x)^2 );
end


  m_t(1) = m_x(1)+m_x(2)+m_x(3)+ m_x(4)+m_x(5)+m_x(6)+m_x(7)+m_x(8)+ m_x(9);
  m_t(2) = m_x(2)+m_x(3)+ m_x(4)+m_x(5)+m_x(6)+m_x(7)+m_x(8)+ m_x(9);
  m_t(3) = m_x(3)+ m_x(4)+m_x(5)+m_x(6)+m_x(7)+m_x(8)+ m_x(9);
  m_t(4) = m_x(4)+m_x(5)+m_x(6)+m_x(7)+m_x(8)+ m_x(9);
  m_t(5) = m_x(5)+m_x(6)+m_x(7)+m_x(8)+ m_x(9);
  m_t(6) = m_x(6)+m_x(7)+m_x(8)+ m_x(9);
  m_t(7) = m_x(7)+m_x(8)+ m_x(9);
  m_t(8) = m_x(8)+ m_x(9);
  m_t(9) = m_x(9);



Gama_x = zeros(1,Np);
for i=1:Np
    Gama_x(i)=m_t(1)/m_t(i);
end

F_y = zeros(1,Np);  %%% Horizontal Component
for i=1:Np
    F_y(i)=F_y_1* alpha_bar_x(i)/Gama_x(i);
end


Nc_x =2 ;
alfa_c_x =31;

F_y_Axial = zeros(1,Np); %%% Axial Component of single brace strength
```

```
for i=1:Np
    F_y_Axial(i) =F_y(i) /(Nc_x * cosd(alfa_c_x));
end


K_s = zeros(1,Np);
for i=1:Np
    K_s(i)=F_y(i)/D_y_1;
end
```

---

*Published with MATLAB® R2018b*

## Benavent-Climent METHOD - CASE-1

```
clear
clc
close all
```

- Existing structure data

```
Np = 3; % Number of the stories
% vector containing information aboutn the masses
m_x(1) = 0.43 ; % Units of the mass are KNxsec2/cm
m_x(2) = 0.43 ; % Units of the mass are KNxsec2/cm
m_x(3) = 0.43 ; % Units of the mass are KNxsec2/cm

Mass_matrix_x=[43.7 0 0  ; 0 43.7 0  ; 0 0 43.7];
Shape_vector_x=[0.4 0.8 1];
r=[1;1;1];
mass_star_x=Shape_vector_x*Mass_matrix_x*r; % 1st mode effective mass

%stiffness (K_f) and yield interstorey displacements (d_yf) at each storey
%of the main structure known from Linear static Analysis

k_f_x(1) = 198.0; % [KN/cm]
k_f_x(2) = 167.5; % [KN/cm]
k_f_x(3) = 201.6; % [KN/cm]

k_f_star_1 = 9.0; %[kN/mm] elastic stiffness

d_yf_x(1) = 2.0; %  [cm]
d_yf_x(2) = 2.0; % [cm]
d_yf_x(3) = 2.0; % [cm]

d_uf_x=3.0;      %  [cm]  ultimate displacemnt from pushover curve

T1_x = 0.63; % [sec] calculated by an eignevalue analysis using intitial stiffness of the mem
bers

% vector containing the height of each story
h(1) = 3.0;     % [m]
h(2) = 3.0;     % [m]
h(3) = 3.0;     % [m]

Max_drift_ratio = 0.5;  % [%]
d_allowable_x = zeros(1,Np);
for t = 1:Np
    d_allowable_x(t) = min( (h(t) * Max_drift_ratio / 100) * 100, d_yf_x(t)) ; % [cm]
end
```

- response spectra and ground motion related data (near-fault ground motion

```
c_1 = 0.23;     % non dimensional
```

```
c_2 = 0.40;      % non dimensional
V_D_max_x = 75.0;    % [cm/sec] spectral velocity,
T_G_x = 0.75;      % [sec] predominant period
T_NH_x = 0.65;     % [sec]
I_d_x = 7.5;       % non dimensional

g = 980.0;           % cm/sec2
```

- Design procedure

```
M_x = sum(m_x);          % Total mass  [KN sec2/cm]
Keq_x=4*(pi^2)*M_x/(T1_x^2);

D_alpha_s_x = 0.01;          % increment of alpha in the procedure below
D_K_x = 0.1;                 % increment of Adimentional K ratios in the procedure below
K_x = zeros(1,Np);           % initialize the vector containing the K ratios = ksi/kfi
for y=1:1:Np
    K_x(y)=0.8;
end

alpha_s1_x=zeros(1,Np);
d_max_x = zeros(1,Np) ;
alpha_bar_x_x = zeros(1,Np);    % initialize the vector containing the alpha adimensional val
ues
for i = 1:1:Np
    % evaluate the alpha_bar_i for the i-th story and put it in the
    % corresponding cell of vector alpha_bar
    Aux_1_x = (1 - 0.02 * (k_f_x(1)/k_f_x(Np)) - 0.16 * (T1_x/T_G_x));
    Aux_2_x = 0.5 - 0.05 * k_f_x(1)/k_f_x(Np) - 0.3 * T1_x/T_G_x;
    % Auxiliary values to be input in the following expression for alpha_bar(e).
    % It is convenient to evaluate these once for all, since 1) they do not
    % depend on the counter "e", and 2) it is always good idea to split
    % long mathematical expressions to better check them!
    x_bar_x = (i-1)/Np;
    alpha_bar_x_x(i) = exp( ( Aux_1_x * x_bar_x) - Aux_2_x *(x_bar_x)^2 );
end


alpha_e_x=(2*pi*V_D_max_x)/(g*T1_x);
X_1_x=k_f_x(1)/Keq_x;


found = 0;      %

while found==0;
    % based on the current values of kfi (stored in the vector k_f) and on
    % the ratios Ki (stored in the vector K), calculate the
    K_x = K_x + D_K_x;

    gama_1_x=zeros(1,Np);
    for i=1:1:Np
        Mass_Ratio(1) = ((m_x(1)+m_x(2)+m_x(3))/M_x);
        Mass_Ratio(2) = ((m_x(2)+m_x(3))/M_x);
        Mass_Ratio(3) = (m_x(3)/M_x);
```

```
        gama_1_x(i)=((alpha_bar_x_x(i)*Mass_Ratio(i)*(K_x(1)+1)/(K_x(i)+1))^2)*(k_f_x(1)*K_x(
i))/(k_f_x(i)*K_x(1));
    end
    Gama_1_x=sum(gama_1_x);

    K_changed=0;
    for i=1:1:Np

        massa(1) = m_x(1)+m_x(2)+m_x(3);
        massa(2) = m_x(2)+m_x(3);
        massa(3) = m_x(3);

        alpha_s1_max_x(i)=d_yf_x(i)*k_f_x(i)*K_x(1)*(K_x(i)+1)/((alpha_bar_x_x(i)*(K_x(1)+1)*
massa(i)*g));
        ffound = 0;
        while ffound==0;
            alpha_s1_x(i) = alpha_s1_x(i)+D_alpha_s_x;
            Alpha_s1_x = alpha_s1_x(i);

            neq_x = 1 + c_1 * I_d_x * sqrt(T_NH_x / T1_x) *( ((K_x(1)*alpha_e_x)/((K_x(1)+1)*
Alpha_s1_x)) -1)^c_2;

            AA_x = alpha_bar_x_x(i) * Alpha_s1_x * (K_x(1)+1) * M_x * g;
            BB_x = k_f_x(i) * (K_x(i)+1);
            CC_x = (2 * neq_x * Gama_1_x /(K_x(1) * X_1_x));
            DD_x = ((alpha_e_x)^2) / (Alpha_s1_x^2) ;
            EE_x = neq_x * Gama_1_x / X_1_x;
            GG_x = (neq_x * Gama_1_x / X_1_x)^2;
            FF_x = sqrt(CC_x+DD_x+GG_x);
            d_max_x(i) = (AA_x/BB_x)* (FF_x - EE_x); % [cm]

            if (d_max_x(i)>d_allowable_x(i) || d_max_x(i)<0.95*d_allowable_x(i)) && alpha_s1_
x(i)<alpha_s1_max_x(i)
                ffound=0;

             elseif (d_max_x(i) >= 0.95*d_allowable_x(i) && d_max_x(i)<= d_allowable_x(i)) &&
 alpha_s1_x(i)<alpha_s1_max_x(i)
                  ffound=1;

             elseif (d_max_x(i)>d_allowable_x(i) || d_max_x(i)<0.95*d_allowable_x(i)) && alph
a_s1_x(i)>alpha_s1_max_x(i)
                alpha_s1_x = zeros(1,Np);
                K_changed = 1;
                break
            end
        end % end of the 2nd "while" loop
        if i == Np && ffound == 1
            found = 1; % I found both the values of K and the alpha_s1
        elseif K_changed == 1
            break
        end

    end % end of the for loop

end % end of the while loop
```

- Brace characteristics evaluation

```
Qy_s_x = zeros(1,Np);     % yield strength of braces in each story
for i=1:Np;
    Qy_s_x(i)=alpha_s1_x(i)*massa(i)*g;
end

k_s_x=zeros(1,Np);  %% [KN/cm]  Brace stiffnes in each story
for i=1:Np;
    k_s_x(i)=k_f_x(i)*K_x(i);
end

N_c_x = 2; % Number of the braces per floor
teta_x = 40 ; %inclination angle of the brace with respect to the horizontal axis

k_s_x_axial = zeros (1,Np); % single brace axial stiffness
for i=1:Np
    k_s_x_axial(i)=k_s_x(i)/(N_c_x * (cosd(teta_x)^2));
end


Mu_x=K_x(1)*((((neq_x*Gama_1_x/X_1_x)^2)+(2*neq_x*Gama_1_x/(K_x(1)*X_1_x))+((alpha_e_x)^2)/((
Alpha_s1_x)^2))^0.5-neq_x*Gama_1_x/X_1_x)-1;

eta_x=neq_x*Mu_x; %% Demand energy coefficent


%%%------------Evaluation of single brace Axial stiffness yield displ and yield force in each
 floor---------

Nc_x=2; %%% Number of braces per floor
alfa_c_x=31; %brace inclination angle in degrees

k_s_req_x = zeros(1,Np); %%% single brace stiffness for each story [KN/cm]
for i=1:Np
    k_s_req_x(i) = k_s_x(i) * (Nc_x^(-1)) * (cosd(alfa_c_x))^(-2);
end

Qy_s_Axial_x = zeros(1,Np); % Axial Force capacity of the brace
for i=1:Np
    Qy_s_Axial_x(i)= Qy_s_x(i)/(Nc_x * cosd(alfa_c_x));
end

Delta_s_y_x= zeros(1,Np); % Axial Yield displacement of brace
for i=1:Np
 Delta_s_y_x(i)= (d_allowable_x(i)/(Mu_x+1))*cosd(alfa_c_x);
end

Delta_axial_x = zeros(1,Np);
for i=1:Np
    Delta_axial_x(i) = Qy_s_Axial_x(i)/k_s_req_x(i);
end
```

*Published with MATLAB® R2018b*

## Benavent-Climent METHOD - CASE-2

```
clear
clc
close all
```

- Existing structure data

```
Np = 5; % Number of the stories

%%%%%%   X-Direction    %%%%%%

% vector containing information aboutn the masses
m_x(1) = 0.43 ; % Units of the mass are KNxsec2/cm
m_x(2) = 0.43 ; % Units of the mass are KNxsec2/cm
m_x(3) = 0.43 ; % Units of the mass are KNxsec2/cm
m_x(4) = 0.43 ; % Units of the mass are KNxsec2/cm
m_x(5) = 0.43 ;

Mass_matrix_x=[43.7 0 0 0 0 ; 0 43.7 0 0 0 ; 0 0 43.7 0 0; 0 0 0 43.7 0; 0 0 0 0 43.7];
Shape_vector_x=[0.2 0.47 0.71 0.89 1];
r=[1;1;1;1;1];
mass_star_x=Shape_vector_x*Mass_matrix_x*r; % 1st mode effective mass

%stiffness (K_f) and yield interstorey displacements (d_yf) at each storey
%of the main structure known from Linear static Analysis

k_f_x(1) = 320.0; % [KN/cm]
k_f_x(2) = 220.5; % [KN/cm]
k_f_x(3) = 220.6; % [KN/cm]
k_f_x(4) = 200.1; % [KN/cm]
k_f_x(5) = 210.5; % [KN/cm]

k_f_star_1 = 65.7; %[kN/cm] elastic stiffness

d_yf_x(1) = 2.0; %  [cm] [5.2]
d_yf_x(2) = 2.0; % [cm]
d_yf_x(3) = 2.0; % [cm] % to be checked for 1.2 as well. Original value = 1.53
d_yf_x(4) = 2.0; %  [cm] [5.2]
d_yf_x(5) = 2.0; % [cm]

d_uf_x=7.0;      %  [cm]  ultimate displacemnt from pushover curve

T1_x = 0.93; % [sec] calculated by an eignevalue analysis using intitial stiffness of the mem
bers

% vector containing the height of each story
h(1) = 3.0;     % [m]
h(2) = 3.0;     % [m]
h(3) = 3.0;     % [m]
h(4) = 3.0;     % [m]
h(5) = 3.0;
```

```
Max_drift_ratio = 0.5;  % [%] As per Fema 356 requirements to achieve IO performace level, th
e story drifts should remain under 1% of the story height
d_allowable_x = zeros(1,Np);
for t = 1:Np
    d_allowable_x(t) = min( (h(t) * Max_drift_ratio / 100) * 100, d_yf_x(t)) ; % [cm]
end
```

- response spectra and ground motion related data (near-fault ground motion

```
c_1 = 0.23;     % non dimensional
c_2 = 0.40;     % non dimensional (c1 and c2 are selected for near-fault ground motion) [72.3
7]
V_D_max_x = 75.0;   % [cm/sec] spectral velocity, Determined from Sv= Se * 1/omega where Omeg
a = 2pi/T1
T_G_x = 0.75;     % [sec] predominant period
T_NH_x = 0.65;    % [sec] Initial period of medium period region in the Newmark and Hall spec
tral representation.
I_d_x = 7.5;      % non dimensional

g = 980.0;           % cm/sec2
```

- Design procedure

```
M_x = sum(m_x);          % Total mass  [KN sec2/cm]
Keq_x=4*(pi^2)*M_x/(T1_x^2);

D_alpha_s_x = 0.01;          % increment of alpha in the procedure below
D_K_x = 0.1;                 % increment of Adimentional K ratios in the procedure below
K_x = zeros(1,Np);           % initialize the vector containing the K ratios = ksi/kfi
for y=1:1:Np
    K_x(y)=0.8;
end



alpha_s1_x=zeros(1,Np);
d_max_x = zeros(1,Np) ;
alpha_bar_x_x = zeros(1,Np);    % initialize the vector containing the alpha adimensional val
ues
for i = 1:1:Np
    % evaluate the alpha_bar_i for the i-th story and put it in the
    % corresponding cell of vector alpha_bar
    Aux_1_x = (1 - 0.02 * (k_f_x(1)/k_f_x(Np)) - 0.16 * (T1_x/T_G_x));
    Aux_2_x = 0.5 - 0.05 * k_f_x(1)/k_f_x(Np) - 0.3 * T1_x/T_G_x;
    % Auxiliary values to be input in the following expression for alpha_bar(e).
    % It is convenient to evaluate these once for all, since 1) they do not
    % depend on the counter "e", and 2) it is always good idea to split
    % long mathematical expressions to better check them!
    x_bar_x = (i-1)/Np;
    alpha_bar_x_x(i) = exp( ( Aux_1_x * x_bar_x) - Aux_2_x *(x_bar_x)^2 );
end
```

```
alpha_e_x=(2*pi*V_D_max_x)/(g*T1_x);
X_1_x=k_f_x(1)/Keq_x;


found = 0;      % initialize this "logical" parameter on "0" meaning "NO, I have not found ye
tth eright values of stiffness,
% stored in vector K" so, please, keep calculating!

while found==0;
    % based on the current values of kfi (stored in the vector k_f) and on
    % the ratios Ki (stored in the vector K), calculate the
    K_x = K_x + D_K_x;

    gama_1_x=zeros(1,Np);
    for i=1:Np
        Mass_Ratio(1) = ((m_x(1)+m_x(2)+m_x(3)+ m_x(4)+m_x(5))/M_x);
        Mass_Ratio(2) = ((m_x(2)+m_x(3)+m_x(4)+m_x(5))/M_x);
        Mass_Ratio(3) = ((m_x(3)+m_x(4)+m_x(5))/M_x);
        Mass_Ratio(4) = ((m_x(4)+m_x(5))/M_x);
        Mass_Ratio(5) = ((m_x(5))/M_x);

        gama_1_x(i)=((alpha_bar_x_x(i)*Mass_Ratio(i)*(K_x(1)+1)/(K_x(i)+1))^2)*(k_f_x(1)*K_x(
i))/(k_f_x(i)*K_x(1));
    end
    Gama_1_x=sum(gama_1_x);

    K_changed=0;
    for i=1:1:Np

        massa(1) = m_x(1)+m_x(2)+m_x(3)+ m_x(4)+m_x(5);
        massa(2) = m_x(2)+m_x(3)+m_x(4)+m_x(5);
        massa(3) = m_x(3)+m_x(4)+m_x(5);
        massa(4) = m_x(4)+m_x(5);
        massa(5) = m_x(5);

        alpha_s1_max_x(i)=d_yf_x(i)*k_f_x(i)*K_x(1)*(K_x(i)+1)/((alpha_bar_x_x(i)*(K_x(1)+1)*
massa(i)*g));
        ffound = 0;
        while ffound==0;        % It means, as long as you have not found the right value of
alpha_s1 for the corrent i-th storey, keep searching!
            alpha_s1_x(i) = alpha_s1_x(i)+D_alpha_s_x;
            Alpha_s1_x = alpha_s1_x(i);

            neq_x = 1 + c_1 * I_d_x * sqrt(T_NH_x / T1_x) *( ((K_x(1)*alpha_e_x)/((K_x(1)+1)*
Alpha_s1_x)) -1)^c_2;

            AA_x = alpha_bar_x_x(i) * Alpha_s1_x * (K_x(1)+1) * M_x * g;
            BB_x = k_f_x(i) * (K_x(i)+1);
            CC_x = (2 * neq_x * Gama_1_x /(K_x(1) * X_1_x));
            DD_x = ((alpha_e_x)^2) / (Alpha_s1_x^2) ;
            EE_x = neq_x * Gama_1_x / X_1_x;
            GG_x = (neq_x * Gama_1_x / X_1_x)^2;
            FF_x = sqrt(CC_x+DD_x+GG_x);
            d_max_x(i) = (AA_x/BB_x)* (FF_x - EE_x); % [cm]

            if (d_max_x(i)>d_allowable_x(i) || d_max_x(i)<0.95*d_allowable_x(i)) && alpha_s1_
x(i)<alpha_s1_max_x(i)
```

```
                ffound=0;

            elseif (d_max_x(i) >= 0.95*d_allowable_x(i) && d_max_x(i)<= d_allowable_x(i)) &&
 alpha_s1_x(i)<alpha_s1_max_x(i)
                    ffound=1;

            elseif (d_max_x(i)>d_allowable_x(i) || d_max_x(i)<0.95*d_allowable_x(i)) && alph
a_s1_x(i)>alpha_s1_max_x(i)
                alpha_s1_x = zeros(1,Np); % In this case, annull each value of alpha_s1 that
you've already stored, and start from the beginning of the 1st "while" cycle, by increasing t
he K values
                K_changed = 1; % if this is the case, meaning that you have to increment the
values of stiffness stored in the vector K, exit the "while" cycle (the 2nd or nested one)
                break
            end
        end % end of the 2nd "while" loop
        if i == Np && ffound == 1
            found = 1; % I found both the values of K and the alpha_s1
        elseif K_changed == 1
            break
        end

    end % end of the for loop

end % end of the while loop
```

- Brace characteristics evaluation

```
Qy_s_x = zeros(1,Np);      % yield strength of braces in each story
for i=1:Np;
    Qy_s_x(i)=alpha_s1_x(i)*massa(i)*g;
end

k_s_x=zeros(1,Np);  %% [KN/cm]  Brace stiffnes in each story
for i=1:Np;
    k_s_x(i)=k_f_x(i)*K_x(i);
end

N_c_x = 2; % Number of the braces per floor
teta_x = 31.0 ; %inclination angle of the brace with respect to the horizontal axis

k_s_x_axial = zeros (1,Np); % single brace axial stiffness
for i=1:Np
    k_s_x_axial(i)=k_s_x(i)/(N_c_x * (cosd(teta_x)^2));
end


Mu_x=K_x(1)*((((neq_x*Gama_1_x/X_1_x)^2)+(2*neq_x*Gama_1_x/(K_x(1)*X_1_x))+((alpha_e_x)^2)/((
Alpha_s1_x)^2))^0.5-neq_x*Gama_1_x/X_1_x)-1; %%Placticity coefficient of the device

eta_x=neq_x*Mu_x; %% Demand energy coefficent that should be smaller than the brace energy di
ssipation capacity coefficent (eta-u), eq-10.


%%%------------Evaluation of single brace Axial stiffness yield displ and yield force in each
```

```
 floor---------

Nc_x=2; %%% Number of braces per floor
alfa_c_x=31; %brace inclination angle in degrees

k_s_req_x = zeros(1,Np); %%% single brace stiffness for each story [KN/cm]
for i=1:Np
    k_s_req_x(i) = k_s_x(i) * (Nc_x^(-1)) * (cosd(alfa_c_x))^(-2);
end

Qy_s_Axial_x = zeros(1,Np); % Axial Force capacity of the brace
for i=1:Np
    Qy_s_Axial_x(i)= Qy_s_x(i)/(Nc_x * cosd(alfa_c_x));
end

Delta_s_y_x= zeros(1,Np); % Axial Yield displacement of brace
for i=1:Np
 Delta_s_y_x(i)= (d_allowable_x(i)/(Mu_x+1))*cosd(alfa_c_x);
end

Delta_axial_x = zeros(1,Np);
for i=1:Np
    Delta_axial_x(i) = Qy_s_Axial_x(i)/k_s_req_x(i);
end
```

---

*Published with MATLAB® R2018b*

## Benavent-Climent METHOD - CASE-3

```
clear
clc
close all
```

- Existing structure data

```
Np = 9; % Number of the stories

% vector containing information aboutn the masses
m_x(1) = 0.66 ; % Units of the mass are KNxsec2/cm
m_x(2) = 0.66 ; % Units of the mass are KNxsec2/cm
m_x(3) = 0.66 ; % Units of the mass are KNxsec2/cm
m_x(4) = 0.66 ; % Units of the mass are KNxsec2/cm
m_x(5) = 0.43 ;
m_x(6) = 0.43 ; % Units of the mass are KNxsec2/cm
m_x(7) = 0.43 ; % Units of the mass are KNxsec2/cm
m_x(8) = 0.43 ; % Units of the mass are KNxsec2/cm
m_x(9) = 0.43 ;

Mass_matrix_x=[0.66 0 0 0 0 0 0 0 0 ; 0 0.66 0 0 0 0 0 0 0 ; 0 0 0.66 0 0 0 0 0 0 ; 0 0 0 0.6
6 0 0 0 0 0 ; 0 0 0 0 0 0.43 0 0 0 0; 0 0 0 0 0 0 0.43 0 0 0; 0 0 0 0 0 0 0 0.43 0 0; 0 0 0 0 0 0 0 0
 0.43 0; 0 0 0 0 0 0 0 0 0 0.43];;
Shape_vector_x=[0.1 0.24 0.38 0.5 0.64 0.77 0.88 0.95 1];
r=[1;1;1;1;1;1;1;1;1];
mass_star_x=Shape_vector_x*Mass_matrix_x*r; % 1st mode effective mass

%stiffness (K_f) and yield interstorey displacements (d_yf) at each storey
%of the main structure known from Linear static Analysis

k_f_x(1) = 442.0; % [KN/cm]
k_f_x(2) = 317.5; % [KN/cm]
k_f_x(3) = 310.6; % [KN/cm]
k_f_x(4) = 311.1; % [KN/cm]
k_f_x(5) = 223.5; % [KN/cm]
k_f_x(6) = 206.5; % [KN/cm]
k_f_x(7) = 215.6; % [KN/cm]
k_f_x(8) = 210.1; % [KN/cm]
k_f_x(9) = 213.5; % [KN/cm]

k_f_star_1 = 70.02; %[kN/cm] elastic stiffness

d_yf_x(1) = 2.0; %  [cm] [5.2]
d_yf_x(2) = 2.0; % [cm]
d_yf_x(3) = 2.0; % [cm] % to be checked for 1.2 as well. Original value = 1.53
d_yf_x(4) = 2.0; %  [cm] [5.2]
d_yf_x(5) = 2.0; % [cm]
d_yf_x(6) = 2.0; % [cm]
d_yf_x(7) = 2.0; % [cm] % to be checked for 1.2 as well. Original value = 1.53
d_yf_x(8) = 2.0; %  [cm] [5.2]
d_yf_x(9) = 2.0; % [cm]
```

```
d_uf_x=7.0;      %  [cm]  ultimate displacemnt from pushover curve

T1_x = 1.5; % [sec] calculated by an eignevalue analysis using intitial stiffness of the memb
ers

% vector containing the height of each story
h(1) = 3.0;     % [m]
h(2) = 3.0;     % [m]
h(3) = 3.0;     % [m]
h(4) = 3.0;     % [m]
h(5) = 3.0;
h(6) = 3.0;     % [m]
h(7) = 3.0;     % [m]
h(8) = 3.0;     % [m]
h(9) = 3.0;


Max_drift_ratio = 0.5;  % [%] As per Fema 356 requirements to achieve IO performace level, th
e story drifts should remain under 1% of the story height
d_allowable_x = zeros(1,Np);
for t = 1:Np
    d_allowable_x(t) = min( (h(t) * Max_drift_ratio / 100) * 100, d_yf_x(t)) ; % [cm]
end
```

- response spectra and ground motion related data (near-fault ground motion

```
c_1 = 0.23;     % non dimensional
c_2 = 0.40;     % non dimensional (c1 and c2 are selected for near-fault ground motion) [72.3
7]
V_D_max_x = 75.0;   % [cm/sec] spectral velocity, Determined from Sv= Se * 1/omega where Omeg
a = 2pi/T1
T_G_x = 0.75;     % [sec] predominant period
T_NH_x = 0.65;    % [sec] Initial period of medium period region in the Newmark and Hall spec
tral representation.
I_d_x = 7.5;      % non dimensional

g = 980.0;           % cm/sec2
```

- Design procedure

```
M_x = sum(m_x);          % Total mass  [KN sec2/cm]
Keq_x=4*(pi^2)*M_x/(T1_x^2);


D_alpha_s_x = 0.01;          % increment of alpha in the procedure below
D_K_x = 0.1;                 % increment of Adimentional K ratios in the procedure below
K_x = zeros(1,Np);           % initialize the vector containing the K ratios = ksi/kfi
for y=1:1:Np
    K_x(y)=0.8;
end
```

```
alpha_s1_x=zeros(1,Np);
d_max_x = zeros(1,Np) ;
alpha_bar_x_x = zeros(1,Np);    % initialize the vector containing the alpha adimensional val
ues
for i = 1:1:Np
    % evaluate the alpha_bar_i for the i-th story and put it in the
    % corresponding cell of vector alpha_bar
    Aux_1_x = (1 - 0.02 * (k_f_x(1)/k_f_x(Np)) - 0.16 * (T1_x/T_G_x));
    Aux_2_x = 0.5 - 0.05 * k_f_x(1)/k_f_x(Np) - 0.3 * T1_x/T_G_x;
    % Auxiliary values to be input in the following expression for alpha_bar(e).
    % It is convenient to evaluate these once for all, since 1) they do not
    % depend on the counter "e", and 2) it is always good idea to split
    % long mathematical expressions to better check them!
    x_bar_x = (i-1)/Np;
    alpha_bar_x_x(i) = exp( ( Aux_1_x * x_bar_x) - Aux_2_x *(x_bar_x)^2 );
end


alpha_e_x=(2*pi*V_D_max_x)/(g*T1_x);
X_1_x=k_f_x(1)/Keq_x;


found = 0;      % initialize this "logical" parameter on "0" meaning "NO, I have not found ye
tth eright values of stiffness,
% stored in vector K" so, please, keep calculating!

while found==0;
    % based on the current values of kfi (stored in the vector k_f) and on
    % the ratios Ki (stored in the vector K), calculate the
    K_x = K_x + D_K_x;

    gama_1_x=zeros(1,Np);
    for i=1:Np
        Mass_Ratio(1) = ((m_x(1)+m_x(2)+m_x(3)+ m_x(4)+m_x(5)+m_x(6)+m_x(7)+m_x(8)+ m_x(9))/M
_x);
        Mass_Ratio(2) = ((m_x(2)+m_x(3)+ m_x(4)+m_x(5)+m_x(6)+m_x(7)+m_x(8)+ m_x(9))/M_x);
        Mass_Ratio(3) = ((m_x(3)+ m_x(4)+m_x(5)+m_x(6)+m_x(7)+m_x(8)+ m_x(9))/M_x);
        Mass_Ratio(4) = ((m_x(4)+m_x(5)+m_x(6)+m_x(7)+m_x(8)+ m_x(9))/M_x);
        Mass_Ratio(5) = ((m_x(5)+m_x(6)+m_x(7)+m_x(8)+ m_x(9))/M_x);
        Mass_Ratio(6) = ((m_x(6)+m_x(7)+m_x(8)+ m_x(9))/M_x);
        Mass_Ratio(7) = ((m_x(7)+m_x(8)+ m_x(9))/M_x);
        Mass_Ratio(8) = ((m_x(8)+ m_x(9))/M_x);
        Mass_Ratio(9) = ((m_x(9))/M_x);


        gama_1_x(i)=((alpha_bar_x_x(i)*Mass_Ratio(i)*(K_x(1)+1)/(K_x(i)+1))^2)*(k_f_x(1)*K_x(
i))/(k_f_x(i)*K_x(1));
    end
    Gama_1_x=sum(gama_1_x);

    K_changed=0;
    for i=1:1:Np
        massa(1) = m_x(1)+m_x(2)+m_x(3)+ m_x(4)+m_x(5)+m_x(6)+m_x(7)+m_x(8)+ m_x(9);
        massa(2) = m_x(2)+m_x(3)+ m_x(4)+m_x(5)+m_x(6)+m_x(7)+m_x(8)+ m_x(9);
        massa(3) = m_x(3)+ m_x(4)+m_x(5)+m_x(6)+m_x(7)+m_x(8)+ m_x(9);
        massa(4) = m_x(4)+m_x(5)+m_x(6)+m_x(7)+m_x(8)+ m_x(9);
        massa(5) = m_x(5)+m_x(6)+m_x(7)+m_x(8)+ m_x(9);
```

```
        massa(6) = m_x(6)+m_x(7)+m_x(8)+ m_x(9);
        massa(7) = m_x(7)+m_x(8)+ m_x(9);
        massa(8) = m_x(8)+ m_x(9);
        massa(9) = m_x(9);

        alpha_s1_max_x(i)=d_yf_x(i)*k_f_x(i)*K_x(1)*(K_x(i)+1)/((alpha_bar_x_x(i)*(K_x(1)+1)*
massa(i)*g));
        ffound = 0;
        while ffound==0;        % It means, as long as you have not found the right value of
alpha_s1 for the corrent i-th storey, keep searching!
            alpha_s1_x(i) = alpha_s1_x(i)+D_alpha_s_x;
            Alpha_s1_x = alpha_s1_x(i);

            neq_x = 1 + c_1 * I_d_x * sqrt(T_NH_x / T1_x) *( ((K_x(1)*alpha_e_x)/((K_x(1)+1)*
Alpha_s1_x)) -1)^c_2;

            AA_x = alpha_bar_x_x(i) * Alpha_s1_x * (K_x(1)+1) * M_x * g;
            BB_x = k_f_x(i) * (K_x(i)+1);
            CC_x = (2 * neq_x * Gama_1_x /(K_x(1) * X_1_x));
            DD_x = ((alpha_e_x)^2) / (Alpha_s1_x^2) ;
            EE_x = neq_x * Gama_1_x / X_1_x;
            GG_x = (neq_x * Gama_1_x / X_1_x)^2;
            FF_x = sqrt(CC_x+DD_x+GG_x);
            d_max_x(i) = (AA_x/BB_x)* (FF_x - EE_x); % [cm]

            if (d_max_x(i)>d_allowable_x(i) || d_max_x(i)<0.95*d_allowable_x(i)) && alpha_s1_
x(i)<alpha_s1_max_x(i)
                ffound=0;

             elseif (d_max_x(i) >= 0.95*d_allowable_x(i) && d_max_x(i)<= d_allowable_x(i)) &&
 alpha_s1_x(i)<alpha_s1_max_x(i)
                  ffound=1;

             elseif (d_max_x(i)>d_allowable_x(i) || d_max_x(i)<0.95*d_allowable_x(i)) && alph
a_s1_x(i)>alpha_s1_max_x(i)
                alpha_s1_x = zeros(1,Np); % In this case, annull each value of alpha_s1 that
you've already stored, and start from the beginning of the 1st "while" cycle, by increasing t
he K values
                K_changed = 1; % if this is the case, meaning that you have to increment the
values of stiffness stored in the vector K, exit the "while" cycle (the 2nd or nested one)
                break
            end
        end % end of the 2nd "while" loop
        if i == Np && ffound == 1
            found = 1; % I found both the values of K and the alpha_s1
        elseif K_changed == 1
            break
        end

    end % end of the for loop

end % end of the while loop
```

- Brace characteristics evaluation

```
Qy_s_x = zeros(1,Np);     % yield strength of braces in each story
for i=1:Np;
    Qy_s_x(i)=alpha_s1_x(i)*massa(i)*g;
end

k_s_x=zeros(1,Np);  %% [KN/cm]  Brace stiffnes in each story
for i=1:Np;
    k_s_x(i)=k_f_x(i)*K_x(i);
end

N_c_x = 2; % Number of the braces per floor
teta_x = 31.0 ; %inclination angle of the brace with respect to the horizontal axis

k_s_x_axial = zeros (1,Np); % single brace axial stiffness
for i=1:Np
    k_s_x_axial(i)=k_s_x(i)/(N_c_x * (cosd(teta_x)^2));
end


Mu_x=K_x(1)*((((neq_x*Gama_1_x/X_1_x)^2)+(2*neq_x*Gama_1_x/(K_x(1)*X_1_x))+((alpha_e_x)^2)/((
Alpha_s1_x)^2))^0.5-neq_x*Gama_1_x/X_1_x)-1; %%Placticity coefficient of the device

eta_x=neq_x*Mu_x; %% Demand energy coefficent that should be smaller than the brace energy di
ssipation capacity coefficent (eta-u), eq-10.


% Evaluation of single brace Axial stiffness yield displ and yield force in each floor-------
--

Nc_x=2; %%% Number of braces per floor
alfa_c_x=31; %brace inclination angle in degrees

k_s_req_x = zeros(1,Np); %%% single brace stiffness for each story [KN/cm]
for i=1:Np
    k_s_req_x(i) = k_s_x(i) * (Nc_x^(-1)) * (cosd(alfa_c_x))^(-2);
end

Qy_s_Axial_x = zeros(1,Np); % Axial Force capacity of the brace
for i=1:Np
    Qy_s_Axial_x(i)= Qy_s_x(i)/(Nc_x * cosd(alfa_c_x));
end

Delta_s_y_x= zeros(1,Np); % Axial Yield displacement of brace
for i=1:Np
 Delta_s_y_x(i)= (d_allowable_x(i)/(Mu_x+1))*cosd(alfa_c_x);
end

Delta_axial_x = zeros(1,Np);
for i=1:Np
    Delta_axial_x(i) = Qy_s_Axial_x(i)/k_s_req_x(i);
end
```

---

*Published with MATLAB® R2018b*

## Ponzo-Di Cesare Method - CASE-1

```
clear
clc
close all
```

- Existing structure data

```
Np = 3 ; % Number of floors []

% storey heights in meters
H(1) = 3.0;
H(2) = 3.0;
H(3) = 3.0;

% DIRECTION 1 (X)
% Hereafter are forces and displacements at each floor obtained by a Linear Static Analysis
% Note that the first number in the label refers to the direction in plant: where 1 stands fo
r X and 2 for Y
Fp_1(1) = 130.1 ; % [kN]
Fp_1(2) = 257.5 ; % [kN]
Fp_1(3) = 369.0 ; % [kN]

Dp_1(1) = 38.2; % [mm] % Interstorey Drifts
Dp_1(2) = 37.4; % [mm]
Dp_1(3) = 18.3; % [mm]

Mass_matrix_1=[43.7 0 0  ; 0 43.7 0  ; 0 0 43.7];
Shape_vector_1=[0.4 0.8 1];
r=[1;1;1];
mass_starr_1=Shape_vector_1*Mass_matrix_1*r; % 1st mode effective mass

% Note that those above are relative displacements
% Hereafter evaluate the total displacements for each direction
Dp_tot_1 = 0.0; % [mm]
for i=1:Np
    Dp_tot_1 = Dp_tot_1 + Dp_1(i);
end


k_star_1 = 9.0; %[kN/mm] elastic stiffness from pushover anlaysis
Fy_star_1 = 238.8; % [kN] yielding strength
dy_star_1 = Fy_star_1/k_star_1 ; % Yield displacement from Pushover
du_star_1 = 100.0; % [mm] ultimate displacement
massa_star_1=mass_starr_1; % [tonn]
mu_c_1 = 8 ; %[ ] equivalent bracing's ductility (you're the one to fix, in advance, that par
ameter

alfa_disp = 0.95; %[ ] this is a parameter defining the amount of the structure ultimate disp
lacement you're accepting as target displacement

% EVALUATION OF EACH STORY'S STIFFNESS (Existing Structure)
```

```
ki_1 = zeros(1,Np);  % Preallocate vector
for i=1:Np
    AUX = 0;
    for j=i:Np
        AUX = AUX + Fp_1(j); % [kN]
        % this is the sum of all the forces from the current i-th floor above
    end
    ki_1(i)= (Dp_1(i)^(-1))* AUX  ; % [kN/mm]
end


% Knowing the Dp_tot, DP_i, and d_star from pushover ,we can define the yield displacement of
 each storey
% Knowing the k(i) and dy(i) ,we can define the Fy_i of each storey

 dy_p_1 = zeros(1,Np);
for i=1:Np
    dy_p_1(i)= Dp_1(i) * (Dp_tot_1^(-1)) * dy_star_1; % [mm] Formulation to be checked!!
end

% Yield Force at each floor
Fy_p_1 = zeros(1,Np);
for i=1:Np
    Fy_p_1(i)= dy_p_1(i) * ki_1(i); % [kN]
end
```

- Input parameters defining the seismic spectrum

```
ag_adim = 0.298 ; % [] it actually is ag/g
Tc_star = 0.356 ; % []
F0 = 2.386 ; % [] maximum amplification factor
% Note that those parameters have been taken from CDS and already takes into account PVR(SLV)

% Soil type
cat_suolo = 3; % [from A to E i.e. from 1 to 5]
% Structural damping
Xsi = 5; % [%]

ST = 1.0 ;% [ ] topographic amplification factor
```

- Brace characteristics evaluation

```
Nc_1 = 2; % []
alfa_c = 31.0; % [°] braces' inclination angle
% note that the assumption is done that all the braces have the same
% inclination with respect to the horizontal

% STEEL BAR ON WHICH THE BRACE IS INSTALLED
Aa = 53.831; % [cm2] cross-section area
Ea = 210000.0; % [N/mm2] Steel Young's Modulus
La = 5.0; % [m] length
fyk = 355.0; % [MPa]
gamma_M_0 = 1.05; % []
```

```
%%%%%%%%%%%%%%%%%%%%%%%%%%%%%%%%%%%%%%%%%%%%%%%%%%%%%%%%%%%%%%%%%%%%%%%%%%%%%%%
%                     Second phase: DERIVED DATA                                %
%%%%%%%%%%%%%%%%%%%%%%%%%%%%%%%%%%%%%%%%%%%%%%%%%%%%%%%%%%%%%%%%%%%%%%%%%%%%%%%

% Seismic Spectrum
% stratigraphic amplification factor SS [] and soil-dependent coefficient CC []
if cat_suolo == 1
    SS = 1.0;
    CC = 1.0;
end
if cat_suolo == 2
    CC = 1.1 * Tc_star^(-0.2);
    aux = 1.4 - 0.4 * F0 * ag_adim;
    if aux>=1.0 && aux<=1.2
        SS = aux;
    elseif aux < 1.0
        SS = 1.0;
    elseif aux > 1.2
        SS =1.2;
    end
end
if cat_suolo == 3
    CC = 1.05 * Tc_star ^(-0.33);
    aux = 1.7 - 0.6 * F0 * ag_adim;
    if aux>=1.0 && aux<=1.5
        SS = aux;
    elseif aux < 1.0
        SS = 1.0;
    elseif aux > 1.5
        SS =1.5;
    end
end
if cat_suolo == 4
    CC = 1.25 * Tc_star^(-0.5);
    aux = 2.4 - 1.5 * F0 * ag_adim;
    if aux>=0.9 && aux<=1.8
        SS = aux;
    elseif aux < 0.9
        SS = 0.9;
    elseif aux > 1.8
        SS =1.8;
    end
end
if cat_suolo == 5
    CC = 1.15 * Tc_star^(-0.4);
    aux = 2.0 - 1.1 * F0 * ag_adim;
    if aux>=1.0 && aux<=1.6
        SS = aux;
    elseif aux < 1.0
        SS = 1.0;
    elseif aux > 1.6
        SS =1.6;
    end
end

Tc = Tc_star * CC; %[sec]
```

```
Tb = Tc/3; %[sec]
Td = 4.0 * ag_adim + 1.6; %[sec]
eta = sqrt(10/(5+Xsi)); % []
S = SS * ST ; % []

% Definition of the target displacement for the brace of both directions. Note that you
% can define it as a certain percentage of the structure's ultimate displacement
d_allowed =zeros(1,Np);
for i=1:Np
    d_allowed(i) = 0.005*H(i)*1000;
end
D_allowed = sum(d_allowed); % The allowed 0.5% limit storey drift for BDE from Code


d_u_pushover_1 = alfa_disp * du_star_1; %[mm] 95 % displacement from pushover

Mu_allowed = 1.5; % Allowed ductility for the existing structures is Mu_allowed = 1.5 [NTC]
if du_star_1/dy_star_1 <= Mu_allowed
    D_allowed_Ductility_1 = du_star_1 ;
elseif du_star_1/dy_star_1 > Mu_allowed
    D_allowed_Ductility_1 = dy_star_1 * Mu_allowed;
end


ds_target_1 = min ([d_u_pushover_1 D_allowed  D_allowed_Ductility_1]); %% The final target di
splacement

% Steel bar elastic stiffness
 ka = 0.0001 * (Ea * Aa) / La; % [kN/mm]                                    dimensionally co
rrect
Fy_a = (Aa * fyk / gamma_M_0) * 0.1; % [kN]

%%%%%%%%%%%%%%%%%%%%%%%%%%%%%%%%%%%%%%%%%%%%%%%%%%%%%%%%%%%%%%%%%%%%%%%%%%%%%%%
%                                  PROCEDURE                                    %
%%%%%%%%%%%%%%%%%%%%%%%%%%%%%%%%%%%%%%%%%%%%%%%%%%%%%%%%%%%%%%%%%%%%%%%%%%%%%%%


% ITERATIVE PROCEDURE TO EVALUATE THE EQUIVALENT BRACE (for the two directions)
% INITIALIZATION
T_star_1 = 2*pi*sqrt(massa_star_1/k_star_1)*sqrt(0.001); % [sec] SDFS's period in the X direc
tion     check dimesionally!!!!!!!!!!!!!!!!!!!!!!!!!!!!!!
wn_star_1= (2*pi)/T_star_1;

% hereabove, I initialize the periods whose values will be successively
% iteratively updated
% ( The values are wrong, Formulation needs to be checked)
if T_star_1 >= 0 && T_star_1 < Tb
    Se_1_T_star_1 = ag_adim * 9.81 * S * eta * F0 * (T_star_1/Tb + (eta*F0)^(-1.0)*(1-T_star_
1/Tb)); % [m/sec2]
elseif T_star_1 >= Tb && T_star_1 < Tc
    Se_1_T_star_1 = ag_adim * 9.81 * S * eta * F0;
elseif T_star_1 >= Tc && T_star_1 < Td
    Se_1_T_star_1 = ag_adim * 9.81 * S * eta * F0 * (Tc/T_star_1);
elseif T_star_1 >= Td
    Se_1_T_star_1 = ag_adim * 9.81 * S * eta * F0 * (Tc * Td * T_star_1^(-2));
end
```

```
% Note that the values of acceleration above are in [m/sec2]

dcy_1 = ds_target_1 / mu_c_1; % [mm] Brace Yield Displacement (Ratio of Target displacement a
nd Brace ductility)

Fc_1=0;
Delta_Fc_1=0.01;
K_Str_Brace_1=k_star_1;


found = 0;
while found == 0;
    Fc_1=Fc_1+Delta_Fc_1;
    K_c_1=Fc_1/dcy_1;
    K_Str_Brace_1=k_star_1 + K_c_1;
    T_Str_Brace_1 = 2*pi* sqrt(massa_star_1/(1000*K_Str_Brace_1));

     if T_Str_Brace_1 >= 0 && T_Str_Brace_1 < Tb
        Se_1_T_Str_Brace_1 = ag_adim * 9.81 * S * eta * F0 * (T_Str_Brace_1/Tb + (eta*F0)^(-1
.0)*(1-T_Str_Brace_1/Tb));
    elseif T_Str_Brace_1 >= Tb && T_Str_Brace_1 < Tc
        Se_1_T_Str_Brace_1 = ag_adim * 9.81 * S * eta * F0;
    elseif T_Str_Brace_1 >= Tc && T_Str_Brace_1 < Td
        Se_1_T_Str_Brace_1 = ag_adim * 9.81 * S * eta * F0 * (Tc/T_Str_Brace_1);
    elseif T_Str_Brace_1 >= Td
        Se_1_T_Str_Brace_1 = ag_adim * 9.81 * S * eta * F0 * (Tc * Td * T_Str_Brace_1^(-2));
    end

    d_e_Str_Brace_1=1000*Se_1_T_Str_Brace_1 *(T_Str_Brace_1/(2*pi))^2 ;
    if T_Str_Brace_1 < Tc

        q_Str_Brace_1=1000*Se_1_T_Str_Brace_1 * 1000*massa_star_1 /Fy_star_1 ;
        d_t_Str_Brace_1= d_e_Str_Brace_1 *(1+(q_Str_Brace_1-1)*Tc/Tb)/q_Str_Brace_1 ;
    elseif T_Str_Brace_1>Tc
        d_t_Str_Brace_1=d_e_Str_Brace_1;
    end

    if d_t_Str_Brace_1 <= ds_target_1 && d_t_Str_Brace_1>=0.95*ds_target_1;
        found=1;

    end
end



% EACH FLOOR'S EQUIVALENT BRACE STIFFNESS AND YIELD FORCE X direction

% Yield Force of Braces for whole story
Fy_c_1 = zeros(1,Np);
for i=1:Np
    Fy_c_1(i)= Fy_p_1(i) * Fc_1 * Fy_star_1^(-1); % [kN]
end
% Brace stiffness for whole story that will be iterated if regularity conditions dont satisfy
kk_c_1 = zeros(1,Np);
for i=1:Np
    kk_c_1(i)= K_c_1 * ki_1(i) * k_star_1^(-1); % [kN/mm]
```

```
end

% Total story stiffness K_tot_1, sum of existing structure stiffness ki_1(i) and brace stiffn
ess(kk_c_1(i)
K_tot_1=zeros(1,Np);
for i=1:1:Np
    K_tot_1(i)=kk_c_1(i)+ki_1(i);
end

% Story stiffness regularity conditions verification, After this step the Brace story stiffne
ss will be named kk_c_req

kk_c_new_1 = zeros(1,Np);
for i=2:Np
    if (K_tot_1(i-1)-K_tot_1(i)) /K_tot_1(i-1)> 0.3;
        kk_c_new_1(i)=0.7*K_tot_1(i-1)-ki_1(i)-kk_c_1(i);

        kk_c_req_1= zeros(1,Np);
        for k=1:Np
    kk_c_req_1(k)=kk_c_new_1(k)+kk_c_1(k);
        end

        K_tot_req_1 = zeros(1,Np);
        for h=1:Np
    K_tot_req_1(h)=ki_1(h)+kk_c_req_1(h);
    K_tot_1(h)= K_tot_req_1(h);
        end



    elseif (K_tot_1(i-1)-K_tot_1(i)) /K_tot_1(i-1)<-0.1;
        kk_c_new_1(i-1)=((K_tot_1(i)/1.1)-ki_1(i-1))-kk_c_1(i-1);

        kk_c_req_1= zeros(1,Np);
        for j=1:Np
    kk_c_req_1(j)=kk_c_new_1(j)+kk_c_1(j);
        end


    kk_c_1 = zeros(1,Np);
    K_tot_req_1 = zeros(1,Np);
        for h=1:Np
    K_tot_req_1(h)=ki_1(h)+kk_c_req_1(h);
    K_tot_1(h)= K_tot_req_1(h);
    kk_c_1(h) = kk_c_req_1(h);
        end

    elseif (K_tot_1(i-1)-K_tot_1(i)) /K_tot_1(i-1)>=-0.1 && (K_tot_1(i-1)-K_tot_1(i)) /K_tot_
1(i-1)<0.3;
         kk_c_req_1=zeros(1,Np);
        for j=1:Np
            kk_c_req_1(j)=kk_c_1(j);
            K_tot_req_1(j)= kk_c_req_1(j)+ki_1(j);
        end

    end
```

```
end


% DISTRIBUTION OF THE FLOOR BRACE
% AS FUNCTION OF THEIR NUMBER AND DISTRIBUTION IN PLAN


kkk_c_1 = zeros(1,Np); %%% single brace stiffness for each story
for i=1:Np
    kkk_c_1(i) = kk_c_req_1(i) * (Nc_1^(-1)) * (cosd(alfa_c))^(-2);
end

% here above the axial stiffness of each brace was evaluated for each floor, having assumed t
he same inclination angle for all of them
ffy_c_1 = zeros(1,Np); %%% single brace lateral strength for each story
for l=1:Np
    ffy_c_1(l) = Fy_c_1(l)/((Nc_1) * (cosd(alfa_c)));
end
% here above the axial yeild force of each brace was evaluated for each floor, having assumed
 the same inclination angle for all of them

d_c_y_axial_1 = zeros(1,Np); % [mm] Yield displacement of the brace at ith floor
for i=1:Np
    d_c_y_axial_1(i) = ffy_c_1(i)/kkk_c_1(i);
end


% DEVICE CHARACTERISTICS AT EACH FLOOR
% yield force
ffy_d_1 = zeros(1,Np);
for i=1:Np
    ffy_d_1(i) = ffy_c_1(i); % the correction is made for A(I) = B , to be checked
    if (Fy_a - ffy_d_1(i))<= 0.0
        warning('bar stiffness smaller than the device stiffness')
    end
end
% stiffness
kkk_d_1 = zeros(1,Np);
for i=1:Np
    kkk_d_1(i) = kkk_c_1(i) * ka / (ka - kkk_c_1(i));
    if (ka - kkk_c_1(i))<= 0.0
        warning('bar stiffness smaller than the device stiffness')
    end
end
% ductility
mu_d_1 = zeros(1,Np);
for i=1:Np
    mu_d_1(i) = ((ka + kkk_d_1(i)) * mu_c_1 - kkk_d_1(i)) / ka; % [kN/mm]
end


% Make also a drawing to have a better representation of the results
```

## Ponzo-Di Cesare Method - CASE-2

```
clear
clc
close all
```

- Existing structure data

```
Np = 5 ; % Number of floors []

% storey heights in meters
H(1) = 3.0;
H(2) = 3.0;
H(3) = 3.0;
H(4) = 3.0;
H(5) = 3.0;

% DIRECTION 1 (X)
% Hereafter are forces and displacements at each floor obtained by a Linear Static Analysis
% Note that the first number in the label refers to the direction in plant: where 1 stands fo
r X and 2 for Y
Fp_1(1) = 63.4 ;  % [kN]
Fp_1(2) = 126.7 ; % [kN]
Fp_1(3) = 190.2 ; % [kN]
Fp_1(4) = 253.6 ; % [kN]
Fp_1(5) = 316.9 ; % [kN]

Dp_1(1) = 29.7; % [mm] % Interstorey Drifts
Dp_1(2) = 39.3; % [mm]
Dp_1(3) = 34.3; % [mm]
Dp_1(4) = 25.8; % [mm]
Dp_1(5) = 14.7; % [mm]

Mass_matrix_1=[43.7 0 0 0 0  ; 0 43.7 0 0 0  ; 0 0 43.7 0 0 ; 0 0 0 43.7 0 ; 0 0 0 0 43.7];
Shape_vector_1=[0.2 0.47 0.71 0.89 1];
r=[1;1;1;1;1];
mass_starr_1=Shape_vector_1*Mass_matrix_1*r; % 1st mode effective mass



% Note that those above are relative displacements
% Hereafter evaluate the total displacements for each direction
Dp_tot_1 = 0.0; % [mm]
for i=1:Np
    Dp_tot_1 = Dp_tot_1 + Dp_1(i);
end


% First phase: INPUT DATA
% input the parameters defining the capacity spectrum for the
% existing structure's two directions. Where, note those informations can be got by means of
% whatever FEM (commercial) software.
```

```
% First Direction (X)
k_star_1 = 6.57; %[kN/mm] elastic stiffness
Fy_star_1 = 480.0; % [kN] yielding strength
dy_star_1 = Fy_star_1/k_star_1 ; % Yield displacement from Pushover
du_star_1 = 107.0; % [mm] ultimate displacement
massa_star_1=mass_starr_1; % [tonn]
mu_c_1 = 8 ; %[ ] equivalent bracing's ductility (you're the one to fix, in advance, that par
ameter

alfa_disp = 0.95; %[ ] this is a parameter defining the amount of the structure ultimate disp
lacement you're accepting as target displacement

% EVALUATION OF EACH STORY'S STIFFNESS (Existing Structure)
% Hereafter, taken as input the information about horizontal forces and displacements at each
 floor, evaluate each floor's stiffness
% Note that those are the stiffnesses of the Structure without bracings
% Direction X (1)
ki_1 = zeros(1,Np);  % Preallocate vector
for i=1:Np
    AUX = 0;
    for j=i:Np
        AUX = AUX + Fp_1(j); % [kN]
        % this is the sum of all the forces from the current i-th floor above
    end
    ki_1(i)= (Dp_1(i)^(-1))* AUX  ; % [kN/mm]
end


% Knowing the Dp_tot, DP_i, and d_star from pushover ,we can define the yield displacement of
 each storey
% Knowing the k(i) and dy(i) ,we can define the Fy_i of each storey

%Yield Displacemts at each floor
 dy_p_1 = zeros(1,Np);
for i=1:Np
    dy_p_1(i)= Dp_1(i) * (Dp_tot_1^(-1)) * dy_star_1; % [mm] Formulation to be checked!!
end

% Yield Force at each floor
Fy_p_1 = zeros(1,Np);
for i=1:Np
    Fy_p_1(i)= dy_p_1(i) * ki_1(i); % [kN]
end
```

- Input parameters defining the seismic spectrum

```
ag_adim = 0.298 ; % [] it actually is ag/g
Tc_star = 0.356 ; % []
F0 = 2.386 ; % [] maximum amplification factor
% Note that those parameters have been taken from CDS and already takes into account PVR(SLV)

% Soil type
cat_suolo = 3; % [from A to E i.e. from 1 to 5]
% Structural damping
Xsi = 5; % [%]
```

```
ST = 1.0 ;% [ ] topographic amplification factor
```

- Brace characteristics evaluation

```
Nc_1 = 2; % []
alfa_c = 31.0; % [°] braces' inclination angle
% note that the assumption is done that all the braces have the same
% inclination with respect to the horizontal

% STEEL BAR ON WHICH THE BRACE IS INSTALLED
Aa = 53.831; % [cm2] cross-section area
Ea = 210000.0; % [N/mm2] Steel Young's Modulus
La = 5.0; % [m] length
fyk = 355.0; % [MPa]
gamma_M_0 = 1.05; % []

%%%%%%%%%%%%%%%%%%%%%%%%%%%%%%%%%%%%%%%%%%%%%%%%%%%%%%%%%%%%%%%%%%%%%%%%%%%%%%%
%                     Second phase: DERIVED DATA                               %
%%%%%%%%%%%%%%%%%%%%%%%%%%%%%%%%%%%%%%%%%%%%%%%%%%%%%%%%%%%%%%%%%%%%%%%%%%%%%%%

% Seismic Spectrum
% stratigraphic amplification factor SS [] and soil-dependent coefficient CC []
if cat_suolo == 1
    SS = 1.0;
    CC = 1.0;
end
if cat_suolo == 2
    CC = 1.1 * Tc_star^(-0.2);
    aux = 1.4 - 0.4 * F0 * ag_adim;
    if aux>=1.0 && aux<=1.2
        SS = aux;
    elseif aux < 1.0
        SS = 1.0;
    elseif aux > 1.2
        SS =1.2;
    end
end
if cat_suolo == 3
    CC = 1.05 * Tc_star ^(-0.33);
    aux = 1.7 - 0.6 * F0 * ag_adim;
    if aux>=1.0 && aux<=1.5
        SS = aux;
    elseif aux < 1.0
        SS = 1.0;
    elseif aux > 1.5
        SS =1.5;
    end
end
if cat_suolo == 4
    CC = 1.25 * Tc_star^(-0.5);
    aux = 2.4 - 1.5 * F0 * ag_adim;
    if aux>=0.9 && aux<=1.8
        SS = aux;
    elseif aux < 0.9
```

```
        SS = 0.9;
    elseif aux > 1.8
        SS =1.8;
    end
end
if cat_suolo == 5
    CC = 1.15 * Tc_star^(-0.4);
    aux = 2.0 - 1.1 * F0 * ag_adim;
    if aux>=1.0 && aux<=1.6
        SS = aux;
    elseif aux < 1.0
        SS = 1.0;
    elseif aux > 1.6
        SS =1.6;
    end
end

Tc = Tc_star * CC; %[sec]
Tb = Tc/3; %[sec]
Td = 4.0 * ag_adim + 1.6; %[sec]
eta = sqrt(10/(5+Xsi)); % []
S = SS * ST ; % []

% Definition of the target displacement for the brace of both directions. Note that you
% can define it as a certain percentage of the structure's ultimate displacement
d_allowed =zeros(1,Np);
for i=1:Np
    d_allowed(i) = 0.005*H(i)*1000;
end
D_allowed = sum(d_allowed); % The allowed 0.5% limit storey drift for BDE from Code


d_u_pushover_1 = alfa_disp * du_star_1; %[mm] 95 % displacement from pushover

Mu_allowed = 1.5; % Allowed ductility for the existing structures is Mu_allowed = 1.5 [NTC]
if du_star_1/dy_star_1 <= Mu_allowed
    D_allowed_Ductility_1 = du_star_1 ;
elseif du_star_1/dy_star_1 > Mu_allowed
    D_allowed_Ductility_1 = dy_star_1 * Mu_allowed;
end


ds_target_1 = min ([d_u_pushover_1 D_allowed  D_allowed_Ductility_1]); %% The final target di
splacement

% Steel bar elastic stiffness
 ka = 0.0001 * (Ea * Aa) / La; % [kN/mm]                                        dimensionally co
rrect
Fy_a = (Aa * fyk / gamma_M_0) * 0.1; % [kN]



% ITERATIVE PROCEDURE TO EVALUATE THE EQUIVALENT BRACE (for the two directions)
% INITIALIZATION
T_star_1 = 2*pi*sqrt(massa_star_1/k_star_1)*sqrt(0.001); % [sec] SDFS's period in the X direc
tion     check dimesionally!!!!!!!!!!!!!!!!!!!!!!!!!!!!!!!!
wn_star_1= (2*pi)/T_star_1;
```

```
% hereabove, I initialize the periods whose values will be successively
% iteratively updated
% ( The values are wrong, Formulation needs to be checked)
if T_star_1 >= 0 && T_star_1 < Tb
    Se_1_T_star_1 = ag_adim * 9.81 * S * eta * F0 * (T_star_1/Tb + (eta*F0)^(-1.0)*(1-T_star_
1/Tb)); % [m/sec2]
elseif T_star_1 >= Tb && T_star_1 < Tc
    Se_1_T_star_1 = ag_adim * 9.81 * S * eta * F0;
elseif T_star_1 >= Tc && T_star_1 < Td
    Se_1_T_star_1 = ag_adim * 9.81 * S * eta * F0 * (Tc/T_star_1);
elseif T_star_1 >= Td
    Se_1_T_star_1 = ag_adim * 9.81 * S * eta * F0 * (Tc * Td * T_star_1^(-2));
end

% Note that the values of acceleration above are in [m/sec2]

dcy_1 = ds_target_1 / mu_c_1; % [mm] Brace Yield Displacement (Ratio of Target displacement a
nd Brace ductility)

Fc_1=0;
Delta_Fc_1=0.01;
K_Str_Brace_1=k_star_1;


found = 0;
while found == 0;
    Fc_1=Fc_1+Delta_Fc_1;
    K_c_1=Fc_1/dcy_1;
    K_Str_Brace_1=k_star_1 + K_c_1;
    T_Str_Brace_1 = 2*pi* sqrt(massa_star_1/(1000*K_Str_Brace_1));

     if T_Str_Brace_1 >= 0 && T_Str_Brace_1 < Tb
        Se_1_T_Str_Brace_1 = ag_adim * 9.81 * S * eta * F0 * (T_Str_Brace_1/Tb + (eta*F0)^(-1
.0)*(1-T_Str_Brace_1/Tb));
    elseif T_Str_Brace_1 >= Tb && T_Str_Brace_1 < Tc
        Se_1_T_Str_Brace_1 = ag_adim * 9.81 * S * eta * F0;
    elseif T_Str_Brace_1 >= Tc && T_Str_Brace_1 < Td
        Se_1_T_Str_Brace_1 = ag_adim * 9.81 * S * eta * F0 * (Tc/T_Str_Brace_1);
    elseif T_Str_Brace_1 >= Td
        Se_1_T_Str_Brace_1 = ag_adim * 9.81 * S * eta * F0 * (Tc * Td * T_Str_Brace_1^(-2));
    end

    d_e_Str_Brace_1=1000*Se_1_T_Str_Brace_1 *(T_Str_Brace_1/(2*pi))^2 ;
    if T_Str_Brace_1 < Tc

        q_Str_Brace_1=1000*Se_1_T_Str_Brace_1 * 1000*massa_star_1 /Fy_star_1 ;
        d_t_Str_Brace_1= d_e_Str_Brace_1 *(1+(q_Str_Brace_1-1)*Tc/Tb)/q_Str_Brace_1 ;
    elseif T_Str_Brace_1>Tc
        d_t_Str_Brace_1=d_e_Str_Brace_1;
    end

    if d_t_Str_Brace_1 <= ds_target_1 && d_t_Str_Brace_1>=0.95*ds_target_1;
        found=1;

    end
end
```

```
% EACH FLOOR'S EQUIVALENT BRACE STIFFNESS AND YIELD FORCE X direction

% Yield Force of Braces for whole story
Fy_c_1 = zeros(1,Np);
for i=1:Np
    Fy_c_1(i)= Fy_p_1(i) * Fc_1 * Fy_star_1^(-1); % [kN]
end
% Brace stiffness for whole story that will be iterated if regularity conditions dont satisfy
kk_c_1 = zeros(1,Np);
for i=1:Np
    kk_c_1(i)= K_c_1 * ki_1(i) * k_star_1^(-1); % [kN/mm]
end

% Total story stiffness K_tot_1, sum of existing structure stiffness ki_1(i) and
% brace stiffness(kk_c_1(i)
K_tot_1=zeros(1,Np);
for i=1:1:Np
    K_tot_1(i)=kk_c_1(i)+ki_1(i);
end

% Story stiffness regularity conditions verification, After this step the Brace story stiffne
ss will be named kk_c_req

kk_c_new_1 = zeros(1,Np);
for i=2:Np
    if (K_tot_1(i-1)-K_tot_1(i)) /K_tot_1(i-1)> 0.3;
        kk_c_new_1(i)=0.7*K_tot_1(i-1)-ki_1(i)-kk_c_1(i);

        kk_c_req_1= zeros(1,Np);
        for k=1:Np
    kk_c_req_1(k)=kk_c_new_1(k)+kk_c_1(k);
        end

        K_tot_req_1 = zeros(1,Np);
        for h=1:Np
    K_tot_req_1(h)=ki_1(h)+kk_c_req_1(h);
    K_tot_1(h)= K_tot_req_1(h);
        end



    elseif (K_tot_1(i-1)-K_tot_1(i)) /K_tot_1(i-1)<-0.1;
        kk_c_new_1(i-1)=((K_tot_1(i)/1.1)-ki_1(i-1))-kk_c_1(i-1);

        kk_c_req_1= zeros(1,Np);
        for j=1:Np
    kk_c_req_1(j)=kk_c_new_1(j)+kk_c_1(j);
        end


    kk_c_1 = zeros(1,Np);
    K_tot_req_1 = zeros(1,Np);
        for h=1:Np
```

```
    K_tot_req_1(h)=ki_1(h)+kk_c_req_1(h);
    K_tot_1(h)= K_tot_req_1(h);
    kk_c_1(h) = kk_c_req_1(h);
        end

    elseif (K_tot_1(i-1)-K_tot_1(i)) /K_tot_1(i-1)>=-0.1 && (K_tot_1(i-1)-K_tot_1(i)) /K_tot_
1(i-1)<0.3;
         kk_c_req_1=zeros(1,Np);
        for j=1:Np
            kk_c_req_1(j)=kk_c_1(j);
            K_tot_req_1(j)= kk_c_req_1(j)+ki_1(j);
        end

    end


end


% DISTRIBUTION OF THE FLOOR BRACE
% AS FUNCTION OF THEIR NUMBER AND DISTRIBUTION IN PLANT


kkk_c_1 = zeros(1,Np); %%% single brace stiffness for each story
for i=1:Np
    kkk_c_1(i) = kk_c_req_1(i) * (Nc_1^(-1)) * (cosd(alfa_c))^(-2);
end

% here above the axial stiffness of each brace was evaluated for each floor, having assumed t
he same inclination angle for all of them
ffy_c_1 = zeros(1,Np); %%% single brace lateral strength for each story
for l=1:Np
    ffy_c_1(l) = Fy_c_1(l)/((Nc_1) * (cosd(alfa_c)));
end

% here above the axial yeild force of each brace was evaluated for each floor, having assumed
 the same inclination angle for all of them

d_c_y_axial_1 = zeros(1,Np); % [mm] Yield displacement of the brace at ith floor
for i=1:Np
    d_c_y_axial_1(i) = ffy_c_1(i)/kkk_c_1(i);
end


% DEVICE CHARACTERISTICS AT EACH FLOOR
% yield force
ffy_d_1 = zeros(1,Np);
for i=1:Np
    ffy_d_1(i) = ffy_c_1(i); % the correction is made for A(I) = B , to be checked
    if (Fy_a - ffy_d_1(i))<= 0.0
        warning('bar stiffness smaller than the device stiffness')
    end
end

% stiffness
kkk_d_1 = zeros(1,Np);
for i=1:Np
```

```
    kkk_d_1(i) = kkk_c_1(i) * ka / (ka - kkk_c_1(i));
    if (ka - kkk_c_1(i))<= 0.0
        warning('bar stiffness smaller than the device stiffness')
    end
end
% ductility
mu_d_1 = zeros(1,Np);
for i=1:Np
    mu_d_1(i) = ((ka + kkk_d_1(i)) * mu_c_1 - kkk_d_1(i)) / ka; % [kN/mm]
end


% Make also a drawing to have a better representation of the results
```

*Published with MATLAB® R2018b*

## Ponzo-Di Cesare Method - CASE-3

```
clear
clc
close all
```

- Existing structure data

```
Np = 9 ; % Number of floors []

% storey heights in meters
H(1) = 3.0;
H(2) = 3.0;
H(3) = 3.0;
H(4) = 3.0;
H(5) = 3.0;
H(6) = 3.0;
H(7) = 3.0;
H(8) = 3.0;
H(9) = 3.0;

% DIRECTION 1 (X)
% Hereafter are forces and displacements at each floor obtained by a Linear Static Analysis
% Note that the first number in the label refers to the direction in plant: where 1 stands fo
r X and 2 for Y
Fp_1(1) = 39.0 ;  % [kN]
Fp_1(2) = 78.0 ; % [kN]
Fp_1(3) = 116.4 ; % [kN]
Fp_1(4) = 157.0 ; % [kN]
Fp_1(5) = 130.0 ; % [kN]
Fp_1(6) = 116.0 ; % [kN]
Fp_1(7) = 182.9 ; % [kN]
Fp_1(8) = 208.0 ; % [kN]
Fp_1(9) = 234.9 ; % [kN]


Dp_1(1) = 28.5; % [mm] % Interstorey Drifts
Dp_1(2) = 38.5; % [mm]
Dp_1(3) = 37.0; % [mm]
Dp_1(4) = 33.0; % [mm]
Dp_1(5) = 39.0; % [mm]
Dp_1(6) = 36.0; % [mm]
Dp_1(7) = 29.0; % [mm]
Dp_1(8) = 21.0; % [mm]
Dp_1(9) = 11.0; % [mm]


Mass_matrix_1=[66 0 0 0 0 0 0 0 0 ; 0 66 0 0 0 0 0 0 0 ; 0 0 66 0 0 0 0 0 0 ; 0 0 0 66 0 0 0
0 0 ; 0 0 0 0 43.7 0 0 0 0; 0 0 0 0 0 43.7 0 0 0; 0 0 0 0 0 0 43.7 0 0; 0 0 0 0 0 0 0 43.7 0;
 0 0 0 0 0 0 0 0 43.7];
Shape_vector_1=[0.1 0.24 0.38 0.5 0.64 0.77 0.88 0.95 1];
r=[1;1;1;1;1;1;1;1;1];
mass_starr_1=Shape_vector_1*Mass_matrix_1*r; % 1st mode effective mass
```

```
% Note that those above are relative displacements
% Hereafter evaluate the total displacements for each direction
Dp_tot_1 = 0.0; % [mm]
for i=1:Np
    Dp_tot_1 = Dp_tot_1 + Dp_1(i);
end


% First phase: INPUT DATA
% input the parameters defining the capacity spectrum for the
% existing structure's two directions. Where, note those informations can be got by means of
% whatever FEM (commercial) software.

% First Direction (X)
k_star_1 = 7.02; %[kN/mm] elastic stiffness
Fy_star_1 = 660.0; % [kN] yielding strength
dy_star_1 = Fy_star_1/k_star_1 ; % Yield displacement from Pushover
du_star_1 = 120.0; % [mm] ultimate displacement
massa_star_1=mass_starr_1; % [tonn]
mu_c_1 = 8 ; %[ ] equivalent bracing's ductility (you're the one to fix, in advance, that par
ameter

alfa_disp = 0.95; %[ ] this is a parameter defining the amount of the structure ultimate disp
lacement you're accepting as target displacement

% EVALUATION OF EACH STORY'S STIFFNESS (Existing Structure)
% Hereafter, taken as input the information about horizontal forces and displacements at each
 floor, evaluate each floor's stiffness
% Note that those are the stiffnesses of the Structure without bracings
% Direction X (1)
ki_1 = zeros(1,Np);  % Preallocate vector
for i=1:Np
    AUX = 0;
    for j=i:Np
        AUX = AUX + Fp_1(j); % [kN]
        % this is the sum of all the forces from the current i-th floor above
    end
    ki_1(i)= (Dp_1(i)^(-1))* AUX  ; % [kN/mm]
end


% Knowing the Dp_tot, DP_i, and d_star from pushover ,we can define the yield displacement of
 each storey
% Knowing the k(i) and dy(i) ,we can define the Fy_i of each storey

%Yield Displacemts at each floor
 dy_p_1 = zeros(1,Np);
for i=1:Np
    dy_p_1(i)= Dp_1(i) * (Dp_tot_1^(-1)) * dy_star_1; % [mm] Formulation to be checked!!
end

% Yield Force at each floor
Fy_p_1 = zeros(1,Np);
for i=1:Np
```

```
    Fy_p_1(i)= dy_p_1(i) * ki_1(i); % [kN]
end
```

- Input parameters defining the seismic spectrum

```
ag_adim = 0.298 ; % [] it actually is ag/g
Tc_star = 0.356 ; % []
F0 = 2.386 ; % [] maximum amplification factor
% Note that those parameters have been taken from CDS and already takes into account PVR(SLV)

% Soil type
cat_suolo = 3; % [from A to E i.e. from 1 to 5]
% Structural damping
Xsi = 5; % [%]

ST = 1.0 ;% [ ] topographic amplification factor
```

- Brace characteristics evaluation

```
Nc_1 = 2; % []
alfa_c = 31.0; % [°] braces' inclination angle
% note that the assumption is done that all the braces have the same
% inclination with respect to the horizontal

% STEEL BAR ON WHICH THE BRACE IS INSTALLED
Aa = 53.831; % [cm2] cross-section area
Ea = 210000.0; % [N/mm2] Steel Young's Modulus
La = 5.0; % [m] length
fyk = 355.0; % [MPa]
gamma_M_0 = 1.05; % []

%%%%%%%%%%%%%%%%%%%%%%%%%%%%%%%%%%%%%%%%%%%%%%%%%%%%%%%%%%%%%%%%%%%%%%%%%%%%%%%
%                     Second phase: DERIVED DATA                                %
%%%%%%%%%%%%%%%%%%%%%%%%%%%%%%%%%%%%%%%%%%%%%%%%%%%%%%%%%%%%%%%%%%%%%%%%%%%%%%%

% Seismic Spectrum
% stratigraphic amplification factor SS [] and soil-dependent coefficient CC []
if cat_suolo == 1
    SS = 1.0;
    CC = 1.0;
end
if cat_suolo == 2
    CC = 1.1 * Tc_star^(-0.2);
    aux = 1.4 - 0.4 * F0 * ag_adim;
    if aux>=1.0 && aux<=1.2
        SS = aux;
    elseif aux < 1.0
        SS = 1.0;
    elseif aux > 1.2
        SS =1.2;
    end
end
if cat_suolo == 3
```

```
    CC = 1.05 * Tc_star ^(-0.33);
    aux = 1.7 - 0.6 * F0 * ag_adim;
    if aux>=1.0 && aux<=1.5
        SS = aux;
    elseif aux < 1.0
        SS = 1.0;
    elseif aux > 1.5
        SS =1.5;
    end
end
if cat_suolo == 4
    CC = 1.25 * Tc_star^(-0.5);
    aux = 2.4 - 1.5 * F0 * ag_adim;
    if aux>=0.9 && aux<=1.8
        SS = aux;
    elseif aux < 0.9
        SS = 0.9;
    elseif aux > 1.8
        SS =1.8;
    end
end
if cat_suolo == 5
    CC = 1.15 * Tc_star^(-0.4);
    aux = 2.0 - 1.1 * F0 * ag_adim;
    if aux>=1.0 && aux<=1.6
        SS = aux;
    elseif aux < 1.0
        SS = 1.0;
    elseif aux > 1.6
        SS =1.6;
    end
end

Tc = Tc_star * CC; %[sec]
Tb = Tc/3; %[sec]
Td = 4.0 * ag_adim + 1.6; %[sec]
eta = sqrt(10/(5+Xsi)); % []
S = SS * ST ; % []

% Definition of the target displacement for the brace of both directions. Note that you
% can define it as a certain percentage of the structure's ultimate displacement
d_allowed =zeros(1,Np);
for i=1:Np
    d_allowed(i) = 0.005*H(i)*1000;
end
D_allowed = sum(d_allowed); % The allowed 0.5% limit storey drift for BDE from Code


d_u_pushover_1 = alfa_disp * du_star_1; %[mm] 95 % displacement from pushover

Mu_allowed = 1.5; % Allowed ductility for the existing structures is Mu_allowed = 1.5 [NTC]
if du_star_1/dy_star_1 <= Mu_allowed
    D_allowed_Ductility_1 = du_star_1 ;
elseif du_star_1/dy_star_1 > Mu_allowed
    D_allowed_Ductility_1 = dy_star_1 * Mu_allowed;
end
```

```
ds_target_1 = min ([d_u_pushover_1 D_allowed  D_allowed_Ductility_1]); %% The final target di
splacement

% Steel bar elastic stiffness
 ka = 0.0001 * (Ea * Aa) / La; % [kN/mm]                                        dimensionally co
rrect
Fy_a = (Aa * fyk / gamma_M_0) * 0.1; % [kN]

%%%%%%%%%%%%%%%%%%%%%%%%%%%%%%%%%%%%%%%%%%%%%%%%%%%%%%%%%%%%%%%%%%%%%%%%%%%%%%%
%                                  PROCEDURE                                    %
%%%%%%%%%%%%%%%%%%%%%%%%%%%%%%%%%%%%%%%%%%%%%%%%%%%%%%%%%%%%%%%%%%%%%%%%%%%%%%%


% ITERATIVE PROCEDURE TO EVALUATE THE EQUIVALENT BRACE (for the two directions)
% INITIALIZATION
T_star_1 = 2*pi*sqrt(massa_star_1/k_star_1)*sqrt(0.001); % [sec] SDFS's period in the X direc
tion     check dimesionally!!!!!!!!!!!!!!!!!!!!!!!!!!!!!!!!
wn_star_1= (2*pi)/T_star_1;

% hereabove, I initialize the periods whose values will be successively
% iteratively updated
% ( The values are wrong, Formulation needs to be checked)
if T_star_1 >= 0 && T_star_1 < Tb
    Se_1_T_star_1 = ag_adim * 9.81 * S * eta * F0 * (T_star_1/Tb + (eta*F0)^(-1.0)*(1-T_star_
1/Tb)); % [m/sec2]
elseif T_star_1 >= Tb && T_star_1 < Tc
    Se_1_T_star_1 = ag_adim * 9.81 * S * eta * F0;
elseif T_star_1 >= Tc && T_star_1 < Td
    Se_1_T_star_1 = ag_adim * 9.81 * S * eta * F0 * (Tc/T_star_1);
elseif T_star_1 >= Td
    Se_1_T_star_1 = ag_adim * 9.81 * S * eta * F0 * (Tc * Td * T_star_1^(-2));
end

% Note that the values of acceleration above are in [m/sec2]

dcy_1 = ds_target_1 / mu_c_1; % [mm] Brace Yield Displacement (Ratio of Target displacement a
nd Brace ductility)

Fc_1=0;
Delta_Fc_1=0.01;
K_Str_Brace_1=k_star_1;


found = 0;
while found == 0;
    Fc_1=Fc_1+Delta_Fc_1;
    K_c_1=Fc_1/dcy_1;
    K_Str_Brace_1=k_star_1 + K_c_1;
    T_Str_Brace_1 = 2*pi* sqrt(massa_star_1/(1000*K_Str_Brace_1));

     if T_Str_Brace_1 >= 0 && T_Str_Brace_1 < Tb
        Se_1_T_Str_Brace_1 = ag_adim * 9.81 * S * eta * F0 * (T_Str_Brace_1/Tb + (eta*F0)^(-1
.0)*(1-T_Str_Brace_1/Tb));
    elseif T_Str_Brace_1 >= Tb && T_Str_Brace_1 < Tc
        Se_1_T_Str_Brace_1 = ag_adim * 9.81 * S * eta * F0;
    elseif T_Str_Brace_1 >= Tc && T_Str_Brace_1 < Td
```

```
        Se_1_T_Str_Brace_1 = ag_adim * 9.81 * S * eta * F0 * (Tc/T_Str_Brace_1);
    elseif T_Str_Brace_1 >= Td
        Se_1_T_Str_Brace_1 = ag_adim * 9.81 * S * eta * F0 * (Tc * Td * T_Str_Brace_1^(-2));
    end

    d_e_Str_Brace_1=1000*Se_1_T_Str_Brace_1 *(T_Str_Brace_1/(2*pi))^2 ;
    if T_Str_Brace_1 < Tc

        q_Str_Brace_1=1000*Se_1_T_Str_Brace_1 * 1000*massa_star_1 /Fy_star_1 ;
        d_t_Str_Brace_1= d_e_Str_Brace_1 *(1+(q_Str_Brace_1-1)*Tc/Tb)/q_Str_Brace_1 ;
    elseif T_Str_Brace_1>Tc
        d_t_Str_Brace_1=d_e_Str_Brace_1;
    end

    if d_t_Str_Brace_1 <= ds_target_1 && d_t_Str_Brace_1>=0.95*ds_target_1;
        found=1;

    end
end



% EACH FLOOR'S EQUIVALENT BRACE STIFFNESS AND YIELD FORCE X direction

% Yield Force of Braces for whole story
Fy_c_1 = zeros(1,Np);
for i=1:Np
    Fy_c_1(i)= Fy_p_1(i) * Fc_1 * Fy_star_1^(-1); % [kN]
end
% Brace stiffness for whole story that will be iterated if regularity conditions dont satisfy
kk_c_1 = zeros(1,Np);
for i=1:Np
    kk_c_1(i)= K_c_1 * ki_1(i) * k_star_1^(-1); % [kN/mm]
end

% Total story stiffness K_tot_1, sum of existing structure stiffness ki_1(i) and brace stiffn
ess(kk_c_1(i)
K_tot_1=zeros(1,Np);
for i=1:1:Np
    K_tot_1(i)=kk_c_1(i)+ki_1(i);
end

% Story stiffness regularity conditions verification, After this step the Brace story stiffne
ss will be named kk_c_req

kk_c_new_1 = zeros(1,Np);
for i=2:Np
    if (K_tot_1(i-1)-K_tot_1(i)) /K_tot_1(i-1)> 0.3;
        kk_c_new_1(i)=0.7*K_tot_1(i-1)-ki_1(i)-kk_c_1(i);

        kk_c_req_1= zeros(1,Np);
        for k=1:Np
    kk_c_req_1(k)=kk_c_new_1(k)+kk_c_1(k);
        end

        K_tot_req_1 = zeros(1,Np);
```

```
        for h=1:Np
    K_tot_req_1(h)=ki_1(h)+kk_c_req_1(h);
    K_tot_1(h)= K_tot_req_1(h);
        end



    elseif (K_tot_1(i-1)-K_tot_1(i)) /K_tot_1(i-1)<-0.1;
        kk_c_new_1(i-1)=((K_tot_1(i)/1.1)-ki_1(i-1))-kk_c_1(i-1);

        kk_c_req_1= zeros(1,Np);
        for j=1:Np
    kk_c_req_1(j)=kk_c_new_1(j)+kk_c_1(j);
        end


    kk_c_1 = zeros(1,Np);
    K_tot_req_1 = zeros(1,Np);
        for h=1:Np
    K_tot_req_1(h)=ki_1(h)+kk_c_req_1(h);
    K_tot_1(h)= K_tot_req_1(h);
    kk_c_1(h) = kk_c_req_1(h);
        end

    elseif (K_tot_1(i-1)-K_tot_1(i)) /K_tot_1(i-1)>=-0.1 && (K_tot_1(i-1)-K_tot_1(i)) /K_tot_
1(i-1)<0.3;
         kk_c_req_1=zeros(1,Np);
        for j=1:Np
            kk_c_req_1(j)=kk_c_1(j);
            K_tot_req_1(j)= kk_c_req_1(j)+ki_1(j);
        end

    end


end


% DISTRIBUTION OF THE FLOOR BRACE AS FUNCTION OF THEIR NUMBER AND DISTRIBUTION IN PLANT


kkk_c_1 = zeros(1,Np); %%% single brace stiffness for each story
for i=1:Np
    kkk_c_1(i) = kk_c_req_1(i) * (Nc_1^(-1)) * (cosd(alfa_c))^(-2);
end

% here above the axial stiffness of each brace was evaluated for each floor, having assumed t
he same inclination angle for all of them
ffy_c_1 = zeros(1,Np); %%% single brace lateral strength for each story
for l=1:Np
    ffy_c_1(l) = Fy_c_1(l)/((Nc_1) * (cosd(alfa_c)));
end

% here above the axial yeild force of each brace was evaluated for each floor, having assumed
 the same inclination angle for all of them

d_c_y_axial_1 = zeros(1,Np); % [mm] Yield displacement of the brace at ith floor
```

```
for i=1:Np
    d_c_y_axial_1(i) = ffy_c_1(i)/kkk_c_1(i);
end


% DEVICE CHARACTERISTICS AT EACH FLOOR
% yield force
ffy_d_1 = zeros(1,Np);
for i=1:Np
    ffy_d_1(i) = ffy_c_1(i); % the correction is made for A(I) = B , to be checked
    if (Fy_a - ffy_d_1(i))<= 0.0
        warning('bar stiffness smaller than the device stiffness')
    end
end

% stiffness
kkk_d_1 = zeros(1,Np);
for i=1:Np
    kkk_d_1(i) = kkk_c_1(i) * ka / (ka - kkk_c_1(i));
    if (ka - kkk_c_1(i))<= 0.0
        warning('bar stiffness smaller than the device stiffness')
    end
end
% ductility
mu_d_1 = zeros(1,Np);
for i=1:Np
    mu_d_1(i) = ((ka + kkk_d_1(i)) * mu_c_1 - kkk_d_1(i)) / ka; % [kN/mm]
end


% Make also a drawing to have a better representation of the results
```

*Published with MATLAB® R2018b*